TAXONOMY AND BIOCHRONOLOGY OF EARLY TRIASSIC CONODONTS

Dissertation

zur

Erlangung der naturwissenschaftlichen Doktorwürde
(Dr. sc. nat.)

vorgelegt der

Mathematisch-naturwissenschaftlichen Fakultät

der

Universität Zürich

von

Nicolas Goudemand

aus

Frankreich

Promotionskomitee

Prof. Dr. Hugo Bucher
(Leiter der Dissertation, Vertreter der Universität Zürich)
PD Dr. Mike Orchard
Prof. Dr. Leopold Krystyn
Prof. Dr. Christoph Zollikofer

Zürich, 2011

Twenty years from now
You will be more disappointed
By the things you didn't do
Than by the things you did.
So throw the bowlines.
Sail away from the safe harbor.
Catch the trade winds in your sails.
Explore. Dream. Discover.

Mark Twain

---

quoted on the
wallboard of the
GSC, Vancouver

CONTENTS

Abstract

The most severe of all metazoan crises occurred about 252 million years ago at the Permo-Triassic boundary. It wiped out more than 90 percent of all marine species. Various scenarios have been proposed, all implying global environmental changes (e.g. pCO2, SO2, climate, sea-level). Such mass extinctions dramatically demonstrate how closely evolution of organismal shapes is related to modifications of the ‚environment' in a broad sense.

Testing the various crisis scenarios and underlying mechanisms ultimately rely on the acquisition of precise biochronological data. Owing to their broad geographical distribution and unrivalled evolutionary rates during the Early Triassic, ammonoids and conodonts are the ideal organisms for this purpose.

Conodonts were marine, eel-shaped predators. Their phosphatic feeding elements are usually abundant and well preserved in marine Triassic sedimentary rocks. Though the debate still goes on, they are now widely accepted as a major group of early vertebrates. Their excellent fossil record, makes them important tools for both evolutionary and biostratigraphical studies.

This PhD thesis is based upon new conodont data from Nevada, India and South China.

In particular I report first on the co-occurrence of conodont *Chiosella timorensis* with typical late Spathian ammonoids such as *Neopopanoceras haugi*. *Chiosella timorensis* was hitherto considered as a good index fossil for the base of the Anisian (Middle Triassic; Olenekian-Anisian boundary=OAB). This led me to question previous phylogenetic hypotheses about the origin of this taxa. Based on my revision of the data from the two best OAB sections in Guandao (China) and Desli Caira (Rumania) I also propose a new biochronological scheme for this interval.

I also describe new conodont faunas from Dienerian/Smithian beds (Induan-Olenekian boundary=IOB) respectively at Mud (Spiti, Himashal Pradesh, India) and Waili (Guangxi, China). They led to the definition of numerous new taxa and to a significant revision of the most important taxa of this time interval (e.g. *Neospathodus* ex. gr. *dieneri*, *Ns*. ex. gr. *cristagalli*, *Novispathodus* ex. gr. *pakistanensis* and *Nv*. ex gr. *waageni*), for which I differentiate numerous new morphotypes. Based on revised determinations of the material from Chaohu (another GSSP candidate section for the definition of the IOB), I demonstrate that these three sections are in good agreement. This suggests a good lateral reproducibility of the proposed biozonation, at least across the Tethys. In Mud, the combination of both conodont and ammonoid datasets allows to constrain the IOB within 10cm and to construct an informal biozonation scheme comprising 11 association zones for the considered 4m interval.

In South China, I discovered also fused clusters of conodont elements of the genera *Neospathodus* and *Novispathodus*. These are the first natural assemblages reported for the Early Triassic. These specimens partly confirm previous reconstructions of the corresponding apparatuses. Yet, they also contradict previous hypotheses of homologies. Consequently I revised the superfamily Gondolelloidea.

One particular fused cluster of S elements of *Novispathodus*, imaged using propagation phase contrast X-ray synchrotron microtomography (PPC-SRμCT) allowed me to reinterpret available natural assemblage data and to develop a dynamical model of the feeding apparatus at work. This model suggests the presence of a pulley-shaped lingual cartilage homologous to that of extant cyclostomes within the conodonts' mouth. This lends additional support to the interpretation of conodonts as early vertebrates and shows that the presence of such a cartilage is a plesiomorphic condition of crown-vertebrates (lost in gnathostomes).

Key words: Early Triassic, biotic recovery, conodonts, fused clusters, lingual cartilage, vertebrates, Induan-Olenekian Boundary, Olenekian-Anisian Boundary, Nevada, Spiti, South China.

Zusammenfassung

Die schlimmste aller Krisen in der Geschichte der vielzelligen Tieren fand vor etwa 252 Millionen Jahren, an der Perm-Trias Grenze statt. Diese löschte mehr als 90 Prozent der marinen Arten aus. Verschiedene Szenarien wurden vorgeschlagen, alle schliessen globale Umweltveränderungen ein (e.g. pCO2, SO2, Klima, Meerespiegel). Solche Massenaussterben veranschaulichen in einer dramatischen Weise wie eng die Evolution der organismischen Formen von Umweltschwankungen abhängt.

Das Prüfen der verschiedenen Krisenszenarien und der zugrunde liegenden Mechanismen beruht letzendlich auf der Erfassung von genauen biochronologischen Daten. Ammonoideen und Conodonten sind dank ihrer weiten geographischen Verbreitung und ihren einzigartigen hohen Evolutionsraten in der frühen Trias optimale Organismen für diesen Zweck.

Conodonten waren marine aalförmige Predatoren. Ihre Fressapparate bestehen aus einzelnenn Elementen welche aus Kalziumphosphat aufgebaut sind. Diese Elemente sind in Triassischen Sedimentgesteinen üblicherweise reichlich vorhanden und gut erhalten. Obwohl die Debatte weiterbesteht werden sie jetzt weitgehend als eine bedeutende Gruppe früher Wirbeltieren angenommen. Dank ihres gewaltigen Fossilbelegs sind sie für Biostratigraphie sowie auch für unser Verständnis der frühen Wirbeltiergeschichte von grosser Bedeutung.

Diese Dissertation basiert auf neuen Conodonten-Daten aus Nevada, Indien und Südchina.

Im Besonderen berichte ich zum ersten Mal vom gemeinsamen Vorkommen von Conodont *Chiosella timorensis* mit typischen spät-Spathium Ammonoideen wie *Neopopanoceras haugi*. *Chiosella timorensis* wurde bisher als gutes Leitfossil für die Basis des Anis (Mitteltrias; Olenekium-Anis Grenze=OAB) betrachtet. Dies leitete mich an vorherigen phylogenetischen Annahmen über deren Ursprung zu zweifeln. Bezogen auf meine Revidierung der Daten aus den zwei besten OAB Profilen in Guandao (China) und Desli Caira (Rumänien) schlage ich auch ein neues biochronologischen Schema für dieses Intervall vor.

Ich beschreibe auch neue Conodontenfaunen aus Bänken des Dienerium/Smithium Intervalls (Induum/Olenekium Grenze=IOB) in Mud (Spiti, Himashal Pradesh, Indien) und Waili (Guangxi, China). Das hat mir ermöglicht viele neue Taxa zu definieren sowie auch die wichtigsten Taxa dieses Intervalls (u.a. *Neospathodus* ex. gr. *dieneri*, *Ns*. ex. gr. *cristagalli*, *Novispathodus* ex. gr. *pakistanensis* and *Nv*. ex gr. *waageni*) bedeutsam zu revidieren, indem ich viele neue Morphotypen dieser Taxa unterscheiden konnte. Basierend auf von mir revidierten Bestimmungen des Materials aus Chaohu (ein anderes GSSP Kandidatprofil für die Definition der IOB) zeige ich, dass diese drei Profile sehr gut miteinander übereinstimmen. Dies deutet auf eine gute laterale Reproduzierbarkeit (mindestens über die Tethys) der vorgeschlagenen Zonierung hin. In Mud ermöglicht die Kombination der beiden Conodonten- und Ammonoideen-Datensätzen die IOB innerhalb von 10 Zentimeter zu orten und ein informelles Biozonierungschema herzustellen, welches für das entsprechende 4 Meter Intervall 11 Assoziationszonen umfasst.

In Südchina habe ich auch verschmolzene Clusters (*fused clusters*) von Conodontenelementen der Gattungen *Neospathodus* und *Novispathodus* entdeckt. Damit liegt der erste Bericht über solche natürlichen Ansammlungen (*natural assemblages*) aus der frühen Trias vor. Diese Funde bestätigen vorherige Rekonstruktionen der entsprechenden Apparate. Jedoch widersprechen sie früheren Homologiehypothesen. Demzufolge revidiere ich die Superfamilie Gondolelloidea.

Ein besonderes, mit Synchrotron Microtomographie (PPC-SRμCT) abgebildetes, Cluster von S-Elementen von *Novispathodus* ermöglichte mir vorhandene *natural assemblage* Daten neu zu deuten und ein dynamisches Modell des Fressapparates aufzubauen. Dieses Modell deutet auf die Anwesenheit eines Flaschenzugsförmigen Zungenknorpels innerhalb des Conodontenmundes hin, der mit dem Zungenknorpel der Rundmäuler homolog wäre. Dies befürwortet die Interpretation, wonach Conodonten frühe Wirbeltiere darstellen und weist drauf hin, dass die Anwesenheit eines solchen Knorpels ein plesiomorphes Merkmal der Kronenwirbeltiere (verloren bei Kiefermäuler) bildet.

Plus tard, des inquiéteurs de pierre demanderont aux volutes,
aux symétries, aux volumes, aux textures, aux concrétions,
de raconter un peu de leurs mystères, de livrer un peu de sens.
Les fossiles témoigneront de ce que fut la vie
quand le temps n'était pas celui d'aujourd'hui...

Michel Onfray (2009:14)

INTRODUCTION

Onfray, M. 2009. Les Formes du Temps: Théorie du Sauternes. Ed. Mollat.

Introduction

This dissertation is part of a multidisciplinary study conducted at the Palaeontological Institute and Museum of the University of Zurich (PIMUZ), in which different aspects of the Early Triassic recovery and its climatic/oceanographic constraints are being investigated.

In paleontology, evolution refers to the change of biological shape through time. This per se dynamical process is best exemplified during particular time intervals such as biotic crises or subsequent recovery periods, during which faunal changes are the most spectacular. The most severe of all metazoan crises occurred about 252 million years ago (Mundil *et al*., 2004), at the Permo-Triassic Boundary (PTB). It wiped out more than 90% of all marine species (e.g. Raup and Sepkoski, 1982) and replaced typical Palaeozoic faunas by typical Mesozoic-Cenozoic communities (Fig. 1; Sepkoski, 1984). It is also generally assumed that the subsequent recovery lasted longer compared with other mass extinctions.

The peculiar Early Triassic geographical configuration of landmasses, with a unique,

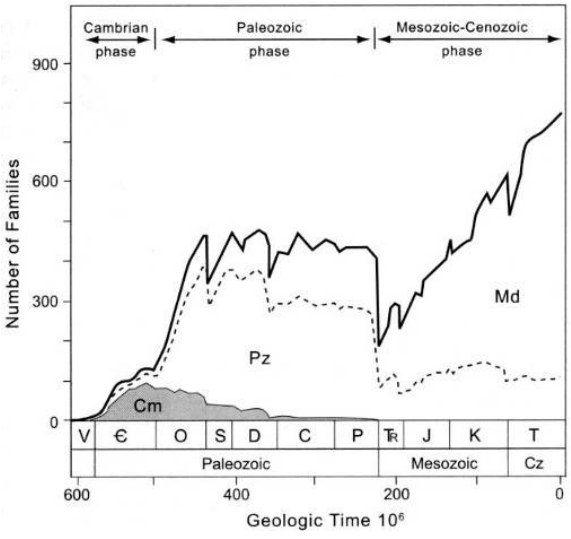

Fig. 1. Marine diversity throughout the Phanerozoic. Cm: Cambrian fauna; Pz: Palaeozoic fauna; Md: Mesozoic-Cenozoic fauna. From Sepkoski (1984).

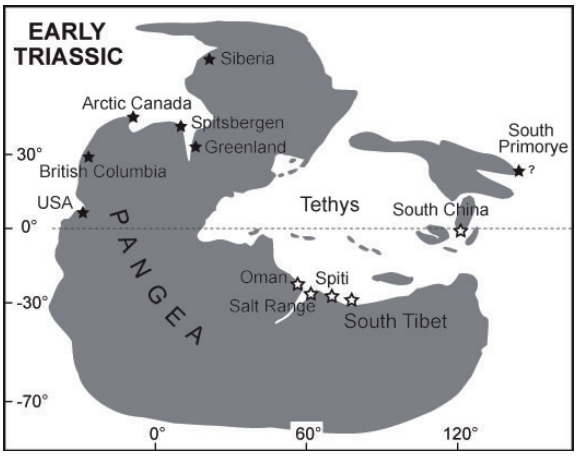

Fig. 2. Simplified palaeogeographical map of the Early Triassic with the palaeoposition of the Salt Range (Pakistan), Spiti (Northern India), Tulong (South Tibet), Oman, South China and other localities mentioned in this thesis (modified after Brayard *et al*., 2006).

crescent-shaped Pangea (or supercontinent) encircled by Panthalassa (Fig. 2), renders this time interval even more compelling for evolutionary studies: we aim indeed at understanding the interrelationships between biotic and abiotic changes, for instance potential causal links between climate and evolution of faunas. The relatively simple and constant configuration prevailing during the Early Triassic, the main continental masses being stable with no ocean closure nor opening, limits the number of potential abiotic factors, which somewhat simplifies the analysis.

Various scenarios have been proposed for the end-Permian extinction, including sea-level regression (Holser *et al*., 1989), voluminous volcanism (Renne *et al*., 1995; Payne and Kump, 2007), extraterrestrial impacts (Becker *et al*., 2004), widespread marine anoxia (Wignall and Twitchett, 1996; Isozaki, 1997; Kakuwa, 2008), hypercapnia (Knoll *et al*., 2007), euxinia (Grice *et al*., 2005; Meyer and Kump, 2008), methane release (Krull and Retallack, 2000), massive release of carbon dioxide via vaporization of coal deposits (Erwin, 2006), and venting of

halocarbons and greenhouse gases induced by metamorphism of the Siberian Traps with evaporites and organic-rich (Svensen *et al*., 2009). Of course, it could be also a combination of these (Berner, 2002; Erwin, 2006).

Testing of these various scenarios requires precise absolute and relative timing of events. It is clear that event A can not cause event B if A does not precede B (see for instance Hoffmann *et al*., submitted). A direct causal link must be also excluded if both events are too timely distant: for instance a presumed meteorite impact, whose dramatic consequences are supposed to be geologically instantaneous (within years or thousands of years) cannot be said to be the cause of a particular major faunal crisis if it predates the latter by more than 100 kyr. One major outcome of our team project has been the calibration of the Early Triassic time scale by means of new U-Pb zircon ages measured from volcanic ash layers discovered in Guangxi (South China) (Ovtcharova *et al*., 2006; Galfetti *et al*., 2007b). These results indicate that the four Early Triassic substages (Griesbachian, Dienerian, Smithian, Spathian) are of extremely uneven duration (Fig. 3).

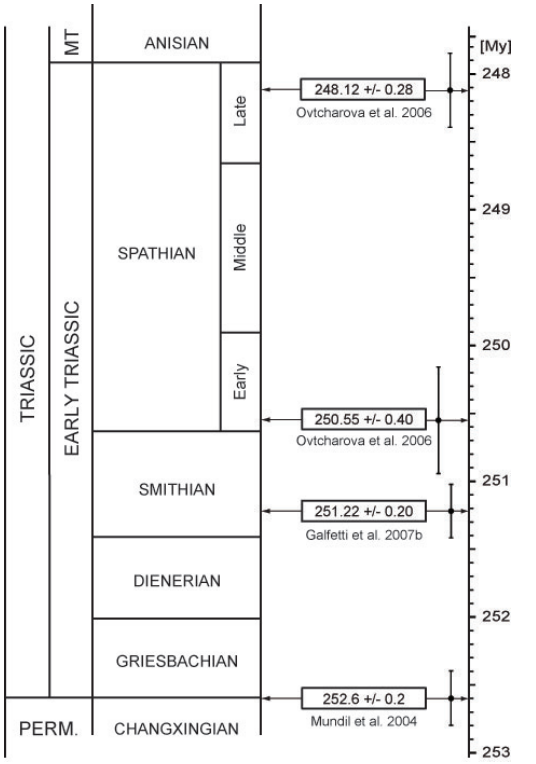

Fig. 3. Early Triassic stage subdivision (Tozer, 1967) calibrated with recently published radiometric ages from South China (Mundil *et al*., 2004; Ovtcharova *et al*., 2006; Galfetti *et al*., 2007b).

Combined with absolute age calibrations, acquisition of precise biochronological data is the cornerstone to which all other aspects of the research on the Early Triassic recovery hinge with. A firm basis for this purpose has been laid by the revision of ammonoid faunas from South China (Brayard and Bucher, 2008; Brühwiler *et al*., 2008; Bucher *et al*., ongoing work). The initial goal of this thesis was a similar refined taxonomic work on South Chinese conodonts (see Chapter 5). Finally, it has been supplemented by high resolution sampling and taxonomic revision of Early Triassic key conodont and ammonoid successions from the Northern Indian Margin (NIM; Salt Range in Pakistan, Spiti in Northern India, Tulong in South Tibet) and from North America (Darwin section, California). Correlation of these sequences with South China, and other areas aim at the construction of a high-resolution Early Triassic conodont and ammonoid zonation (see Chapters 3, 4, 5; Goudemand *et al*., ongoing work; Brühwiler *et al*., 2009, 2010a-c; Ware *et al*., ongoing work; Bucher *et al*., ongoing work).

In the aftermath of the end-Permian mass extinction, conodonts and ammonoids were among the fastest clades to recover. A recent analysis of a global diversity data set of ammonoid genera from the Late Carboniferous to the Late Triassic shows that Triassic ammonoids actually reached levels of diversity higher than in the Permian less than 2 million years after the PTB (Brayard *et al*., 2009b). Similarly, and during the same two million year interval, conodonts experienced their most important evolutionary radiation since the Devonian (see Orchard, 2007, modified by Goudemand *et al*., 2008). As for ammonoids, this exceptional radiation

is interrupted at the end of the Smithian by a major extinction event, related to global climate changes (Galfetti *et al*., 2007a, c).

The necessary, refined biochronologic conodont data was obtained using multi-element taxonomy, which takes into account the fact that morphologically different conodont elements represent different skeletal parts of the same individual animal. The latter is evident from both bedding plane *natural assemblages* and from *fused clusters* in acid residues.

The general architecture of the conodont oral skeleton (Fig. 4) is a bilaterally symmetrical array of usually 15 phosphatic elements: one unpaired 'S_0' element on the axis of bilateral symmetry; four pairs of 'ramiform' (grasping) elements located on both sides of the S_0 (S_{1-4}, subscript number indicates distance ordering from the symmetry axis); one pair of anteriorly located, obliquely pointed, 'makelliform' elements (M); and two pairs of caudally located pectiniform elements (P_1, P_2) (Fig. 4C). The latter would have processed food by crushing and/or slicing (Purnell, 1995; Purnell and Donoghue, 1997).

The multi-element taxonomic approach is not only biologically more meaningful, it is also potentially capable of providing higher biochronologic resolution. Because the morphology of the ramiform elements is more conservative than that of pectiniform elements, standard biochronology was usually based on the P_1 'platform' element only, as were also most interpretations of phyletic relationships. Yet, the restricted number of available characters and the numerous observed morphological convergences within pectiniform elements render this very difficult. This problem is best solved using multi-element reconstructions (Chapters 3-5), relying ultimately upon rare, but crucial findings of natural clusters (Chapter 1).

We discovered exceptional, new fused clusters of the conodont *Novispathodus*. These clusters not only led us to important taxonomic revisions (Chapter 1), but also to a new functional model of the apparatus of euconodonts (Chapter 2), with consequences both for the affinity of conodonts and for our understanding of early vertebrates, before the apparition of jaws. In the near future, these results should help better understanding the biology and ecology of conodonts, recognizing major evolutionary innovations and revising suprageneric classification, which in turn may lead to a refined biochronological scheme.

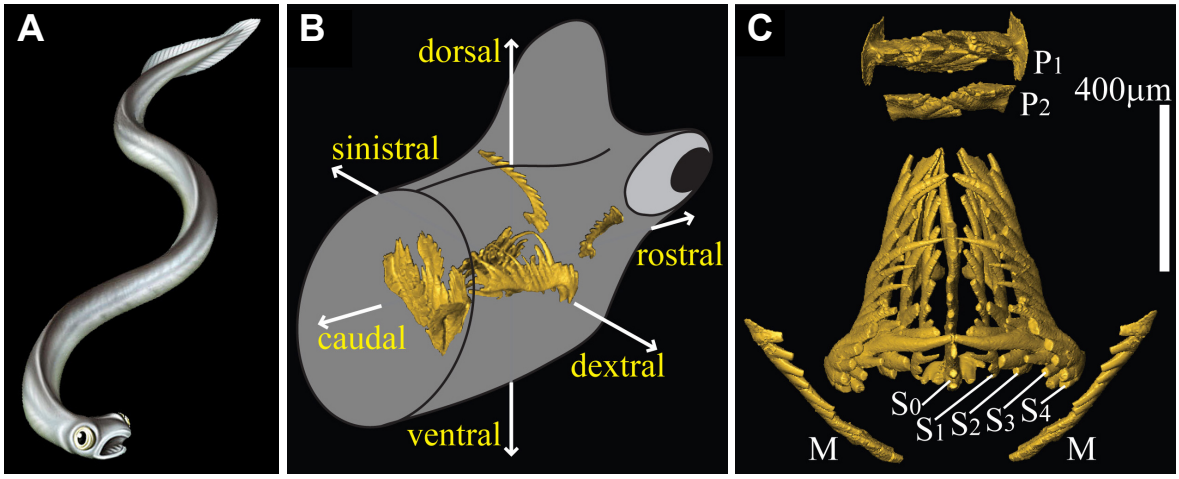

Fig. 4. A: Conodonts were marine, eel-shaped animals. **B**: Orientation of the apparatus within the conodont's head. **C**: Dorsal view of the reconstructed, closed apparatus of *Novispathodus*. From Goudemand *et al*. in prep. see also Chapter 2; Anatomical notation follows that of Purnell *et al*. (2000).

References

Becker, L., R. J. Poreda, A. R. Basu, K. O. Pope, T. M. Harrison, C. Nicholson, and R. Iasky. 2004. Bedout: a possible end-Permian impact crater offshore of northwestern Australia. Science, 304:1469-1476.

Berner, R. A. 2005. The Carbon and Sulfur Cycles and Atmosphere Oxygen from Middle Permian to Middle Triassic. Geochimica et Cosmochimica Acta, 69(13):3211-3217.

Brayard, A., and H. Bucher. 2008. Smithian (Early Triassic) ammonoid faunas from northwestern Guangxi (South China): Taxonomy and Biochronology. Fossils and Strata, 55:179 pp.

Brayard, A., H. Bucher, G. Escarguel, F. Fluteau, S. Bourquin, and T. Galfetti. 2006. The Early Triassic Ammonoid Recovery: Paleoclimatic Significance of Diversity Gradients. Palaeogeography, Palaeoclimatology, Palaeoecology.

Brayard, A., G. Escarguel, H. Bucher, C. Monnet, T. Brühwiler, N. Goudemand, T. Galfetti, and J. Guex. 2009. Good genes and good luck: ammonoid diversity and the end-Permian mass extinction. Science, 325:1118-1121.

Brühwiler, T., A. Brayard, H. Bucher, and K. Guodun. 2008. Griesbachian and Dienerian (Early Triassic) ammonoid faunas from northwestern Guangxi and southern Guizhou (South China). Palaeontology, 51:1151-1180.

Brühwiler, T., Goudemand, N., Galfetti, T., Bucher, H., Baud, A. Ware, D., Hermann, E., Hochuli, P.A. & Martini, R. 2009. The Lower Triassic sedimentary and carbon isotope records from Tulong (South Tibet) and their significance for Tethyan palaeoceanography. Sedimentary Geology 222:314-332.

Brühwiler, T., Ware, D., Bucher, H., Krystyn, L. & Goudemand, N. 2010a. New Early Triassic ammonoid faunas from the Dienerian/ Smithian boundary beds at the Induan/ Olenekian GSSP candidate at Mud (Spiti, Northern India). Journal of Asian Earth Sciences.

Brühwiler, T., Bucher, H. & Goudemand, N. 2010b. Smithian (Early Triassic) ammonoids from Tulong, South Tibet. Geobios 43: 403-431.

Brühwiler, T., Bucher, H., Brayard, A. & Goudemand, N. 2010c. High-resolution biochronology and diversity dynamics of the Early Triassic ammonoid recovery: the Smithian faunas of the Northern Indian Margin. Palaeogeography, Palaeoclimatology, Palaeoecology. doi:10.1016/j.palaeo.2010.09.001.

Erwin, D. H. 2006. Extinction: How Life on Earth Nearly Ended 250 Millions Years Ago. Princeton University Press, 296 p.

Galfetti, T., H. Bucher, A. Brayard, P. A. Hochuli, H. Weissert, G. Kuang, V. Atudorei, and J. Guex. 2007a. Late Early Triassic climate change: Insights from carbonate carbon isotopes, sedimentary evolution and ammonoid paleobiogeography. Palaeogeography, Palaeoclimatology, Palaeoecology, 243(2007):394-411.

Galfetti, T., H. Bucher, M. Ovtcharova, U. Schaltegger, A. Brayard, T. Brühwiler, N. Goudemand, H. Weissert, P. A. Hochuli, F. Cordey, and G. Kuang. 2007b. Timing of the Early Triassic carbon cycle perturbations inferred from new U-Pb ages and ammonoid biochronozones. Earth and Planetary Science Letters, 258:593-604.

Galfetti, T., P. A. Hochuli, A. Brayard, H. Bucher, H. Weissert, And J. O. Vigran. 2007c. Smithian-Spathian boundary event: Evidence for global climatic change in the wake of the end-Permian biotic crisis. Geology, 35(4):291-294.

Goudemand, N., Orchard, M., Bucher, H., Brayard, A., Brühwiler, T., Galfetti, T., Hochuli, P.A., Hermann, E. & Ware, D., 2008. Smithian-Spathian Boundary: The Biggest Crisis in Triassic Conodont History. Geological Society of America, Houston. Paper No. 318-3.

Grice, K., C. Cao, G. D. Love, M. E. Böttcher, R. J. Twitchett, E. Grosjean, R. E. Summons, S. C. Turgeon, W. Dunning, and Y. Jin. 2005. Photic Zone Euxinia During the Permian-Triassic Superanoxic Event. Science, 307:706-709.

Holser, W. T., H. P. Schönlaub, M. Attrep, K. Boeckelmann, P. Klein, M. Magaritz, C. J. Orth, A. Fenninger, C. Jenny, M. Kralik, H. Mauritsch, E. Pak, J.-M. Schramm, K. Stattegger, and R. Schmöller. 1989. A unique geochemical record at the Permian/ Triassic boundary. Nature, 337:39-44.

Isozaki, Y. 1997. Permo-Triassic boundary superanoxia and stratified superocean: record from lost deep sea. Science, 276:235-238.

Kakuwa, Y. 2008. Evaluation of palaeo-oxygenation of the ocean bottom across the Permian-Triassic boundary. Global and Planetary Change, 63:40-56.

Knoll, A. H., R. K. Bambach, J. L. Payne, S. Pruss, AND W. W. Fischer. 2007. Paleophysiology and end-Permian mass extinction. Earth and Planetary Science Letters.

Krull, E. S., AND G. J. Retallack. 2000. $\delta^{13}C$ depth profiles from paleosols across the Permian-Triassic boundary: Evidence for methane release. Geological Society of America Bulletin, 112:1459-1472.

Meyer, K. M., AND L. R. Kump. 2008. Oceanic euxinia in Earth history: Causes and consequences. Annu. Rev. Earth Planetary Sci., 36:251-288.

Mundil, R., K. R. Ludwig, I. Metcalfe, AND P. R. Renne. 2004. Age and Timing of the Permian Mass Extinctions: U/Pb Geochronology on Closed-System Zircons. Science, 305:1760-1763.

Orchard, M. J. 2007. Conodont diversity and evolution through the latest Permian and Early Triassic upheavals. Palaeogeography, Palaeoclimatology, Palaeoecology, 252:93-117.

Ovtcharova, M., H. Bucher, U. Schaltegger, T. Galfetti, A. Brayard, AND J. Guex. 2006. New late Early Triassic and Anisian U-Pb ages from South China: calibration with the ammonoid time scale and implications for the timing of the Triassic biotic recovery. Earth and Planetary Science Letters.

Payne, J. L., AND L. R. Kump. 2007. Evidence for recurrent Early Triassic massive volcanism from quantitative interpretation of carbon isotope fluctuations Earth and Planetary Science Letters.

Purnell, M. A. 1995. Microwear on conodont elements and macrophagy in the first vertebrates. Nature, 374:798-800.

Purnell, M. A., AND P. C. J. Donoghue. 1997. Architecture and functional morphology of the skeletal apparatus of ozarkodinid conodonts. Philosophical Transactions of the Royal Society London B, 352:1545-1564.

Raup, D. M., AND J. J. Sepkoski. 1982. Mass extinctions in the marine fossil record. Science, 215:1501-1503.

Renne, P. R., Z. Zhang, M. A. Richardson, M. T. Black, AND A. R. Basu. 1995. Synchrony and causal relations between Permo-Triassic boundary crises and Siberian flood volcanism. Science, 269:1413-1416.

Sepkoski, J. J. 1984. A Kinetic-model of Phanerozoic taxonomic diversity. 3. Post-Paleozoic families and mass extinctions. Paleobiology, 10(246-267).

Svensen, H., S. Planke, A. G. Polozov, N. Schmidbauer, F. Corfu, Y. Y. Podladchikov, AND B. Jamtveit. 2009. Siberian gas venting and the end-Permian environmental crisis. Earth and Planetary Science Letters, 277:490-500.

Wignall, P. B., AND R. J. Twitchett. 1996. Oceanic anoxia and the end Permian mass extinction. Science, 272:1155-1158.

CHAPTER 1

Early Triassic conodont clusters from South China: Revision of the architecture of the 15-element apparatuses of the superfamily Gondolelloidea

Nicolas Goudemand[a] , Michael J. Orchard[b], Paul Tafforeau[c], Séverine Urdy[a], Thomas Brühwiler[a], Arnaud Brayard[d], Thomas Galfetti[e] & Hugo Bucher[a]

[a]Palaeontological Institute and Museum, University of Zurich, Karl Schmid-Strasse 4, CH-8006 Zürich, Switzerland.
[b]Geological Survey of Canada, 101-605 Robson St., Vancouver, BC, V6B 5J3 Canada.
[c]European Synchrotron Radiation Facility, 6 rue Jules Horowitz, BP 220, 38043 Grenoble cedex, France.
[d]UMR-CNRS 5561 Biogéosciences, Université de Bourgogne, 6 Bd Gabriel, 21000 Dijon, France.
[e]Holcim Group Support Ltd, Materials Technology, 5113 Holderbank, Switzerland.

Several fused clusters of conodont elements of the genera *Neospathodus* and *Novispathodus* were recovered from limestone beds at the Dienerian-Smithian and Smithian-Spathian boundaries respectively, from several localities in Guangxi province, South China.
Conodont clusters are otherwise extremely rare in the Triassic and these are the first reported for the Early Triassic. The exceptional specimens partially preserve the relative three-dimensional position and orientation of ramiform elements and are therefore extremely important for testing hypotheses on the architecture of apparatuses.
These specimens partly confirm the previous reconstruction of the *Novispathodus* apparatus by Orchard. Yet, they also demonstrate that the elements previously identified as occupying the S_1 and S_2 positions occupy in fact the S_2 and S_1 positions respectively. This affects our interpretation of all apparatuses of superfamily Gondolelloidea, which was based on bedding plane natural assemblages from the Middle Triassic of Switzerland. The same applies to the elements in the S_3 and S_4 positions, whose positions are actually reversed, at least for the subfamily Novispathodinae.
It was possible to reach these conclusions thanks to a X-ray synchrotron microtomography. A pink beam setup at 17.6 keV, recently developed at the European Synchrotron Radiation Facility on the ID19 beamline, and allowing submicron resolution (voxel size 0.23µm), has been successfully tested on these fossils.
Several new forms of early Spathian P_1 elements are described but pending detailed analysis of better preserved representatives mostly from Darwin canyon (California), these forms are kept in open nomenclature.

Key words: conodont, fused cluster, Triassic, South China, Luolou Fm., multielement taxonomy.

Since Hinde's presumed cluster from the Devonian of New York (Hinde, 1879), conodont workers held two opposing views about whether conodont taxonomy should rely only on the shape of individual, isolated specimens (*form taxonomy*) or whether it should reflect the fact that morphologically different elements represent different skeletal parts of the same individual animal (Briggs *et al*., 1983; Aldridge, 1993). The latter is evident from both bedding plane *natural assemblages* and from *fused clusters* in acid residues.

The continued discovery of assemblages from the early 1950s on soon questioned traditional form taxonomy. However, since

conodonts were predominantly used as biochronologic tools, many conodont workers continued to use form taxonomy arguing that collections were too scarce and that multi-element taxonomy, though biologically more meaningful and potentially capable of providing higher resolution, was consequently impossible to apply. With growing collections multi-element taxonomy progressively took a predominant part in the literature, but Triassic studies remain an exception.

The scarcity of data and the preponderance of pectiniform elements within collections even led some Triassic workers (Sweet, 1970, p. 210; Kozur, 1971, pp.11-12) to regard ramiform and pectiniform elements as pertaining to separate apparatuses. The discovery of fused clusters (Ramovs, 1977; 1978) and natural assemblages (Rieber, 1980) demonstrated the natural association of 'platform' and ramiform elements and invalidated this view. As previously suggested, the evidence for the diagnosis of a conodont multi-element species is provided by a natural assemblage or a fused cluster. Yet, except for two examples of fused platforms discovered by Mietto in Ladinian rocks around Trento (Mietto, 1982), the above mentioned specimens were, until recently, the only published examples of conodont clusters for the entire Triassic. Just a few months ago, Huang *et al*. (2010) reported new clusters from the Yunnan Province, China (see comments below).

Since the morphology of the ramiform elements is more conservative than that of pectiniform elements, standard biochronology was usually based on the P_1 'platform' element only, as were also most interpretations of phyletic relationships. Yet, the restricted number of available characters and the numerous observed morphological convergences render this very difficult. This problem is best solved using multi-element reconstructions, which again underlines the importance of finding natural clusters upon which provide the ultimate test for these hypothetical reconstructions.

We first report here fused clusters from the Early Triassic. They enable us to test previous reconstructions of the *Novispathodus* and *Neospathodus* apparatuses.

Previous multi-element reconstructions

Huckriede was the first in 1958 to attempt a reconstruction of Triassic apparatuses. He empirically identified recurrent associations of discrete elements in his collections (Huckriede, 1958). Note that this method is still the most employed by conodont workers today. Various clustering methods can be applied also in the case of large collections of discrete elements. This is for instance the approach Sweet (1970) adopted for analyzing his Lower Triassic collection from the Salt Range of Pakistan. Unfortunately it led him to distinguish ramiform apparatuses (then referred to *Ellisonia*) from pectiniform apparatuses (including *Neogondolella* and *Neospathodus*), which, as previously discussed, was later invalidated by the discovery of natural assemblages of *Neogondolella* (Rieber, 1980).

Several authors proposed empirical apparatuses' reconstructions of Triassic species (Kozur and Mostler 1971; Ramovs 1977; Mietto 1982; Bagnoli, 1985; Zhang, 1991; Koike, 1996; 1999; 2004), but most of these appear incomplete and/or lack modern notation.

The Middle Triassic *Neogondolella* natural assemblages discovered by Rieber at the Monte San Giorgio in Switzerland (Rieber, 1980) were reinterpreted by Orchard and Rieber (1999). As a result they proposed a common 15-element architectural template for all apparatuses of the Gondolelloidea superfamily: paired P_1, P_2, M, S_1, S_2, S_3 and S_4, and an unpaired alate S_0 (see Text-Fig. 4 in Orchard and Rieber, 1999). Moreover, the superfamily was said to be characterized by a breviform digyrate, 'enantiognathiform' S_1

element. Note that we adopt the anatomical notation by Purnell *et al*. (2000). This template subsequently provided Orchard (2005) with a basis for his 26 multielement reconstructions within this superfamily.

However, it should be noted that the nature of the Monte San Giorgio (smashed) assemblages rendered them difficult to interpret unambiguously and Orchard himself clear-sightedly noted:

"…*there is some evidence that the pair of elements identified as occupying the S_1 and S_2 (= S_b) positions in fact occupy, respectively, the S_2 and S_1 positions but the evidence is inconclusive. Similar uncertainty surrounds the relative position of some element pairs identified as S_3 and S_4*…"

Material

Several fused clusters were found in the acid residues of Lower Triassic rock samples from the Jinya/Waili, Youping/Leye and Tsoteng areas respectively, all located within the Nanpanjiang Basin in the northwestern Guangxi Province, South China (Text-Fig. 1A).

A composite section of the Jinya/Waili area with the main lithological and formational subdivisions is shown in Text-Fig. 1B. Late Permian skeletal reef limestones of the Wujiaping Fm. are overlain by the ~80 m thick, ammonoid- and conodont-rich Early Triassic mixed carbonate-siliciclastic series of the Luolou Fm. (further details can be found for instance in Galfetti *et al*., 2008). The Middle Triassic Baifeng Formation consists generally of a very thick (>1000 meters) prograding turbiditic sequence. The sample from this area, numbered W148-C3, was collected within the uppermost part of Unit II (as defined in Galfetti, 2008) about half a meter below the prominent and cliff-forming "*Flemingites rursiradiatus*" beds (see Text-Fig. 1C). Its age, based both on ammonoids ("*Kashmirites kapila*" beds) and conodonts (e.g. *Borinella* cf. *nepalensis*, see also Chapter 5), is early Smithian.

The lithological succession in the Youping/Leye area is very similar to that observed in the Jinya/Waili area. Clusters were found in this area in sample Y3-C1. It corresponds to small-sized, early diagenetic limestone nodules within black shales (see Text-Fig. 1D). It contains a typical *Xenoceltites* ammonoid fauna, which was diagnosed by Brayard & Bucher (2008) as latest Smithian in age. Yet, the occurrence of *Novispathodus pingdingshanensis* in this sample and the co-occurrence of *Nv. pingdingshanensis* and *Icriospathodus collinsoni* in a correlative sample (JIN 33, ammonoid-based correlation) indicate more affinities with Spathian faunas than with Smithian faunas.

The succession in the classical Tsoteng section (Zhang, 2005), almost exclusively consists of limestones. Clusters were found in sample TQ84-C30, from a decimetre-thick limestone bed within an intercalation of very thin limestone beds and dark shales (see Text-Fig. 1E). It is bracketed by two ash layers, which unfortunately did not yield reliable radiometric ages. The presence of *Nv. pingdingshanensis* again indicates an early Spathian age.

Most of these clusters (see Pl. 1) consist of two elements only. A first observation is that many of these clusters are fused S_3 and S_4 elements. We will later address considerations on their relative position (see the revision part), but let us already note that their relative frequent occurrence may indicate that these elements were lying very close to one another in the living animal. More than the other elements, the S_3 and S_4 may have functioned together (see also Chapter 2). Similarly, associations of two paired pectiniform P_1 elements are found relatively often (both in our samples and in the literature).

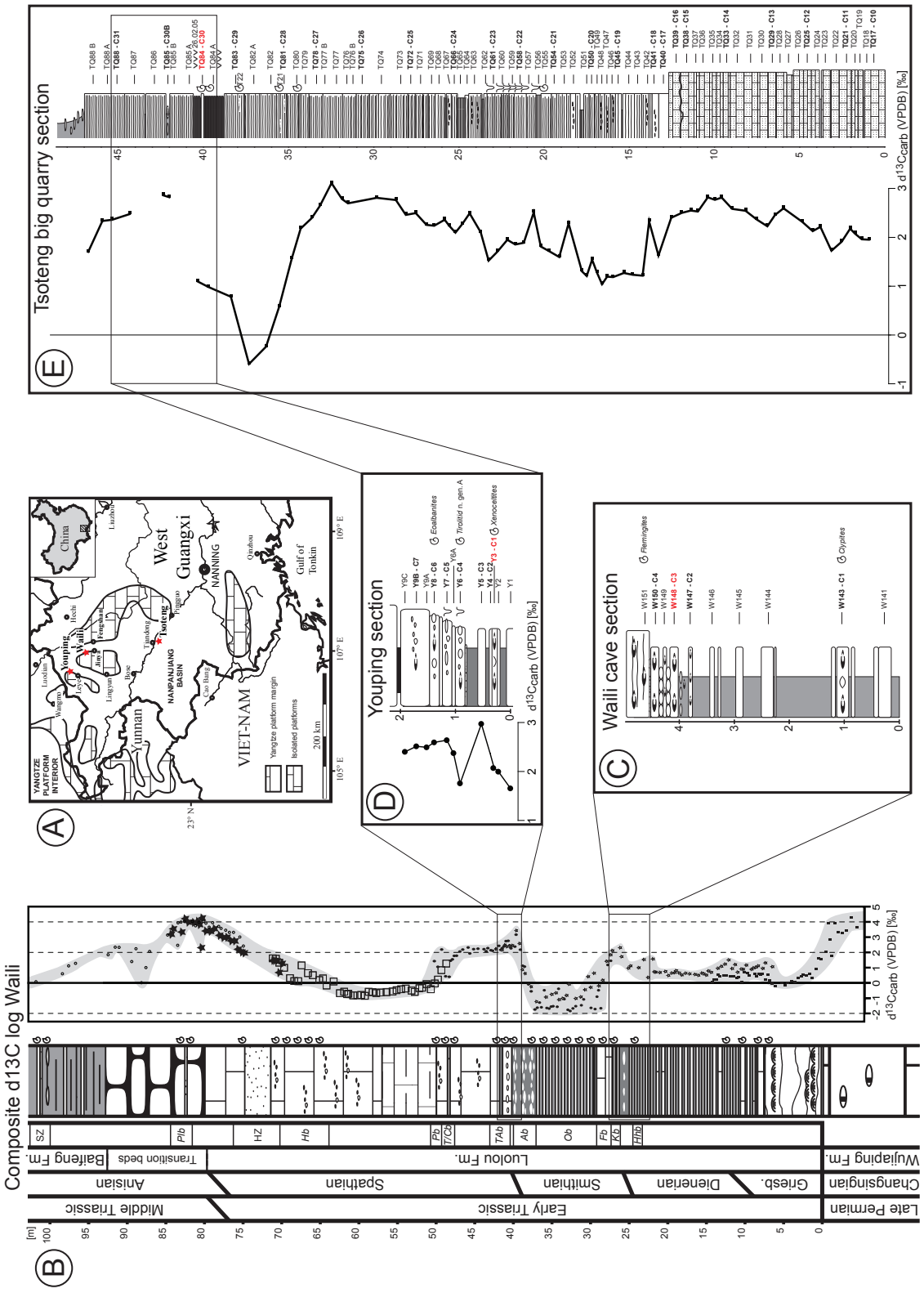

TEXT-FIG. 1. Geographical and geological setting. A: the specimens were found within the Nanpanjiang Basin in the northwestern Guangxi Province, South China; B: composite section of the Jinya/Waili area with the main lithological and formational subdivisions; C: log profile of the cave section in Waili area; D: log profile of the section in the Youping area; E: log profile of the section in the classical Tsoteng area.

X-ray synchrotron microtomography

Fused clusters are potentially more informative than most bedding-plane assemblages in the sense that the compound-elements may remain intact as opposed to crushed bedding-plane assemblages and the clusters may also better record the three-dimensional, relative positions between those elements. Yet, they are very fragile and tricky to manipulate. In particular, if more than two or three elements are involved, it becomes very complicated to see all elements without removing any of them.

One way to circumvent this problem is to use a non-destructive inspection method, such as tomography. The principle of tomography, or volume imaging, is to record a series of 2D-slice images through the studied object. In computer tomography for instance, the object or the sensor is rotated around an axis such that many cross-sectional images are recorded under different view angles. Reconstruction software is then used to compute and visualize a three-dimensional image of the inside of the object under study. Conventional microtomography has many limitations in terms of achievable resolution and contrast. These can be best overcome by using X-ray synchrotron microtomography (Tafforeau, 2006). Third-generation synchrotrons producing hard X-rays, such as the European Synchrotron Radiation Facility (ESRF) in Grenoble (France), yield the best images. The monochromatised intense beam of beamline ID19 at ESRF effectively avoids beam hardening effects. Its high intensity (up to 100 keV) allows very fast data acquisition (much less than one second per projection using the new set-up; see below) at very high spatial resolution (voxel size down to 0.2 µm). Moreover, its partial transverse coherence enables phase contrast imaging (vs. standard absorption contrast imaging). Phase contrast SR-µCT yields volumetric data with edge detection superimposed on absorption contrast and this technique reveals tiny details otherwise invisible (Tafforeau, 2006). The pink beam setup we used had been developed very recently at the ESRF on the ID19 beamline. It allows submicron resolution with a speed and an overall quality never reached before. It has been successfully tested on our conodonts. This technique appears as very successful for high quality and high resolution imaging of microfossils. It will certainly allow the non-destructive study or restudy of other known specimens, particularly of fused clusters, for which only exposed surfaces are otherwise accessible.

One particular cluster from the Tsoteng sample (TQ84-C30) is composed of four ramiform elements, identified as the S_1, S_2, S_3 and S_4 elements of the *Novispathodus* apparatus (see Text-Fig. 2). This exceptional cluster apparently preserves the relative three-dimensional positions and orientations of these elements and is therefore extremely important. This conclusion however was confirmed only after having scanned this specimen using phase contrast SR-µCT, which enabled us to virtually eliminate the matter of unidentified origin that acted as cement between the elements and to virtually extract the various individual elements (segmentation). Since *Novispathodus pingdingshanensis* highly predominates within the low-diversity TQ84-C30 sample, isolated elements from the same sample and presumably pertaining to the same multi-element species were also scanned and then compared with the segmented cluster elements. This allowed to confirm this taxonomic indentification, at least at the generic level.

The reconstruction of the *Novispathodus* apparatus by Orchard (2005) is re-illustrated on Text-Fig. 3A. The P_1 element is usually segminate, sometimes carminate with the initiation of a posterior process. The angulate P_2 element has a relatively high blade, the posterior process is half the length of the anterior one. The antero-lateral processes

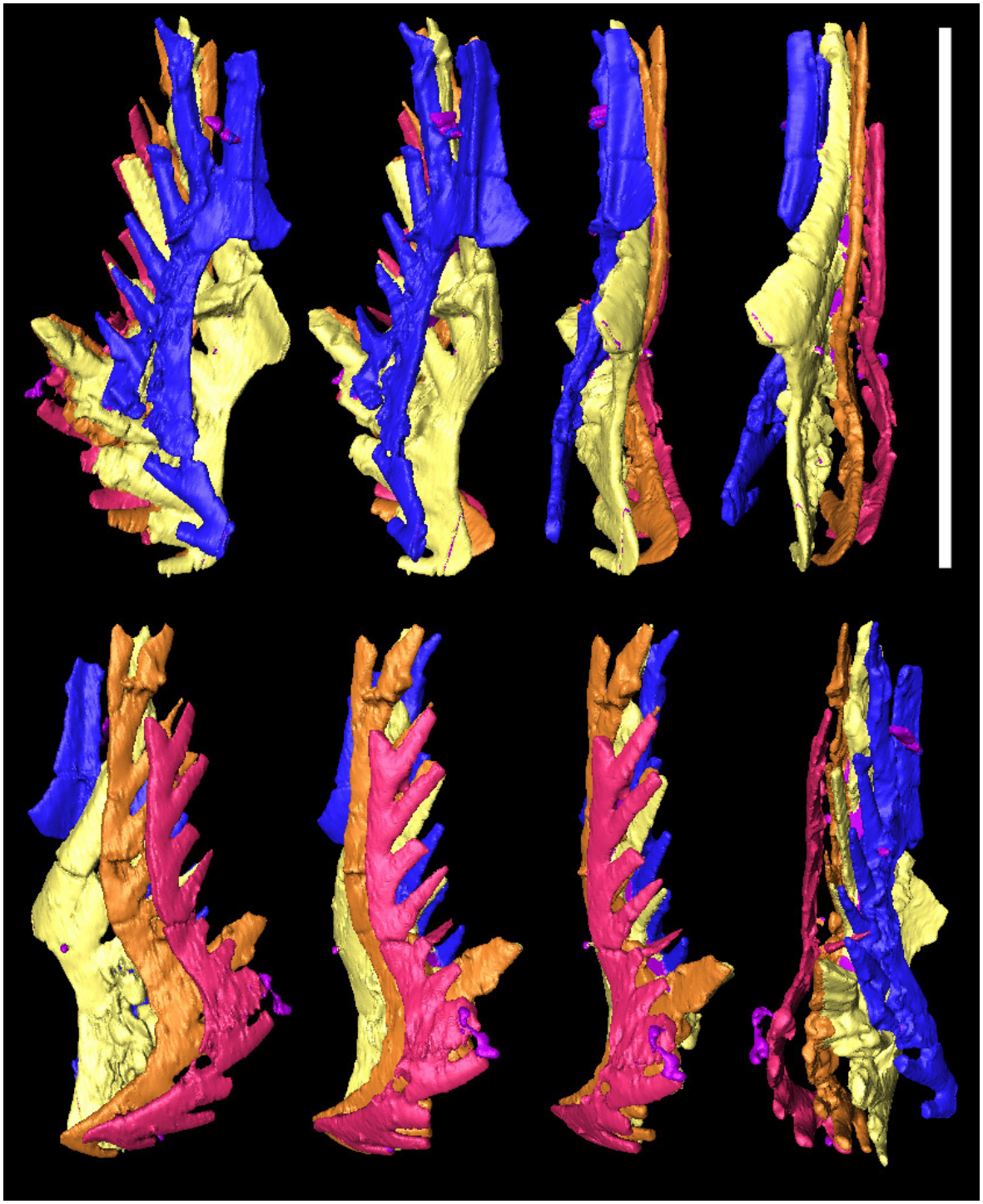

TEXT-FIG. 2. Several views of a fused cluster of S_{1-4} elements. PIMUZ 27900. Scale bar 400µm. SR-µCT images.

of the alate or modified alate S_0 element originate two or three denticles anterior of the cusp. The 'enantiognathiform' (both lateral processes make an angle of about 90 degrees) breviform digyrate element is interpreted to lie in the S_1 position. The characteristic S_2 (interpreted as such) is essentially a 'dolabrate' element, which would have developed a short antero-lateral process comprising two or three denticles. Both S_3 and S_4 are bipennate elements with slightly different degrees of downturning and flexure

of the anterior and posterior processes.

Text-Fig. 3B shows the corresponding scanned elements and their new assigned positions (see explanation below). The cluster partly confirms Orchard's reconstruction by demonstrating the natural association of the proposed S_{1-4} elements.

Relative positions of S elements

Yet, the relative positions of these elements are strikingly different from that previously inferred using Rieber's natural assemblages. Note as a reminder that in the modern notation (Purnell *et al*., 2000) the lowercase index corresponds to the position of the element relative to the symmetry axis. The higher this index, the more distal the element lies from this axis. The unpaired bilaterally symmetrical S_0 element lies on the symmetry axis itself.

The 'enantiognathiform' breviform digyrate element is not in the S_1 but S_2 position. The dolabrate element on the contrary lies in the S_1 rather than in the S_2 position. Without any other evidence concerning the members of the Gondolelloidea superfamily and considering the uncertainty attached to Orchard's initial interpretations, it seems more reasonable to think that Rieber's natural assemblages were simply misinterpreted, rather than assuming that this inversion of relative positions would concern only this multi-element genus. Therefore, the definition of the superfamily must be revised to take this into account (see the Systematic Palaeontology part of this manuscript).

Note that the very recent report by Huang *et al*. (2010) of new conodont clusters from the Yunnan Province lends strong support to our reinterpretation of the relative positions of the respective dolabrate and enantiognathiform elements: we interpret one of their clusters (Huang *et al*., 2010, Fig. 2A) as composed of the S_{1-4} elements (not S_{0-3}); it is apparently very similar to our cluster and the relative positions and orientations of the S_{1-4} elements are identical to those in our specimen. Huang and coauthors did not assign their specimens to any multi-element taxa but previous reports of conodonts from the same section (Huang *et al*., 2009; Zhang, QiYue *et al*., 2009) suggests that they should belong to *Nicoraella* spp., whose apparatus is very similar to both *Novispathodus* and *Mosherella* (as reconstructed by Orchard (2005), with the herein introduced modifications).

A similar switch of relative positions applies to the S_3 and S_4 elements: Orchard suggested that the most sinuous (both in lateral and lower views) hindeodelliform element would lie in the S_3 position. But, numerous fused clusters (Pl. 1, figs. 1-4; 18, 29-33) show that: 1) S_3 and S_4 lower profiles do not necessarily differ as much as illustrated in Orchard, 2005 (D, E on Text-Fig. 16; see also Text-Fig. 3A, herein) but look subparallel along most of their length (except for the anterior process but including the initial downturning of the posterior process); 2) when posterior processes are aligned, it becomes clear that the anterior process of the S_4 element is usually larger and more downturned than that of the S_3 (in lateral view, they are both equally wide but the anterior process of the S_4 is higher); 3) the most sinuous element (best seen in lower view, for instance Pl. 1, fig. 1b) is also the most distal, i.e. lies in the S_4 position; 4) the cusp of the element in S_3 position is subparallel to or more inclined (up to about 20 degrees) than the cusp in the S_4. The latter observation suggests that by analogy the relative location of S_3 and S_4 elements assigned to *Triassospathodus* by Orchard (2005, pp. 93, 94) was right.

In our view, Orchard's illustrated specimens (*Novispathodus*, specimens D, E on Text-Fig. 16, p. 91) could be both S_3 or, most probably, both S_4 elements. They must have pertained to two different animals though. They probably illustrate intraspecific variation in the initial downturning of the posterior

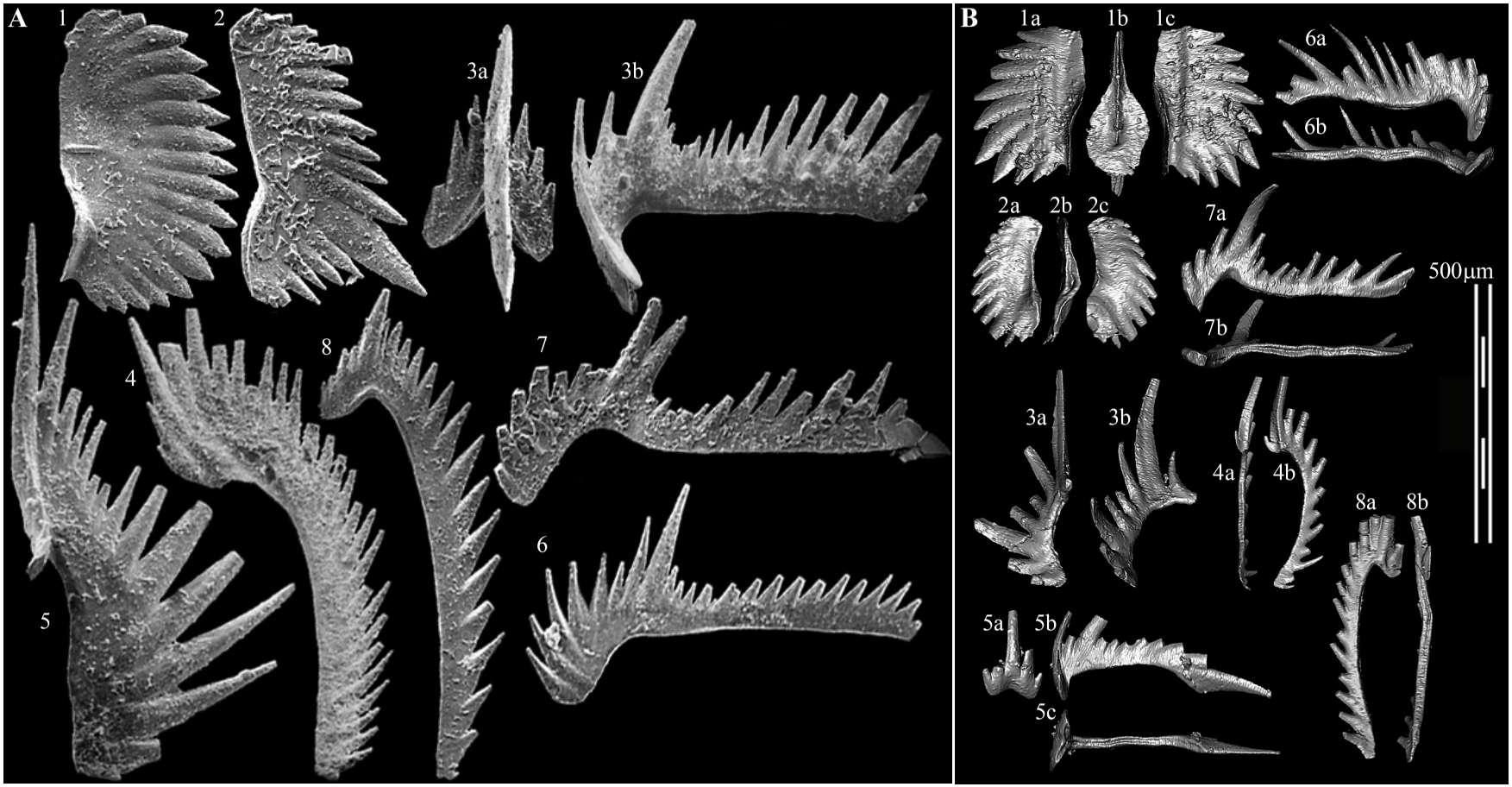

TEXT-FIG. 3. Reconstruction of the *Novispathodus* apparatus. A. Original reconstruction by Orchard (modified after Orchard, 2005). 1, P_1; 2, P_2; 3a-b, S_0; 4, S_1; 5, S_2; 6, S_3; 7, S_4; 8, M. All ×80 SEM photographs. B. This work's reconstruction. 1a-c, *Novispathodus pingdingshanensis*, P_1, resp. inner, lower, and outer views, PIMUZ 27901. 2a-c, P_2, resp. inner, lower, and outer views, PIMUZ 27902. 3a-b, S_2, resp. ventral and inner views, PIMUZ 27903. 4a-b, S_1, resp. ventral and inner views, PIMUZ 27904. 5a-c, S_0, resp. anterior, lateral, and lower views, PIMUZ 27905. 6a-b, S_4, resp. inner and lower views, PIMUZ 27906. 7a-b, S_3, resp. inner and lower views, PIMUZ 27907. 8a-b, M, resp. inner and lower views, PIMUZ 27908. All ×80 SR-μCT images.

process.

Nevertheless, the cluster illustrated on Pl. 1, fig. 29 and assigned to the genus *Neospathodus*?, suggests that the initial interpretation concerning the position of these elements was probably right for those subfamilies where the S_3 element possesses a bifurcated anterior process.

This leads us to revise a few taxa (see below), including the Novispathodinae subfamily, for which, on the contrary, none of the hindeodelliform elements has a bifid anterior process.

Systematic Palaeontology (Goudemand and Orchard)

Figured specimens are housed in the Paleontological Institute and Museum of the University of Zurich (PIMUZ), Karl Schmid-Strasse 4, 8006 Zurich, Switzerland.

Suprageneric classification mostly follows Donoghue *et al.* (2008).

Class CONODONTA Eichenberg, 1930
Division PRIONIODONTIDA Dzik, 1976
Order OZARKODINIDA Dzik, 1976
Superfamily GONDOLELLOIDEA (Lindström, 1970)

The Gondolelloidea were predominant from the mid-Permian until the end of the Triassic. They bore a 15-element apparatus: seven paired element types ($P_{1, 2}$, S_{1-4}) and an unpaired bilaterally symmetrical element S_0. The superfamily is characterized by an 'enantiognathiform' S_2 element. Apart from the diagnostic P elements, the most distinctive elements for the classification within the superfamily are the S_0 (position of the antero-lateral processes relative to the cusp), S_1 (character of the second antero-lateral process), and S_3 (presence and position of a secondary anterior process) elements.
Contrary to known Palaeozoic apparatuses where all S elements seem to be oriented in the same direction, our cluster shows that at least for the *Novispathodus* apparatus but probably within the entire superfamily, both S_1 and S_2 were oriented with the cusps pointing caudally (see also Huang *et al*., 2010). This again confirms a previous suggestion by Orchard and Rieber (1999).

Family GONDOLELLIDEA Lindström, 1970
Subfamily NEOGONDOLELLINAE Hirsch, 1994

As in Orchard (2005), except that the elements previously identified as occupying the S_1 and S_2 positions occupy in fact the S_2 and S_1 positions respectively. Most other gondolelloids evolved from members of this subfamily, especially from the genus *Neogondolella*, which emphasizes the importance of Rieber's natural assemblages (Rieber, 1980).

Genus NEOGONDOLELLA Bender and Stoppel, 1965

1965 *Neogondolella* Bender and Stoppel, p.343.
1970 *Xaniognathus* Sweet, pp. 261-262.
1989 *Clarkina* Kozur, pp. 428-429.
1989 *Pridaella* Budurov and Sudar, pp. 250, 253.

Type species and holotype. *Gondolella mombergensis* Tatge, 1956, p.132, pl. 6, fig. 2a-c.
Type stratum and locality. Upper Muschelkalk, Schmidtdiel Quarry, Momberg, near Marburg.

Original diagnosis and type species. Bender and Stoppel introduced *Neogondolella* for segminiplanate P_1 elements with strong, partly fused carina of variable height ending in a (sub)terminal cusp. These elements were previously included in *Gondolella* Stauffer and Plummer.

Multielement diagnosis. As described by Orchard (2005) or Orchard and Rieber (1999), except that the dolobrate element is now considered to be in the S_1 position and the S_2 position is occupied by the 'enantiognathiform' breviform digyrate element. A thorough discussion can be found in Orchard and Rieber (1999).

Neogondolella? n. sp. A
Pl. 2, fig. 29

Diagnosis. A species with narrow, lanceolate segminiplanate P_1 elements with slightly upturned platform margins that extend the entire length of the element, tapering gradually anteriorly. The broadest point lies at mid-length. A narrow posterior platform brim develops on the rounded but asymmetrical posterior margin. The carinal denticles are numerous, moderately high, partly fused, and triangular in shape. The cusp is indistinctive. In lateral view, the unit is straight for

most of its length and strongly downcurved in the posterior quarter. A smaller denticle lies posterior of the cusp, offset from the carinal main axis, which is reminiscent of *Borinella buurensis* Dagis (1984). Contrary to the latter however its carinal denticles are not gradually higher anteriorly but subequal in height (this in turn is reminiscent of *Ng*. *regale* of which it may represent an early representative). Moreover, the posterior margin of the latter is somewhat rectangular and its attachment surface on the aboral side is much broader posteriorly than the present specimen.

Remarks. This element closely resembles the specimen figured next to it on Plate 2 (fig. 28) and herein assigned with question mark to '*Gladigondolella'* n. sp. A, but that specimen has a much narrower platform and its posterior part is conspicuously deflected, which is somehow more typical of the latter genus.
Similar, more numerous and sometimes better preserved specimens were found in residues of earliest Spathian rocks at other Chinese sections (Waili area, Goudemand *et al*., in prep.), and also in correlative collections from Darwin Canyon (California, Goudemand *et al*., in prep.), from where they will be formally described.

Genus NEOSPATHODUS Mosher, 1968

Type species and holotype. *Spathognathodus cristagalli* Huckriede, 1958, pp. 161-162, pl. 10, fig. 15.
Type stratum and locality. Lower 'Ceratitenschichten', Mittiwali near Chhidru, Salt Range, Pakistan.

Original diagnosis and type species. Orchard, 2005: The type species is a segminate P_1 element with a width:height:length ratio of 1:3:4, a posterior lower margin that is upturned beneath the posterior one-third of the element, and a short terminal cusp (Mosher, 1968). Mosher included forms with variable arching and denticulation.

Multielement diagnosis (revised). As described by Orchard (2005), except that the elements previously identified as occupying the S_1 and S_2 positions occupy in fact the S_2 and S_1 positions respectively. Note that, as defined by Orchard, the S_3 element would have a more posteriorly located bifurcation of the anterior process compared with the homologous element in the *Neogondolella* apparatus.

Neospathodus? spp.
Pl. 1, figs. 29-31

Considering the above observations about the relative shape of S_3 and S_4 elements, Orchard's illustrated specimens (resp. D, E on Text-Fig. 14, p. 89) are most probably both S_3 elements (it is not perfectly clear on the photograph but it has a single denticle outgrown from the 6th denticle of the anterior process). Yet, they must have pertained to two different apparatuses hence to two different species or even genera (see remark below about the generic assignment of *N. dieneri* forms). Except for the more posteriorly located bifurcation of the anterior process, specimen E (*ibid*.) most closely resembles the homologous element of *Neogondolella*. The anterior process of specimen D is more anteriorly bifurcated and much less downturned than in *Neogondolella*. In lateral view, the anterior process of the S_3 of both *Neogondolella* and specimen E makes an angle of about 90 or more degrees with the posterior process, whereas in specimen D this angle is only about 45 degrees. In that respect, the present specimens more closely resemble specimen D and are somewhat intermediate (similar downturning of the anterior process and displacement of the bifurcation towards the anterior until complete loss) towards homologous elements of *Novispathodus*.

Remarks. Figured ramiform specimens 29-31 (Pl. 1) are here tentatively assigned to *Neospathodus*, based on the predominant co-occurrence of P_1 elements pertaining to the *Neospathodus dieneri* group. It should be noted however that some uncertainty surrounds the generic assignment of this species. Previous attempts at reconstructing its multielement apparatus suggest that different morphotypes of the P_1 element may correspond to significantly different apparatuses that would deserve further generic differentiation.

Subfamily NOVISPATHODINAE Orchard, 2005

Genus NOVISPATHODUS Orchard, 2005
Text-Fig. 3; Pl. 1, figs. 1-28, 32; Pl. 2, figs. 1-26, 30-31.

Type species and holotype. *Neospathodus abruptus* Orchard, 1995, pp. 118-119, figs. 3.23-24.
Type stratum and locality. Contrary to what appeared in the publication of the original description of the genus, the type locality is the same as for the type species, that is Jabral

Safra, Oman.

Revised multielement diagnosis. As described by Orchard (2005), except again that the elements previously identified as occupying the S_1 and S_2 positions occupy in fact the S_2 and S_1 positions respectively. Bipennate S_3-S_4 elements, whose sinuous lower profiles are subparallel along most of their length except for the anterior process, but including the initial downturning of the posterior process. The anterior process of the S_4 element is commonly larger and more downturned than that of the S_3. The most sinuous element (in lower view) is the S_4 element. Yet, in early Smithian forms (see Pl. 1, figs. 32a-b) both elements might be even less differentiated from one another.

Novispathodus pingdingshanensis (Zhao & Orchard, 2007)
Text-Fig. 3B; Pl. 1, figs. 19-20; Pl. 2, figs. 2, 6, 7?, 9, 10, 13, 16?, 17, 30

Original diagnosis (Zhao & Orchard, 2007). Small segminate elements characterized by a length: height ratio in the range of 1.32–2.34, and about 4–9 robust, wide, and mostly fused denticles. In lateral view, the basal margin is straight. A large, broadly expanded oval to subrounded basal cavity is upturned on the inner margin and flat to downturned on the outer margin.
Revised diagnosis. The basal margin of the P_1 element is not necessarily straight, but may vary from sub-straight to slightly upturned posteriorly as in *Nv. waageni* (Sweet). As a consequence, this can not be used as a diagnostic feature upon which the species would be differentiated. In our view, they most strikingly differ in the denticulation: the denticles axes of *Nv. pingdingshanensis* are distinctively curved in the posterior direction and consequently the two or three (wide) denticles anterior of the cusp are often conspicuously asymmetrical, the posterior edge of the free tip being much shorter than the anterior one. In this respect *Nv. pingdingshanensis* superficially resembles *Neospathodus soleiformis* Zhao & Orchard (2008) but the latter is much shorter and higher. In both *Nv. waageni* and *Nv. abruptus*, the denticles are straight, even when those are reclined or radiating.
Remarks. P_1 elements of *Novispathodus pingdingshanensis* predominate in both lower Spathian samples herein described, as it usually does in most worldwide samples of the *Xenoceltites* Zone. Note that, as previously mentioned, the ammonoid literature refers this biozone as latest Smithian but it is here considered to be already of Spathian age: we indeed consider *Nv*. *pingdingshanensis* and *Nv*. *abruptus* as the rootstock of all Spathian neospathodid forms (Goudemand *et al*., 2006). The position of this boundary is arbitrary but in terms of conodonts the most important faunal turnover occurs between the older *Wasatchites tardus* Zone and the *Xenoceltites* Zone. This will be discussed at length in a future paper describing our material from Darwin, California (Goudemand *et al*., in prep.).

Novispathodus aff*. pingdingshanensis*
Pl. 2, fig. 11?, 12

Diagnosis. Very similar to *Nv. pingdingshanensis* but with much lower and more strongly curved denticles. As a consequence the outer margin appears almost smooth. The specimens figured on Pl. 2, fig. 11 strikingly resembles *Nv. pakistanensis* (Sweet, 1970), to which it could belong too. Its denticles however seem to have the characteristic *pindingshanensis*-like curvature. It is not clear how the elongate, subrectangular *Nv. pakistanensis* relates to the shorter, subquadrate *Nv. waagen*i, with which it otherwise shares similarities, but a similar relationship exists between *Nv*. aff. *pingdingshanensis* and *Nv. pingdingshanensis*.

Novispathodus aff. *abruptus* A
Pl. 2, figs. 1, 18?, 26?

Original diagnosis. A species in which segminate elements representing all growth stages are relatively short and high with a length:height ratio of about 1.5-1.8:1, and up to about 14 upright to reclined denticles that increase in height toward the posterior except for the terminal 1-3 progressively smaller denticles that descend rapidly to the posterior tip of the blade. The lower margin of the basal cavity is irregularly oval to subcircular in outline (Orchard, 1995).
Remarks. This large specimen (Pl. 2, fig. 1), though about as large as the holotype of *Nv. abruptus* from Oman, more closely resembles juvenile forms of the latter species, hence its taxonomic separation. The substraight lower margin and the somewhat curved anterior denticles recall *Nv. pingdingshanensis*. Yet, its denticles are not as wide and posteriorly they miss the characteristic curvature of the latter. Except for the posteriormost part of the element, it also superficially

resembles *Nv. eotriangularis* (Zhao & Orchard, 2007) in lateral view.
Specimens illustrated on Pl. 2, figs. 18, 26 are also reminiscent of *Nv. abruptus* but with wide and slightly curved *pingdingshanensis*-like anterior denticles. Both specimens also closely resemble *Nv. pakistanensis* but they lack the posterior downturning of the lower margin.

Novispathodus aff. *abruptus* B
Pl. 1, fig. 21

Remarks. Only small (juvenile?) P_1 elements of *Novispathodus* aff. *abruptus* B were found in these samples. These fused elements may actually belong to *Nv. abruptus*. Yet, in the definition of this species, the terminal 1-3 denticles are progressively smaller. Unpublished material from Pakistan suggests that elements like those of the present cluster, where the terminal denticles are subequal in height but conspicuously smaller than the cusp, may deserve assignment to a separate species. Orchard (1995) assigned elements like this to *Nv*. *abruptus* and similar elements with a more developed posterior process to *Triassospathodus homeri* (see Orchard 1995, Pl. 3, figs. 17-18 and Pl. 2, fig. 9 respectively, both from sample 103A-2, Jabral Safra, Oman). The distinction is based on the number of denticles worn by the posterior process, the deflection of this process and the shape of the basal cavity beneath it. In the Oman material, some *Nv*. *abruptus* dominated samples seem to lack these forms completely. Hence their differentiation may have some stratigraphic utility. In Oman samples where they do occur, they can be quite common and then *Tr*. *homeri* occurs too, but this is clearly not the case in the present Tsoteng sample.

Novispathodus waageni (Sweet, 1970)
Pl. 2, figs. 3?, 4, 5?, 8, 14?, 19, 20?

Original diagnosis. In lateral view, P_1 elements of this species have a subquadrate form and a blade profile with a distinctive arcuate crest. Original description by Sweet stressed that the (rather variable) basal margin is often conspicuously upturned beneath the posterior half of the element. They feature a subcircular basal cavity. Orchard and Krystyn (2007) recognized 6 morphotypes, one of which being recently differentiated by Orchard and Zonneveld (2009) as a new species (*Nv. latiformis*).

Remarks. This species was previously assigned to *Neospathodus*. Yet, unpublished reconstructions show that its ramiform elements are like those of *Novispathodus abruptus* (see Orchard, 2005). *Nv. waageni* is a typical Smithian form. It might have been the ancestor of *Nv. pingdingshanensis*, which is itself thought of as the rootstock of most Spathian species with segminate P_1 elements. Their co-occurrence in this sample (the youngest known occurrence of *Nv. waageni*) suggests that *Nv. waageni* survived the end-Smithian crisis (Galfetti *et al*., 2007) and became extinct only shortly after.

Novispathodus radialis (Zhao & Orchard, 2007)
Pl. 2, figs. 21, 25

Revised diagnosis. A species with segminate P_1 elements, which have 6-9 wide and axial denticles radiating from a point half way along the midst of the unit. In lateral view, the free tips of denticles anterior of the cusp are sub-equilaterally triangular, and the basal margin is slightly uparched in both directions. The basal cavity is subcircular and broadly expanded, occupying about two-third to three-fourth of the lower surface.

Novispathodus n. sp. C
Pl. 2, fig. 15

Diagnosis. This small segminate element has a large, rounded basal cavity, rather straight denticles that are strongly reclined to the posterior. The cusp is subterminal: a needle-like denticle appears to be mostly fused to the straight, posterior margin of the cusp. The base of this denticle lies well in front (anteriorly) of the posterior edge of the basal cavity. Similar elements are found in our collections from Darwin canyon, California.

Novispathodus n. sp. D
Pl. 2, figs. 22-24

Diagnosis. Small segminate elements with a big basal cavity, and subtriangular, upright denticles. The upper margin is similar to that of *Nv*. *abruptus*: a posterior denticle stands behind the cusp, and the maximal height is reached at the cusp. These elements most closely resemble *Nv*. *pingdingshanensis* but their denticles are not posteriorly recurved as it is typical in the latter. They

are also somewhat similar to *Nv*. *radialis* but their denticles are more erect. The denticulation of these elements recalls also that of *Icriospathodus*? *crassatus*, especially of early forms of the latter that were found in rocks from Darwin canyon (California) and to which they may actually be related. Yet, elements of *Ic.*? *crassatus* are usually relatively longer. Very similar elements are also found in collections of the *Xenoceltites* Zone from Georgetown, Idaho.

Subfamily Uncertain
Genus BORINELLA Budurov and Sudar, 1994
Pl. 2, figs. 27

1988 *Pseudogondolella* Kozur, p. 244.
1993 *Kozurella* Budurov and Sudar, p. 24.
1994 *Borinella* Budurov and Sudar (June), p. 30.
1994 *Chengyuania* Kozur (September), pp. 529-530.

Type species and holotype. Neogondolella buurensis Dagis, 1984, pp.12-13, pl. XI, figs. 1, 2.
Type stratum and locality. Buur River basin, Taion-Uiolaakh River, Hedenstromia hedenstromi Zone.

Remarks. Species of this genus have in common P_1 elements with discrete blade-carinal denticles that lengthen towards the anterior. Though the apparatus of the type species *Bo. buurensis* has not been described yet, limited available material resemble that of *Wapitiodus*, itself similar to *Gladigondolella* and *Cratognathodus* (Orchard, 2005). The apparatus of the older *Bo. chowadensis* is the same as that of *Neogondolella* (Orchard, 2007), which suggests derivation of *Borinella* from *Neogondolella*.

Borinella aff. *buurensis* Dagis
Pl. 2, fig. 27

Diagnosis. A species with segminiplanate P_1 elements,with discrete blade-carinal denticles that become bigger towards the anterior, except for the two anteriormost denticles. The width of very narrow, microreticulated and asymmetrical platform is maximal at about one-third of the unit from the posterior end. On the inner side, the platform tapers rapidly at mid-length and barely extends to the anterior end.

Remarks. This element closely resembles *Bo. buurensis*, but is more asymmetrical and much narrower. *Bo*. *sweeti* differs in being subsymmetrical and having a platform whose margins are parallel for most its length, a more conspicuous cusp and more closely spaced anterior denticles. The present element looks also similar to the specimen here below assigned to '*Gladigondolella'*, except that its more discrete and increasingly taller denticles to the anterior are more typical of *Borinella* and it lacks the conspicuous posterior deflection that is somehow characteristic of '*Gladigondolella'*. Note however that specimens of *Bo. buurensis* may have a smaller accessory posterior node, which is offset from the main axis of the carina (Orchard, 2008). By analogy, if more material is found in the future, it may appear that the posterior end is variably deflected (intraspecific variation), in which case both specimens (Pl. 2, figs. 27-28) could be included in the same species.

Subfamily GLADIGONDOLELLINAE Hirsch, 1994
Genus GLADIGONDOLELLA Müller, 1962

1968 *Dichodella* Mosher, p. 923.

Type species and holotype. *Polygnathus tethydis* Huckriede, 1958, pp. 157-158, pl. 2, fig. 38a-b.
Type stratum and locality. *Trachyceras austriacum* bed (Julian), Feuerkogel near Röthelstein, Austria.

Original diagnosis. The name was first used for a carminiplanate P_1 element with a narrow platform, a low carina, and a relatively short posterior process and corresponding keel posterior of the pit (Müller 1962, p. 116).

Remarks. Revision as for superfamily. Owing to the morphological similarity of their multi-element apparatuses, *Gladigondolella* was considered (Orchard, 2005) to have evolved from *Cratognathodus* during early Spathian time. The Middle Triassic type species might have been significantly different; hence the uncertainty about the generic assignment of these Spathian forms ('*Gladigondolella*' *carinata*). The herein reported occurrence of a somewhat similar P_1 element in earliest Spathian rocks suggests that *Gladigondolella* or '*Gladigondolella*' may alternatively have evolved from *Borinella* and have given rise later to *Cratognathodus* (Orchard, 2007). The M and S_1 elements of these apparatuses differ markedly and could be used as diagnostic features to distinguish them. Unfortunately no such element was found in the material of this sample.

'Gladigondolella'? n. sp. A
Pl. 2, fig. 28.

Diagnosis. A species with segminiplanate P_1 elements with a relatively narrow platform whose oral surface is microreticulated, low and discrete denticles, and a very short free blade. A short deflected process with two denticles is budding posteriorly but it still lacks the corresponding keel posterior of the pit.

Remarks. The P_1 element of this new species shares characters of both *Borinella* and *Gladigondolella* (see discussion above). Its generic assignment is uncertain but it may be a primitive representative of the Spathian '*Gladigondolella*'.

Acknowledgements

This research is supported by the Swiss NSF project 200020-113554 (to H.B.).
We acknowledge the European Synchrotron Radiation Facility for provision of synchrotron radiation facilities and for granting access to beamline ID19. Julia Huber and Leonie Pauli are thanked for having dissolved and concentrated the conodont samples.

References

Aldridge, R. J. 1993. The Anatomy of Conodonts. Philosophical Transactions: Biological Sciences, 340(1294):405-421.

Bagnoli, G., M. C. Perri, AND A. Gandin. 1985. Ladinian conodont apparatuses from northwestern Sardinia, Italy. Bolletino della Società Paleontologica Italiana, 23:311-323.

Bender, H., AND D. Stoppel. 1965. Perm-Conodonten. Geologisches Jahrbuch, 82:331-364.

Brayard, A., AND H. Bucher. 2008. Smithian (Early Triassic) ammonoid faunas from northwestern Guangxi (South China): Taxonomy and Biochronology. Fossils and Strata, 55:179 pp.

Briggs, D. E. G., E. N. K. Clarkson, AND R. J. Aldridge. 1983. The conodont animal. Lethaia, 16:1-14.

Budurov, K. J., AND M. N. Sudar. 1989. New Conodont Taxa from the Middle Triassic, p. 250-254. *In* V. J. Gupta (ed.), Geology of Himalayas - Palaeontology, Stratigraphy and Structure.Volume 4. Hindustan Publishing Corporation (India).

Budurov, K. J., AND M. N. Sudar. 1993. *Kozurella* gen. n. (Conodonta) from the Olenekian (Early Triassic). Geologica Balkanica, 23(4):24.

Budurov, K. J., AND M. N. Sudar. 1994. *Borinella* Budurov & Sudar, nomen novum for the Triassic Conodont Genus *Kozurella* Budurov and Sudar. Geologica Balkanica, 24(3):30.

Dagis, A. A. 1984. Lower Triassic Conodonts from Northern Central Siberia. Nauka Publishers, Moscow, 554.

Donoghue, P. C. J., M. A. Purnell, R. J. Aldridge, AND S. Zhang. 2008. The interrelationships of 'complex' conodonts (Vertebrata). Journal of Systematic Palaeontology, 6(2):119-153.

Dzik, J. 1976. Remarks on the evolution of Ordovician conodonts. Acta Palaeontologica Polonica, 21:395-455.

Eichenberg, W. 1930. Conodonten aus dem Culm des Harzes. Palaeontol. Zeitschr., 12:177-182.

Galfetti, T., H. Bucher, A. Brayard, P. A. Hochuli, H. Weissert, G. Kuang, V. Atudorei, AND J. Guex. 2007. Late Early Triassic climate change: Insights from carbonate carbon isotopes, sedimentary evolution and ammonoid paleobiogeography. Palaeogeography, Palaeoclimatology, Palaeoecology, 243(2007):394-411.

Galfetti, T., H. Bucher, R. Martini, P. A. Hochuli, H. Weissert, S. Crasquin-Soleau, A. Brayard, N. Goudemand, T. Brühwiler, AND G. Kuang. 2008. Evolution of Early Triassic outer platform paleoenvironments in the Nanpangjiang Basin (South China) and their significance for the biotic recovery. Sedimentary Geology, 204:36-60.

Goudemand, N., M. J. Orchard, G. Li, T. Galfetti, AND H. Bucher. 2006. A new early Spathian (Early Triassic) Conodont Succession from North America. First International Conodont Symposium (ICOS 2006), July 12-30, 2006, University of Leicester, Leicester, UK, Programme and Abstracts:35.

Hinde, G. J. 1879. On conodonts from the Chazy and Cincinnati group of the Cambro-Silurian, and from the Hamilton and Geneseeshale divisions of the Devonian in Canada and the United States. Quart. J. Geol. Soc. London, 35:351-369.

Hirsch, F. 1994. Triassic conodonts as ecological and eustatic sensors, p. 949-959, Pangea: Global Environments and Resources.Volume Memoir 17. Canadian Society of Petroleum Geologists.

Huang, J.-Y., K.-X. Zhang, Q.-Y. Zhang, T. Lü, C.-Y. Zhou, AND J.-K. Bai. 2009. Conodonts stratigraphy and sedimentary environment of the Middle Triassic at Daaozi section of Luoping County, Yunnan Province, South China. Acta Micropalaeontologica Sinica, 26(3):211-224.

Huang, J.-Y., K.-X. Zhang, Q.-Y. Zhang, T. Lü, C.-Y. Zhou, AND S.-X. Hu. 2010. Discovery of Middle Triassic Conodont Clusters from Luoping Fauna, Yunnan Province. Earth Science, Journal of China University of Geosciences, 35(4):512-514.

Huckriede, R. 1958. Die Conodonten der mediterranen Trias und ihr stratigraphischer Wert. Paläontologisches Zeitschrift, 32(3/4):141-175.

Koike, T. 1996. Skeletal Apparatuses of Triassic Conodonts of *Cornudina*. Prof. H. Igo Commem. Vol.:113-120.

Koike, T. 1999. Apparatus of a Triassic Conodont Species *Cratognathodus multihamatus* (Huckriede). Paleontological Research, 3(4):234-248.

Koike, T. 2004. Early Triassic *Neospathodus* (Conodonta) Apparatuses from the Taho Formation, Southwest Japan. Paleontological

Research, 8(2):129-140.

Kozur, H. 1988. The Taxonomy of the Gondolellids Conodonts in the Permian and Triassic. 1st International Senckenberg Conference and 5th European Conodont Symposium (ECOS V): Contributions III, Papers on Ordovician to Triassic Conodonts, 117:409-469.

Kozur, H. 1994. *Chengyuania*, A New Name for *Pseudogondolella* Kozur 1988 (Conodonta) [non *Pseudogondolella* Yang 1984 (hybodont fish teeth)]. Paläontologisches Zeitschrift, 68(3/4):529-530.

Kozur, H., AND H. Mostler. 1971. Probleme der Conodontenforschung in der Trias. Geol. Paläont. Mitt. Innsbruck, 1(4):1-19.

Lindström, M. 1970. A Suprageneric Taxonomy of the Conodonts. Lethaia Norwegia, 3:427-445.

Mietto, P. 1982. A Ladinian Conodont-Cluster of *Metapolygnathus mungoensis* (Diebel) from Trento Area (NE Italy). Neues Jahrbuch für Geologie und Paläontologie. Monatshefte, 1982(10):600-606.

Mosher, L. C. 1968. Triassic Conodonts from Western North America and Europe and Their Correlation. Journal of Paleontology, 42(4):895-946.

Müller, K. J. 1962. Zur systematischen Einteilung der Conodontophoridae. Paläontologisches Zeitschrift, 36:109-117.

Orchard, M. J. 2005. Multielement conodont apparatuses of Triassic Gondolelloidea, p. 73-101. *In* M. A. Purnell and P. C. J. Donoghue (eds.), Conodont Biology and Phylogeny: Interpreting the Fossil Record.Volume 73. Special Papers in Palaeontology.

Orchard, M. J. 2008. Lower Triassic conodonts from the Canadian Arctic, their intercalibration with ammonoid-based stages and a comparison with other North American Olenekian faunas. Polar Research, 27(3):393-412.

Orchard, M. J., AND L. Krystyn. 2007. Conodonts from the Induan-Olenekian boundary interval at Mud, Spiti. Albertiana, 35:30-34.

Orchard, M. J., AND H. Rieber. 1999. Multielement *Neogondolella* (Conodonta, upper Permian - middle Triassic). Bolletino della Società Paleontologica Italiana, 37(2-3):475-488.

Orchard, M. J., AND J.-P. Zonneveld. 2009. The Lower Triassic Sulphur Mountain Formation in the Wapiti Lake area: lithostratigraphy, conodont biostratigraphy, and a new biozonation for the lower Olenekian (Smithian). Canadian Journal of Earth Sciences, 46:757-790.

Purnell, M. A., P. C. J. Donoghue, AND R. J. Aldridge. 2000. Orientation and anatomical notation in conodonts. Journal of Paleontology, 74:113-122.

Ramovs, A. 1977. Skelettapparat von *Pseudofurnishius murcianus* (Conodontophorida) im Mitteltrias Sloweniens (NW Jugoslawien) / The reconstructed skeletal apparatus of Pseudofurnishius murcianus (Conodontophorida) in the Middle Triassic of Slovenia (NW Jugoslavia). Neues Jahrbuch für Geologie und Paläontologie. Abhandlungen, 153(3):361-399.

Ramovs, A. 1978. Mitteltriassische Conodontenclusters in Slowenien, NW Jugoslawien. Paläontologisches Zeitschrift, 52(1/2):129-137.

Rieber, H. 1980. Ein Conodontencluster aus der Grenzbitumenzone (Mittlere Trias) des Monte San Giorgio. Ann. Naturhist. Mus. Wien, 83:265-274.

Sweet, W. C. 1970. Uppermost Permian and Lower Triassic Conodonts of the Salt Range and Trans-Indus Ranges, West Pakistan, p. 207-275. *In* B. Kummel and C. Teichert (eds.), Stratigraphic Boundary Problems: Permian and Triassic of West Pakistan.Volume Special Publication 4. The University Press of Kansas.

Sweet, W. C. 1988. The Conodonta: Morphology, Taxonomy, Paleoecology and Evolutionary History of a Long-Extinct Animal Phylum. Oxford University Press, 10, 212 p.

Tafforeau, P., R. Boistel, E. Boller, A. Bravin, M. Brunet, Y. Chaimanee, P. Cloetens, M. Feist, J. Hoszowska, J.-J. Jaeger, R. F. Kay, V. Lazzari, L. Marivaux, A. Nel, C. Nemoz, X. Thibault, P. Vignaud, AND S. Zabler. 2006. Applications of X-ray synchrotron microtomography for non-destructive 3d studies of paleontological specimens. Applied Physics A, 83(2006):195-202.

Tatge, U. 1956. Conodonten aus dem germanishen Muschelkalk. Paläontologisches Zeitschrift, 30(1/2):108-127.

Zhang, H., J. Tong, AND J. Zuo. 2005. Lower Triassic and Carbon Isotope Excursion in West Guangxi, Southwest China. International Symposium on Triassic Chronostratigraphy and Biotic Recovery, Chaohu, China (May 23-25, 2005), 33 (Part I: Program and

Abstracts):103-104.

Zhang, Q.-Y., C.-Y. Zhou, T. Lü, T. Xie, X.-Y. Lou, W. Liu, Y.-Y. Sun, J.-Y. Huang, AND L. Zhao. 2009. A conodont-based Middle Triassic age assignment for the Luoping Biota of Yunnan, China. Science in China Series D-Earth Sciences, 52(10):1673-1678.

Zhang, S., AND Z. Yang. 1991. On Multielement Taxonomy of the Early Triassic Conodonts. Stratigraphy and Paleontology of China, 1:17-47.

Zhao, L., M. J. Orchard, J. Tong, Z. Sun, J. Zuo, S. Zhang, AND A. Yun. 2007. Lower Triassic conodont sequence in Chaohu, Anhui Province, China and its global correlation. Palaeogeography, Palaeoclimatology, Palaeoecology, 252:24-38.

Zhao, L., J. Tong, S. Zhang, AND Z. Sun. 2008. An update of conodonts in the Induan-Olenekian boundary strata at West Pingdingshan section, Chaohu, Anhui Province. Journal of China University of Geosciences, 19(3):207-216.

PLATE 1

Figs 1-28. *Novispathodus* sp. indet.
1-4, fused cluster of S_3 and S_4 elements; a, `lateral´ view; b, `aboral´ view. 1a-b, PIMUZ 29001. 2a-b, PIMUZ 29002. 3a-b, PIMUZ 29003. 4, PIMUZ 29004.
5a-b, fused cluster, P_1 and S_3 or S_4, PIMUZ 29005.
6a-b, fused cluster, M and ?, PIMUZ 29006.
7a-b, fused cluster, M and $S_{4?}$, PIMUZ 29007.
8a-b, fused cluster, S_3 and S_4, PIMUZ 29008.
9a-b, fused cluster, S_0 and S_2, PIMUZ 29009.
10-11, S_0. 10a-b, PIMUZ 29010. 11a-b, PIMUZ 29011.
12-13, teratological? S_3 or S_4. 12, PIMUZ 29012. 13, PIMUZ 29013.
14-16, S_2. 14, PIMUZ 29014. 15, juvenile form with distal denticles ‘buds’, PIMUZ 29015. 16, PIMUZ 29016.
17a-b, M, PIMUZ 29017.
18a-c, fused cluster, S_3 and S_4, resp. inner, outer and lower views, PIMUZ 29018.
19-20, *Novispathodus pingdingshanensis*, fused clusters of P_1 elements. 19a-b, PIMUZ 29019. 20a-b, PIMUZ 29020.
21a-b, *Novispathodus* aff. *abruptus* B, fused cluster of P_1 elements, PIMUZ 29021.
22-28, *Novispathodus* spp., fused clusters. 22a-b, PIMUZ 29022. 23, PIMUZ 29023. 24a-b, PIMUZ 29024. 25, PIMUZ 29025. 26a-b, PIMUZ 29026. 27a-b, PIMUZ 29027. 28a-b, PIMUZ 29028.
29-31, *Neospathodus*? sp. indet. 29a-b, fused cluster of M, S_3 and S_4 elements, PIMUZ 29029. 30a-b, fused cluster, M, S_3 and S_4, juvenile forms, PIMUZ 29030. 31a-b, bifid S_3, PIMUZ 29031.
32a-b, *Novispathodus* sp. indet., fused cluster, S_3 and S_4, PIMUZ 29032.
33a-b, gen. indet. sp. indet., fused cluster, S_3 and S_4, PIMUZ 29033.

1-18, sample TQ84C30, Tsoteng section, Guangxi, South China, Lowest Spathian;
19-28, sample Y3C1, Youping section, Guangxi, South China, Lowest Spathian;
29-33, sample W148C3, Waili cave section, Guangxi, South China, Lowest Smithian.
All ×80 SEM photographs, except figs. 9b, 17a-b, and 18a-c, which are ×80 SR-µCT images.

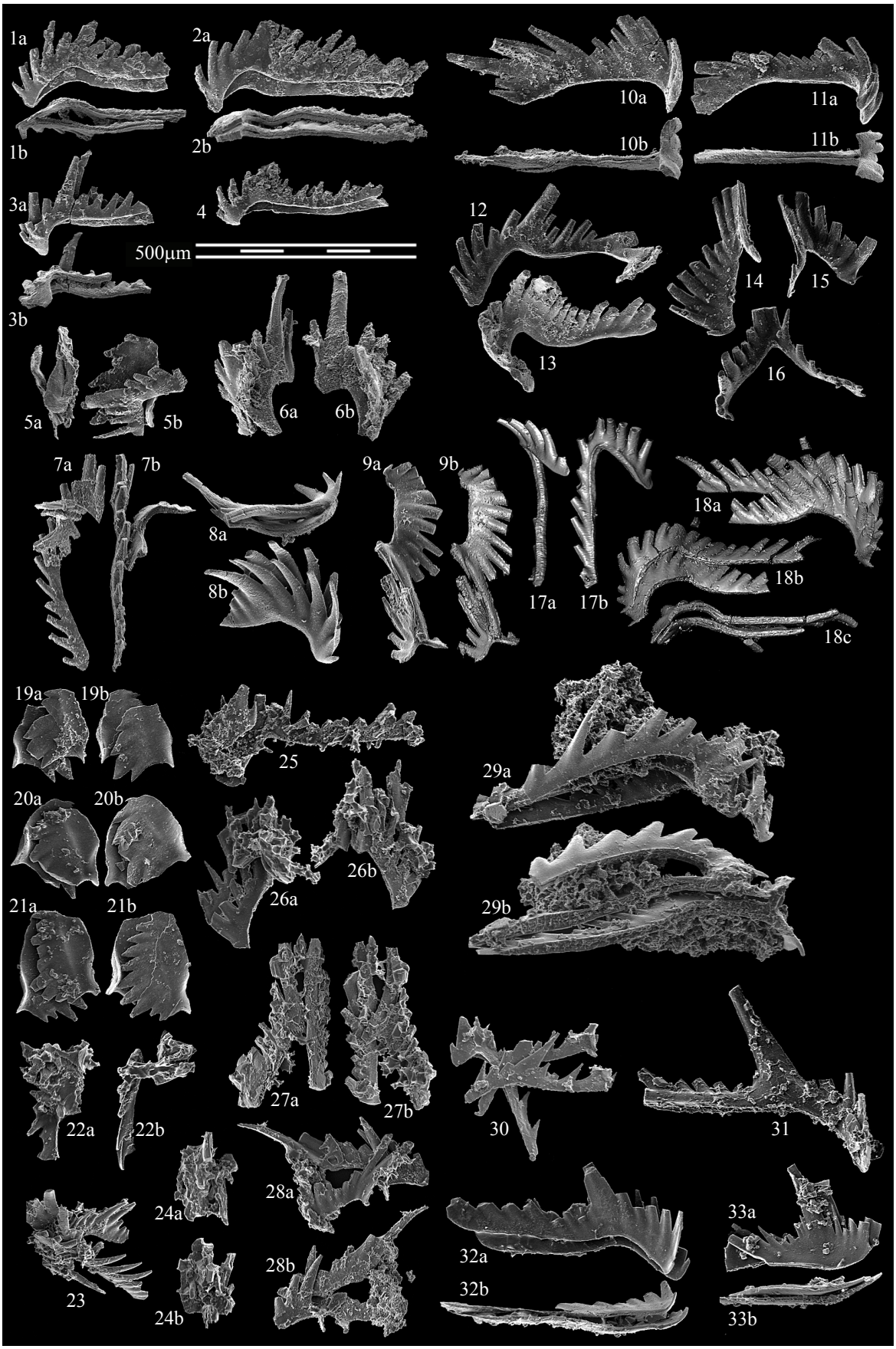
1a
1b
2a
2b
10a
10b
11a
11b
3a
3b
4
500µm
12
13
14
15
16
5a
5b
6a
6b
7a
7b
8a
8b
9a
9b
17a
17b
18a
18b
18c
19a
19b
20a
20b
21a
21b
22a
22b
23
24a
24b
25
26a
26b
27a
27b
28a
28b
29a
29b
30
31
32a
32b
33a
33b

PLATE 2

Figs 1-26, 30-31. *Novispathodus* spp.; a, `lateral´ view; b, `aboral´ view.
1, 18?, 26?, *Nv*. aff. *abruptus* A. 1a-b, PIMUZ 29001. 18a-b, PIMUZ 29018. 26a-b, PIMUZ 29026. 2, 6, 7?, 9, 10, 13, 16?, 17, 30, *Nv. pingdingshanensis*. 2a-b, PIMUZ 29002. 6a-b, PIMUZ 29006. 7, PIMUZ 29007. 9a-b, PIMUZ 29009. 10a-b, PIMUZ 29010. 13a-b, PIMUZ 29013. 16a-b, PIMUZ 29016. 17a-b, M, PIMUZ 29017. 30a-b, PIMUZ 29030.
3?, 4, 5?, 8, 14?, 19, 20, *Nv. waageni*. 3a-b, PIMUZ 29003. 4a-b, PIMUZ 29004. 5a-b, PIMUZ 29005. 8a-b, PIMUZ 29008. 14a-b, PIMUZ 29014. 19a-b, PIMUZ 29019. 20a-b, PIMUZ 29020.
11?, 12, *Nv*. aff. *pingdingshanensis*. 11a-b, PIMUZ 29011. 12a-b, PIMUZ 29012.
15a-b, *Nv.* n. sp. C. PIMUZ 29015.
21, 25, *Nv. radialis*. 21a-b, PIMUZ 29021. 25a-b, PIMUZ 29025.
22-24, *Nv*. n. sp. D. 22a-b, PIMUZ 29022. 23a-b, PIMUZ 29023. 24a-b, PIMUZ 29024.
27a-b, *Bo*. aff. *buurensis*, PIMUZ 29027.
28a-b, '*Gladigondolella"*? n. sp. A, PIMUZ 29028.
29a-b, *Ng*.? n. sp. A, PIMUZ 29029.
31a-b, *Nv*. sp. indet., M, PIMUZ 29031.

All from sample TQ84C30, Tsoteng section, Guangxi, South China, Lowest Spathian.
All P_1 elements except fig. 31. All ×80 SEM photographs, except figs. 30a-b, and 31a-c, which are ×80 SR-µCT images.

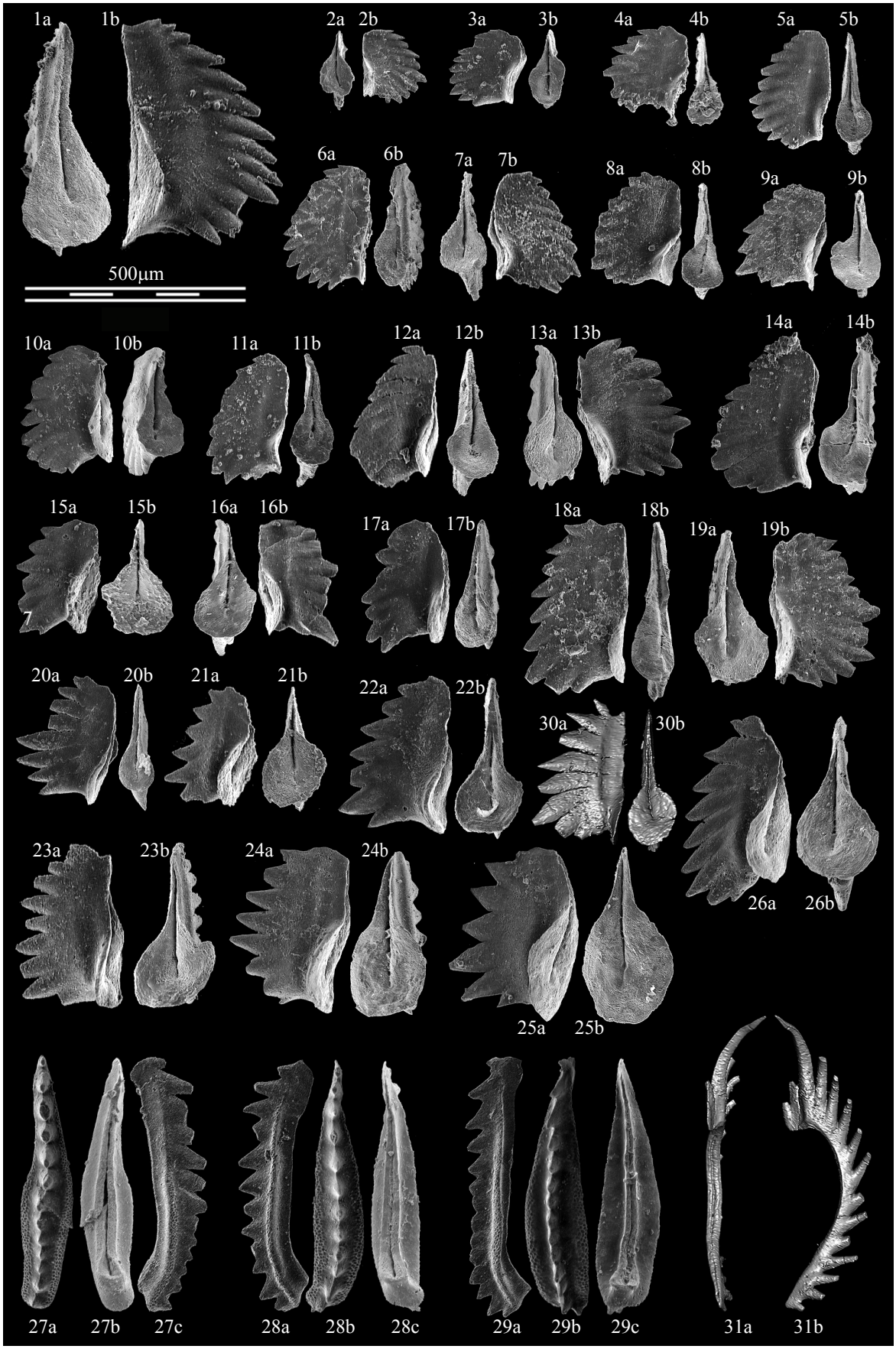
1a
1b
2a
2b
3a
3b
4a
4b
5a
5b
6a
6b
7a
7b
8a
8b
9a
9b
500µm
10a
10b
11a
11b
12a
12b
13a
13b
14a
14b
15a
15b
16a
16b
17a
17b
18a
18b
19a
19b
20a
20b
21a
21b
22a
22b
30a
30b
23a
23b
24a
24b
25a
25b
26a
26b
27a
27b
27c
28a
28b
28c
29a
29b
29c
31a
31b

CHAPTER 2

Synchrotron light gives euconodonts new bite: indirect evidence for a lingual cartilage

Nicolas Goudemand[a] , Michael J. Orchard[b], Séverine Urdy[a], Hugo Bucher[a] & Paul Tafforeau[c]

[a]Palaeontological Institute and Museum, University of Zurich, Karl Schmid-Strasse 4, CH-8006 Zürich, Switzerland.
[b]Geological Survey of Canada, 101-605 Robson St., Vancouver, BC, V6B 5J3 Canada.
[c]European Synchrotron Radiation Facility, 6 rue Jules Horowitz, BP 220, 38043 Grenoble cedex, France.

The origin of jaws remains largely a mystery that is best addressed by studying fossil and living jawless vertebrates. Conodonts were macrophagous, eel-shaped jawless predators, whose vertebrate affinity is still disputed. The geometrical analysis of exceptional three-dimensionally preserved clusters of oro-pharyngeal elements of the Early Triassic *Novispathodus*, imaged using propagation phase contrast X-ray synchrotron microtomography (PPC-SRμCT) suggests the presence of a pulley-shaped lingual cartilage homologous to that of extant cyclostomes within the feeding apparatus of euconodonts ('true' conodonts). This would lend strong support to their interpretation as vertebrates and demonstrate that the presence of such cartilage is a plesiomorphic condition of crown-vertebrates rather than a specialization associated with a parasitic feeding mode.

The transition from "agnathans" to gnathostomes ("jawed" vertebrates) is one of the most intriguing problems of evolutionary biology (1). Little is known about the endoskeleton of fossil jawless vertebrates (e.g. fossil cyclostomes (hagfishes and lampreys) and "ostracoderms"). Though the view is still debated, euconodonts would have possessed the very first vertebrate mineralized skeleton, in the form of their oral denticles (2, 3).

The general architecture of the conodont oral skeleton is a bilaterally symmetrical array of usually 15 phosphatic elements, which generally gets disarticulated after the decay of the supporting tissues. Hence most conodonts are known only as isolated elements. From the detailed study of hundreds of articulated 'natural assemblages' and photographic simulation of their collapse, Purnell and Donoghue (4) constructed a three-dimensional model of the *Idiognathodus* apparatus (presumably a template for all ozarkodinid apparatuses, see also (5)): one pair of obliquely pointed M elements are located rostrally; behind them, one unpaired 'S_0' element lying on the axis of bilateral symmetry and four pairs of elements (S_{1-4}) located on both sides of the S_0 (subscript number indicates distance ordering from the symmetry axis) would have grasped food and, more caudally, two pairs of pectiniform elements (P_1, P_2) would have processed this food by crushing and/or slicing (4, 6, 7) (Figs. 1A-B; for 'standard' orientation of single elements, see Fig. S1). Purnell and Donoghue's reconstruction of a generalized resting (dead) position is very well supported and in most aspects very convincing. It is therefore adopted herein as a basis upon which we build our new, dynamic reconstruction of the feeding apparatus at work.

How could these elements actually grasp or cut prey tissues? Purnell and Donoghue's functional model (2nd part of (4)) was based chiefly on analogies with extant agnathans.

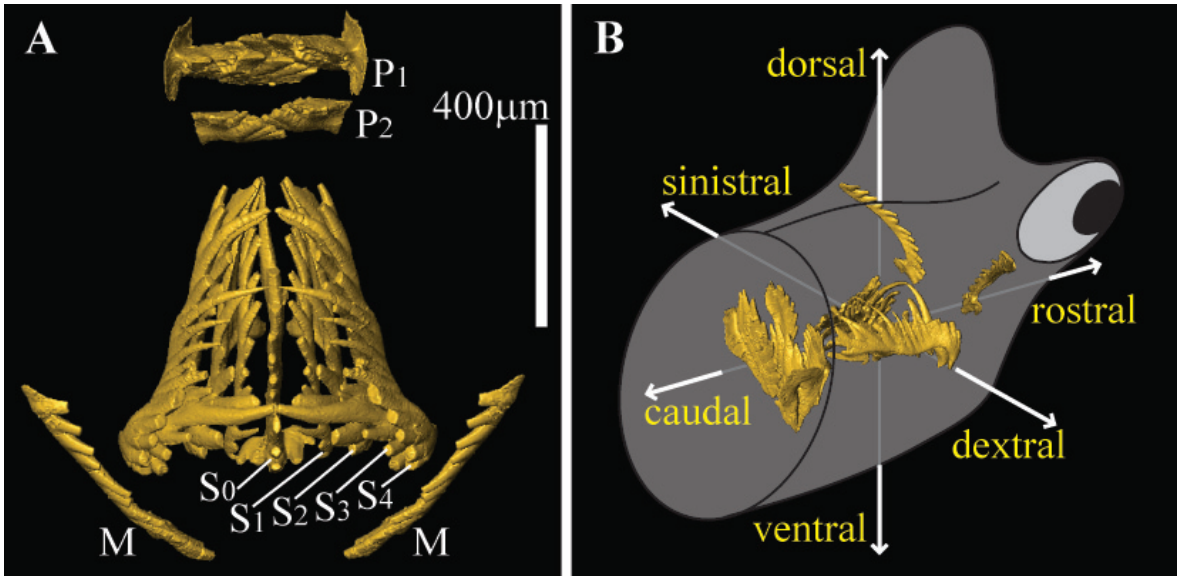

Fig. 1. Anatomical notation and orientation**. A.** Dorsal view of the reconstructed, closed apparatus of *Novispathodus*. Anatomical notation after Purnell *et al*. (8). **B.** Orientation of the apparatus within the conodont's head.

Indeed, the quite 'simple' geometry of the *Idiognathodus* elements does not provide much indication on what motions are possible or not (except for uncommon natural assemblages, see below). Thus, hypotheses were inferred from extant putative closest relatives. In our view, the more 'complicated' *Novispathodus* apparatus (particularly the presence of the peculiar 'enantiognathiform' S_2 element that characterizes the superfamily Gondolelloidea) imposes additional constraints that enable us to reconstruct the movement of the elements independently of phylogenetic considerations. Despite the absence of any preserved traces of oral cartilages in the rare specimens of conodonts with partly preserved soft-tissue (10), we show that partial reconstruction of their mouth is possible through biomechanical analysis.

Results

We recently discovered several fused clusters (rare occurrences of exceptional preservation where several elements of the same animal were diagenetically cemented together) of the Early Triassic conodont *Novispathodus* (10). One of these specimens (Fig. 2A), found in lowermost Spathian rocks of the Tsoteng section (Tiandong District, Guangxi Province, China; 11, 12), consists of four 'grasping' elements (S_{1-4} elements).

Fused clusters partially preserve the relative, three-dimensional positions and orientations of the involved elements. Yet, they are very small, fragile, tricky to manipulate and if more than two or three elements are involved, very complicated to analyse. One way to circumvent this is to use a non-destructive imaging method such as X-ray microtomography. In our case, the required resolution and contrast could not be achieved with conventional microtomography. Hence, we scanned this Chinese cluster, as well as a complete set of isolated elements (catalogue numbers PIMUZ 28001-9) found in the same sample and belonging to the same multi-element species, at the European Synchrotron Radiation Facility, on the ID19 beamline, using sub-micron resolution PPC-SRµCT (13; see Methods). Based on (5, 10, 14), we reconstructed a virtual three-dimensional apparatus of *Novispathodus*. The relative sizes of the S_{1-4} elements were inferred from the cluster. The other relative sizes (M, S_0, P_1, P_2 relative to S_{1-4}) were derived from the few known *Neogondolella* na-

tural assemblages (Figs. 2B-C, 14, 15, and unpublished material from Rieber).

Both our *Novispathodus* cluster and the *Neogondolella* natural assemblages (*ibid*) show that the cusps of the S_1 and S_2 elements were oriented more caudally than those of the S_0 and $S_{3, 4}$ elements, a feature that Orchard and Rieber considered to be unique to the 'gondolellaceans' (14, p. 480). Its recurrence in all known Triassic assemblages (see also (16, 17)) independently of their collapse angle suggests that it is not due to a taphonomic bias (post-mortem rotation of elements) and indeed records a configuration that differs from the *Idiognathodus* reconstruction (4). Natural assemblages of *Ozarkodin*a, the presumed rootstock of the Ozarkodinida (18) indicate that this caudal orientation of the cusp of the S_1 is not restricted to the Gondolelloideans (see (19), reinterpreted in (5), Text-Fig. 13A; or also (20)).

Fused clusters involving only the two hindeodelliform S_3 and S_4 elements are relatively more frequent in our collections. This can be partly explained by their very close morphological similarity but suggests also that they were located close and subparallel to one another (their recurrent relative position in those clusters) and had probably a common motion within the living animal. In (ab)oral view, their respective posterior processes are substraight posteriorly and outwardly deflected behind the cusp, and their anterior processes are laterally bowed inwards, which results in an overall sitar-like profile; the 'belly' of the more distal S_4 being larger and more rounded than that of the S_3.

The shape of the S_2 fits those of the S_3 and S_4 in the following aspects: (*1*) in the 'cluster position' (see above) where the cusp of the S_2 is subparallel to the posterior processes of the S_3 and S_4 elements, the outer profile (oral view) of the S_2 is similar to the inner profile of the S_3 and the largest denticle of its antero-lateral process is aligned with the cusps of the S_3 and S_4 (Figs. 2A, 3B); (*2*) in a presumed 'growth position' where the respective basal cavities (initial growth centres) of the S_{2-4} elements are approximately aligned and the inner lateral process of the S_2 is parallel to the posterior processes of the S_3 and S_4 (Fig. 3C), their respective profiles in ventral view still match, as their lower margins in lateral view; in this 'growth

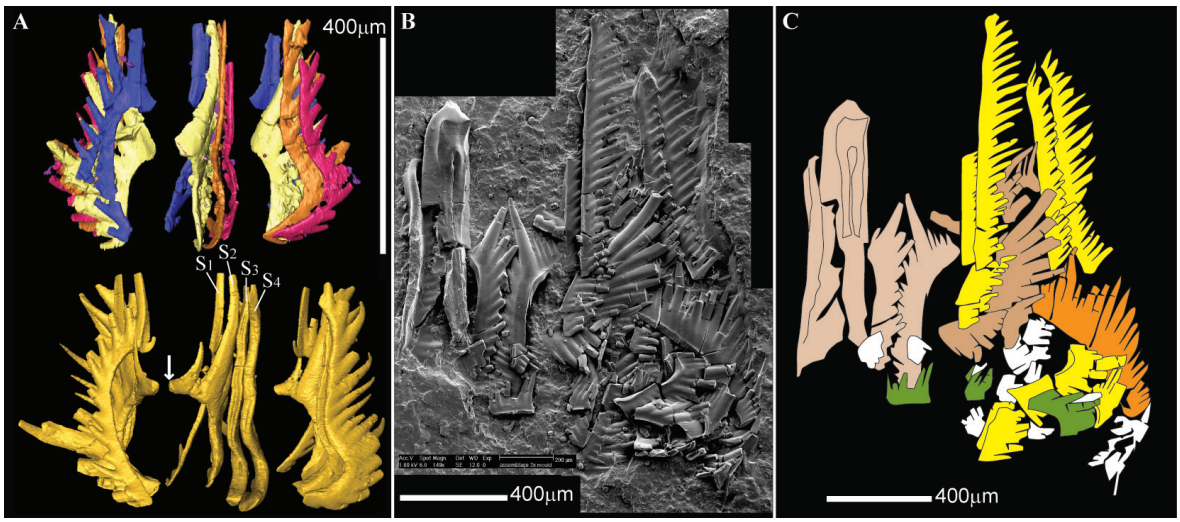

Fig. 2. Fossil material and interpretation. **A.** Comparison of the scanned cluster specimen (top) with a partial reconstruction based on isolated elements (bottom). Arrow: broken process. **B.** SEM composite microphotograph and interpretation (**C**) of a natural assemblage of *Neogondolella* found by Rieber (unpublished specimen, see also (15)), Middle Triassic, Monte San Giorgio, Switzerland. Beige: P elements; orange: S_0; brown: S_1 and S_2; yellow: S_3 and S_4; green: M elements.

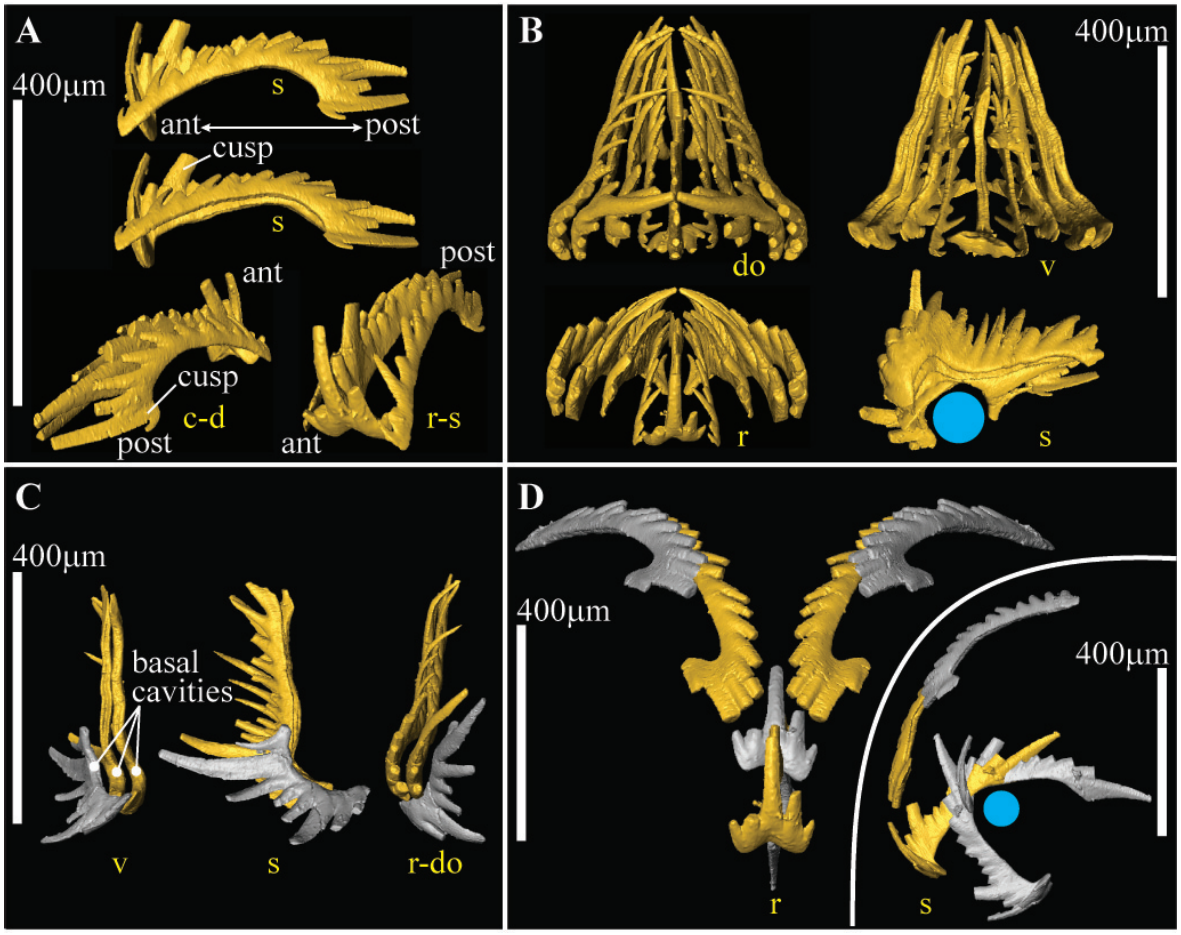

Fig. 3. Geometrical correspondences between elements**. A.** The S_1 elements match the posterior process of the S_0. Per definition, the tip of the cusp points posteriorly; ant, anterior; post, posterior. **B.** Closed arrangement of S elements. **C.** Presumed 'growth' position of the S_2 (silver) as inferred by geometrical correspondences with the S_3 and S_4 elements (gold). **D.** Proposed movement of the S_0 against the M elements; silver: start and end positions; gold: pinching position. **A-D**. Views: c, caudal; d, dextral; do, dorsal; r, rostral; s, sinistral; v, ventral. Blue: hypothetical cartilage.

position' (which also corresponds to the resting position of *Idiognathodus*, 4) the antero-lateral process of the S_2 extends more rostrally than the anterior processes of the S_3 and S_4 and is outwardly deflected in a way that somehow complements the rostral denticulation of the S_3 and S_4 (Fig. 3D, ventral view, note the alignment of the anteriormost denticles of the S_2 with the tangent of the S_4's outline at the anterior end). This indicates that at least in gondolelloideans the S_2 had a pivot motion relative to the S_3 and S_4 elements.

If we assume that the various elements moved along trajectories approximately parallel to the curvature of the cusp and denticles (4), then the movements of the $S_{2\text{-}4}$ elements must have included an opening/closing pivot motion around an axis parallel to the posterior processes of the S_3 and S_4. Consequently the net motion of the S_2 element was the composition of at least two pivot motions around two nearly perpendicular axes and hence its trajectory must have been subhelicoidal, which is compatible with the peculiar right-angled configuration of its processes. The minimal distance between sinistral and dextral sets of $S_{2\text{-}4}$ elements is constrained by the dimensions of their respective cusps and denticles and of the inner lateral processes of both S_2 elements (here broken; Fig. 2A, arrow; see also Fig. S1). Moreover, an efficient grasping could have been achieved only if the tips of the

denticles were directed subrostrally, that is towards the prey in an opened position (Fig. 4Aa).

The curvature of the cusp and denticles of the S_0 element suggest both a rotation about a point located posteriorly on the posterior process and an arched antero-posterior translation. Similarly the movement of the S_1 must have included an arched antero-posterior translation accompanied by an opening/closing pivot about its main axis. Interestingly the outline of the latter element very closely matches the outline of the posterior process of the S_0 (Fig. 3A), which suggests that the S_0 and the two S_1 elements grew and probably functioned together.

This position of the S_0 respective to the S_1 is compatible with the relative positions of the S_{1-4}, as recorded by our cluster. In fact, if all S elements are reconstructed in these respective positions (Fig. 3B), we get a very compact arrangement where all denticles tips end up close to the mid-plane (as here represented by the length axis of the S_0 element) and the lower margins are subparallel in lateral view. We propose that this particular spatial configuration, partly recorded by our cluster, corresponds to the maximal closing position of the grasping S 'module' (Fig. 4Ag).

This arrangement is rather uncommon for a natural assemblage and it differs substantially from the 'at rest' arrangement, as reconstructed by Purnell and Donoghue (4, 5). Yet, several published natural assemblages (for an exhaustive list of those published before 1998, see appendix in (5)) record also relative orientations of elements that differ significantly from the Purnell and Donoghue's reconstruction (that is in a way that is not convincingly explained by ad-hoc post-mortem displacements of the elements). In particular, a 'very uncommon' sub-parallel arrangement of the S_{2-4} and M elements of *Gnathodus*, originally figured by Schmidt (21; re-illustrated in (5), Text-figs. 7-8) or a specimen of *Bispathodus* where the converging cusps of the M elements come in contact with one another (Text-fig. 14 and Pl. 3 in (5)). Furthermore, we consider that some of the variation observed among the numerous specimens of *Idiognathodus* natural assemblages is best explained if one assumes that they record several slightly differing 'living' positions rather than one single 'resting' position affected by taphonomic noi-

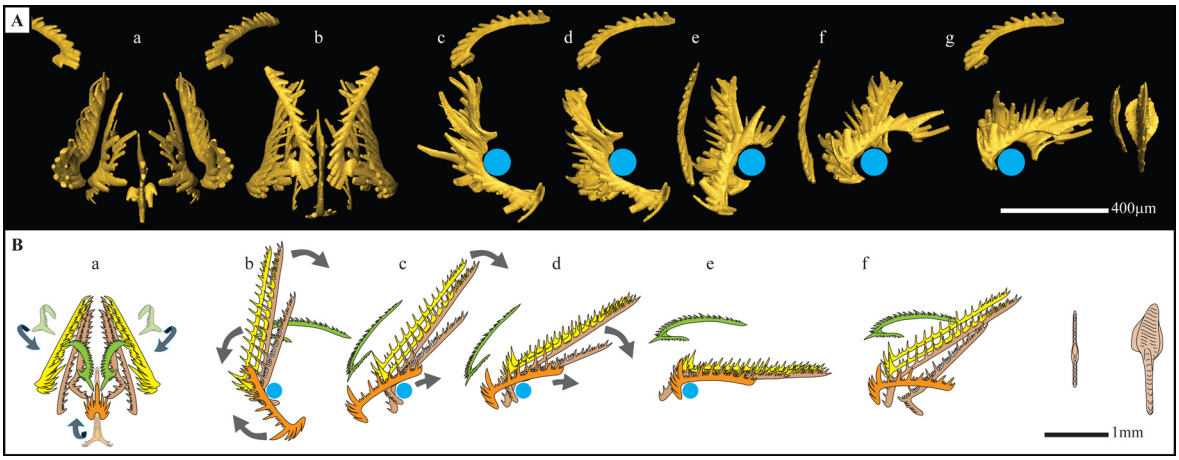

Fig. 4. Proposed relative positions and movements of the elements in *Novispathodus* (**A**) and *Idiognathodus* (**B**). Colour coding as in Fig. 2C; blue: hypothetical cartilage. **Aa, c / Ba, b.** Resp. rostral and sinistral views of the opened (protracted) apparatus. **Ac, d.** S_3 and S_4 elements of *Novispathodus* could have closed independently in the protracted position and performed grasping before the S_0 and M elements cut the prey's tissues. **Ab, e / Ba, c.** Pinching position. **Af / Bd.** Intermediate position. **Ag / Be.** Closed (retracted) position. **Bf.** Original 'at rest' reconstruction of *Idiognathodus* (compare with **Bd**); redrawn after Purnell and Donoghue (4). **A, B.** In lateral views, only the dextral 'half' of the apparatus is represented. P elements are represented only in **Ag** and **Bf**.

se. Hence, in our view, they are potentially informative about the relative motions of the elements.

Theoretically, the geometrical analysis of the flattening of a few pairs of bilaterally symmetrical elements is sufficient for solving the inverse mapping problem of estimating the three-dimensional angle of collapse. The relative orientation and spacing of these pairs of elements can then be solved independently for each (obliquely collapsed) specimen and analysis of numerous specimens not only allows smoothing taphonomically induced discrepancies but also gives insights about the relative motions of the elements.

The integration of this information, in particular from our cluster (see also Fig. 5a-b and Pl. 6, Fig. 1 in (21)), into a comprehensive, dynamic model implies a rotation of the $S_{3, 4}$ elements relative to the S_0 about a medio-lateral axis approximately located below the cusp of the S_0. From the 'at rest' position, maximal closing of the apparatus is most plausibly attained by dorso-caudal retraction of the $S_{3, 4}$ towards the P elements rather than by rostral eversion of the S_0. Note that the longitudinal dimensions of the largest S elements approximately equal the distance between this presumed rotation axis and the P_2 elements and are thus compatible with this interpretation (Figs. 4Af-g, 4Be-f).

Each euconodont element is composed of two parts: a crown and a basal body. The latter is preserved only in exceptional cases. In S or M elements, the basal body, when present, smoothes out the lower margin (ventral outline) of the element (see for instance Figs. 5C-D). In *Novispathodus*, the lower margins of the S elements are already 'smooth' (low three-dimensional curvature) and we therefore assume that their respective basal bodies, if mineralized, were relatively thin, filled up the basal grooves but did not alter the shape of their lower margins substantially (Fig. S1).

If the later holds, then it is clear from Figs. 3B and 4A that a single and simple mechanism can explain all the above deduced motions of the elements: a pulley-like system with protractor and retractor muscles that would have rotated the elements about a ventral, medio-laterally oriented, cylinder- or possibly U-shaped (both slightly curved ends pointing dorso-rostrally) supporting element of unknown but most probably cartilaginous nature (Figs. 3-5, blue circle). Only three pairs of antagonistic muscles (inserted resp. on $S_{0, 1}$; S_2; $S_{3, 4}$) would have been necessary to operate the 9 S elements the way here described.

Interestingly, this 'pulley hypothesis' also possibly accounts for the presence of the two inward and forward pointing M elements: the lower profile of the *Novispathodus* S_0, especially the arched part of its posterior process suggests that during opening it was first rostro-ventrally translated and then rotated (its arched posterior end 'gliding' on the ventral cartilage), and vice versa during closure; its dimensions are compatible with its initial rotation being synchronized with the closure of the M elements (Figs. 3D and 4Ae). Together their overall Y-shaped (in rostral view) converging motion would have performed (as an ice cube grabber) an efficient pinching, seizing function. The uncommon arrangement of *Bispathodus* figured by Purnell and Donoghue (5, Pl.3 and Text-fig. 14) lends partial support to this scenario. The subsequent dorso-caudal retraction of the S_0 and S_1 elements would have torn off preys' tissues and brought them towards the pectiniform elements. Then, the other S elements would have close, further channelling the food towards the pharynx (Fig. 4A, Movies S2, S3).

Discussion

Our model strongly recalls the operation of the lingual laminae of lampreys such as the flesh-feeder species *Geotria australis* (22) (Fig.5A). In the fully protracted position, a pair of longitudinal lingual laminae can open and close independently and pinch the prey's

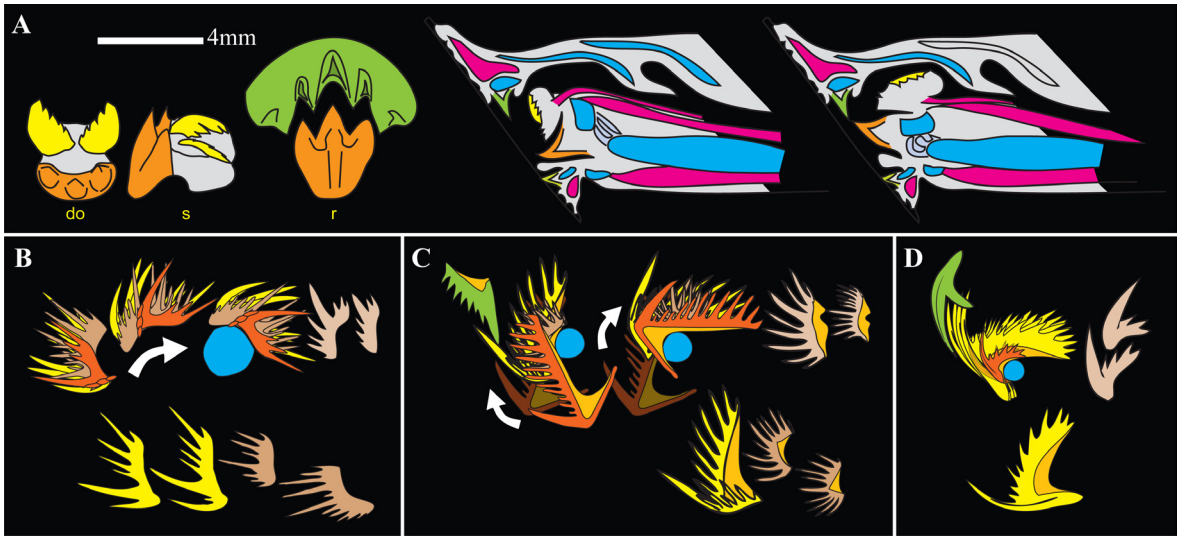

Fig. 5. Comparison with extant lamprey and other conodont taxa. **A.** Left: supraoral tooth (green) and lingual laminae (orange: transverse lamina; yellow: longitudinal laminae) of the lamprey *Geotria australis*. Right: sagittal sections of the lamprey head in protracted (middle) and retracted (right) positions. Red: muscles; cyan: cartilages. Redrawn after Hilliard (22). **B-D.** Proposed relative positions and movements of the elements of *Ellisonia* (**B**), *Hibbardella* (**C**) and *Paracordylodus* (**D**). Isolated S_{1-4} in lower row. Colour coding as in Fig. 2C; light orange: basal body. Modified resp. after Koike (23), Nicoll (24), and Tolmacheva and Purnell (25). **B**. M is missing.

tissues. During subsequent retraction, the interlocking of the transverse lingual lamina with the supraoral tooth cuts the flesh off and the longitudinal laminae brings it towards the pharynx (22). The growth and phosphatic composition of the conodont elements prevent homology of the conodont elements themselves with the keratin 'teeth' of extant agnathans (3, 26*, contra* 27). Yet, our model supports the view that the conodonts' oral apparatus as a whole is homologous with the lingual apparatus of lampreys. We tentatively homologize the presumed ventral cartilage with the *cartilago apicalis* of extant lampreys (28). In lampreys this cartilage is flexibly attached to a larger piston cartilage (22, Fig. 5A). In *Novispathodus*, the available data does not constrain its shape caudoventrally and a similar mechanism can only be hypothesized.

In our view, the S elements were not necessarily lying on dental plates (*contra* 4). At least for *Novispathodus* the location of the ventral cartilage is constrained by the shape and motion of the S_2 elements and space considerations contradict the presence of such plates. In *Novispathodus*, if cartilaginous dental plates were present, they were restricted to the posterior processes of the S_3 and S_4, and thus analogous to the paired *cartilago apicalis lateralis* of lampreys (28). By analogy with lampreys, additional muscles located between the apical lobes and the apicalis (22) would have allowed performing independent opening/closing of these elements (analogous to the longitudinal lingual laminae) in the protracted position.

Further work is necessary to assess to what extent this reconstruction is compatible with other conodont taxa, but we consider that the presence of a ventral 'apical' cartilage and the proposed seizing movement of the S_0 and M elements were possibly shared by most euconodonts (Figs. 5B-D, Fig. 6). Though we consider the presence of a flexible, half-circular ventral cartilage as obvious in the Ordovician balognathid *Promissum pulchrum* (described by Aldridge *et al*. (32)), the closure of the S elements occurred certainly in a ventral rather than dorsal position (see uncommon arrangement, Text-figs. 7-9 in (32)). Thus, the shape of the ventral cartilage and the putative pulley-like motion of the various S elements must have varied within

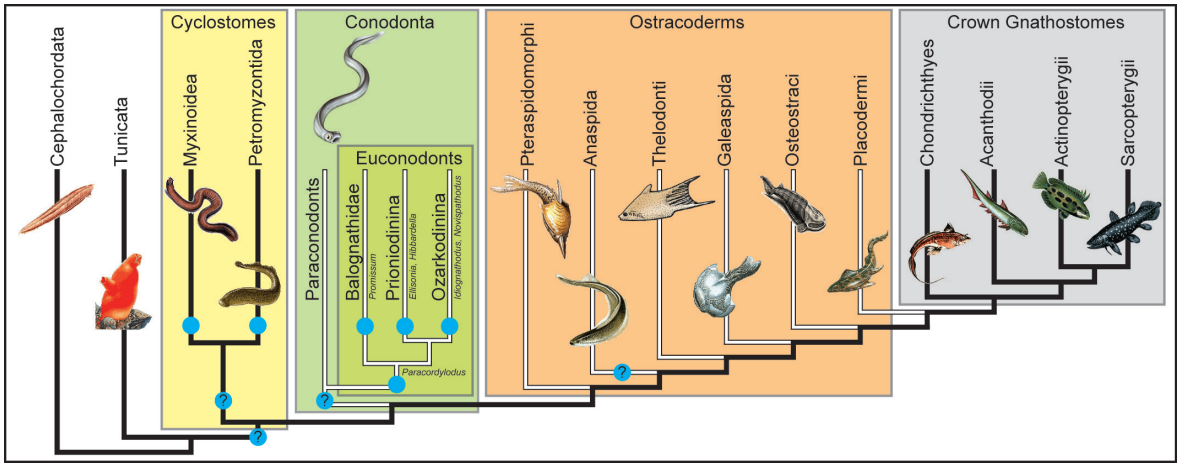

Fig. 6. Hypothesis of relationships among chordates. Primarily based on (26, 29). Evidence from molecular data supports monophyly of cyclostomes and shows that the closest relatives of vertebrates are the tunicates, not the cephalochordates (30). The relationships among euconodonts are from (31). Blue circle indicates presence of a lingual cartilage.

the clade. Yet, if, as suggested, the presence of such cartilage is established in even the most 'basal' forms of complex conodonts (31), such as the Early Ordovician (ca 480 million year old) *Paracordylodus* (Fig. 5D), then it should reflect a plesiomorphic condition of euconodonts. It cannot be confirmed yet whether conodonts, whose apparatus is composed of coniform elements only, could have shared this character but similarities between the apparatuses of panderodontids and euconodonts (6, p. 90) favour this hypothesis.

The presence of such 'lingual' cartilage has been asserted only in extant lampreys and hagfishes so far (25), but also suggested in euphaneropids (33), anaspids (34) and fossil lampreys (35, 36) (all however significantly younger than *Paracordylodus*). Besides lending strong support to a vertebrate affinity of conodonts, possibly as the most 'primitive' stem-gnathostomes (i.e. between lampreys and "ostracoderms") (Fig. 6), our reconstruction suggests that this cartilage associated with protractor and retractor muscles is a plesiomorphic condition of crown-vertebrates (lost in gnathostomes)(37) and not, as often suggested (36), a specialized feature associated with a parasitic feeding habit.

Acknowledgements

This work was supported by the Swiss NSF project 200020-113554 (H.B.). We acknowledge the European Synchrotron Radiation Facility for provision of synchrotron radiation facilities and for granting access to beamline ID19 (proposal ec432). We thank also T. Brühwiler for his help at ESRF, C. Zollikofer for access to FoRM-IT, C. Monnet, R. Lebrun and C. Zollikofer for assistance with Amira™ and FoRM-IT, T. Galfetti and A. Brayard for assistance in the field, as well as J. Huber and L. Pauli for their help with the processing of conodont samples. We are very indebted to H. Rieber for providing the natural assemblage illustrated in Fig. 2B, which was imaged at GSC Vancouver with the help of P. Krauss. M. Purnell reviewed a previous version of this manuscript.

References and Notes

1. Janvier, P. (2007) in *Major transitions in vertebrate evolution*, eds. Anderson, J. S. & Sues, H.-D. (Indiana University Press, Bloomington, USA), pp. 57-121.
2. Donoghue, P. C. J. & Sansom, I. J. (2002) Origin and early evolution of vertebrate skeletonization. *Microsc. Res. Techniq.* **59,** 352-372.
3. Donoghue, P. C. J. (1998) Growth and patterning in the conodont skeleton. *Philos. T. Roy. Soc. B* **353,** 633-666.
4. Purnell, M. A. & Donoghue, P. C. J. (1997) Architecture and functional morphology of the skeletal apparatus of ozarkodinid conodonts. *Philos. T. Roy. Soc. B* **352,** 1545-1564.
5. Purnell, M. A. & Donoghue, P. C. J. (1998) Architecture, Taphonomy and Homologies of the Skeletal Apparatus of Ozarkodinid Conodonts. *Palaeontology* **41,** 57-102.
6. Purnell, M. A. & Von Bitter, P. H. (1992) Blade-Shaped Conodont Elements Functioned as Cutting Teeth. *Nature* **359,** 629-630.
7. Purnell, M. A. (1995) Microwear on conodont elements and macrophagy in the first vertebrates. *Nature* **374,** 798-800.
8. Purnell, M. A., Donoghue, P. C. J. & Aldridge, R. J. (2000) Orientation and anatomical notation in conodonts. *J. Paleontol.* **74,** 113-122.
9. Orchard, M. J. (2005) in *Conodont Biology and Phylogeny: Interpreting the Fossil Record*, eds. Purnell, M. A. & Donoghue, P. C. J. (*Spec. Pap. Palaeontol*., **73**), pp. 73-101.
10. Briggs, D. E. G., Clarkson, E. N. K. & Aldridge, R. J. (1983) The conodont animal. *Lethaia* **16,** 1-14.
11. Zhang, H., Tong, J. & Zuo, J. (2005) in *International Symposium on Triassic Chronostratigraphy and Biotic Recovery* (Albertiana, Vol. 33, Part I: Program and Abstracts), pp. 103-104.
12. Galfetti, T., et al. (2008) Evolution of Early Triassic outer platform paleoenvironments in the Nanpangjiang Basin (South China) and their significance for the biotic recovery. *Sed. Geol.* **204,** 36-60.
13. Tafforeau, P., et al. (2006) Applications of X-ray synchrotron microtomography for non-destructive 3d studies of paleontological specimens. *Appl. Phys. A-Mater.* **83,** 195-202.
14. Orchard, M. J. & Rieber, H. (1999) Multielement *Neogondolella* (Conodonta, upper Permian - middle Triassic). *Boll. Soc. Paleontol.* **37,** 475-488.
15. Rieber, H. (1980) Ein Conodontencluster aus der Grenzbitumenzone (Mittlere Trias) des Monte San Giorgio. *Ann. Naturhist. Mus. Wien* **83,** 265-274.
16. Ramovs, A. (1978) Mitteltriassische Conodonten-clusters in Slowenien, NW Jugoslawien. *Paläont. Z.* **52,** 129-137.
17. Huang, J.-y., et al. (2010) Discovery of Middle Triassic Conodont Clusters from Luoping Fauna, Yunnan Province. *Earth Science, Journal of China University of Geosciences* **35,** 512-514.
18. Sweet, W. C. (1988) The Conodonta: Morphology, Taxonomy, Paleoecology and Evolutionary History of a Long-Extinct Animal Phylum. *Oxford Monographs on Geology and Geophysics* **10** (Clarendon Press, Oxford), 212pp.
19. Mashkova, T. V. (1972) *Ozarkodina steinhornensis* (Ziegler) apparatus, its conodonts and biozone. *Geologica et Palaeontologica* **1,** 81-90.
20. Nicoll, R. S. & Rexroad, C. B. (1987) in *Palaeobiology of Conodonts*, ed. Aldridge, R. J. (Ellis Horwood Limited, Chichester), pp. 49-61.
21. Schmidt, H. (1934) Conodonten-Funde in ursprünglichen Zusammenhang. *Paläont. Z.* **16,** 105-135.
22. Hilliard, R. W., Potter, I. C. & Macey, D. J. (1985) The dentition and feeding mechanism in adults of the southern-hemisphere lamprey *Geotria australis* Gray. *Acta Zool.-Stockholm* **66,** 159-170.
23. Koike, T., Yamakita, S. & Kadota, N. (2004) A natural assemblage of *Ellisonia* sp. cf. *E. triassica* Müller (Conodonta) from the Permian- Triassic boundary in the Suzuka Mountains, Central Japan. *Paleontol. Res.* **8,** 241-253.
24. Nicoll, R. S. (1977) Conodont apparatus in an Upper Devonian palaeoniscoid fish from the Canning Basin, Western Australia. *BMR J. Aust. Geol. Geop.* **2,** 217-228.
25. Tolmacheva, T. Y. & Purnell, M. A. (2002) Apparatus composition, growth, and survivorship of the Lower Ordovician conodont *Paracordylodus gracilis* Lindström, 1955. *Palaeontology* **45,** 209-228.
26. Donoghue, P. C. J., Forey, P. L. & Aldridge, R. J. (2000) Conodont affinity and chordate phylogeny. *Biol. Rev.* **75,** 191-251.

27. Krejsa, R. J., Bringas, P. J. & Slavkin, H. C. (1990) A neontological interpretation of conodont elements based on agnathan cyclostome tooth structure, function, and development. *Lethaia* **23,** 359-378.
28. Yalden, D. W. (1985) Feeding mechanisms as evidence of cyclostome monophyly. *Zool. J. Linn. Soc.-Lond.* **84,** 291-300.
29. Donoghue, P. C. J. & Purnell, M. A. (2005) Genome duplication, extinction and vertebrate evolution. *Trends in Ecology and Evolution (TREE)* **20,** 312-319.
30. Donoghue, P. C. J., Graham, A. & Kelsh, R. N. (2008) The origin and evolution of the neural crest. *BioEssays* **30,** 530-541.
31. Donoghue, P. C. J., Purnell, M. A., Aldridge, R. J. & Zhang, S. (2008) The interrelationships of 'complex' conodonts (Vertebrata). *J. Syst. Palaeontol.* **6,** 119-153.
32. Aldridge, R. J., Purnell, M. A., Gabbott, S. E. & Theron, J. N. (1995) The apparatus architecture and function of *Promissum pulchrum* Kovacs-Endrody (Conodonta, Ordovician) and the prioniodontid plan. *Philos. T. Roy. Soc. B* **347,** 275-291.
33. Janvier, P. & Arsenault, M. (2007) The anatomy of *Euphanerops longaevus* Woodward, 1900, an anaspid-like jawless vertebrate from the Upper Devonian of Miguasha, Quebec, Canada. *Geodiversitas* **29,** 143-216.
34. Stensiö, E. (1964) in *Traité de Paléontologie*, ed. Piveteau, J. (Masson, Paris), pp. 96-383.
35. Gess, R. W., Coates, M. I. & Rubidge, B. S. (2006) A lamprey from the Devonian period of South Africa. *Nature* **443,** 981-984.
36. Bardack, D. & Zangerl, R. (1968) First fossil lamprey - a record from Pennsylvanian of Illinois. *Science* **162,** 1265-1267.
37. A similar hypothesis has been proposed by Janvier, P. (1981) The phylogeny of the Craniata, with particular reference to the significance of fossil "agnathans." *J. Vertebr. Paleontol.* **1,** 121-159.

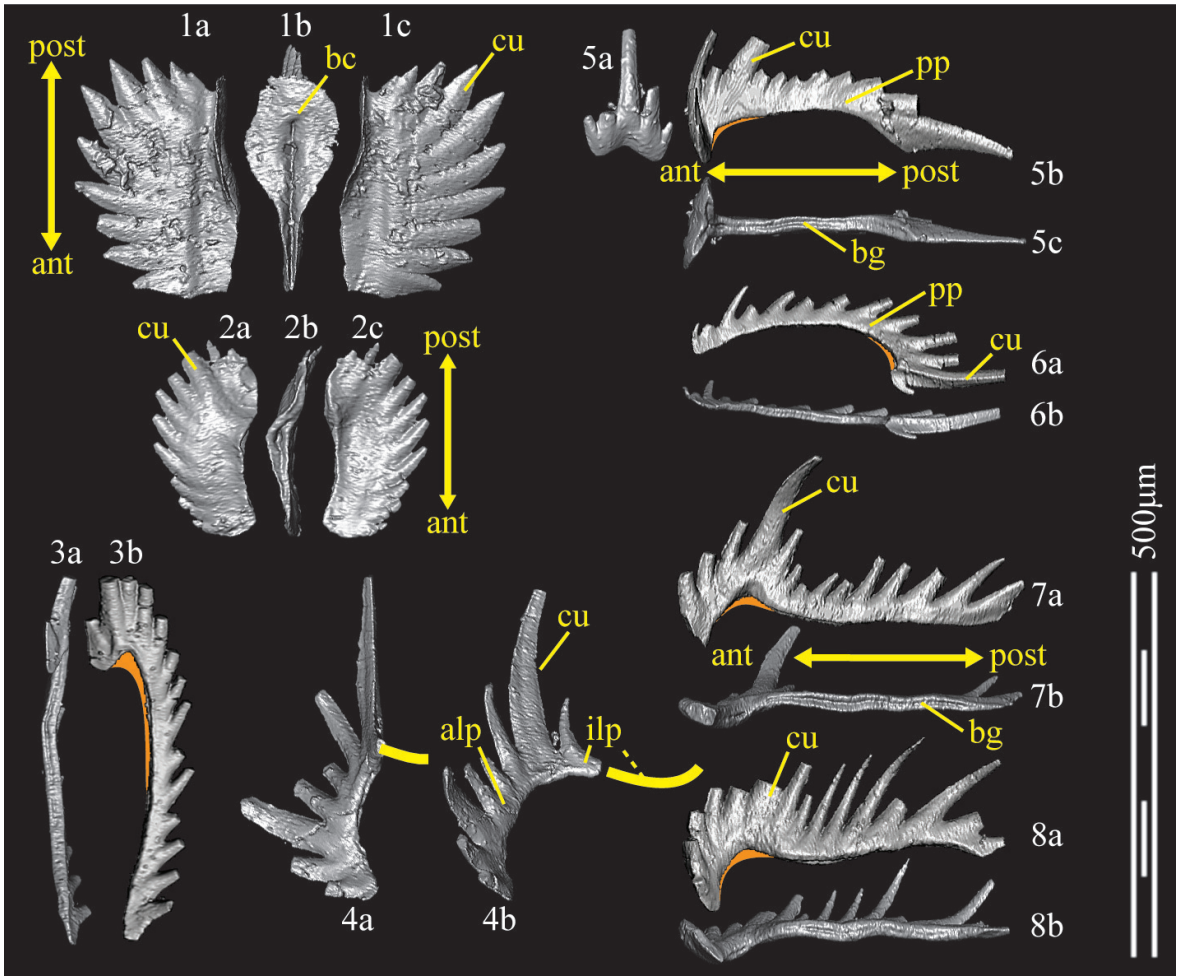

Supporting Information

Methods

Propagation phase contrast X-ray synchrotron microtomography (PPC-SRμCT). The specimens were scanned at the ESRF on the beamline ID19. We used a pink beam with a critical energy of 17.68 keV delivered by a U17.6 undulator. This insertion device is delivering a single harmonic with a narrow bandwidth (ΔE/E of 5 %). The original source monochromaticity is good enough to perform high quality scans at sub-micron resolution without a monochromator. It allows rapid scans of microfossils, nearly free of ring artefacts. Regarding to the sample size, we used a detector composed of a 6 μm thick GGG scintillator, of a revolver microscope, and of a FReLoN CCD camera (S1). The isotropic voxel sizes ranged from 0.23 to 0.46 microns. Phase contrast was obtained using a propagation distance of 10 mm. Absorption contrast being often low in fossils, phase contrast can reveal much more structures (13, S2, S3).

Processing of raw data. Radiographs were processed using in-house tools developed at the ESRF. They were corrected by flatfield and darkfield, using a protocol that reduces ring artefacts. Sample movements were measured and corrected later during the tomographic reconstruction. An average of the processed radiographs was computed and filtered to obtain a correction map for ring artefacts. The volumes were then reconstructed using filtered back-projection algorithm (PyHST, ESRF). After reconstruction, the remaining ring artefacts were corrected slice by slice. The final slices were converted into stacks of 16-bit TIFF files for the 3D processing.

3D processing. The 3d model was constructed using both the commercially available Amira™ imaging software and the in-house software FoRM-IT, developed by Christoph Zollikofer (Univ. Zurich).

References

S1. Labiche, J.-C. (2007) The fast readout low noise camera as a versatile X-ray detector for time resolved dispersive extended X-ray absorption fine structure and diffraction studies of dynamic problems in materials science, chemistry, and catalysis. *Rev Sci Instrum* **78,** 091301.

S2. Feist, M., Liu, J. & Tafforeau, P. (2005) New insights into Paleozoic charophyte morphology and phylogeny. *Am. J. Bot.* **92,** 1152-1160.

S3. Friis, E. M., et al. (2007) Phase-contrast x-ray microtomography links Cretaceous seeds with Gnetales and Bennettitales. *Nature* **450,** 549-552.

Supplementary Movie S2. Animated reconstruction of the feeding apparatus of conodont *Novispathodus*. In the protracted (opened) arrangement of the apparatus, S_3 and S_4 elements can close and grasp the prey. S_{2-4} elements start to retract and pull on the prey's tissues while the symmetrical S_0 and the M elements come to close in an opposing, Y-shaped converging motion. The S_0 and S_1 then retract caudally, tear off the seized tissues and bring them towards the cutting/shearing P elements. The accompanying closure of the S_{2-4} elements helps channelling the food. Especially in lateral and caudal views, it is clear that all S elements rotate about a sub-cylindrical, presumably cartilaginous support: the inferred lingual (apical) cartilage.

Supplementary Movie S3. 3d animated reconstruction of the feeding apparatus of conodont *Novispathodus*. Red/cyan anaglyph (3d) version of Movie S2. Please use appropriate glasses.

Fig. S1. 'Standard' orientation of the single elements of *Novispathodus*. The pit of the basal cavity (**bc**) corresponds to the growth centre. The denticle directly above this growth centre is called the cusp (**cu**). Per definition, the cusp is curved towards the posterior end of the element. Other abbreviations: **ant**: anterior; post: posterior; **alp**: antero-lateral process; **ilp**: inner-lateral process; **pp**: posterior process; **bg**: basal groove. 1a-c: P1; 2a-c: P2; 3a-b: M; 4a-b: S2, the common extension of the broken inner-lateral process is indicated in yellow (9); 5a-c: S0; 6a-b: S1; 7a-b: S3; 8a-b: S4. The light orange area below the cusp of each ramiform element (figs. 3-8) shows the hypothesized potential extension of the basal body.

CHAPTER 3

The Elusive Origin of *Chiosella timorensis* (Conodonts, Triassic)

Nicolas Goudemand[a], Michael J. Orchard[b], Hugo Bucher[a], Jim Jenks[c]

[a] Paläontologisches Institut und Museum der Universität Zürich, Karl Schmid-Strasse 4, CH-8006 Zürich, Switzerland.
[b] Geological Survey of Canada, 101-605 Robson St., Vancouver, BC, V6B 5J3 Canada.
[c] 1134 Johnson Ridge Lane, West Jordan, Utah 84084.

The First Appearance Datum (FAD) of the conodont *Chiosella timorensis* has been recently proposed has an index for the worldwide recognition of the Olenekian-Anisian Boundary (OAB, Early-Middle Triassic boundary). We here report the co-occurrence of *C. timorensis* with the ammonoids *Neopopanoceras haugi* (Hyatt & Smith), *Keyserlingites pacificus* (Hyatt & Smith), *Subhungarites yatesi* (Hyatt & Smith) and *Pseudacrochordiceras inyoense* (Smith), which are diagnostic of the late Spathian *Haugi* Zone. This shows that the previously published occurrences of *C. timorensis* were still too poorly constrained, and it questions the presumed adequacy of its FAD as a marker of the OAB. It weakens also the usual assumption that *C. gondolelloides* would occur stratigraphically lower than *C. timorensis*. We reject the current criterion for their taxonomic separation and define a new *Chiosella* species (left in open nomenclature). The origin of *Chiosella timorensis* remains unknown but multi-element analyses suggest an affinity with the late Olenekian *Neogondolella* ex gr. *regalis* group of forms.

Key words: conodont, Triassic, South China, North America, Olenekian-Anisian Boundary.

Platforms are frequently reduced/lost or on the contrary (re-)developed during the evolutionary course of conodonts' pectiniform elements. During the Early Triassic, progressive reduction of the platform is presumably exemplified by the *Neogondolella – Sweetospathodus – Neospathodus* lineage. Similarly Nogami defined '*Gondolella' timorensis* as a 'Gondolella' with noticeably reduced platform (Nogami, 1968). Kozur, on the contrary (following Bender, 1968), erected the genus *Chiosella* (Kozur, 1988) on the assumption that forms like *Chiosella gondolelloides* and *C. timorensis* were transitional forms along a *Triassospathodus - Chiosella- Neogondolella* lineage, by which neospathodid (segminate) elements would have developed midlateral ridges and later gained platforms. This view is shared by most conodont workers at least since the 70's (Bender, 1968) and it has historical grounds: at that time it was thought that elements like the P_1 of *Neogondolella* would have disappeared at the PTB and would have re-evolved around the OAB through the proposed platform gain scenario. The type species of *Neogondolella* is a post-OAB species, so this naturally led Kozur to erect the pre-PTB genus *Clarkina* (1988). More recently however it was showed that such elements were actually present throughout the Early Triassic (Orchard, 1994). Moreover, multi-element reconstructions demonstrated that some neogondolellid species of respectively late Permian, Smithian and early Anisian age shared this same apparatus

(Orchard and Rieber, 1999). As the reconstructions by Orchard (2005) impressively show, the ramiform elements were able to evolve quite rapidly too during the Early Triassic. So the fact that several species share the same apparatus tends to prove that they were pertaining to the same long-ranging taxa and assuming instead that their apparatuses are only homeomorphic, i.e that they evolved several times independently, does not seem to be the most parsimonious. Yet, and though it is largely contradicted by multi-element analyses, this view is still the one advocated in a recent publication by Gradinaru *et al.* (2006), and this apparently encouraged them to redefine *C. timorensis* on the basis of the extension of its mid-lateral ridge. Indeed, this paper was meant to reflect a newly reached consensus of its authors on an exact definition of *C. timorensis* relative to its presumed forerunner *C. gondolelloides*, because authors used to disagree on whether and how both species should be separated. In other occasions this question could appear subsidiary, but it had been recognized that the first occurrence of *C. timorensis* appeared frequently very close to the Anisian base as defined by ammonoids (*Japonites welteri* beds; Bucher, 1989; see discussion). Its wide distribution (North America, Southern Europe, Pakistan, Japan, Timor, Australia) makes it particularly helpful for global correlations. Subsequently its First Appearance Datum (FAD) has been suggested as a potential index for a global definition of the Olenekian-Anisian Boundary (OAB, Early-Middle Triassic boundary).

The confusion concerning the recognition of *C. timorensis* arose in part from the impossibility to distinguish between juveniles of *C. timorensis* and juveniles or even adult specimens of *C. gondolelloides*. Orchard (1995) noted that adult specimens of both *Chiosella* species are usually distinguished by their relative length and the relative width of the rudimentary platform. Yet, the '*Neospathodus' timorensis* illustrated by Sweet (1970) is a demonstrative example of the difficulties herewith involved: in all the above mentioned aspects (relative length of the element and relative width of the rudimentary platform) it appears identical to both Nogami's holotype (1968) and Gradinaru *et al*.'s figured specimen of *C. timorensis* (Pl. 1, figs. 1, 2 in Gradinaru *et al*., 2006); it is nevertheless regarded as an (upper Spathian?) 'advanced' form of *C. gondolelloides*. In fact the difference lies in the posterior extension of the median ridge which, according to the new definition (Gradinaru *et al*., 2006) (see also Kozur, 1988 and Bachmann and Kozur, 2004), "reaches the posterior denticle of the unit at least on one side […] of the blade". This particular criterion was convenient as long as it enabled the 'exact' correspondance of the FAD of *C. timorensis* with the ammonoid-defined Anisian base (note the past tense). We will see below that it is not necessarily appropriate.

New occurrences of *C. timorensis*

Geological settings

The present study is based on the analysis of a rock sample collected by one of us (J.J.) from his JJ7-07 locality, south of John Brown Canyon, in the Northern Humboldt Range, Nevada (N40 29' 8.8", W118 07' 38.2", see Fig. 1). This locality is believed to correspond to the M2834 locality from which Norm Silberling reported Haugi zone ammonoids (Silberling, 1969). No outcrop is visible at this locality and the sample corresponds to the matrix of a floated block full of ammonoids. The ammonoid fauna is composed of: *Neopopanoceras haugi* (Hyatt & Smith), *Keyserlingites pacificus* (Hyatt & Smith), *Subhungarites yatesi* (Hyatt & Smith) and *Pseudacrochordiceras inyoense* Smith. "*Acrochordiceras*" *inyoense* has been reassigned by Tozer (1994) to the new genus *Pseudacrochordiceras*, which clearly differs from the exclusively Anisian *Paracrochord-*

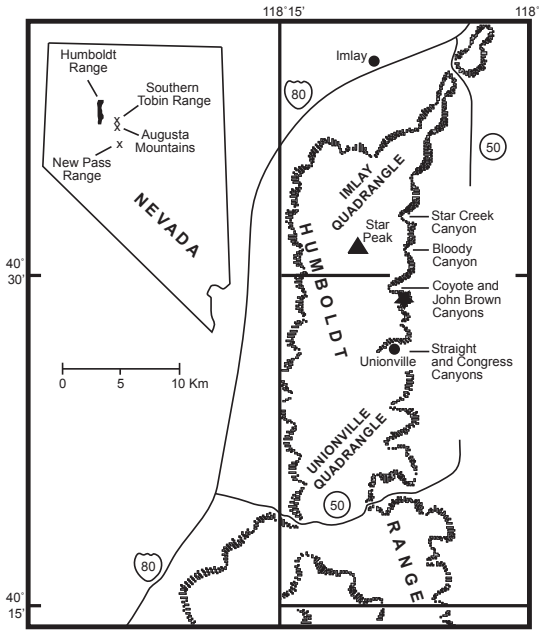

TEXT-FIG. 1. Geographical setting. The mentioned JJ7-07 locality is indicated by a star.

iceras. This association is diagnostic of the late Spathian Upper *Haugi* Zone. It is found at the top of the carbonate unit of the lower Member of the Prida Fm. (Star Peak Gr.), i.e. some 20 to 30m stratigraphically below the base of the Anisian (Fossil Hill Member, *J. welteri* beds). It is separated from the *J. welteri* beds by the Brown calcareous Sst., which is a lateral equivalent of the deltaic Dixie Valley Fm., which crops out in the eartern part of the basin (Bucher, 1989). It records the world-wide regression straddling the Lower-Middle Triassic boundary.

Material and methods

About 3 kg of rocks were dissolved in buffered acetic acid (Jeppsson *et al*., 1999). The residues were then treated for concentration by density separation using Sodium-Polytungstate (Jeppsson and Anehus, 1999). Several independent runs were processed, which invariably yielded the same results in terms of conodont faunal content: namely the presence of *Triassospathodus homeri, Neogondolella* ex. gr. *regalis*, and *Chiosella timorensis.* Indeed, as illustrated on Plates 1, 2, some *Chiosella* specimens do exhibit the distinctive *timorensis*' posterior extension of the midlateral ridge, and, following the criterion suggested by Gradinaru *et al*. (2006), are therefore referred to *C*. *timorensis*. Furthermore, as explained in part 4 of this manuscript, we no longer assign elements like *C*. *timorensis* (for a description of what this 'like' includes, see part 4) that lack the posterior extension of the midlateral ridge to *C*. *gondolelloides* but include them in *C*. *timorensis*. *C*. *gondolelloides* is also redefined and a new *Chiosella* species is described.

The preservation of the present material is moderate and the colour of the elements is dark brown.

Discussion

The above mentioned co-occurrence of *C. timorensis* with ammonoids classically regarded as late Spathian questions both the nature of *C. timorensis* as a presumed index for the O-A boundary and its presumed higher stratigraphic occurrence compared with *C. gondolelloides*, which until now lend some support to the platform gain scenario. Indeed, the best argument (Kozur, 1988; Orchard, 1995) for the separation of both *Chiosella* species using the current criterion is the apparent earlier occurrence of *C. gondolelloides* in several sections over the world, notably at the Desli Caira section in Romania, where the OAB can also be placed using the ammonoid faunal succession (Orchard *et al*., 2007a). The First Occurrence (FO) of *C. gondolelloides* is about 3 meters below the proposed OAB (sample 9038), whereas the FO of *C. timorensis* would be in sample GR7 (before reassessment, see below), which contains also the oldest Anisian ammonoids of the section. Footnote: the reader should be warned that the abrupt excursion of the carbon stable isotope curve, the apparent absence of several ammonoid associations, and the lithology (Hallstatt-type limestones)

require caution about the possible incompleteness of the record at this section..

In the Pietra dei Saracini section (Sicily) and in several sections in Turkey, the relative locations of both FOs are apparently similar as in the Desli Caira section (Gradinaru *et al*., 2006) but no published data is available yet.

At the type locality of *C. gondolelloides* in Marathovuno on Chios island, Greece (section CM II, Bender, 1968), if we trust the occurrence table (p. 488; vs. captions, see below), the FO of *C. gondolelloides* (8,5m) is about two meters below that of '*Neogondolella*' *aegea* (10,5m ; this name is now considered a junior synonym of *C. timorensis*, see Nicora, 1977 and Gradinaru *et al*., 2006). Note also that the (erroneous?) caption of two illustrated specimens of '*Neogondolella*' *aegea* (Pl. III, figs. 21, 22; caption p. 537; '*Neogondolella*' *timorensis benderi* Nicora) indicates an occurrence three meters (5,5m level) below the FO of *C. gondolelloides*. Furthermore, a later report by Asseretto *et al*. (1980), who re-examined Bender's localities, outlined problems of fissure fillings and erosion channels. They mentioned more especially the considered interval (CMII, 8.5-10m), for which their conodont faunas differ completely from those of Bender (*ibid*., 1980, p. 730, last paragraph). They could not confirm a lower occurrence of *C. gondolelloides* (CMII, 8.5m) and suggested that the corresponding report by Bender might be due to erroneous sampling.

At the much more expanded Guandao section in South China the FOs of both species are almost synchronous (same bed in Upper Guandao, only 10cm difference in Lower Guandao) (Orchard *et al*., 2007b). Unfortunately, as for the Chios section, no ammonoid data is available that would provide an independent age control. If the respective Chinese FOs are in the Welteri Zone then we may expect (if additional sampling were available) a lower FO of *C. gondolelloides* in the Chinese section (as assumed by Orchard *et al*., 2007b). Alternatively, if they are in the Haugi Zone as we show to be the case in Nevada, we will rather expect a lower FO of *C. timorensis* in Romania (if we assume that both FOs have similar relative positions globally, but of course the FO of one or both species can be diachronous on a global scale). However, it is important to note that especially at the Lower Guandao section, these first *Chiosella* occurrences are relatively rare (*Triassospathodus homeri* still predominates in the fauna). Furthermore, and in absence of any clear facies change, several beds where *Chiosella* is apparently absent (a dozen samples corresponding to 1-2 meters at the Lower Guandao section) separate these first occurrences from the interval where *Chiosella* eventually predominates. This even led Orchard and coauthors (2007b) to suggest that the OAB (defined as the FAD of *C. timorensis*) could actually be located up to three meters below the base of Upper Guandao samples (OU numbers).

What if the same applies to the Desli Caira section? In China, among the first and rare *Chiosella*, pectiniform elements assigned to *C. timorensis* represent less than 4% (2 specimens over about 60) of all *Chiosella* pectiniform elements. A similar distribution of those taxa in the lowest *Chiosella*-bearing rocks may explain the apparent absence of *C. timorensis* in those beds.

In fact *C. timorensis* is not absent from these beds: a close re-examination of the material available at the GSC in Vancouver revealed that at least one specimen (in sample 9038) exhibits the posterior extension of the midlateral rib. As in some Nevadan specimens, it is very faint, which explains why the corresponding element was previously identified as *C. gondolelloides*, but in lateral view a conspicuous bump of the posterior edge of the cusp or posteriormost denticle is clearly visible. This is similar to what is observed in the Nevadan collection, except that in the latter, the number of specimens available is much higher, which enhanced the chance of

finding at least some specimens that have a more conspicuous and hence more easily identifiable rib posteriorly. Actually the same applies also to the Upper Guandao section where again a specimen of sample OU2 can been assigned to *C. timorensis* using the platform extension criterion.

How reliable is then the evidence that the FO of *C. gondolelloides* is older than that of *C. timorensis*? And if they are contemporeaneous, how are they related to each other? Could the observed distribution of both taxa alternatively reflect intraspecific variation (*C. timorensis* as big, robust variant of *C. gondolelloides*) and/or ontogenetic trajectory (*C. timorensis* as adult, or gerontic form of *C. gondolelloides*)? In fact, if *Neogondolella* was already present in the Permian and ranges through the Lower Triassic, as it is here assumed, then the close affinity of the *Chiosella* apparatus to that of *Neogondolella* should reflect an origination of *Chiosella* from *Neogondolella* rather than from *Triassospathodus* (i.e. through platform loss in P_1 elements rather than through platform gain). In this case it is quite surprising that the presumed precursor (*C. gondolelloides*) of *C. timorensis* has even less prominent platforms/ribs.

Let us take another example of presumed platform loss in the course of Early Triassic evolution, namely the case of *Sweetospathodus kummeli*. '*Neospathodus*' *kummeli* was introduced by Sweet (1970) to designate a species whose P_1 elements are comblike, twice as long as high; with up to 16 subequal denticles; a straight or downwardly convex basal margin; and a prominent midlateral rib. Its generic reassignment to *Sweetospathodus* by Kozur, Mostler and Krainer (1998) reflects the widely accepted idea that P_1 elements like this should have evolved from neogondolellid (platform-bearing, segminiplanate) forms, presumably from *Neogondolella* and are transitional to neospathodid (*Neospathodus*-like, i.e. short segminate) forms. Sweet (1970, p. 251) describes that the midlateral rib "varies greatly in prominence from one specimen to another" and "may be produced laterally into a platform-like brim in specimens representing intermediate and late growth stages.

We consider that within known *Chiosella* populations the extension of the platform is probably an intraspecific variable character that bears no clear stratigraphic information. Separation of both taxa should rather be based on other criteria. Some relative short and high forms previously included in *C. gondolelloides* are absent from our Nevadan collection, and these deserve separation from *C. timorensis*. Due to the poor preservation of Bender's holotype, their assignment to a new species is here favoured (*Chiosella*? n. sp. B, see below).

Using our new definitions (see part 4), we reassessed the collections of the two currently best OAB sequences (Desli Caira and Guandao). The corresponding new occurrence tables are found in Fig. 2. Highlighted are the proposed association zones. The color coding enables to recognize them easily and to see how these zones or rather 'beds' are correlated from one place to the other.

The (blue) '*triangularis* beds' are defined by the local occurrence of '*Neospathodus*' *triangularis*. In our Chinese collections this species is usually restricted to the mid-upper Spathian *Prohungarites* beds. Its occurrence very close below the FO of *Chiosella* spp. suggests that it partly extends into the *Haugi* Zone in this region. A single element occurs in bed G7B at Desli Caira and it may well be an example of reworking. Nevertheless, in the Salt Range (Pakistan) Sweet (1970) reported the co-occurrence (in samples K1-50 and T63-167) of this species with *Chiosella timorensis*. Hence this informal biozone may be only local and not laterally reproducible.

The (yellow) '*carinata* beds' are characterized by the co-occurrence of *Gladigondolella carinata* with either *Chiosella timorensis* or *Chiosella* n. sp. B. It correlates with

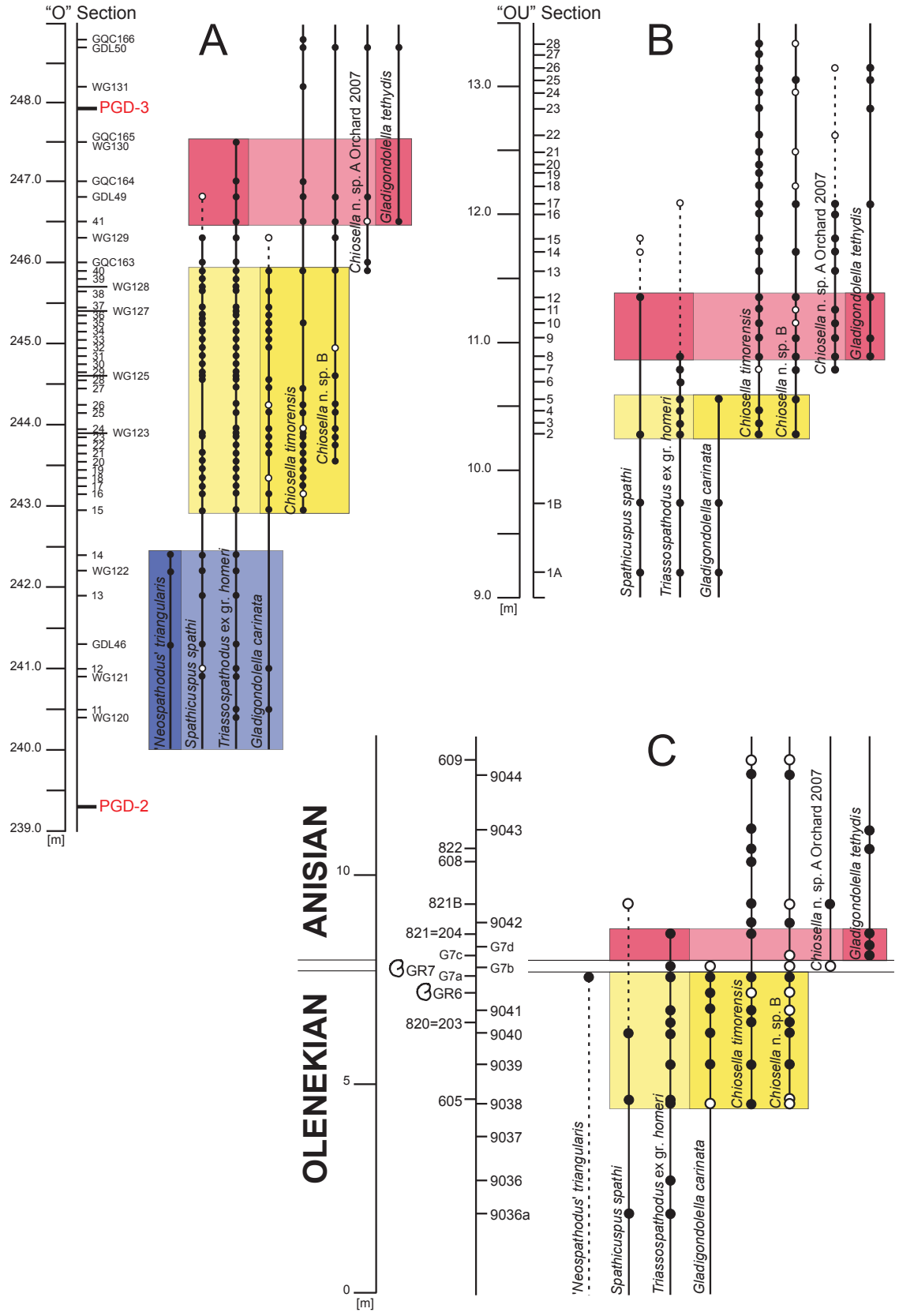

TEXT-FIG. 2. Revised distribution of conodont taxa around the OAB at both Guandao sections (A, B) and at the Desli Caira section (C). Modified after Orchard *et al*., 2007a-b. Full circle: confirmed occurrence; open circle: questionable occurrence. Note that the scale of the Lower Guandao section has been corrected to be congruent with data from Lehrmann (2007).

the late Spathian, *Haugi* Zone (upper part) and the *Stevensi* Zone (latest Spathian). It is not clear yet whether *Gl*. *carinata* extends into the (classically Anisian) *Welteri* Zone.

The (red) '*tethydis* beds' are characterized by the co-occurrence of *Gladigondolella tethydis* with either *Triassospathodus homeri* or *Spathicuspus spathi*. It correlates with the early Anisian, *Welteri* Zone (lower part).

Further work is necessary in order to assess the lateral reproducibility of these biozones. Hence, they are provisory not given the formal status of zones but are rather called 'beds'. As far as the conodonts are concerned, the OAB should preferably be located between the '*carinata'* and the '*tethydis* beds'. The corresponding uncertainty interval is about 50cm in Lower Guandao section (Text-Fig. 2).

Note that in the Lower Guandao section, the local maximal horizon corresponding to the '*carinata* beds' is sample O40, where *Gl*. *carinata* is also associated with *Ch*. n. sp. A. This association is still uncertain in Desli Caira but if it is confirmed there and in other sections in the future, it may enable to add another association zone and to refine the biochronological scheme within this critical interval.

Based on the above definition, the OAB remains bracketed by the two ash layers PGD-2 and PGD-3 at Lower Guandao section (Lehrmann *et al*., 2006, 2007) and the previous 247.2 Ma age estimate of the Early-Middle Triassic boundary given by Lehrmann *et al*. (2007) still holds. Adjustment in the boundary position yields a new slightly younger age estimate comprised between 247.16 Ma and 247.17 Ma, these two values corresponding respectively to the lower and upper bounds of the uncertainty interval within which the OAB should be located.

Finally, Gradinaru *et al*. (2006) claimed that transitional forms would document an evolutionary lineage leading from *C. timorensis* to *Ng*. ex gr. *regalis* (see also Nicora, 1977, p. 98). This putative lineage was first described by Bender and Kockel (1963) and Bender (1968), and actually led to the establishment of *Neogondolella* (see Orchard and Rieber, 1999 for a discussion). However, *Ng*. ex gr. *regalis* forms occur much lower than *Chiosella* in the Spathian (Orchard, 1994), which contradicts their derivation from *C. timorensis*. If the presumed phylogenetic relationship holds, as also reflected by their similar apparatuses, it should be interpreted as directed in the opposite way, i.e. *Chiosella timorensis* should derive from *Neogondolella* ex gr. *regalis*. Furthermore, we observe that the earliest *Chiosella* representatives appear comparatively longer and lower than later representatives (including *C*. n. sp. A sensu Orchard *et al*., 2007a-b or *C*. n. sp. B) and early juveniles of *C*. *timorensis* (for instance in sample OU3 of the Upper Guandao section) most closely resemble subcontemporaneous juveniles of *Neogondolella*, except that they miss the platform of the latter. This again is an argument in favour of the platform loss scenario contra an origin in *Triassospathodus*. Yet, pending taxonomic revision of the neogondolellids of this time interval including *Ng*. ex gr. *regalis*, the origin of *C*. *timorensis* remains unclear.

Systematic Palaeontology (Goudemand and Orchard)

Figured specimens are housed with the Paleontological Institute and Museum of the University of Zurich (numbers designated below by PIMUZ), Karl Schmid-Strasse 4, 8006 Zurich, Switzerland.

Suprageneric classification mostly follows Donoghue *et al.* (2008).

Class CONODONTA Eichenberg, 1930
Division PRIONIODONTIDA Dzik, 1976
Order OZARKODINIDA Dzik, 1976
Superfamily GONDOLELLOIDEA (Lindström, 1970)
Family GONDOLELLIDEA Lindström, 1970

Subfamily NEOGONDOLELLINAE Hirsch, 1994

Genus CHIOSELLA Kozur, 1989

Type species and holotype. *Gondolella timorensis* Nogami, 1968, pp.127-128, pl. 10, fig. 17a-c.
Type stratum and locality. Lacan, Manatuto county, Timor.

Original diagnosis and type species. Based on segminate to segminiplanate P1 elements with a very narrow or rudimentary platform developed, commonly asymmetrically, on each side of a high carina (Kozur 1988, pp. 415-416).
Multielement diagnosis. As for *Neogondolella* (see Goudemand *et al*. Chapter 1), except for the characteristic P1 element (Orchard 2005).

Chiosella? gondolelloides
Bender, 1968, Pl. 5, fig. 17; re-illustrated in Orchard, 1995, figs. 2.4, 2.5

Diagnosis. Species distinguished by relatively elongate segminate elements with a blade that in later growth stages bears a low longitudinal ridge along most of its length. The denticles are moderately fused and increasingly reclined to the posterior, where a larger, posteriorly projecting denticle is located. The lower margin of the basal cavity is elliptical in outline and is expanded beneath the posterior one-third to one-half of the element (Orchard, 1995).

Remarks. The holotype was re-illustrated and described by Orchard (1995). It is partly broken and its preservation does not allow unambiguous determination of similar elements. It was for instance compared with and said to be similar to '*Neospathodus*' *symmetricus*, except that the latter would lack a conspicuous lateral rib. However, in the type collection of '*N*'. *symmetricus* from Oman a few specimens apparently do have a lateral rib. The latter is faint and not really conspiscuous but the same applies to the holotype of *C*. *gondolelloides*. Its denticulation appears to be different but again the fact that most of the holotype's denticles are broken is not particularly helpful. For these reasons we consider that this species may include only its holotype. Previously this species included also elements that were in all aspects similar to *C*. *timorensis* but lacked the posterior extension of the midlateral rib. These are now included in *C*. *timorensis*. It included also relatively shorter and higher elements that we now assign to *C*. n. sp. B.

Chiosella timorensis
Pl. 1, figs. 1-14; Pl. 2, figs. 1-8

Remarks. Available specimens correspond to the thorough description given by Sweet (1970), except that a secondary posterior process bearing one or two denticles is not necessarily present. At all stages of growth, the cusp may or may not be terminal (note that elements with big terminal cusp have been differentiated already by Orchard: see *Chiosella* n. sp. A sensu Orchard *et al*., 2007a, b). The downward deflection of the posterior end varies also more than suggested by Sweet: in most specimens the basal margin is straight or substraight for most of the unit's length and deflected downwardly posterior of the cusp, but in some specimens (see for instance Pl. 1, fig. 7) the basal margin is curved along the whole length of the element and no distinctive deflection can be observed posterior of the cusp. These forms may deserve differentiation in the future but for now they are retained within the present taxa. This species is also rather variable in general profile, development of lateral ribs (that extend or not to the posteriormost denticle), shape, number and extent of fusion of denticles. Yet, we consider that some forms with distinctively smaller length:height ratio should be separated (see *Chiosella*? n. sp. B). We illustrate also two presumably teratological specimens of *C*. cf. *timorensis* on Pl. 2, figs. 4 and 7.

Chiosella n. sp. B

2005 *Chiosella*? sp. A, Orchard, Text-Fig. 12, part A.
2006 *C. gondolelloides*, Gradinaru *et al*., Pl. 1, figs. 8-12.
2007a *C. gondolelloides*, Orchard *et al*., Fig. 5, parts 13-15, 23-25.
2007b *C. gondolelloides*, Orchard *et al*., Fig. 6, parts 25-29.

Description. Segminate elements with moderate length:height ratio (2.5-2.7:1), about 9 to 12 gradually more reclined to the posterior, and relatively broad denticles whose free tips are subequilaterally triangular in shape. The height is maximal on the third or fourth denticle from the posterior end and decreases slowly in both directions from there. The cusp is the broadest denticle. One or two smaller denticles stand behind the cusp, the terminal one being conspicuously less broad than the adjacent ones.
Remarks. Compared with *C*. *timorensis*, which it most closely resembles, this species is relatively shorter and higher and it has less numerous and broader denticles of distinctive triangular shape.

Genus NEOGONDOLELLA Bender and Stoppel, 1965

1989 *Clarkina* Kozur, pp. 428-429.

Type species and holotype. *Gondolella mombergensis* Tatge, 1956, p.132, pl. 6, fig. 2a-c.
Type stratum and locality. Upper Muschelkalk, Schmidtdiel Quarry, Momberg, near Marburg.

Original diagnosis and type species. Bender and Stoppel introduced *Neogondolella* for segminiplanate P1 elements with strong, partly fused carina of variable height ending in a (sub)terminal cusp. These elements were previously included in *Gondolella* Stauffer and Plummer.

Multielement diagnosis. As described by Orchard (2005) or Orchard and Rieber (1999), except that the dolobrate element is now considered to be in the S1 position and the S2 position is occupied by the 'enantiognathiform' breviform digyrate element (see Goudemand *et al*., Chapter 1). A thorough discussion can be found in Orchard and Rieber (1999).

Neogondolella ex. gr. *regalis*
Pl. 2, figs. 9, 11-14

Diagnosis. P1 elements of *Ng. regale* have a platform extending full length of the unit and a prominent carina of mostly fused, nearly subequal denticles (Mosher, 1970).

Remarks. Mosher (1970) included Spathian forms within the range of this species. Nicora (1977) noted however that older specimens (from the *Subrobustus* Zone) differ substantially by having a large, flat platform and a lower carina, and should be referred to another species. This was also the opinion of Orchard (1994) who considered that these forms are only superficially similar to the type species. Hence their assignment to *Ng*. ex gr. *regalis*, pending revision of the neogondolellids of this interval. The herein illustrated specimens strongly resemble *Neogondolella* elements illustrated by Orchard *et al*. and occurring around the OAB at Guandao and Desli Caira respectively (Orchard *et al*., 2007a, b). They also closely resemble much older (early Spathian) ***Neogondolella*** elements that occur in our collections from Darwin canyon, California (Goudemand *et al*., in prep.).

Neogondolella n. sp. A
Pl. 2, fig. 10

Diagnosis. This (juvenile) element has a platform, which is broadest at about one-third of the unit from the anterior end and tapers gradually at both ends. Anteriorly the platform is conspicuously serrated and the corresponding carinal denticles are laterally expanded in a manner that recalls those of *Icriospathodus collinsoni*. The terminal cusp is very big and markedly separated from the moderately high denticles of the anterior process. In lateral view the unit is strongly arched.

Remarks. This species is based on a single specimen. Hence it is kept in open nomenclature.

Acknowledgements
This research is supported by the Swiss NSF project 200020-113554 (to HB).
We thank Julia Huber and Leonie Pauli, who dissolved and concentrated the samples; and Peter Krauss (GSC, Vancouver), who took some of the SEM photographs. Prof. Hans Thierstein (ETH, Zurich) is acknowledged for granting access to his lab's SEM. Sandra Hermann (ETH, Zurich) is warmly thanked for her help with the SEM.

References

Assereto, R., V. Jacobshagen, G. Kauffmann, AND A. Nicora. 1980. The Scythian/Anisian Boundary in Chios, Greece. Rivista Italiana di Paleontologia, 85(3-4):715-736.

Bachmann, G. H., AND H. W. Kozur. 2004. The Germanic Triassic: correlations with the international scale, numerical ages and Milankovitch cyclicity. Hallesches Jahrbuch für Geowissenschaften, Reihe B, 26:17-62.

Bender, H. 1968. Zur Gliederung der Mediterranen Trias II. Die Conodontenchronologie der Mediterranen Trias. Annales Géologiques des Pays Hélléniques, 19:465-540.

Bender, H., AND C. W. Kockel. 1963. Die Conodonten der Griechischen Trias. Annales Géologiques des Pays Hélléniques, 1(14):436-445.

Bender, H., AND D. Stoppel. 1965. Perm-Conodonten. Geologisches Jahrbuch, 82:331-364.

Bucher, H. 1989. Lower Anisian Ammonoids from the Northern Humboldt Range (northwestern Nevada, USA) and their bearing upon the Lower-Middle Triassic boundary. Eclogae Geologicae Helvetiae, 82(3):945-1002.

Donoghue, P. C. J., M. A. Purnell, R. J. Aldridge, AND S. Zhang. 2008. The interrelationships of ‹complex› conodonts (Vertebrata). Journal of Systematic Palaeontology, 6(2):119-153.

Dzik, J. 1976. Remarks on the evolution of Ordovician conodonts. Acta Palaeontologica Polonica, 21:395-455.

Eichenberg, W. 1930. Conodonten aus dem Culm des Harzes. Palaeontol. Zeitschr., 12:177-182.

Gradinaru, E., H. W. Kozur, A. Nicora, AND M. J. Orchard. 2006. The *Chiosella timorensis* lineage and correlation of the ammonoids and conodonts around the base of the Anisian in the GGSP candidate at Desli Caira (North Dobrogea, Romania). Albertiana, 34:34-38.

Hirsch, F. 1994. Triassic conodonts as ecological and eustatic sensors, p. 949-959, Pangea: Global Environments and Resources.Volume Memoir 17. Canadian Society of Petroleum Geologists.

Hyatt, A., AND J. P. Smith. 1905. The Triassic cephalopod genera of North America. U.S. Geological Survey - Professional Paper, 40:1-394.

Jeppsson, L., AND R. Anehus. 1999. A New Technique to Separate Conodont Elements from Heavier Minerals. Alcheringa, 23:57-62.

Jeppsson, L., R. Anehus, AND D. Fredholm. 1999. The Optimal Acetate Buffered Acetic Acid Technique for Extracting Phosphatic Fossils. Journal of Paleontology, 73(5):964-972.

Kozur, H. 1988. The Taxonomy of the Gondolellids Conodonts in the Permian and Triassic. 1st International Senckenberg Conference and 5th European Conodont Symposium (ECOS V): Contributions III, Papers on Ordovician to Triassic Conodonts, 117:409-469.

Kozur, H., H. Mostler, AND K. Krainer. 1998. *Sweetospathodus* n. gen. and *Triassospathodus* n. gen., Two Important Lower Triassic Conodont Genera. Geologia Croatica, 51(1):1-5.

Lehrmann, D. J., J. Ramezani, S. A. Bowring, M. W. Martin, P. Montgomery, P. Enos, J. L. Payne, M. J. Orchard, H. Wang, And J. Wei. 2006. Timing of recovery from the end-Permian extinction: Geochronologic and biostratigraphic constraints from south China. Geology, 34(12):1053-1056.

Lehrmann, D. J., J. Ramezani, S. A. Bowring, M. W. Martin, P. Montgomery, P. Enos, J. L. Payne, M. J. Orchard, H. Wang, And J. Wei. 2007. Timing of recovery from the end-Permian extinction: Geochronologic and biostratigraphic constraints from south China: Reply. Geology, 35:e136-e137.

Mosher, L. C. 1970. New Conodonts Species as Triassic Guide Fossils. Journal of Paleontology, 44:737-742.

Nicora, A. 1977. Lower Anisian Platform Conodonts from the Tethys and Nevada, Taxonomic and Stratigraphic Revision. Palaeontographica Abt. A, 157:88-107.

Nogami, Y. 1968. Trias-Conodonten von Timor, Malaysien und Japan (Paleontological Study of Portuguese Timor, 5). Memoirs of the Faculty of Science, Kyoto University, Series of Geology and Mineralogy, XXXIV(2):115-136.

Orchard, M. J. 1994. Conodont Biochronology Around the Early-Middle Triassic Boundary: New Data from North America, Oman and Timor. Proc. of the Triassic Symposium, Lausanne, Switzerland (1992), 22:105-114.

Orchard, M. J. 1995. Taxonomy and Correlation of Lower Triassic (Spathian) Segminate Conodonts from Oman and Revision of Some Species of Neospathodus. Journal of Paleontology, 69(1):110-122.

Orchard, M. J., E. Gradinaru, AND A. Nicora. 2007a. A summary of the conodont succession around the Olenekian-Anisian boundary at Desli Caira, North Dobrogea, Romania. The Global Triassic, Albuquerque, New Mexico, 41:341-346.

Orchard, M. J., D. J. Lehrmann, J. Wei, H. Wang, AND H. J. Taylor. 2007b. Conodonts from the Olenekian-Anisian boundary beds, Guandao, Guizhou Province, China. The Global Triassic, Albuquerque, New Mexico, 41:347-354.

Orchard, M. J., AND H. Rieber. 1999. Multielement *Neogondolella* (Conodonta, upper Permian - middle Triassic). Bolletino della Società Paleontologica Italiana, 37(2-3):475-488.

Silberling, N. J., AND R. E. Wallace. 1969. Stratigraphy of the Star Peak Group (Triassic) and overlying Lower Mesozoic rocks, Humboldt Range, Nevada. Prof. Pap. U.S. geol. Surv., 592.

Smith. 1914. The Middle Triassic marine invertebrate faunas of North America. Washington DC Department of the Interior, U. S. Geological Survey Professional Paper, 83:1-254.

Sweet, W. C. 1970. Uppermost Permian and Lower Triassic Conodonts of the Salt Range and Trans-Indus Ranges, West Pakistan, p. 207-275. *In* B. Kummel and C. Teichert (eds.), Stratigraphic Boundary Problems: Permian and Triassic of West Pakistan.Volume Special Publication 4. The University Press of Kansas.

Tatge, U. 1956. Conodonten aus dem germanishen Muschelkalk. Paläontologisches Zeitschrift, 30(1/2):108-127.

Tozer, E. T. 1994. Significance of Triassic stage boundaries defined in North America. Mémoires de Géologie (Lausanne), 22:155-170.

PLATE 1.

Figs 1-14. *Chiosella timorensis*, PIMUZ XXXX1-14. Aboral and lateral views.

All from sample JJ7-07, Nevada. Spathian. All ×80.

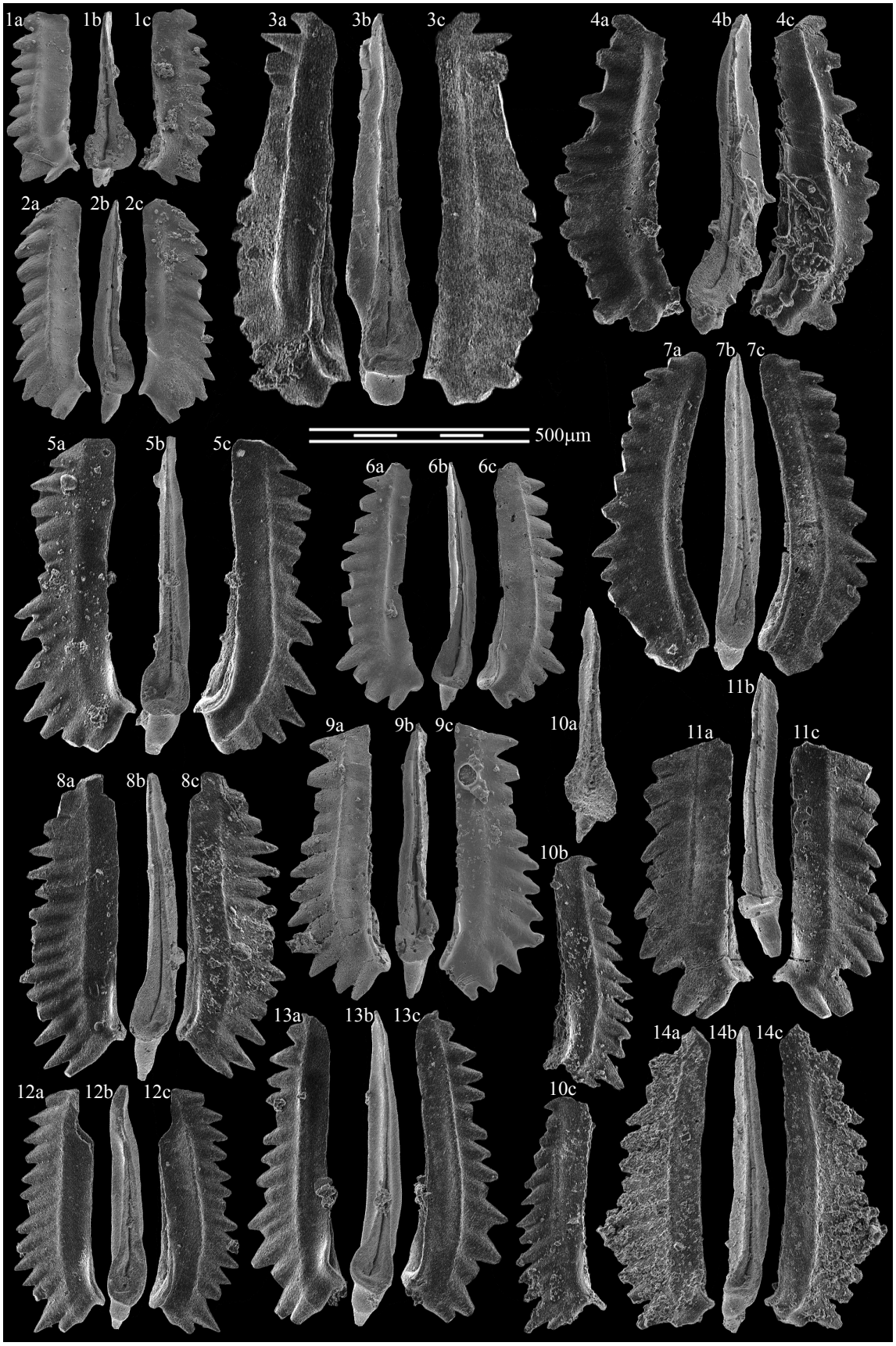
1a
1b
1c
3a
3b
3c
4a
4b
4c
2a
2b
2c
7a
7b
7c
500µm
5a
5b
5c
6a
6b
6c
11b
9a
9b
9c
10a
11a
11c
8a
8b
8c
10b
13a
13b
13c
14a
14b
14c
12a
12b
12c
10c

PLATE 1

PLATE 2.

Figs 1-8. *Chiosella timorensis*, PIMUZ XXXX15-23. Aboral and lateral views.
Figs 9, 11-14. *Neogondolella* ex. gr. *regalis*, PIMUZ XXXX24, 26-29. Aboral, oral and lateral views.
Figs 10. *Neogondolella* sp. indet., PIMUZ XXXX25. Aboral, oral and lateral views.

All from sample JJ7-07, Nevada. Spathian. All ×80.

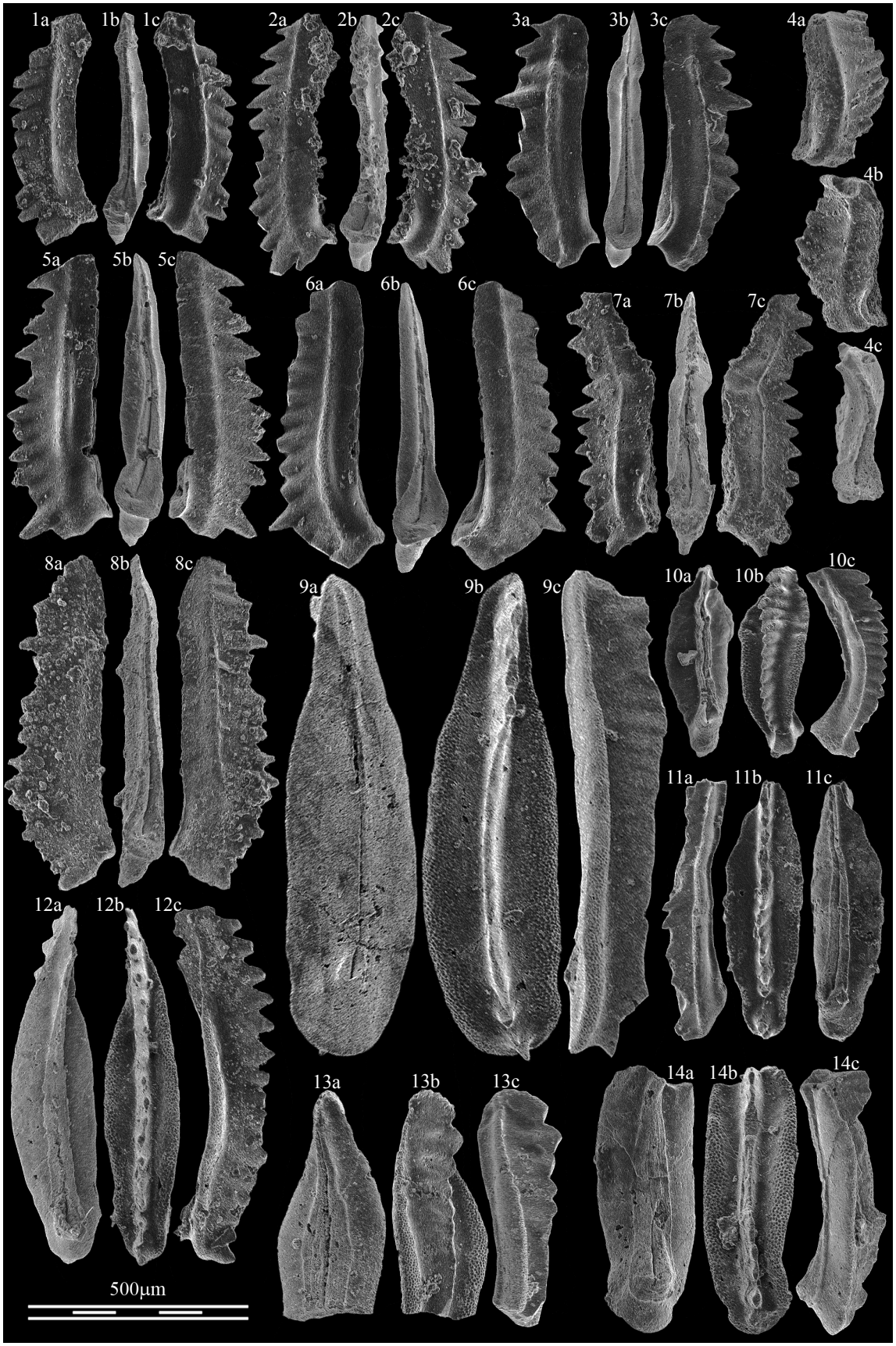
1a
1b
1c
2a
2b
2c
3a
3b
3c
4a
4b
4c
5a
5b
5c
6a
6b
6c
7a
7b
7c
8a
8b
8c
9a
9b
9c
10a
10b
10c
11a
11b
11c
12a
12b
12c
13a
13b
13c
14a
14b
14c
500µm

PLATE 2

The first step in wisdom is to know the things themselves; this notion consists in having the true idea of the objects; objects are distinguished and known by their methodical classification and appropriate naming; therefore Classification and Naming will be the Foundation of our Science.

Linnaeus (1735), quoted in Stevens (1994:201)

CHAPTER 4

Stevens, P. F. 1994. The Development of Biological Systematics: Antoine-Laurent de Jussieu, Nature and the Natural System. New York, Columbia University Press.

New Early Triassic conodont faunas from the Dienerian/Smithian boundary beds at Mud (Himashal Pradesh, India)

N. Goudemand[1], M. J. Orchard[2], L. Krystyn[3], T. Brühwiler[1], D. Ware[1], H. Bucher[1]

[1]Paläontologisches Institut und Museum der Universität Zürich, Karl Schmid-Strasse 4, CH-8006 Zürich, Switzerland.
[2]Geological Survey of Canada, 101-605 Robson St., Vancouver, BC, V6B 5J3 Canada.
[3]Institut für Paläontologie-Geozentrum, A-1090 Wien, Althanstrasse 14, Austria.

Based on new collections at the Induan/Olenekian boundary GSSP candidate at Mud (Himashal Pradesh, Northern India) we describe new, well preserved conodont faunas. We also revise many taxa of this time interval including the important *Neospathodus* ex gr. *dieneri*, *Ns*. ex gr. *cristagalli*, *Novispathodus* ex gr. *pakistanensis* and *Nv*. ex gr. *waageni*, for which we differentiate numerous new morphotypes. This leads us to a new, better resolved biozonation of this section around the proposed GSSP level. In ascending order the new biostratigraphical sequence comprises: the *Nv*. aff. *waageni* 1 beds, the *Borinella* beds, the *Eurygnathodus costatus* beds, the *Discretella* beds and the *Neospathodus spitiensis* beds. Based on revised determinations of the material from Chaohu (another GSSP candidate section), we show that both sequences agree very well, which suggests a good lateral reproducibility of this zonation at least at the Tethyan scale. The faunas from Bed 10, located about 1 meter below the proposed GSSP level have a typical Smithian affinity and it seems preferable to set the IOB just below this level, in congruence with the ammonoid boundary. Many new taxa are described, including several new species (left in open nomenclature).

Key words: Early Triassic, Dienerian/Smithian boundary, Induan/Olenekian boundary, GSSP, conodonts.

The End-Permian mass extinction was the most severe metazoan crisis of Earth history. Detailed recovery patterns of Early Triassic marine fauna in time and space can only be retrieved by using a global biostratigraphic scheme based on those organisms with the highest recovery rates (i.e. ammonoids and conodonts; Brayard *et al*., 2006, 2009; Orchard, 2007). In this respect, a clear and adequate definition of the stage subdivisions of the Early Triassic is needed. Yet, these subdivisions remain controversial. A two-stage scheme (Induan and Olenekian - Kiparisova and Popov, 1956; the Induan encompasses the Griesbachian and the Dienerian, the Olenekian comprises the Smithian and the Spathian; Tozer, 1965; Tozer, 1967; Silberling and Tozer, 1968) has been approved as the standard stage subdivision by the Triassic Subcommission of the International Stratigraphic Commission (Visscher, 1992). The Tethyan-defined Induan and the Boreal-defined Olenekian have resulted in persistent contradictions in the correlations of Early Triassic zonations across paleolatitudes. A Tethyan section near the village

of Mud in the Himalayas (Lahul and Spiti district, Himachal Pradesh, Northern India) may potentially solve this issue: ammonoid and conodont faunas show partial affinity with the Boreal realm (e.g., the occurrence of the conodont *Borinella nepalensis*). Furthermore, ammonoids from this somewhat classical locality have been reported already more than 100 years ago (Diener, 1897; Krafft and Diener, 1909), and conodonts are abundant and well preserved too (Krystyn *et al*., 2007a, b; Orchard, 2007b; Orchard and Krystyn, 2007). This partially explains that this section has been recently selected as the best Global Stratotype Section and Point (GSSP) candidate for the Induan/Olenekian boundary (Krystyn *et al*., 2007a, b). The First Appearance Datum (FAD) of the conodont species *Novispathodus waageni* sensu lato at the base of subbed 13A3 (within the lower part of the *Flemingites* beds) has been suggested as a good index for the Induan/Olenekian boundary (IOB).

However, ammonoids and conodont faunas from the beds underlying the proposed GSSP level were only insufficiently known. These beds were sampled thoroughly for ammonoids during a field trip in 2008 and several new and well preserved ammonoid faunas were discovered. These new ammonoid faunas are the topic of a separate paper (Brühwiler *et al*., in press). Here, we focus on the stratigraphic distribution and the taxonomic description of new conodont faunas associated with these ammonoids. Several conodont elements of typical Smithian affinity were found in a relatively low stratigraphical position compared to the previously proposed GSSP.

We then compare these faunas from Mud with those from its rival GSSP candidate, i.e. the West Pingdingshan section in Chaohu (Anhui Province, China; Tong *et al*., 2003, 2004).

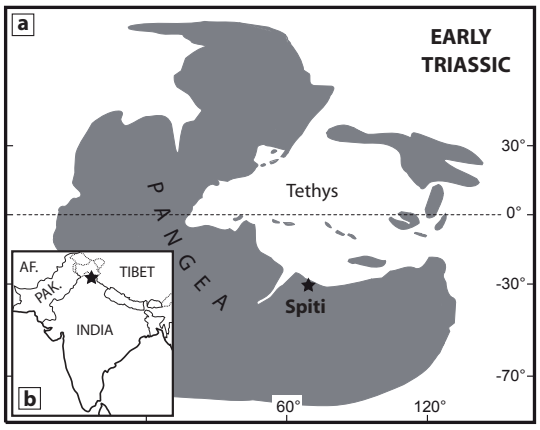

Fig. 1. (a) Simplified Early Triassic palaeogeography (modified after Brayard *et al*., 2006) and position of the Northern Indian Margin (NIM). (b) Present-day location of the Induan/Olenekian GSSP candidate Mud, in Himachal Pradesh, Northern India (see Krystyn *et al*. 2007a for a detailed description).

Geological setting

During Early Triassic times the Spiti area was located on the peri-Gondwanan margin, on the southern side of the Tethys Ocean (e.g. Smith *et al*., 1994) (Fig. 1). The Kuling Shales of Late Permian (Dzulfian) age are disconformably overlain by the Lower Triassic Mikin Formation (Bucher *et al*., 1997). The described faunas are from the Limestone and Shale Member (LSM) of the Mikin Formation (see Fig. 2). The LSM is subdivided into three parts: the Dienerian *Ambites* Beds (equivalent to the *Meekoceras* Beds of Krafft and Diener, 1909 and the *Gyronites* Beds of Bhargava *et al*., 2004) consisting of dark shales with intercalated limestone beds and nodules; the early Smithian *Flemingites* Beds, consisting of grey, slightly nodular limestone; and the middle-late Smithian *Parahedenstroemia* Beds, consisting of alternating shales and limestone beds.

New conodont faunas

Figure 3 gives the detailed conodont stratigraphic distributions within the critical interval at Mud. The bed numbers are those of Krystyn *et al*. (2007a, b). Some of these

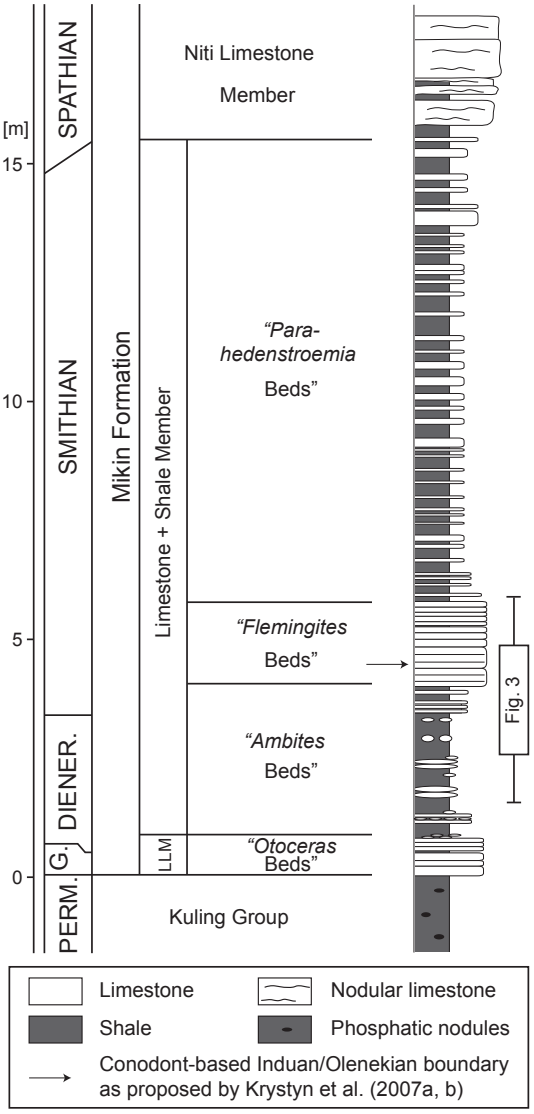

Fig. 2. Stratigraphic section of the Lower Triassic at Mud with indication of the detailed section in Fig. 3 (modified after Bhargava *et al*., 2004). PERM.= Permian; G.= Griesbachian; DIENER.= Dienerian; L.L.M.= Lower Limestone Member. The "*Ambites* beds" correspond to the "*Gyronites* beds" of Krystyn *et al*. (2007a, b) and to the "*Meekoceras* beds" of Krafft and Diener (1909); these beds need to be renamed here because they do not yield *Gyronites* nor *Meekoceras* but do contain abundant representatives of *Ambites* (Brühwiler *et al*., in press).

beds were subdivided in subbeds. The M0X-prefixes correspond to the different Mud sections (*ibid*), between which the different beds can be easily traced laterally. Additional samples (Mudxx numbers) were recently collected during intense and detailed ammonoid sampling (Brühwiler *et al*., in press).

The most striking difference with previous reports from Mud is the huge number of conodont taxa occurring in this interval, in particular in bed 10. This is principally due to the intentional splitting of the most important taxa (*Ns*. *dieneri*, *Ns*. *cristagalli*, *Nv*. *waageni* and *Nv*. *pakistanensis*) in numerous new morphotypes (see below) but also to the subdivision of bed 10 in three subbeds and the recognition that the middle part (samples Mud10 and Mud33) was much richer in conodonts (higher abundance, higher diversity and better preservation) than the previously sampled lowest part.

In particular this bed contains a relative abundant fauna of finely denticulated P1 and P2 elements that we consider to be the first representatives of the *Novispathodus* genus. Some of these forms are known from Chaohu and were assigned by Zhao *et al*. (2007, 2008) to '*Neospathodus*' *waageni eowaageni* and '*Neospathodus*' *posterolongatus* respectively. They are here temporarily termed *Novispathodus* aff. *waageni* (morphotype 1) and *Nv*. aff. *pakistanensis* (morphotype 5) and will be formally described in another paper dealing with our material from Waili, Guangxi, South China, where beautifully preserved specimens were recovered (Goudemand *et al*., Chapter 5).

Discussion

Based on figure 3, (confirmed occurrences only), we recognize four, possibly five local maximal horizons (Guex, 1991). Sample M03-16 (M. H. 5?) is a local maximal horizon relative to underlying samples, but without data above this level, it is not possible to assess whether it is also maximal relative to overlying samples. Strictly speaking there are more local maximal horizons (see for instance, bed 14C) but some are due to artificially truncated ranges (in the case of bed 14C, we actually know that *Spathicuspus* and *Discretella* occur further above bed 16) or based on single occurrences of

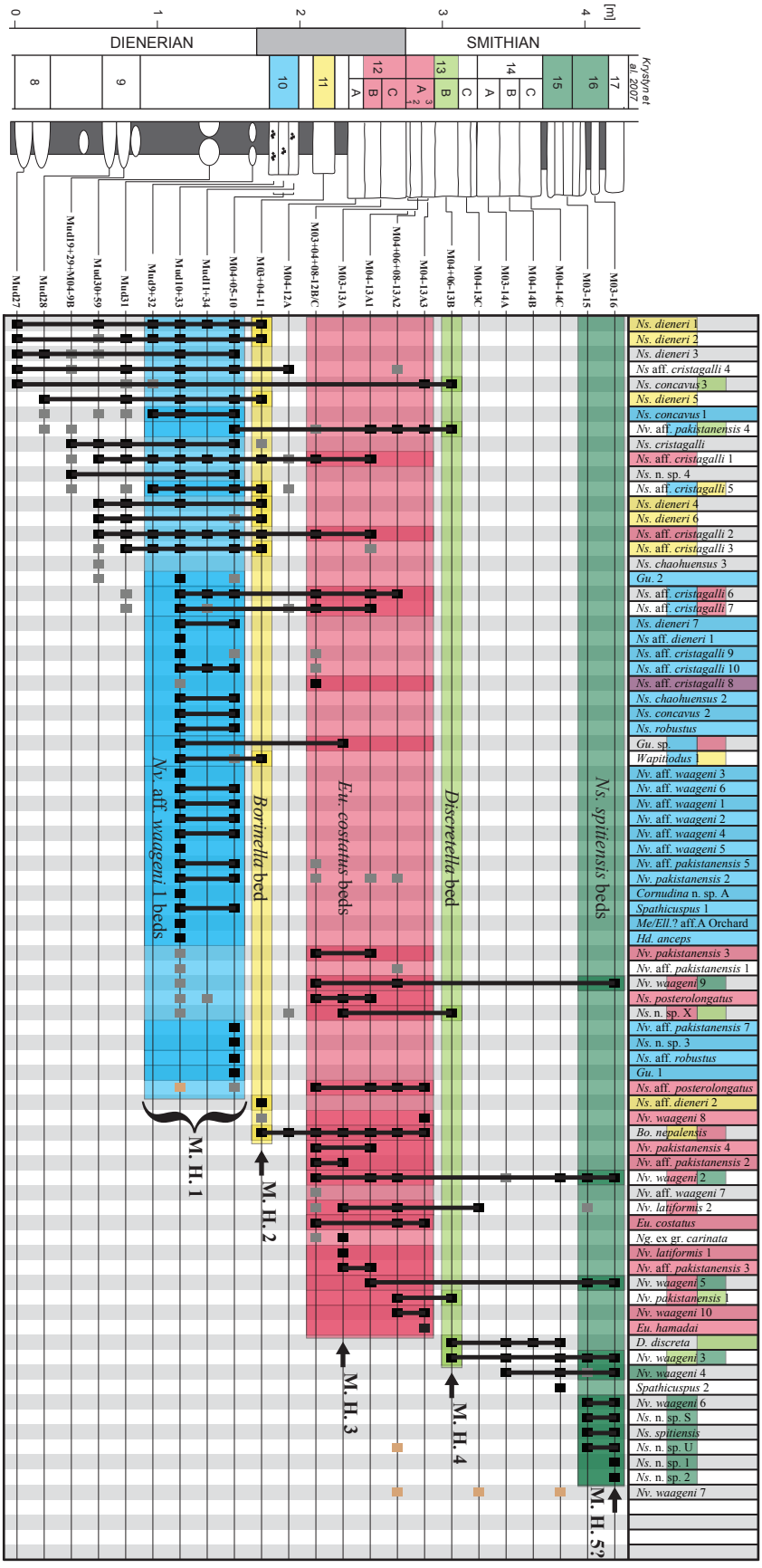
[m]
DIENERIAN
SMITHIAN
Krystyn et al. 2007
Mud27
Mud28
Mud19+29+M04-9B
Mud30+59
Mud31
Mud9+32
Mud10+33
Mud11+34
M04-05-10
M03+04-11
M04-12A
M03+04+08-12B/C
M03-13A
M04-13A1
M04+06+08-13A2
M04-13A3
M04+06-13B
M04-13C
M03-14A
M04-14B
M04-14C
M03-15
M03-16
Ns. dieneri 1
Ns. dieneri 2
Ns. dieneri 3
Ns aff. cristagalli 4
Ns. concavus 3
Ns. dieneri 5
Ns. concavus 1
Nv. aff. pakistanensis 4
Ns. cristagalli
Ns. aff. cristagalli 1
Ns. n. sp. 4
Ns. aff. cristagalli 5
Ns. dieneri 4
Ns. dieneri 6
Ns. aff. cristagalli 2
Ns. aff. cristagalli 3
Ns. chaohuensus 3
Gu. 2
Ns. aff. cristagalli 6
Ns. aff. cristagalli 7
Ns. dieneri 7
Ns aff. dieneri 1
Ns. aff. cristagalli 9
Ns. aff. cristagalli 10
Ns. aff. cristagalli 8
Ns. chaohuensus 2
Ns. concavus 2
Ns. robustus
Gu. sp.
Wapitiodus 1
Nv. aff. waageni 3
Nv. aff. waageni 6
Nv. aff. waageni 1
Nv. aff. waageni 2
Nv. aff. waageni 4
Nv. aff. waageni 5
Nv. aff. pakistanensis 5
Nv. pakistanensis 2
Cornudina n. sp. A
Spathicuspus 1
Me/Ell.? aff.A Orchard
Hd. anceps
Nv. pakistanensis 3
Nv. aff. pakistanensis 1
Nv. waageni 9
Ns. posterolongatus
Ns. n. sp. X
Nv. aff. pakistanensis 7
Ns. n. sp. 3
Ns. aff. robustus
Gu. 1
Ns. aff. posterolongatus
Ns. aff. dieneri 2
Nv. waageni 8
Bo. nepalensis
Nv. pakistanensis 4
Nv. aff. pakistanensis 2
Nv. waageni 2
Nv. aff. waageni 7
Nv. latiformis 2
Eu. costatus
Ng. ex gr. carinata
Nv. latiformis 1
Nv. aff. pakistanensis 3
Nv. waageni 5
Nv. pakistanensis 1
Nv. waageni 10
Eu. hamadai
D. discreta
Nv. waageni 3
Nv. waageni 4
Spathicuspus 2
Nv. waageni 6
Ns. n. sp. S
Ns. spitiensis
Ns. n. sp. U
Ns. n. sp. 1
Ns. n. sp. 2
Nv. waageni 7
Nv. aff. waageni 1 beds
Borinella bed
Eu. costatus beds
Discretella bed
Ns. spitiensis beds
M. H. 1
M. H. 2
M. H. 3
M. H. 4
M. H. 5?

rare forms whose range is still too poorly constrained. An informal biozone can be associated with each of these local maximal horizons. These are color coded in figure 3. Pending thorough assessment of their lateral reproducibility in various basins (ongoing work), these biozones are not introduced as formal zones and are here termed 'beds' instead. They are association zones separated by interval of uncertainty, and each one is characterized by the exclusive occurrence of species and/or pairs of species. These species or pairs of species are their characteristic elements: they make it possible to identify the association zone in stratigraphic sections, or inversely, to assign the species content of a bed to a specific Zone. Instead of listing here the (numerous) characteristic elements of each biozone, we refer again the reader to figure 3, where the latter are displayed in a new, color-coded way: in the upper row, if a particular form is a characteristic element of an association (both FO and LO are within the biozone), its cell is completely filled with the corresponding color; if it is part of one or several characteristic element(s) or pair(s) (its FO OR its LO is within the biozone and only its association with a matching form, whose LO resp. FO is also within the same biozone, is considered a characteristic element of this zone) then only half of its cell (the lower part if its LO is within the association zone, for example) is filled with the corresponding color and potential 'pairing' species are found by looking for species whose cell is half filled with the same color but on the opposite side (the upper part in our example; which means its FO is within the biozone). For instance the *Borinella* bed is characterized by the co-occurrence of *Bo*. *nepalensis* with either *Ns*. *dieneri* (morphotypes 1, 2, 4, 5, or 6) or *Ns*. aff. *cristagalli* 3. Note that since a species can be part of characteristic elements in up to two biozones, some cells appear subdivided in two and the same as above applies then to each subdivision.

Both the *Novispathodus* aff. *waageni* 1 beds and the *Eurygnathodus costatus* beds are recognized also in Chaohu, where they roughly correspond to the two successive *Neospathodus waageni eowaageni* and *Neospathodus waageni waageni* subzones (Zhao *et al*., 2007). In Mud, the *Borinella* beds intercalates between these two biozones. Furthermore, in our view '*Neospathodus*' *waageni eowaageni*, here termed *Nv*. *waageni* 3 is different from *Nv*. aff. *waageni* 1 (see below) and it occurs much higher than the latter (from bed 26 in at the West Pingdingshan section), above the *Eu*.*costatus* beds. In Mud, it occurs also above the *Eu*.*costatus* beds, from bed 13B on, and it partly characterizes both the *Discretella* beds and the *Ns*. *spitiensis* beds. A similar faunal succession (*Nv*. aff. *waageni* 1, *Bo*. cf. *nepalensis*, *Eu*. *costatus*, *Nv*. *waageni* 3) is known also from Waili, Guangxi (Goudemand *et al*., Chapter 5). Not only the IOB interval of the Mud section correlates very well with those of China, but as much as it can be inferred from the published material from Chaohu, it is also better in terms of biochronological resolution than the West Pingdingshan section.

In Mud, bed 10 records the first occurrences of the *Wapitiodus*, *Guangxidella, Cornudina* and *Spathicuspus*? genera, which until now are known only from Smithian or younger strata. Moreover, it records the first occurrence of high-bladed P2 elements that we consider to be associated with the similarly denticulated P1 elements assigned here to *Novispathodus* aff. *waageni* 1-5 and *Nv*. aff. *pakistanensis* 5. New reconstructions from nearly monospecific samples demonstrate that at least some forms currently assigned

Fig. 3. Detailed stratigraphic section of the Dienerian/Smithian boundary at Mud with the distribution of conodont taxa and indicated local maximal horizons. Black rectangles indicate confirmed occurrences, gray (50%) rectangles indicate occurrences based on fragmentary or poorly preserved material, light brown rectangles indicate occurrences of new, undescribed forms that have affinity with the corresponding taxa.

to '*Ns*.' *waageni* and '*Ns*.' *pakistanensis* had a *Novispathodus* apparatus (erected by Orchard, 2005; revised by Goudemand *et al*., Chapter 1). This lends strong support to a close affinity between the latter forms and the widely distributed *Nv*. *waageni*, whose FAD has been proposed as a global index for the definition of the IOB. Hence, in our view, the IOB is below bed 10 in Mud and these new forms are potentially good indexes for the boundary (be they considered as variants of a *Nv*. *waageni* sensu lato or as separate species).

Unfortunately, the current conodont data from Mud (the same remark applies to Chaohu) does not allow recognizing a local maximal horizon below bed 10 that would consist of typically Dienerian faunas. Hence using only conodonts it is not possible to give a lower bound for the location of the IOB. Indeed, the explosive radiation of conodonts during this critical time interval occurs without significant faunal turnover and proceeds essentially by addition of new taxa.

Yet, in contrast with Chaohu, we can use Mud's abundant and well-preserved ammonoids to reliably constrain the uncertainty interval within which the IOB should be set. As is the case for conodonts (see above), ammonoids with typical Smithian affinity (Flemingitidae, Kashmiritidae) first occur in bed 10 at Mud (Brühwiler *et al*., in press), which confirms the validity of this upper bound for the location of the boundary. Based on ammonoids, several local maximal horizons are recognized below bed 10, the highest being located in a thin, lenticular limestone horizon about 10cm below bed 10. The co-occurrence of *Prionolobus rotundatus*, *Clypites typicus* and *Kingites korni* clearly suggests a latest Dienerian age. Hence this horizon can be considered as a lower bound for the IOB, which is consequently bracketed by this level (Mud17, Mud31) and bed 10, within a 10cm-thick interval.

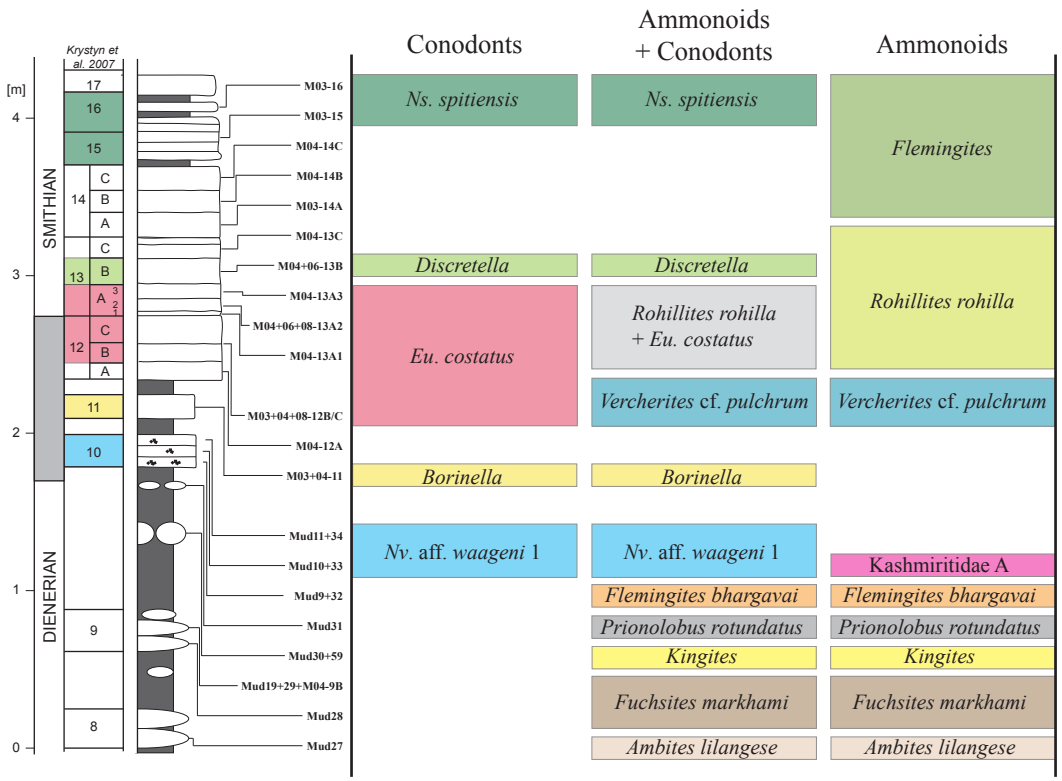

Fig. 4. Detailed stratigraphic section of the Dienerian/Smithian boundary at Mud with the proposed conodont, ammonoid and integrated conodont/ammonoid biozonation schemes. The local ammonoid biozonation is from Brühwiler *et al*., 2010.

Finally, note that the biochronological resolution that can be achieved using conodont data is about the same as that attained with ammonoids (it is in both cases equal to 4 biozones from bed 10 to and including bed 13). More interestingly, if we combine both data (see Fig. 4) we end up with 11 (!) local zones within the considered 4m interval.

Conclusions

Based on new collections, several new conodont faunas have been found at the Induan-Olenekian Boundary near the village of Mud (Himashal Pradesh, Himalaya, India). Additionally many important taxa of this interval have been revised and their variation documented in details. These new data enables to recognize five association zones, which are in very good agreement with the IOB sequence in Chaohu, South China. Not only Mud's conodont sequence can be recognized across the Tethys, but its biochronologic resolution is higher than in Chaohu (absence of the *Borinella* beds). As for ammonoids, the conodont faunas of Bed 10 of Krystyn *et al*., 2007 have an early Smithian affinity. The combination of both conodont and ammonoid datasets allows to constrain the IOB within 10cm below this level and to construct an informal biozonation scheme comprising 11 association zones for the considered 4m interval.

Systematic palaeontology

Preliminary remarks.
The morphology of S and M elements is considered to be more conservative than that of P elements, especially of the P_1 element. Hence, differentiation at the generic and suprageneric levels is usually based on characters of the S and M elements (absence/presence of processes, location of secondary processes, etc…) and is closely tied to reconstructions of the multi-element apparatuses (see for instance Orchard, 2005). Yet, such reconstructions require high quality data, which is unavailable in most cases. Consequently, and this is particularly true for the material from the Early Triassic where multi-element data is relatively sparse, generic assignment is prone to revisions. Pending multi-element reconstructions, many of the taxa discussed below are based on the morphology of the P_1 element only and their generic assignment is made with reservation.
Most of the P_1 elements described here are blade-like elements, whose mode of growth has been studied in details by Donoghue (1997, p. 649): maximal growth is in posterior and anterior directions, essentially through marginal addition of new denticles. Compared to the corresponding adult forms, the juvenile specimens are smaller, have a smaller length/height ratio, less developed platforms or transverse ribs and their denticles are less fused. Usually the P_1 elements of juvenile conodonts cannot be determined because some of the diagnostic characters develop only in adult forms and several different species may have very similar P_1 elements in juvenile stages. Whenever it was possible, growth series were reconstructed. Otherwise, determinations were based on relative large, presumably adult specimens and comparisons were made between elements of similar size.

Suprageneric classification mostly follows Donoghue *et al.* (2008).

Class CONODONTA Eichenberg, 1930
Division PRIONIODONTIDA Dzik, 1976
Order OZARKODINIDA Dzik, 1976
Superfamily GONDOLELLOIDEA (Lindström, 1970)
Family GONDOLELLIDEA Lindström, 1970

Subfamily CORNUDININAE Orchard, 2005

Genus CORNUDINA Hirschmann, 1959

Type species and holotype. *Ozarkodina breviramulis* Tatge, 1956, p. 139, pl. 5, fig. 12a-b.
Type stratum and locality. Lower Muschelkalk, Kalkwerk Quarry, Trubenhausen, Germany.

Original diagnosis and type species. Based on a small angulate P2 element with a large and prominent medial cusp and very short upturned processes (Hirschmann, 1959, p. 44).

Multielement diagnosis. We follow here the interpretation of *Cornudina* by Orchard (2005), where the P1 element has a long cusp, at least twice the length of the adjacent denticles, a very short anterior process, and a broadly excavated basal cavity (Orchard 2005).

***Cornudina* n. sp. A** – Pl. 1.

Included here are forms with a broadly excavated basal cavity, a very short or absent anterior process and a very large (about four times longer than the basal cavity) and strongly reclined cusp. The cusp is strongly recurved to the posterior at its base and then substraight and makes an angle of about 20-30 degrees with the line of the basal margin.
This species will be fully described in a future paper based on better preserved material from northwestern Guangxi, where it commonly occurs in the Smithian *Owenites* beds. Note already that the occurrence of such forms in the early Smithian considerably enlarges the known stratigraphic range of the genus, as it was previously thought to originate in the Spathian (Orchard, 2005). Several specimens of this species were found by Zhao in Smithian strata at Chaohu (unpublished illustrations) but they were misinterpreted as *Aduncodina unicosta*, a Spathian related form in which the posterior processes are much more developed.

Genus SPATHICUSPUS Orchard, 2005

Type species and holotype. *Neospathodus spathi* Sweet, 1970, pp. 257-258, pl. 1, fig. 5.
Type stratum and locality. Mittiwali Member, Mianwali Formation, Narmia, Salt Range, Pakistan.

Original diagnosis and type species. The type species is a segminate P1 element in which the posteriorly located cusp is large but not markedly higher than the denticles of the anterior process.
Multielement diagnosis. see Orchard 2005.

***Spathicuspus* spp.** – Pl. 3.

Included here are forms of various lengths that have a large terminal cusp that is strongly reclined to the posterior. Those from a deeper stratigraphic level (morphotype 1, Pl. 3, figs. 9, 10) are small and have 5-6 recurved denticles (the cusp is unfortunately broken in both specimens), whereas those from a higher level (morphotype 2, Pl. 3, figs. 6, 7) are longer with 8-9 denticles. The latter closely resemble *N*. n. sp. R Orchard (2008) from the Smithian (Tardus Zone) of the Canadian Arctic, but the basal cavity is not as large and the cusp is here (sub)terminal. The generic assignment arises from multielement consideration of Spathian examples (Orchard, 2005) but these Smithian examples may not have the same apparatus.

Subfamily MULLERINAE Orchard, 2005

Genus DISCRETELLA Orchard, 2005

Type species and holotype. *Ctenognathodus discreta* Müller, 1956, pp. 821-822, pl. 95, fig. 28.
Type stratum and locality. Smithian ammonoid bed, Crittenden Springs, Elko Co., Nevada.

Original diagnosis and type species. The type species is a carminate P1 element in which the basal margin is upturned and inverted in the posterior one-third to one-half of the element. The cusp is usually larger than other discrete and upright denticles but not conspicuously (Orchard, 2005).
Multielement diagnosis. see Orchard 2005.

***Discretella discreta* (Müller) 1956** – Pl. 5

These elements have markedly discrete denticles and a large cusp. The generic assignment arises from multielement reconstructions in larger populations (Orchard, 2005).

Genus GUANGXIDELLA Zhang and Yang, 1991

Type species and holotype. *Guangxidella typica* Zhang and Yang, 1991, pp. 35-37.
Type stratum and locality. Lower Triassic Luolou Formation, *N. waageni* Zone, Zuodeng (Tsoteng),Tiandong County, Guangxi, Province, South China.

Original diagnosis and type species. Zhang and Yang (1991, pp. 33-36) introduced the genus as a seximembrate apparatus, whose P1 element is segminate, anteriorly bent, with distinct midlateral ribs which disappear posteriorly (Zhang and Yang, 1991), but it was later reinterpreted as septimembrate by Orchard (2005).

***Guangxidella* n. sp. 1** - Pl. 3, figs. 3, 8.

2007 *Neospathodus chii* – Orchard and Krystyn, 2007, Pl. 1, figs. 1, 2.

The original diagnosis of *Neospathodus chii* Zhao and Orchard (2007) refers to a short segminate element with a broad, deep and oval basal cavity and a terminal cusp, which is "conspicuously higher, thinner and flatter than the other denticles" and whose "cross-section forms a narrow ellipse" (Zhao *et al*., 2007). This Spiti specimen differs in having a cusp whose cross-section is subcircular or slightly expanded to the anterior and it is not necessarily related to *N. chii*. The posterior edge of the cusp is substraight and the anterior edge is elbowed at midheight, just above the apices of the rather small denticles anterior to it. Above that, the anterior edge is straight or slightly concave. This peculiar shape of the cusp is shared by several forms belonging to the present genus, including the holotype of *Gu*. *bransoni* (Müller, 1956), with which this element shares also the posterior extension of the basal cavity (see Pl. 3, fig. 3). The present element is neither markedly arched nor laterally bowed (*Gu*. *bransoni*) and its basal cavity is neither heart-shaped (*Gu*. *bicuspidata*) nor strongly asymmetrical (*Gu*. *bransoni*), but the presence of this distinctive cusp suggests that it should be referred to *Guangxidella*.

***Guangxidella* n. sp. 2** - Pl. 3, fig. 1.

The P1 element has a big, terminal cusp, a downarched anterior process, and a rounded basal cavity with a shallow pit. The cusp is largely inflated at its base. A flange is developed laterally. A similar, better preserved element was found by Orchard (unpublished material) in early-mid Smithian (Romunderi Zone) collections from North America.
Unlike *Gu*. *typica* Zhang and Yang (1991), which more closely resemble '*Neoprioniodus*' *bicuspidatus* Müller (1956) (see also Orchard and Zonneveld, 2009, p. 780) in having the denticle directly anterior to the cusp about as high as the cusp and either standing very close to (Müller, 1956, Pl. 95, fig. 15; Zhang and Yang, 1991, Pl. 1, figs. 2a, b) or being even fused with the cusp (Müller, 1956, Pl. 95, figs. 16, 17; Zhang and Yang, 1991, Pl. 1, figs. 1a, b), the large, terminal cusp of this element was probably much higher than the denticles to the anterior. Its base is also conspicuously inflated and the basal cavity beneath it differs in being subcircular rather than heart-shaped. Note however that the latter character may be associated with intraspecific variation of the midlateral thickening: similar elements occurring in our collections from South China (Goudemand *et al*., Chapter 5) show a similar pattern where the basal cavity is generally heart-shaped and becomes subcircular in variants whose midlateral rib extends posteriorly (in which case the cusp is markedly inflated at its base). *Gu*. *bransoni* is conspicuously bowed laterally and its basal cavity extends posteriorly and is asymmetrical.

***Guangxidella* sp.** – Pl. 3, fig. 4.

This element has a very large cusp that is oriented perpendicular to the base, and a rounded basal cavity. Orchard (2009, p. 780) observed that elements sharing these features were associated with *Gu*. *bicuspidata* (Müller, 1956) in topotype material from Nevada and suggested that such elements should be assigned to *Guangxidella*.

Genus WAPITIODUS Orchard, 2005.

Type species and holotype. *Wapitiodus robustus* Orchard, 2005, pp. 98-99, Text-fig. 24.
Type stratum and locality. Sulphur Mountain Formation, AD Ridge, Wapiti Lake, British Columbia, Canada.

Original diagnosis and type species. see Orchard 2005.

***Wapitiodus* n. sp. 1** – Pl. 3, fig. 2.
This element has a large, terminal cusp that is slightly reclined to the posterior. Denticles of the anterior process are finer but may be as long as the cusp. They are discrete and suberect. The subcircular basal cavity is large, flat and shallow. A furrow extends posteriorly. This element occurs in association with smaller, but similar elements (see Pl. 3, figs. 11, 15), which closely resemble juveniles of *Wapitiodus robustus* Orchard (2005) as illustrated by Orchard and Zonneveld (2009, fig. 14.28). This suggests a relationship between both species and leads us to assign this element to the present genus.

Subfamily NEOGONDOLELLINAE Hirsch, 1994

Genus NEOGONDOLELLA Bender and Stoppel, 1965

1989 *Clarkina* Kozur, pp. 428-429.

Type species and holotype. *Gondolella mombergensis* Tatge, 1956, p.132, pl. 6, fig. 2a-c.
Type stratum and locality. Upper Muschelkalk, Schmidtdiel Quarry, Momberg, near Marburg.

Original diagnosis and type species. Bender and Stoppel introduced *Neogondolella* for segminiplanate P1 elements with strong, partly fused carina of variable height ending in a (sub)terminal cusp. These elements were previously included in *Gondolella* Stauffer and Plummer.
Multielement diagnosis. As described by Orchard (2005) or Orchard and Rieber (1999), except that the dolobrate element is now considered to be in the S1 position and the S2 position is occupied by the 'enantiognathiform' breviform digyrate element (see Goudemand *et al*., Chapter 1). Synonymies are thoroughly discussed in Orchard and Rieber (1999).

***Neogondolella* ex gr. *carinata* (Clark)** 1959 – Pl. 6, figs. 6, 10.

Elements of this species were asssumed to have become extinct in the Griesbachian (hence "*Clarkina*"), but it extends into the Smithian in several regions.

Genus NEOSPATHODUS Mosher, 1968

Type species and holotype. *Spathognathodus cristagalli* Huckriede, 1958, pp. 161-162, pl. 10, fig. 15.
Type stratum and locality. Lower 'Ceratitenschichten', Mittiwali near Chhidru, Salt Range, Pakistan.

Original diagnosis and type species. The type species is a segminate P1 element with a width: height:length ratio of 1:3:4, a posterior lower margin that is upturned beneath the posterior one-third of the element, and a short-terminal cusp (Mosher, 1968, pp. 929-930).
Multielement diagnosis. As described by Orchard (2005), except that the elements previously identified as occupying the S_1 and S_2 positions occupy in fact the S_2 and S_1 positions respectively. Note that, as defined by Orchard, the S3 element would have a more posteriorly located bifurcation of the anterior process than in *Neogondolella*.

Remarks. Based on strong similarities in their respective apparatuses, this genus is thought to have evolved from *Neogondolella* during the Induan. Segminate P1 elements of this time interval are typically assigned to species of *Neospathodus*. New, unpublished material suggests that their multi-element apparatuses rather belong to several, distinct genera. Pending reconstruction of these apparatuses and subsequent taxonomic revision of their generic assignment, the following taxa are provisory included in this genus and the specific determination is based solely on the morphology of the P1 element.

***Neospathodus chaohuensis* Zhao & Orchard 2007**- Pl. 2, figs. 7, 8.

The original diagnosis referred to short segminate elements with a length/height ratio of ~1:1.4, and 5-8 variably discrete, erect to slightly reclined, pointed to apically rounded denticles. Denticles are subequal in width and length, the basal margin is straight anteriorly and upwardly deflected in the posterior part, the basal cavity is broadly expanded and rounded.
Specimens from Spiti differ in having invariably upright denticles. The angle between anterior and posterior parts of the basal margin is less conspicuous (about 20 degrees) and the basal cavity is compressed antero-posteriorly and hence has a flattened heart- or eight-shape. These elements are almost perfect homeomorphs of unpublished earliest Spathian segminate elements occurring at least in the western US and temporarily assigned to *Novispathodus* aff. *brevissimus* (Goudemand *et al*., in prep.).

***Neospathodus concavus* Zhao & Orchard 2007**- Pl. 2, fig. 1.

2007 *Neospathodus concavus* – Orchard and Krystyn, 2007, Pl. 1, fig. 4.
2007 *Neospathodus concavus* n. sp. Zhao and Orchard, Pl. 1, figs. 1A-C.

The original diagnosis referred to relatively large and long segminate elements with a length/height [not length/width] ratio of ~1.9-2.6:1, and about 9-10 denticles, the sixth denticle from the posterior end being large and conspicuous and similar in size to that of the cusp. Also, the basal margin is slightly or conspicuously concave below the anterior four-fifths of the blade; the basal

cavity is rounded with a shallow medium pit.
Spiti specimens correspond to the Chinese types in their lower profile and basal configuration, but the denticulation is variable. Several large denticles occur in the mid blade of a large specimen (Pl. 2, fig. 1). The concavity of the lower profile is also much more pronounced in this specimen than in type *concavus*. This however has been observed also in other taxa (for instance in *Chiosella timorensis*, Goudemand *et al*., Chapter 3; see also Pl. 4, fig. 2) and does not necessarily imply that these forms should be separated from the type species. Specimens here referred as *Ns*. cf. *concavus* have apparently more uniform denticles, even if the sixth denticle is usually broken. The lower profile is also judged to be less diagnostic than previously assumed: several very different pectiniform elements may have a concave lower profile (see for instance, Pl. 4, fig. 2; P. 7, fig. 8; or Pl. 13, fig. 15). Some specimens seem to have a faint heart-shaped configuration posteriorly just above the basal cavity. This configuration is (Pl. 2, figs. 5, 6) or is not (Pl. 2, fig. 4) reflected in the shape of the basal cavity (deflection of the posterior lip). Specimens like Pl. 2, fig. 4, which apparently correspond to 'Ns'. n. sp. K Zhao (PhD2005, Pl. 11, figs. 7, 8), a variant of *Ns. concavus*, resemble also *N*. n. sp. Q Orchard and Zonneveld (2009) but in the latter the lower margin is entirely concave, and it is not clear yet whether these forms are included within the intraspecific variation of the present species.

***Neospathodus cristagalli* (Huckriede) 1958** – Pl. 7, figs. 1, 2.

1958 *Spathognathodus cristagalli* n. sp. Huckriede, Pl. 10, fig. 15.

Elements typically combined in this species have a broad, triangular terminal cusp that is often separated from the anterior denticles. The cusp is markedly shorter than the denticles to the anterior and its posterior edge is shallowly concave except for a small incipient denticle developed at its base. The basal cavity is elongate-oval, with a pit and anterior furrow lying beneath and anterior of the anterior edge of the cusp. In lateral view, the lower margin is weakly to moderately upturned beneath the posterior one-quarter to one-third of the element.
It has been already recognized that this definition includes many different forms that may actually deserve assignment to separate species. Yet, until now they remained undistinguished, hence the recent usage of the ex gr. abbreviation for this taxon (Orchard, 2007). We here tentatively distinguish different morphotypes of *N*. ex gr. *cristagalli*. Pending detailed study of type material from the Salt Range (Pakistan), morphotypes thought to differ from the holotype are kept in open nomenclature and subsequently named *N*. aff. *cristagalli* morph 1-9 (see below).
Among the illustrated specimens with a *cristagalli* affinity (Pl. 7, 8), the one on Pl. 7, fig. 2 most closely resembles the holotype (Huckriede, 1958, Pl. 10, fig. 15) and best fits the original description of the species (*op. cit*., pp. 161, 162). The lower margin is concave ("the proximal, aboral edge with the expansion above the basal pit, is highly bent in oral direction"; translated from the German, *ibid*.), the cusp is "strikingly more obtuse angled than the other denticles", and the basal cavity is inverted ("over the proximally located basal cavity, the keel divides into two narrow, laterally upturned lobes"; translated from the German, *ibid*.).
The very shape of the subpyramidal cusp varies greatly within the population and specimens like the one figured on Pl. 7, fig. 1 are here retained in *N. cristagalli*. The basal cavity is invariably inverted, elongate and pointed posteriorly. The overall shape is rather elongate with a length/height ratio of ~1.7-1.9:1.

***Neospathodus* aff. *cristagalli* (Huckriede) 1958** - Pl. 7, 8.

The following morphotypes correspond to the most frequently encountered forms. Note however that intermediate forms may occur.

morphotype 1 – Pl. 7, fig. 3.

The length/height ratio of this morphotypes is distinctly smaller (~1.35-1.5:1). In all other respects it is very similar to type *cristagalli*. The inverted and elongate basal cavity may appear either pointed or rounded posteriorly. This morphotype is somehow intermediate between *N. cristagalli* and *N*. aff. *cristagalli* morphotype 2 (see below).

morphotype 2 – Pl. 7, figs. 6-13,15; Pl. 8, fig. 2.

1970 *Neospathodus cristagalli* n. sp., Sweet, Pl. 1, figs. 14, 15.
2005 *Neospathodus* cf. *cristagalli* - Orchard, Text-fig. 14, p. 89.

The overall shape of this rather short morphotype (length/height ratio: ~1.2-1.4:1) is close to that of *morphotype 1* but the basal cavity occupies only one-third to half of the length of the element, is oval, posteriorly rounded and only partly inverted. As Sweet observed (1970, p. 248; he was discussing the morphology of *N. cristagalli*), the 'typical *cristagalli*' basal cavity is morphologically complex, being "convex downward in transverse profile, and downwardly sigmoidal in longitudinal profile". Though there is some variation depending on the degree of 'inversion' of the basal cavity, this holds for most or all *cristagalli*-related forms. The denticles are erect to slightly reclined posteriorly (Pl. 7, figs. 10, 11), and more importantly they are laterally flattened and sharp-edged (biconvex in cross-section). This latter character is again common to all forms within the *cristagalli* group. Together with the nature of the basal cavity they constitute the main criteria for differentiating this group from the *dieneri* one (see below). The cusp is markedly shorter and usually broader than the denticles to the anterior but it tends to be more slender than in *N. cristagalli* and it is usually not conspicuously separated from the anterior denticles.

morphotype 3 – Pl. 7, figs. 4, 5.

1981 *Neospathodus srivastavai* - Chhabra and Sahni, Pl. 1, fig. 30.

This morphotype is similar to morphotype 2 but the denticles are almost fully discrete and the posterior edge of the first denticle anterior to the cusp is slightly concave at its base. Subsequently the cusp is strikingly separated from the anterior denticles. The overall shape is highly reminiscent of *N. tongi*, its pendant within the *dieneri* group. Though the holotype of *N. srivastavai* Chhabra and Sahni (1981) might be better included in *N. spitiensis* Goel (1977), its paratype (fig. 30) may fall within this taxa.

morphotype 4 – Pl. 7, fig. 14; Pl. 8, figs. 1, 12.

This morphotype looks like a high length/height ratio version of *morphotype 2* with reclined posterior part: it shares with the latter a complex ('cristagallid') basal cavity, mostly fused, laterally flattened, sharp-edged denticles and an undifferentiated cusp. Besides the higher length/height ratio (~1.5-1.6:1), the posterior denticles (cusp inclusive) are clearly reclined to the posterior and the posterior upturning of the lower margin is here either missing or much less marked. As a consequence the apex of the cusp is located as or more posteriorly than the posteriormost edge of the basal cavity. In overall shape, the element looks (yet only superficially) like *Nv. pakistanensis* Sweet (see discussion below).

morphotype 5 – Pl. 8, figs. 3, 4.

The length-height ratio is the same as for *morphotype 4* (~1.5-1.6:1) with which it shares most characters. It differs in having a rather long and inverted basal cavity that more closely resembles that of *N. cristagalli* (as described above) and in having a fan-shaped denticulation: posterior denticles are reclined posteriorly and anterior denticles are either erect or slightly inclined anteriorly; the cusp is not differentiated (i.e. looks similar to other denticles to the anterior); the lateral profile is arcuate with maximal height at about one third or more from the posterior. Except for the inverted basal cavity this morphotype closely resembles *Nv. posterolongatus* Zhao and Orchard with which it may be related.

morphotype 6 – Pl. 8, figs. 5, 10.

This morphotype corresponds to an elongated *morphotype 2* (or a rather upright *morphotype 4*) by which the incipient denticle at the posterior base of the cusp would have developed significantly into a denticle bud. This form is intermediate towards *morphotype 7*, by which the denticle is small but fully grown.

morphotype 7 – Pl. 8, figs. 9, 11.

As *morphotype 6* but the denticle bud is replaced by a small but 'real' denticle, beneath which the basal cavity extends posteriorly in a manner reminiscent of *N. spitiensis* Goel, to which it may be related (see below). Again in common with or similar to *N. spitiensis* note the presence on the aboral side of a narrow furrow beneath the posteriormost denticle. This furrow is separated from the basal pit and is observed only in the narrowly pointed posterior part of the basal cavity. Except for its basal cavity, which is distinctly different, the shorter and higher specimen with radiating denticles that is figured here on Pl. 8, fig. 9 strongly recalls some morphotypes of *Nv. waageni* (Sweet).

morphotype 8 – Zhao *et al*., 2007, Pl. 1, figs. 11A-C.

This morphotype is a *morphotype 2*, by which the incipient denticle at the posterior base of the cusp would have developed into a small but 'real' denticle. This form is consequently very close to *morphotype 6* or *morphotype 7* but its length /height ratio is smaller (~1.2:1). Zhao and Orchard distinguished three morphotypes of *N*. *dieneri*, based on the height of the cusp relative to the first denticle anterior of it. In our view, their illustred specimen of *N*. *dieneri* morphotype 3 in Zhao *et al*., 2007, Pl. 1, figs. 11A-C does not belong to the *dieneri* group but is instead a good representative of our *N*. aff. *cristagalli* morphotype 8. Its complex ('cristagallid') basal cavity and its laterally flattened, sharp-edged denticles are typical of the *cristagalli* group not of the *dieneri* one (see below). Yet, we agree with Zhao *et al*. (2008) that *Novispathodus waageni* may find its origin in these forms. Indeed very similar specimens from the Sulphur Mountain Formation (Wapiti Lake, BC, Canada), yet with more upright und more fused denticles, were assigned to *Nv*. *waageni* by Orchard and Zonneveld (2009, figs. 13.9-10).

morphotype 9 – Pl. 8, fig. 7; Pl. 10, fig. 1.

This morphotype is similar to *morphotype 8* but its denticles are more fused, and more importantly its basal cavity is fully inverted. In this respect it resembles more closely *morphotype 1*, except for the additional posterior denticle and a markedly more upturned posterior lower margin.

morphotype 10 – Pl. 8, fig. 8.

This morphotype has a substraight lower margin, including a flat (but 'cristagallid') basal cavity and subequally broad, erect denticles. The upper margin is similar to that of *morphotype 4* or *Nv*. *pakistanensis*, but the posterior denticles are not reclined. This element also closely resembles elements like that illustrated in Pl. 11, fig. 12, which may be assigned to *Nv*. *waageni* morphotype 9, but from which it differs in having a larger length/ height ratio (~1.55:1), and a flat, rhomboid basal cavity.

Remarks – In best preserved specimens, we observe that except for the anterior- and posteriormost denticles, the posterior edge of the denticles is substraight whereas the anterior edge is composed of two straight segments making an angle of 10 to 20 degrees. Such bladed P1 elements operated in a pair and were used to cut food (Purnell and Von Bitter, 1992). In our view the more reclined upper part of the anterior edge is the cutting part of the denticle. Further study is necessary to check whether microwear patterns are found exclusively on those segments, but these elements probably functioned as serrated scissors: in lateral view, several consecutive cutting planes either intersect in the same focal point, that we interpret as a virtual hinge around which the elements are rotated, or are subparallel, suggesting that the corresponding denticles cut the food at different points but synchronously (Goudemand *et al*., in prep.).

***Neospathodus dieneri* Sweet 1970** – Pl. 4.

The P1 element is a relatively short (length/ height ratio is about 1-1.2:1) segminate element. Typically, the outer margin of the circular basal cavity is somewhat swollen and the rather discrete denticles are rounded in cross-section.
As for *N*. *cristagalli*, *N*.*dieneri* has been often used almost as a generic name for very numerous morphologies that may actually deserve the status of separate species. The first attempt at differentiating this group is indeed quite recent: based on the relative size of the terminal cusp (or posteriormost denticle) to those to its anterior, Zhao & Orchard (in Zhao *et al*., 2007) distinguished three morphotypes. Based on the Spiti material, we here introduce several new morphotypes. Note that additional morphotypes are recognized in our Chinese material from the Guangxi province (Goudemand *et al*., Chapter 5).

morphotype 1 – Zhao *et al*., 2007, Pl. 1, figs. 12A-B.

This morphotype corresponds to the morphotype 1 Zhao and Orchard but it is here restricted to elements like the one they illustrated (*op. cit*.). In our view, the sole character based on a cusp larger than the denticles anterior of it is not sufficient: in our material from Guangxi, several different forms would fit this diagnosis.

morphotype 2 – Zhao *et al*., 2007, Pl. 1, figs. 9A-C.

This morphotype corresponds to the morphotype 2 Zhao and Orchard but for the same reason as for *morphotype 1* it is here restricted to elements like the one they illustrated (*op. cit*.). In particular, elements with erect and more fused denticles and a straight posterior margin of the cusp (Pl. 4, fig. 8, *morphotype 6*) as well as elements which are markedly more elongate (Pl. 4, fig. 9, *morphotype 5*) are considered distinct.

morphotype 3 –Pl. 4, figs. 12, 13.

1970 *Neospathodus dieneri* n.sp., Sweet, Pl. 1, figs. 1, 4.

This morphotype corresponds to the description of the morphotype 3 Zhao and Orchard but in our view Sweet's holotype of the species better corresponds to the pendant of *morphotypes 1* and *2* with a posteriormost denticle smaller than those to the anterior. The element figured by Zhao *et al*. as *N*. *dieneri* morphotype 3 (2007, Pl. 1, figs. 11A-C) is here regarded as belonging to the *cristagalli* group (*N*. aff. *cristagalli* morphotype 8, see above).

morphotype 4 –Pl. 4, fig. 19.

Unlike *morphotype 2*, which is otherwise very similar, its lower margin is conspicuously convex in lateral view and its denticles tend to be more erect and the basal cavity broader.

morphotype 5 –Pl. 4, fig. 9.

This morphotype corresponds to a high length/height ratio (~1.6:1) *morphotype 2* with more fused denticles. Note that similar elements with conspicuous lateral thickening and posteriorly downcurved lower margin were assigned by Trammer to *Neospathodus svalbardensis* (in Birkenmaier and Trammer, 1975, Pl. 2, fig. 1). He considered variants with more erect denticles (*ibid*, Pl. 2, figs. 2, 4) as conspecific (see also remark 1).

morphotype 6 –Pl. 4, fig. 8.

Close to *morphotype 2*, this morphotype has erect, straight denticles (those of *morphotype 2* are usually reclined and recurved to the posterior) and the posterior margin of the cusp misses the conspicuous concavity, which is common to *morphotypes 1-5*.

morphotype 7 –Pl. 4, fig. 18.

This morphotype is very close to *morphotype 3* but its denticles are less recurved posteriorly and as in *morphotype 6* the posterior margin of the relative small cusp is not concave but straight. It is also very similar to *Nv*. aff. *waageni* morphotype 1 to which it may be related, but the latter has laterally flattened, more erect and more fused denticles.

Neospathodus aff. *dieneri* Sweet 1970

morphotype 1 –Pl. 3, fig. 14.

The overall shape of this element is similar to that of *N*. *dieneri* (morphotype 1 or 2) but the morphology of the basal cavity, whose posterior margin is deflected downwards, is significantly different. In aboral view the subcircular basal cavity appears consequently flattened posteriorly.

morphotype 2 –Pl. 3, fig. 18.

Unlike *N*. *dieneri*, the posteriorly reclined cusp of this element is markedly separated from the erect denticles of the anterior process.

Neospathodus posterolongatus Zhao & Orchard 2007 – Pl. 10, fig. 9.

2007 *Neospathodus posterolongatus* n. sp. Zhao and Orchard, Pl. 1, figs. 2A-C.
2008 *Neospathodus posterolongatus*, Zhao *et al*., Pl. 1, fig. 10a.
2009 *Neospathodus posterolongatus* – Orchard and Zonneveld, fig. 14, parts 16, 17.

A rather elongate, rectangular, segminate element with a length/height ratio ranging from 1.3-1.6:1. The greatest height is located at element midlength or in the posterior part. In lateral view, the basal margin is straight to slightly concave anteriorly, with slightly upturned margins in the posterior one-third to one-fourth of the unit. Consequently, the lower margin may appear conspicuously convex beneath the anterior part of the basal cavity, especially in rather short specimens (Zhao *et al*, 2008, Pl. 1, fig. 10a). A short secondary posterior process is developed posteriorly beneath which the relatively elliptical basal cavity extends. The quite numerous (~15)

denticles are subequally narrow in lateral width, straight, orally pointed and fused for about half of their length. The upper margin is arcuate. In specimens where the denticles are less reclined posteriorly (*ibid*.), the basal cavity appears relatively shorter and rounded posteriorly and the element closely resembles *Novispathodus waageni* (Sweet) to which it may be related. Apparently, the higher the length/height ratio, the more elongate the basal cavity. In elements like the holotype (length/height ratio ~1.4:1), the basal cavity is not more elongate than in *Nv*. *pakistanensis* (compare with Sweet, 1970, Pl. 1, figs. 16, 17, and with the typical *Nv*. *pakistanensis* element figured in Orchard and Zonneveld, 2009, fig. 13, parts 20, 21). Hence this criterion can not be used to separate both species as it was previously suggested. In *Nv*. *pakistanensis* the size of the posterior denticles diminishes more abruptly and the highest point is located more posteriorly than in *N*. *posterolongatus*, and the lower margin is also distinctly different. *N*. *spitiensis* has a more posteriorly extended basal cavity, which occupies about half the length of the element, and often a more upturned posterior part. *N*. *posterolongatus* also closely resembles *N*. aff. *cristagalli* morphotype 5 with its fan-shaped denticulation, but the latter differs in having a larger and inverted basal cavity.

***Neospathodus* aff. *posterolongatus* Zhao & Orchard 2007** – Pl. 11, fig. 14.

2009 *Neospathodus posterolongatus* – Orchard and Zonneveld, fig. 14, parts 21, 22.
1988 *Kashmirella albertii* n. sp. Budurov, Sudar and Gupta, figs. 1g, h, j.

Elements similar to large *N*. *posterolongatus* with a higher length/height ratio (*ibid*; ~1.7:1), but whose basal cavity is posteriorly pointed and whose longest denticles are not straight but rather recurved posteriorly, are here included in *N*. aff. *posterolongatus*. As observed on Pl. 11, fig. 14 they may develop a lateral platform flange like that of *Neospathodus novaehollandiea* McTavish (1973; see *Nv*. *pakistanensis*) or that of *Nv*. *latiformis* Orchard and Zonneveld (2009; see *Nv*. *waageni*). In this particular case it could even be compared with '*Kashmirella*' *alberti* Budurov, Sudar and Gupta (1988) (one paratype of which might be included here, *ibid*, figs. 1g, h, j) but the denticulation of the holotype of the latter is more reminiscent of *Nv*. *pakistanensis* (including *Nv*. *novaehollandiea*). The development of a posterior process wearing several denticles of diminishing height and the extension of the pointed basal cavity beneath it are somewhat reminiscent of *N*. *spitiensis* Goel, but here they are less conspicuous than in the latter.

***Neospathodus robustus* Koike 1982** – Pl. 4, figs. 1-6.

1968 *Spathognathodus cristagalli* n. sp. Huckriede, Pl. 10, figs. 18a, b.
2008 *Neospathodus cyclodontus* n. sp. Zhao and Orchard, Pl. 1, fig. 8.

Neospathodus robustus is a very robust and short segminate element with a shallow but widely flared basal cavity. The element is conspicuously thickened at mid-height. The denticles are mostly fused. The free apices of at least the anterior denticles appear as sub-equilateral triangles in lateral view. As observed in the Spiti material (Pl. 4), the lower margin is interpreted as being intraspecifically variable, from concave (fig. 2; see holotype in Koike, 1982, Pl. VI, figs. 34, 35) to convex (fig. 3; see also the paratype in op. cit., figs. 32, 33). Juvenile elements may look like the one illustrated on Pl. 3, fig. 19, which shares with the mature ones a large, rounded basal cavity and a peculiar anterior denticulation with sub-equilaterally triangular free apices. It is not clear how *N. cyclodontus* Zhao & Orchard (2008), whose holotype closely resembles the (juvenile?) paratype of *N. robustus*, should differ from *N. robustus* and we therefore synonymise it with *N. robustus*. The P1 elements of this species resemble homologous elements of the genus *Wapitiodus* Orchard (2005), to which this species may actually belong. Pending reconstruction of its apparatus, *N*. *robustus* Koike is yet provisionally retained within *Neospathodus* (note that this species is in any case distinct from *Wapitiodus robustus* Orchard 2005).

***Neospathodus* aff. *robustus* Koike 1982** – Pl. 3, fig. 13.

This element is similar to *N*. *robustus* in its overall shape and denticulation, but it misses both the broad basal cavity and the medial lateral thickening of the latter.

***Neospathodus* n. sp. S** – Pl. 10, figs. 5, 6.

This species resembles *N.* n. sp. U (see below) but the posterior basal margin is extended beneath an incipient posterior process. As in *N.* n. sp. U the basal outline tends to have a rhomboid shape.

***Neospathodus spitiensis* Goel 1977** – Pl. 9, figs. 7, 8, 10-12.

1977 *Neospathodus spitiensis* n. sp. Goel, p. 1094, Pl. 1, figs. 14-18.
1990 *Neospathodus pamirensis* n. sp. - Dagis, pp. 79-80, Pl. VI, fig. 9.
1992 *Neospathodus conservativus* - Nicora, p. 252, Pl. 26, fig. 5.

Unlike *Ns*. n. sp. U, this species has more numerous denticles and does not feature a distinctive terminal cusp but rather has a series of posterior denticles that diminish in size. The pit lies beneath about the middle of the element and the posterior process is slightly to strongly upturned (Pl. 9, fig. 10, see also *N*. *pamirensis* Dagis, 1990); the basal cavity is strongly extended and tapers to a point. In lateral view, the lower side of the anterior process tends to be sinuous. One large (broken) specimen has a thickened basal cup.
The holotype of this species has an anterior lower margin that is straight in contrast to the paratypes illustrated by Goel (1977), in which it is slightly concave. In this respect, the paratypes closely resemble '*N'*. *conservativus* (Müller). The Spiti specimens can be distinguished by their more reclined posterior denticles (when comparing specimens with similar lower margins) or more strongly upturned posterior lower margin (when comparing specimens with similar orientations of the denticles). However, these features are also variable in the Spiti specimens (note that apparently within our population of *N*. *spitiensis*, the more upturned the posterior lower margin the more erect the posterior denticles, and *vice versa*) and the two species are very close: it remains to be seen whether the Indian and American forms could be the same. Note that the apparatus of *C*. *conservativa*, as reconstructed by Orchard (2005) from both topotype (Nevada) and Oman collections, is quite different from that of *Neospathodus*. This may further help differentiating both species. So far, no distinctive *Conservatella* ramiform element was found in our Spiti collection.
The flat to inverted basal cavity of this species suggests that it may be derived from *N*. aff. *cristagalli* morphotype 7 by increased posterior growth and extension of the basal cavity, combined with increased upturning of the posterior part. Both species also share in common the presence of a narrow furrow in the posteriormost part of the basal cavity. In *N*. *spitiensis* this furrow extends further anteriorly sometimes all the way through to the basal pit. Alternatively it may also have derived from *N*. n. sp. U by addition of posterior denticles (compare for instance juveniles of both species, Pl. 9, figs. 4, 5).

***Neospathodus* n. sp. U** – Pl. 9, figs. 1, 3, 5.

A derivative of *Ns. cristagalli* in which the denticles are more posteriorly inclined and the basal cavity is relatively larger, posteriorly extended, and narrowly pointed. In lateral view, the lower margin is moderately to strongly upturned beneath the posterior one-third to one-half of the element. The subtriangular cusp and the three or four denticles anterior of it are slightly curved to the posterior and radiate from a point roughly located at mid-lower margin. The basal cavity is not inverted and hence resembles more that of *Novispathodus* than that of the *Ns*. *cristagalli* group. Rather discrete juvenile specimens (Pl. 9, fig. 9) resemble *N*. aff. *cristagalli* morphotype 3 but they lack the slight concavity of the posterior edge of the first denticle anterior to the cusp and their basal cavity is posteriorly pointed.

***Neospathodus* n. sp. X** – Pl. 3, figs. 5, 21, 22.

Small segminate elements whose cusp is terminal, slightly reclined to the posterior, and diagnostically inflated at its base. The basal cavity is rounded in aboral view and concavely arched in lateral view. The lower margin is similar to that of specimens figured on Pl. 3, fig. 9, 10 and assigned to *Spathicuspus*? n. sp. 1, but the denticles of the latter are strongly recurved to the posterior and the cusp much larger than the denticles to the anterior. The cusp of *N*. n. sp. X is slightly smaller than the denticles of the anterior process and of subequal breadth in its upper half (the part of it that is not inflated).

***Neospathodus* n. sp. 1** – Pl. 4, fig. 7.

This relative high specimen with long, radiating

and laterally curved denticles somehow resembles *N*. *dieneri* but its subcircular, slightly posteriorly expanded basal cavity is closest to *Nv*. *posterolongatus* or *N*. n. sp. 2 except that it is more strongly upturned posteriorly.

***Neospathodus* n. sp. 2** – Pl. 10, fig. 2.

The overall shape of this P1 element closely resembles both *Ns*. n. sp. U and *Ns*. n. sp. S. Yet, the basal cavity is not narrowly pointed but rather rhomboid instead. Characteristically, a tiny denticle develops anteriorly at mid-height. The posterior margin of the cusp is basally straight as in *Ns*. n. sp. U not projected posteriorly as typical of *Ns*. n. sp. S.

***Neospathodus* n. sp. 3** – Pl. 10, fig. 3.

As in *Ns*. n. sp. 2 (see above), a budding denticle develops at mid-height posteriorly. But this element differs in being relatively lower and in having a circular basal cavity that more closely resembles that of *Ns*. *dieneri*. Hence both elements may not be related.

***Neospathodus*? n. sp. 4** – Pl. 3, fig. 16; Pl. 13, fig. 29.

This species resembles *Nv*. aff. *pakistanensis* morphotype 5 (see below), but the terminal cusp is about as high as the penultimate denticle and the denticles are less fused than in the latter. Its denticulation is more like that of *Ns*. ex gr. *dieneri* and it actually resembles *Ns*. *dieneri* morphotype 5 (see above). Yet, the lower margin is not upturned posteriorly but rather straight to downcurved as in *Nv*. *pakistanensis*. The generic assignment is uncertain.

Subfamily NOVISPATHODINAE Orchard, 2005

Genus NOVISPATHODUS Orchard, 2005

Type species and holotype. *Neospathodus abruptus* Orchard, 1995, pp. 118-119, figs. 3.23-24.
Type stratum and locality. Oman, see type species in Orchard, 1995 contra Orchard, 2005.

Revised multielement diagnosis. As described by Orchard (2005), except again that the elements previously identified as occupying the S_1 and S_2 positions occupy in fact the S_2 and S_1 positions respectively. Bipennate S3-S4 elements, whose sinuous lower profiles are subparallel along most of their length except for the anterior process, but including the initial downturning of the posterior process. The anterior process of the S4 element is commonly larger and more downturned than that of the S3. The most sinuous element (in lower view) is the S4 element.

***Novispathodus latiformis* Orchard and Zonneveld 2009** – Pl. 12.

Elements previously assigned to *Nv*. *waageni* morphotype 1 (Orchard and Krystyn, 2007) by which platform flanges are developed on the flanks of the unit, especially at the posterior end are now assigned to *Nv*. *latiformis*. We distinguish two new morphotypes.

morphotype 1 – Pl. 12, fig. 1.

This morphotype has a semi-circular upper margin and maximal height is attained at midlength.

morphotype 2 – Pl. 12, figs. 2 (holotype), 6.

2007 *Neospathodus waageni* morphotype 1 – Orchard and Krystyn, figs. 8-10 (holotype).
2009 *Novispathodus latiformis* – Orchard and Zonneveld, fig. 13, parts. 11-13.

This rather long morphotype corresponds to the holotype of the species. The upper margin is straight anteriorly and rises slowly to the posterior, and then falls quite abruptly with the posteriormost 5 denticles. The maximal height is at about one third from the posterior of the element.

Remarks. In both morphotypes, the posteriormost one or two denticles seem to develop from the convex part of the posterior margin that corresponds to the posterior extension of the flange, and they extend beyond (more posteriorly to) the posterior edge of the basal cavity. There is a conspicuous, anisotropic constriction around the basal cavity (between the basal margin and the flange). This constriction is less pronounced laterally and as a consequence the basal cavity is antero-posteriorly compressed, i.e. it has an elliptical shape, whose major axis is perpendicular to the main axis (blade) of the element.

***Novispathodus pakistanensis* (Sweet) 1970**

1973 *Neospathodus novaehollandiea* n. sp. McTavish, Pl. 1, figs. 4, 5, 14, 16-23.
1988 *Kashmirella albertii* n. sp. Budurov, Sudar and Gupta, pp. 111-112, figs. 1i, k, l.

P1 elements of this species have a rounded basal cavity, are relatively long (length/height ratio ~1.8:1) and have posterior denticles of abruptly diminishing height. Sweet (1970) noted that a mid-lateral rib strengthened with growth in this species, and large specimens develop a lateral platform flange like that of '*Neospathodus' novaehollandiea*. McTavish (1973) distinguished the latter species from *Nv*. *pakistanensis* by its straight lower margin and differing distribution of white matter. Although the white matter distribution is impossible to evaluate in blackened material, the lower margin profile has been considered as an intraspecific variable by both Matsuda (1983) and Nicora (1992), who regarded the two species as synonyms. In fact both holotypes have the same circular basal cavity shape (confirmed in McTavish's material, pers. obs., M.O.) even though the material of Matsuda (1983) included both rounded and posteriorly elongate basal cavities. Specimens illustrated by both Nicora (1992) and Goel (1977) show the same variation of the basal cavity, which was considered an ontogenetic feature by McTavish (1973, p. 295, variation VI), but size and shape of the basal cavity are independant variables in this group. Forms with an elongated basal cavity are excluded from *N*. *pakistanensis*. They were previously referred to *N*. *posterolongatus* (Zhao *et a*l., 2007; see discussion of this taxa above), but are now referred to *Nv*. aff. *pakistanensis*. The generic assignment reflects our feeling that this species is intimately related to *Nv*. *waageni* Sweet (see remark 1).
As for the other important taxa of this time interval (see *N*. *cristagalli*, *N*. *dieneri* and *Nv*. *waageni*) several different morphologies of P1 element with roughly the same profile as type *pakistanensis* were grouped into this species but at least some of them may deserve assignment to separate species. As already mentioned, the definitions of the latter taxa were all based on material from the Salt Range, Pakistan and the revision of these taxa and the formal definition of new, related taxa is pending the detailed analysis of abundant, new topotype material collected in recent years by the Zurich team. In the mean time the following morphotypes are placed in open nomenclature.

morphotype 1 – Sweet, 1970, Pl. 1, figs. 16, 17 (holotype of *Nv*. *pakistanensis*).

2009 *Neospathodus pakistanensis* – Orchard and Zonneveld, fig. 13, parts. 20, 21.

This morphotype corresponds to Sweet's holotype. The cusp is here big and subterminal: only one small, needle-like denticle develops posterior of the cusp.

morphotype 2 – Pl. 2, fig. 10; Pl. 11, fig. 2 (juvenile?).

This morphotype has a big (sub)terminal triangular cusp. It consequently resembles *Nv*. *waageni* morphotype 5 but its relative proportions and the flat to downwardly arched posterior margin of its basal cavity are more typical of *Nv*. *pakistanensis*.

morphotype 3 – Pl. 11, fig. 7.

This morphotype has a terminal cusp and the posterior margin of the subcircular basal cavity is not distinctly arched downwards as in type *pakistanensis*. As for other morphotypes a lateral flange may develop.

morphotype 4 – Pl. 11, figs. 6, 10, 13.

1973 *Neospathodus novaehollandiae* n. sp. – McTavish, Pl. 1, figs. 14, 16, 19, 22.

This morphotype corresponds to McTavish's holotype of '*Neospathodus*' *novaehollandiae*. Yet, the Spiti specimens tend to have a smaller length/height ratio. We do not differentiate this morphotype based on the presence/absence of a lateral flange but rather on the posterior denticulation: the cusp is not distinctly broader than the other denticles and one or two denticles develop posterior of the cusp. The circular basal cavity is rather big and shallow. In the posterior part there is a conspicuous constriction around the basal cavity just above the lower margin. Consequently, in lateral view, the margin of the posteriormost denticle is markedly concave at its very base. Above that, the margin is straight and suberect or slightly reclined to the posterior.

***Novispathodus* aff. *pakistanensis* (Sweet) 1970**

morphotype 1 – Pl. 10, fig. 8.

This morphotype has a large, triangular terminal cusp. The posterior margin of the basal cavity is not distinctly arched downwards as in type *pakistanensis*, and the basal cavity more closely resembles that of *N*. *posterolongatus*, to which it is somewhat intermediate except for the cusp.

morphotype 2 – Pl. 10, fig. 10.

1973 *Neospathodus novaehollandiae* n. sp. – McTavish, Pl. 1, figs. 18, 21.
1988 *Kashmirella albertii* n. sp. Budurov, Sudar and Gupta, figs. 1c, d.

This morphotype is very similar to *Nv*. *pakistanensis* morphotype 4 but the posterior denticles are broader and strongly reclined to the posterior. Furthermore, the basal cavity is pointed and it may be asymmetrical. Compared with *N*. aff. *posterolongatus* (see above), the length/height ratio (~2:1) is much larger, the upper margin is not arcuate but straight anterior of the cusp and downcurved posteriorly, and the denticles are straight not recurved.

morphotype 3 – Orchard, 2008, Figs. 8.3, 8.4.

The specimen from the Canadian Arctic illustrated by Orchard (2008, Figs. 8.3, 8.4) is very similar to the Spiti specimens of *Nv*. *pakistanensis* morphotype 4 (see for instance Pl. 11, fig. 6) in most respects, except for a slightly more posteriorly elongated and less laterally flared basal cavity. It apparently misses the basal constriction but this entire element looks thinner. Based on the elongated basal cavity, it was assigned to *N*. *posterolongatus* by Orchard but both the downward orientation of the posterior lower margin and the posterior denticulation differ from the latter. If, as we suggest (see remark 3), both characters covary, this specimen illustrates an intermediate form between both species (compare with Pl. 10, fig. 9 and Pl. 11, fig. 6).

morphotype 4 – Pl. 11, fig. 9; Pl. 13, fig. 18.

2009 *Ns. pakistanensis* – Orchard, figs. 8.11, 8.12.

This morphotype is very similar to the holotype of *Nv*. *pakistanensis* but the element is relatively higher (length/height ratio ~1.5-1.6:1). The cusp is almost as high as the denticles to its anterior, and consequently the upper margin (except for the posteriormost denticle) is much less downarched posteriorly but almost straight and parallel to the lower margin. The denticles (including the cusp) are finer than in *Nv*. *pakistanensis* and subequally broad. Elements like that figured by Orchard and Zonneveld (2009, figs. 8.11, 8.12) differ only in having a relative broader cusp and are somewhat intermediate between this morphotype and *Nv*. *pakistanensis*.

morphotype 5 – Pl. 13, figs. 6, 8.

2009 *Ns. pakistanensis* – Orchard, fig. 8.10.
2008 *Ns. posterolongatus* – Zhao *et al*., fig. 3, parts 7, 8.

These small segminate elements closely resemble *morphotype 4* but differ in having a terminal cusp. Smaller elements like that figured by Orchard and Zonneveld (2009, fig. 8.10), by Zhao *et al*. (fig. 3, parts 7, 8) or like that figured here on Pl. 13, fig. 6 may be either short variants of this morphotype or juveniles. They also closely resemble *N*. *dieneri* morphotype 5 and could be juveniles of this species too, which suggests a relationship between both forms.

morphotype 6 – Nakrem *et al*., 2008, figs. 5.11, 5.14.

We group under this morphotype moderately elongate elements (length/height ratio ~1.6-1.7:1) whose lower margin is posteriorly downarched in a typically '*pakistanensis*'-like manner. Their upper margin on the other hand is more similar to that of *Nv*. *waageni*. These elements resemble *morphotype 4* and *morphotype 5* but the posterior upper margin is more gradually diminishing. Such elements have been reported by Nakrem *et al*. (2008) from the late Smithian of Svalbard.

morphotype 7 – Pl. 13, figs. 10, 15.

This morphotype is very close to morphotype 5 but the anterior process is more developed and distinctly downarched beneath the anterior quarter of the element. They differ also in having suberect denticles (rather than posteriorly reclined as in the latter) and a less expanded cavity whose 'lip' is missing. This is particularly visible in lateral view: in other '*pakistanensis*'-like elements this lip extends posteriorly in a posteroaboral direction and give these elements their typical outline.

***Novispathodus waageni* (Sweet) 1970**

This species features a circular basal cavity and a blade profile with a distinctive arcuate crest. It is relatively short compared with *Nv*. *pakistanensis*, but shares its posterior denticles profile and its rather variable lower margin. Six morphotypes were differentiated by Orchard and Krystyn (2007). One of these corresponded to *Neospathodus waageni eowaageni* Zhao and Orchard (=morphotype 3) and another was recently assigned to a new species *Nv*. *latiformis* Orchard and Zonneveld (=morphotype 1).

morphotype 2 – Pl. 12, figs. 7, 8.

1970 *Ns. waageni* n.sp., Sweet, Pl. 1, figs. 11, 12.

This correponds to *Nv*. *waageni* holotype (*Nv*. *w*. *waageni*) and has slightly reclined denticles forming an arcuate crest.

morphotype 3 – Pl. 13, figs. 1-4.

2007 *Ns. waageni eowaageni* n.subsp., Zhao and Orchard, Pl. 1, figs. 5A, B.

This small morphotype corresponds to *Nv*. *waageni eowaageni*. It has a length/height ratio close to 1:1 and upright denticles. The basal margin may be straight, upturned posteriorly, or upturned at both ends. The holotype of the subspecies (CUG030007 from sample CP27-1, not CUG030006 from CP24-6-2 as mentioned later by Zhao *et al*., 2008b, Pl. 1, figs. 11a-c) is from bed 27 at the West Pingdingshan section, Chaohu, China. This is markedly higher than other related forms (Zhao *et al*., 2008b, Pl. 1, fig. 11; Zhao *et al*., 2008a, fig. 3, parts. 1-4) that we here exclude from *morphotype 3* (see *Nv*. aff. *waageni*).

morphotype 4 – Pl. 12, figs. 9, 15.

In this form, there are a few posterior denticles that are abruptly lower than those to the anterior.

morphotype 5 – Pl. 12, figs. 10-13.

This morphotype has an unusually large (sub)terminal triangular cusp.

morphotype 6 – Pl. 12, fig. 4.

1977 *Neospathodus* aff. *waageni* – Goel, Pl. 2, figs. 5, 6.

This morphotype has denticles that tend to radiate from the base.

morphotype 7 – Orchard and Zonneveld, 2009, figs. 13.9, 13.10.

This morphotype, which is known from the Canadian Arctic (Orchard and Zonneveld, 2009), has a peculiar posterior denticulation: the cusp is almost as big as the denticles to its anterior and only a thin, erect, needle-like denticle develops on the posterior margin from the base of the cusp. Except for this posterior denticle and a somewhat more circular basal cavity, this morphotype is strongly reminiscent of *N*. aff. *cristagalli* morphotype 2, from which it may have evolved. It is hence also very close to *N*. aff. *cristagalli* morphotype 8, but the latter has reclined and more discrete denticles and a more upturned posterior lower margin.

morphotype 8 – Pl. 12, fig. 16.

This morphotype is very close to *morphotype 7*, with which it shares a similar erect denticulation with rather broad denticles. It differs of the latter by having not only one needle-like posterior denticle, but two. Its basal cavity is also more strongly upturned anteriorly and it is posteriorly flat, which is more typical for the *waageni* group. With the additional posterior denticle, the upper margin looks more regular and arcuate, and this is again more typical of the group.

morphotype 9 – Pl. 12, fig. 5.

This morphotype has more discrete denticles than the type of *waageni*. Forms like Pl. 10, figs. 7, 11 differ only in having a more elongate (and 'cristagallid') basal cavity and may be intermediate forms between *morphotype 9* and the *cristagalli*/*posterolongatus* groups (see for instance *N*. aff. *cristagalli* morphotype 8).

morphotype 10 – Pl. 11, fig. 11.

This morphotype has a flat lower margin and except for its low length/height ratio (~1.4:1), it is identical to *Nv*. *pakistanensis* morphotype 4 (ratio ~1.75:1).

***Novispathodus* aff. *waageni* (Sweet) 1970**

We regroup here various, rather small segminate elements that constitute a distinctive fauna with generally very fine and numerous denticles. This peculiar denticulation is particularly striking in better preserved collections from South China (Goudemand *et al*., Chapter 5), from which some of the following morphotypes will be fully described.

morphotype 1 – Pl. 14, figs. 14, 20.

2008 *Neospathodus waageni eowaageni* – Zhao *et al*., fig. 3, parts 1-4.
1977 Neospathodus waageni – Goel, Pl. 2, fig. 2.

These small segminate elements closely resemble *Nv*. aff. *pakistanensis* morphotype 5 but their length/height ratio is distinctly smaller (~1:1) and their denticles are not reclined posteriorly but rather straight, upright or sometimes recurved to the posterior (Pl. 14, fig. 14; Zhao *et al*., 2008, fig. 3.1). Height is maximal at about one third from the posterior of the element and diminishes regularly both posteriorly and anteriorly. Hence the upper margin is arcuate. The basal cavity is rounded, the lower margin either straight or slightly upturned posteriorly. Note that the high variability of this morphotype may allow further differentiation.

morphotype 2 – Pl. 14, figs. 17, 18.

This morphotype differs from *morphotype 1* only in having a bigger length/height ratio (~1.5:1). Their basal cavity is flat or partly inverted (in which case it is upturned posteriorly and somehow resembles the basal cavity of typical *cristagalli* elements except that it is rounded; compare in particular with *N*. aff. *cristagalli* morphotype 2, Pl. 7), but a similar variation is also observed in populations of *morphotype 1* from South China (Goudemand *et al*., Chapter 5). *Nv*. aff. *pakistanensis* morphotype 5 closely resembles but it has posteriorly reclined denticles (see *morphotype 4*).

morphotype 3 – Pl. 14, figs. 19, 23.

This morphotype is very similar to *morphotype 1* but a lateral flange develops at midheight. and creates a posterior bump, which is clearly visible on lateral view. The denticles tend to slightly radiate. In bigger specimens (Pl. 14, fig. 23) the basal cavity may be partly inverted posteriorly.

morphotype 4 – Pl. 14, figs. 6, 11, 24, 25.

This morphotype is also very similar to *morphotype 1* but in this case the denticles are posteriorly reclined and the lower margin is distinctly upturned beneath the posterior third of the element. Posteriorly the tangent of the lower margin is either horizontal (the posterior part of the basal cavity is flat) or oriented slightly aborally (the posterior part of the basal cavity is downcurved). Elements having a bigger length/height ratio and a lower margin that is more downarched posteriorly (a typical '*pakistanensis*' feature) have been here assigned to *Nv*. aff. *pakistanensis* morphotype 5.

morphotype 5 – Pl. 14, figs. 3, 12, 21.

Unlike *morphotype 1*, this morphotype has a big and strongly upturned basal cavity. The upper margin is straight and makes an angle of about 20 degrees with the horizontal (the height of the denticles diminish regularly towards the anterior end).

morphotype 6 – Pl. 14, figs. 2, 4.

1977 *Neospathodus waageni* – Goel, Pl. 2, fig. 4.

This morphotype is similar to *morphotype 5* but maximal height is at midlength rather than posteriorly. The lower margin is convex, being upturned both posteriorly and anteriorly and the denticles tend to radiate. Similar elements were reported by Goel from a section at Khar (1977). This morphotype somewhat resembles *Nv*. *waageni* morphotype 6 but the posterior denticulation, especially the size and orientation of the posteriormost denticle differs markedly: in the latter it is strongly reclined and recurved posteriorly and here it is only slightly reclined and of subtriangular shape.

Subfamily Uncertain

Genus BORINELLA Budurov and Sudar, 1994.

Type species and holotype. *Neogondolella buurensis* Dagis, 1984, pp.12-13, pl. XI, figs. 1, 2.
Type stratum and locality. Buur River basin, Taion-Uiolaakh River, *Hedenstromia hedenstromi* Zone.

Multielement diagnosis. Limited material of 'Neogondolella' buurensis available for study resembles elements of *Wapitiodus* (Orchard 2005).

***Borinella nepalensis* (Kozur & Mostler)** 1976 – Pl. 5, 6.

Variation in this species ranges from those with a very narrow platform (Pl. 5, fig. 9), to those with a uniformly tapered platform (Pl. 5, fig. 8), to those with a markedly asymmetric platform (Pl. 5, fig. 7). All have blades composed of long discrete denticles that rise to the anterior.
Borinella (type species *N. buurensis*) is senior synonym of *Chengyuania* because species with this characteristic discrete denticulation are brought together (see also Orchard, 2007 and Orchard, 2008).

Genus EURYGNATHODUS Staesche, 1964.

Type species and holotype. *Eurygnathodus costatus* Staesche, 1964, pp.269-271, Pl. 28, figs. 1-4.
Type stratum and locality. middle Campil Member, St. Vigil, Enneberg, South Tyrol.

***Eurygnathodus* spp.** – Pl. 5, 6.

Both the costate *E. costatus* and the smooth *E. hamadai* occur in our collections (Fig. 3). Similar forms assigned to *Platyvillosus* occur in the early Spathian, but they are not clearly related. Hence the present species are assigned to *Eurygnathodus* (as originally defined by Staesche, 1964).

New Genus A – Pl. 1, fig. 13.

This S2 element has a bifurcated inner lateral process.

New Genus B – Pl. 1, fig. 14.

This S2 element has a bifurcated antero-lateral process.

New Genus C – Pl. 1, fig. 16.

This is in our view the broken anterior part of a S3 element. A similar element has been recognized by Orchard (2005, fig. D in Text-Fig. 14) as the S4 element of *Neospathodus*. Orchard did not mention the distal bifurcation of the anterior process of this putative S4 element but it is clearly visible on his illustration (on the fifth denticle anterior of the cusp, as in *Neogondolella*). Furthermore, Orchard (2005, p. 89) suggests that the S3 element of *Neospathodus* (see Fig. E in Text-Fig. 14) has a more posteriorly located bifurcation of the anterior process than the homologous element in *Neogondolella*. New conodont clusters from South China (Goudemand *et al*., Chapter 1) suggest however that the S4 element corresponding to Orchard's illustrated S3 element (E) should have a similar lower profile and possibly no bifurcation. It is still unclear which configuration corresponds to the type species but both illustrated elements should probably been assigned to two different taxa. If Orchard's multi-element diagnosis of *Neospathodus* holds, then Orchard's illustrated specimen D should rather be the S3 element of another genus (see Chapter 1) in which the anterior process of S3/4 elements is less conspicuously downturned than in *Neogondolella* and *Neospathodus*. The downturning of the anterior process in the present specimen is similar to the latter (fig. D in Text-Fig. 14) but the bifurcation is located more posteriorly (on the third or fourth denticle anterior of the cusp), which may or may not justify taxonomic separation depending on the yet unknown populational variability of this character.

Suborder PRIONIODININA

***Merillina*?/*Ellisonia*? cf sp. A** Orchard, 2007 – Pl. 1, fig. 1.

This element strongly resembles the Dienerian element illustrated by Orchard from the late Griesbachian of the Arctic, and assigned to *Me*.?/*Ell*.? n. sp. A. The only partial preservation precludes any confident assignment.

Hadrodontina* cf. *anceps Staesche, 1964 – Pl. 1, fig. 12.

Though it is not obvious from this illustration, this quite badly preserved P1 element exhibits the typical secondary row of denticles (see reconstruction by Perri and Andraghetti, 1987, pp. 306-308).

***Remarks*:**
1) At least within the three dominant *cristagalli*, *dieneri* and *waageni* groups of related species, to almost each relative short morphotype of the P1 element there exists a distinct but coeval and morphologically similar, corresponding morphotype with a high length/height ratio. Such a recurrent pattern excludes that it is a pure coincidence. It rather suggests that either the intraspecific variation within the corresponding populations was underestimated, which led to the splitting of both extreme variants (and mixing with other, yet distinct variants under the categories 'relatively short' or 'relatively long'); or that these conodonts' P1 elements were affected by some kind of yet unrecognized dimorphism. Work is in progress to assess the former hypothesis (Goudemand, in prep.).
2) A similar remark may apply to the presence/absence of a lateral platform-like flange. This character may be highly variable but traditionally its presence may be sufficient for distinguishing different species (in some cases it has been also suggested that its extension could be diagnostic (see for instance *Chiosella gondolelloides vs*. *C*. *timorensis* in Gradinaru *et al*. 2006, discussed in Chapter 3). It remains unclear whether forms with or without lateral flange are coeval or not and whether this variability might be somehow generic and hence common to most if not all P1 elements, and if so, whether it might be related to some ecological factor (Goudemand, in prep.).
3) In some occasions we mentioned that apparently some characters such as the elongation of the basal cavity, the upturning of the posterior lower margin and the shape and reclination of the posterior denticles might covary within one species or group of species. Such laws of covariation have never been stated for conodont elements and their reliability has to be tested (Goudemand, in prep.). It may lead to the recognition of generic rules (or mechanical constraints) bound to the growth of the P1 elements.

Acknowledgements

This research is supported by the Swiss NSF project 200020-113554 (to H.B.).
We are much indebted to Séverine Urdy for her help with the SEM photographs and the preparation of the plates. Peter Krauss (Vancouver), Leonie Pauli and Julia Huber (Zurich) are acknowledged for having dissolved and concentrated the conodont samples.

References

Bender, H., AND D. Stoppel. 1965. Perm-Conodonten. Geologisches Jahrbuch, 82:331-364.

Bhargava, O. N., L. Krystyn, M. Balini, R. Lein, AND A. Nicora. 2004. Revised Litho- and Sequence Stratigraphy of the Spiti Triassic. Albertiana, 30 Supplement:21-38.

Birkenmajer, K., AND J. Trammer. 1975. Lower Triassic Conodonts from Hornsund, South Spitsbergen. Acta Geologica Polonica, 25(2):299-308.

Brayard, A., H. Bucher, G. Escarguel, F. Fluteau, S. Bourquin, AND T. Galfetti. 2006. The Early Triassic Ammonoid Recovery: Paleoclimatic Significance of Diversity Gradients. Palaeogeography, Palaeoclimatology, Palaeoecology.

Brayard, A., G. Escarguel, H. Bucher, C. Monnet, T. Brühwiler, N. Goudemand, T. Galfetti, AND J. Guex. 2009. Good genes and good luck: ammonoid diversity and the end-Permian mass extinction. Science, 325:1118-1121.

Brühwiler, T., D. Ware, H. Bucher, L. Krystyn, AND N. Goudemand. 2010. New Early Triassic ammonoid faunas from the Dienerian/Smithian boundary beds at the Induan/Olenekian GSSP candidate at Mud (Spiti, Northern India). Journal of Asian Earth Sciences:doi:10.1016/j.jseaes.2010.1004.1032.

Bucher, H., W. W. Nassichuk, AND C. Spinosa. 1997. A new occurrence of the upper Permian ammonoid *Stacheoceras trimurti* Diener from the Himalayas; Himachal Pradesh, India. Eclogae Geologicae Helvetiae, 90:599-604.

Budurov, K. J., AND M. N. Sudar. 1994. *Borinella* Budurov & Sudar, nomen novum for the Triassic Conodont Genus *Kozurella* Budurov and Sudar. Geologica Balkanica, 24(3):30.

Budurov, K. J., M. N. Sudar, AND V. J. Gupta. 1988. *Kashmirellla*, A New Early Triassic Conodont Genus. Bulletin of the Indian Geologists› Association, 21(2):107-112.

Chhabra, N. L., AND A. Sahni. 1981. Late Lower Triassic and Early Middle Triassic Conodont Faunas from Kashmir and Kumaun Sequences in Himalaya. Journal of the Palaeontological Society of India, 25:135-147.

Clark, D. L. 1959. Conodonts from the Triassic of Nevada and Utah. Journal of Paleontolo-

gy, 33(2):305-312.

Dagis, A. A. 1984. Lower Triassic Conodonts from Northern Central Siberia. Nauka Publishers, Moscow, 554.

Dagis, A. A. 1990. Conodonts from the Lower Triassic of the Southeastern Pamirs, p. 73-89. *In* A. S. Dagis and V. N. Dubatolov (eds.), Trias of Siberia.Volume 767. Trudy Instituta Geologii i Geofiziki [Proceedings of the Institute of Geology and Geophysics of the Siberian Department of the USSR Academy of Sciences], Novosibirsk.

Diener, C. 1897. The Cephalopoda of the Lower Trias. Palaeontologia Indica, ser. 15, Himalayan Fossils, 2:1-181.

Donoghue, P. C. J. 1998. Growth and patterning in the conodont skeleton. Philosophical Transactions of the Royal Society London B, 353:633-666.

Donoghue, P. C. J., M. A. Purnell, R. J. Aldridge, AND S. Zhang. 2008. The interrelationships of ‹complex› conodonts (Vertebrata). Journal of Systematic Palaeontology, 6(2):119-153.

Dzik, J. 1976. Remarks on the evolution of Ordovician conodonts. Acta Palaeontologica Polonica, 21:395-455.

Eichenberg, W. 1930. Conodonten aus dem Culm des Harzes. Palaeontol. Zeitschr., 12:177-182.

Goel, R. K. 1977. Triassic Conodonts from Spiti (Himachal Pradesh), India. Journal of Paleontology, 51(6):1085-1101.

Guex, J. 1991. Biochronological correlations. Springer-Verlag, 252 p.

Hirsch, F. 1994. Triassic conodonts as ecological and eustatic sensors, p. 949-959, Pangea: Global Environments and Resources.Volume Memoir 17. Canadian Society of Petroleum Geologists.

Hirschmann, C. 1959. Über Conodonten aus dem oberen Muschelkalk des Thüringer Beckens. Freiberger Forschungshefte, 76:35-86.

Huckriede, R. 1958. Die Conodonten der mediterranen Trias und ihr stratigraphischer Wert. Paläontologisches Zeitschrift, 32(3/4):141-175.

Kiparisova, L. D., AND Y. D. Popov. 1956. Subdivision of the lower series of the Triassic System into stages. Doklady Akad. Nauk SSSR, 109(4):842-845.

Koike, T. 1982. Triassic Conodont Biostratigraphy in Kedah, West Malaysia. Contributions to the Geology and Palaeontology of Southeast Asia, 23:9-65.

Kozur, H. 1988. The Taxonomy of the Gondolellids Conodonts in the Permian and Triassic. 1st International Senckenberg Conference and 5th European Conodont Symposium (ECOS V): Contributions III, Papers on Ordovician to Triassic Conodonts, 117:409-469.

Kozur, H., AND H. Mostler. 1976. Neue Conodonten aus dem Jungpaläozoikum und der Trias. Geol. Paläont. Mitt. Innsbruck, 6(3):1-33.

Krafft, A. v., AND C. Diener. 1909. Lower Triassic cephalopoda from Spiti, Malla Johar, and Byans. Palaeontologia Indica, ser. 15, , 6:1-186.

Krystyn, L., O. N. Bhargava, AND S. Richoz. 2007a. A candidate GSSP for the base of the Olenekian Stage: Mud at Pin Valley; district Lahul & Spiti, Himachal Pradesh (Western Himalaya), India. Albertiana, 35:5-29.

Krystyn, L., S. Richoz, AND O. N. Bhargava. 2007b. The Induan-Olenekian Boundary (IOB) in Mud – an update of the candidate GSSP section M04. Albertiana, 36:33-45.

Lindström, M. 1970. A Suprageneric Taxonomy of the Conodonts. Lethaia Norwegia, 3:427-445.

Matsuda, T. 1983. Early Triassic Conodonts from Kashmir, India. Part 3: *Neospathodus* 2. Journal of Geosciences, Osaka City University, 26(Article 4):87-110.

McTavish, R. A. 1973. Triassic Conodont Faunas from Western Australia. Neues Jahrbuch für Geologie und Paläontologie. Abhandlungen, 143(3):275-303.

Mosher, L. C. 1968. Triassic Conodonts from Western North America and Europe and Their Correlation. Journal of Paleontology, 42(4):895-946.

Müller, K. J. 1956. Triassic Conodonts from Nevada. Journal of Paleontology, 30(4):818-830.

Nakrem, H. A., M. J. Orchard, W. Weitschat, M. W. Hounslow, T. W. Beatty, AND A. Mork. 2008. Triassic conodonts from Svalbard and their Boreal correlations. Polar Research, 27(3):523-539.

Nicora, A. 1992. Conodonts from the Lower Triassic Sequence of Central Dolpo, Nepal. Rivista Italiana di Paleontologia e Stratigrafia, 97(3-4):239-268.

Orchard, M. J. 1995. Taxonomy and Correlation of Lower Triassic (Spathian) Segminate Conodonts from Oman and Revision of Some Species of Neospathodus. Journal of Pa-

leontology, 69(1):110-122.

Orchard, M. J. 2005. Multielement conodont apparatuses of Triassic Gondolelloidea, p. 73-101. *In* M. A. Purnell and P. C. J. Donoghue (eds.), Conodont Biology and Phylogeny: Interpreting the Fossil Record.Volume 73. Special Papers in Palaeontology.

Orchard, M. J. 2007. Conodont diversity and evolution through the latest Permian and Early Triassic upheavals. Palaeogeography, Palaeoclimatology, Palaeoecology, 252:93-117.

Orchard, M. J. 2007b. Report on 2007 conodonts collections from Mud, Spiti. Albertiana, 36:46-49.

Orchard, M. J. 2008. Lower Triassic conodonts from the Canadian Arctic, their intercalibration with ammonoid-based stages and a comparison with other North American Olenekian faunas. Polar Research, 27(3):393-412.

Orchard, M. J., AND L. Krystyn. 2007. Conodonts from the Induan-Olenekian boundary interval at Mud, Spiti. Albertiana, 35:30-34.

Orchard, M. J., AND H. Rieber. 1999. Multielement *Neogondolella* (Conodonta, upper Permian - middle Triassic). Bolletino della Società Paleontologica Italiana, 37(2-3):475-488.

Orchard, M. J., AND J.-P. Zonneveld. 2009. The Lower Triassic Sulphur Mountain Formation in the Wapiti Lake area: lithostratigraphy, conodont biostratigraphy, and a new biozonation for the lower Olenekian (Smithian). Canadian Journal of Earth Sciences, 46:757-790.

Purnell, M. A., AND P. H. Von Bitter. 1992. Blade-Shaped Conodont Elements Functioned as Cutting Teeth. Nature, 359:629-630.

Silberling, N. J., AND E. T. Tozer. 1968. Biostratigraphic classification of the marine Triassic in North America. Geological Society of America (GSA), Boulder, CO, United States, 110, 63 p.

Staesche, U. 1964. Conodonten aus dem Skyth von Südtirol. Neues Jahrbuch für Geologie und Paläontologie. Abhandlungen, 119(3):247-306.

Sweet, W. C. 1970. Uppermost Permian and Lower Triassic Conodonts of the Salt Range and Trans-Indus Ranges, West Pakistan, p. 207-275. *In* B. Kummel and C. Teichert (eds.), Stratigraphic Boundary Problems: Permian and Triassic of West Pakistan.Volume Special Publication 4. The University Press of Kansas.

Tatge, U. 1956. Conodonten aus dem germanishen Muschelkalk. Paläontologisches Zeitschrift, 30(1/2):108-127.

Tong, J., Y. D. Zakharov, M. J. Orchard, H. Yin, AND H. J. Hansen. 2003. A Candidate of the Induan-Olenekian Boundary Stratotype in the Tethyan Region. Science in China (series D), 46(11).

Tong, J., Y. D. Zakharov, M. J. Orchard, H. Yin, AND H. J. Hansen. 2004. Proposal of Chaohu Section as the GSSP Candidate of the Induan-Olenekian Boundary. Albertiana, 29:13-28.

Tozer, E. T. 1965. Lower Triassic stages and ammonoid zones of Arctic Canada. Geologic Survey of Canada Paper, 65-12:14 pp.

Tozer, E. T. 1967. A standard for Triassic time. Geologic Survey of Canada Bulletin, 156:141 pp.

Visscher, H. 1992. The new STS Triassic stage nomenclature. Albertiana, 10:1.

Zhang, S., AND Z. Yang. 1991. On Multielement Taxonomy of the Early Triassic Conodonts. Stratigraphy and Paleontology of China, 1:17-47.

Zhao, L., M. J. Orchard, J. Tong, Z. Sun, J. Zuo, S. Zhang, AND A. Yun. 2007. Lower Triassic conodont sequence in Chaohu, Anhui Province, China and its global correlation. Palaeogeography, Palaeoclimatology, Palaeoecology, 252:24-38.

Zhao, L., J. Tong, AND M. J. Orchard. 2005. Study on the Lower Triassic conodont sequence and the Induan-Olenekian boundary in Chaohu, Anhui Province. PhD thesis, China University of Geosciences Press, Wuhan, Hubei, China, 140 p.

Zhao, L., J. Tong, Z. Sun, AND M. J. Orchard. 2008a. A detailed Lower Triassic conodont biostratigraphy and its implications for the GSSP candidate of the Induan-Olenekian boundary in Chaohu, Anhui Province. Progress in Natural Science, 18:79-90.

Zhao, L., J. Tong, S. Zhang, AND Z. Sun. 2008b. An update of conodonts in the Induan-Olenekian boundary strata at West Pingdingshan section, Chaohu, Anhui Province. Journal of China University of Geosciences, 19(3):207-216.

PLATE 1

Fig. 1. *Merillina*?/*Ellisonia*? cf. sp. A Orchard, 2007. P1 element.
Figs. 2, 4, 5. *Wapitiodus*? spp., P2 elements.
Fig. 3. *Neospathodus*? sp. indet., P2 element. Note the bifurcating anterior process.
Fig. 6. *Cornudina* n. sp. A, P1 element.
Figs. 7, 8. *Novispathodus* sp. indet., P2 elements.
Figs. 9-11. *Novispathodus*? sp. indet. S1 elements. The specimen on fig. 10 could also be assigned to *Neospathodus*.
Fig. 12. *Hadrodontina* cf. *anceps*, P1?/S0? element.
Fig. 13. new genus A, S2 element.
Fig. 14. new genus B, S2 element.
Fig. 15. *Novispathodus*? sp. indet., S3/4 element.
Fig. 16. new genus C, S3 element.

All ×80. All from sample Mud33.

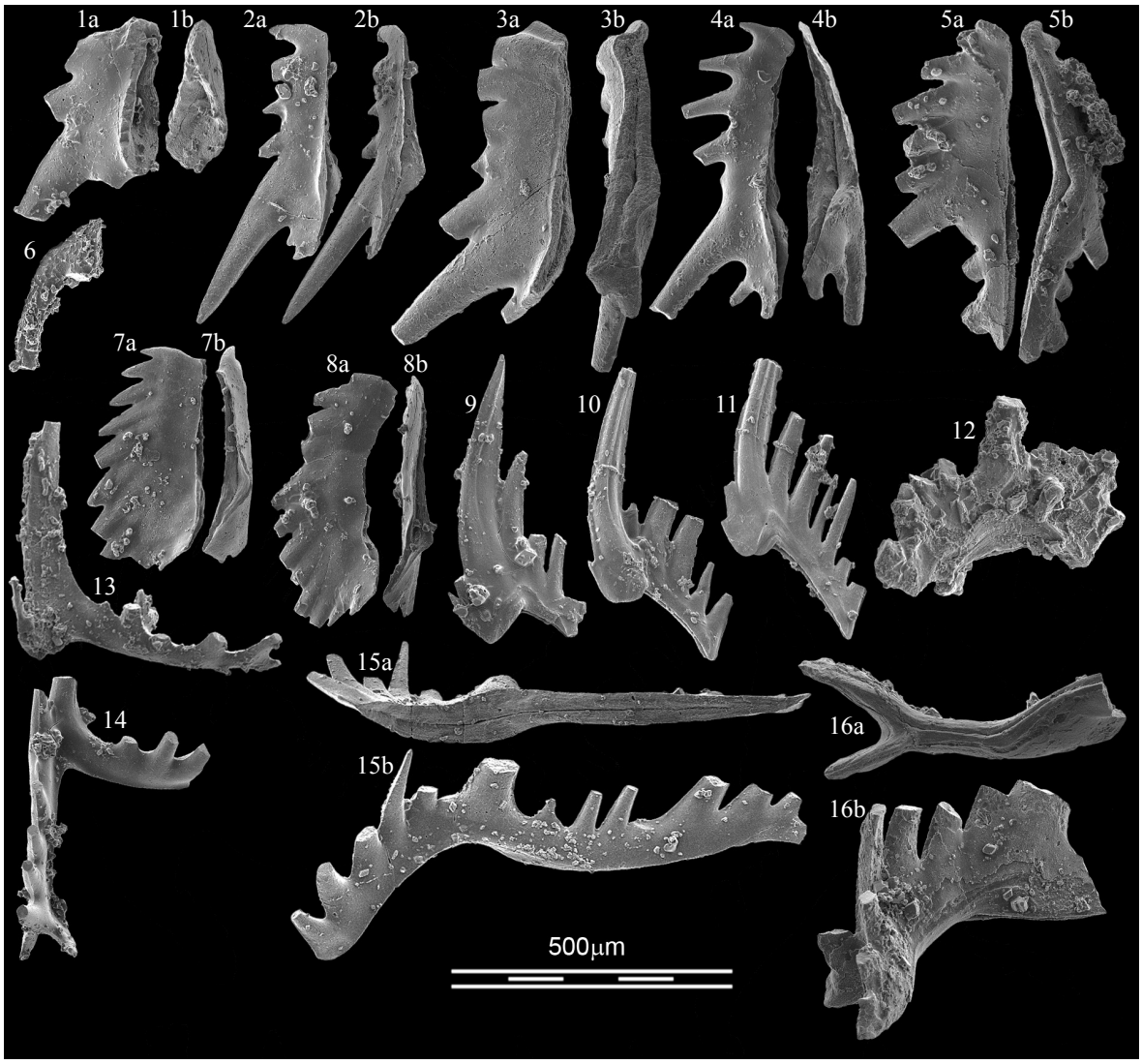
1a
1b
2a
2b
3a
3b
4a
4b
5a
5b
6
7a
7b
8a
8b
9
10
11
12
13
14
15a
15b
16a
16b
500μm

PLATE 1

PLATE 2

Fig. 1. *Ns*. *concavus*. M04-10.
Figs. 2-6. *Ns*. cf. *concavus*. 2: M04-10; 3, 6: Mud33; 4: M04A-13A3; 5: M04A-13B1.
Figs. 7, 8. *Ns*. *chaohuensis*. 7: Mud33; 8: M04-10.
Fig. 9. *Nv*.? aff. *crassatus*. M05-10.
Fig. 10. *Nv. pakistanensis* 2. M05-10.
Fig. 11. Ns.? sp. indet. Mud33.
Fig. 12. *Ns*. aff. *dieneri*. M04-10.
Fig. 13. Ns.? sp. indet. Mud33.

All P1 elements, all ×80.

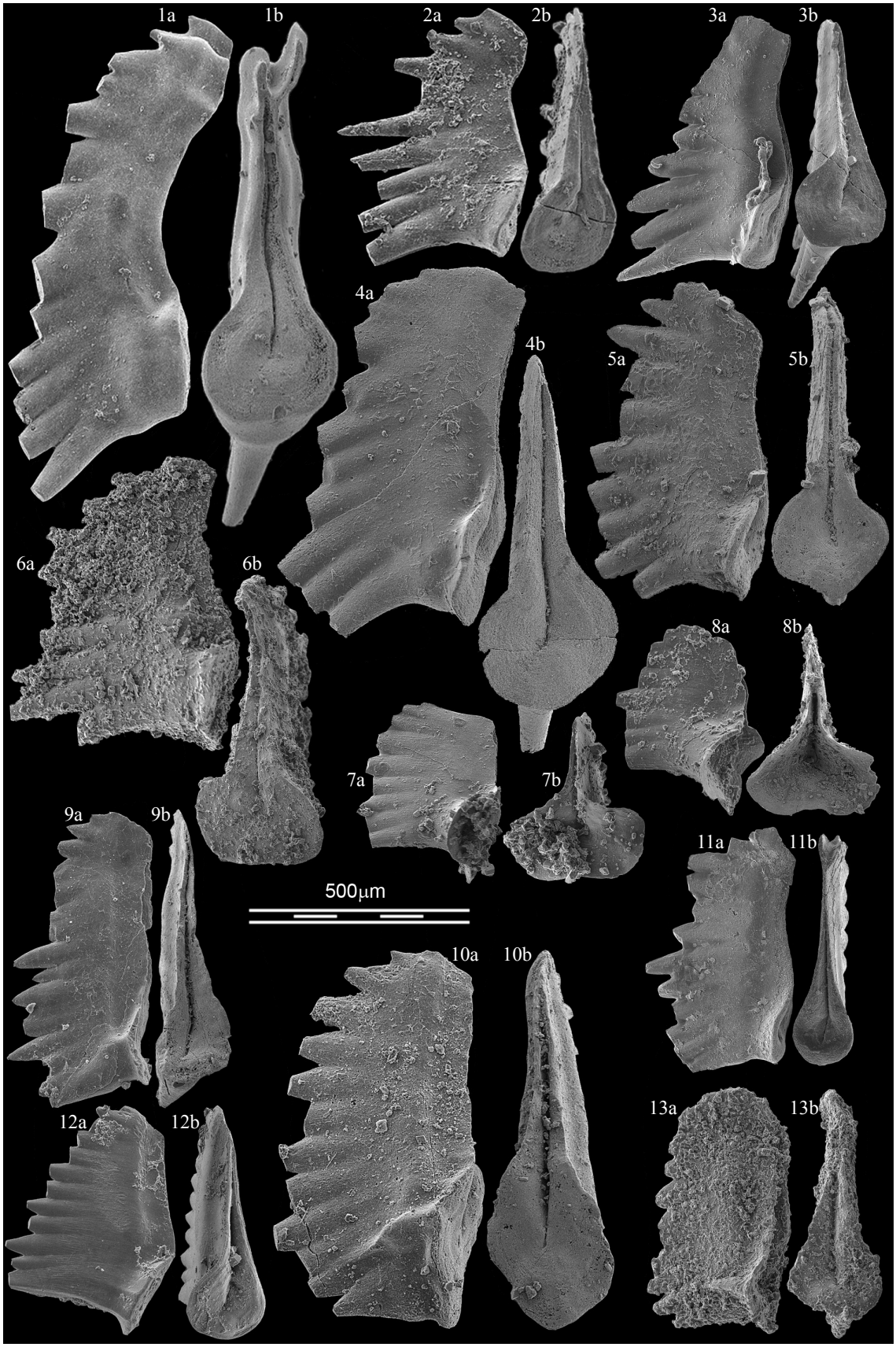
1a
1b
2a
2b
3a
3b
4a
4b
5a
5b
6a
6b
7a
7b
8a
8b
9a
9b
500µm
10a
10b
11a
11b
12a
12b
13a
13b

PLATE 2

PLATE 3

Fig. 1. *Guangxidella* n. sp. 2. Mud33.
Figs. 2, 8?, 11, 12?, 15. *Wapitiodus*? n. sp. 1. 2, 11, 12: Mud33; 8: M05-10; 15: M03-11.
Fig. 3. *Guangxidella* n. sp. 1. M04-10.
Fig. 4. *Guangxidella*? sp. indet. M03-13A.
Figs. 5, 21, 22?. *Ns*. n. sp. X. 5: M03-13A; 21: M04-13B1; 22: Mud33.
Figs. 6, 7. *Spathicuspus*? n. sp. 2. 6: M03-14C; 7: M04-14C.
Figs. 9, 10. *Spathicuspus*? n. sp. 1. 9: M05-10; 10: Mud33.
Fig. 13. *Ns*. aff. *robustus*. 13: M05-10.
Fig. 14. *Ns*. aff. *dieneri* morphotype 1. Mud33.
Figs. 16, 17?. *Ns*. n .sp. 4. 16: M04-10; 17: Mud33.
Fig. 18. *Ns*. aff. *dieneri* morphotype 2. M03-11.
Fig. 19. *Guangxidella*? sp. indet. (compare with Orchard&Zonnenfeld 2010, Fig. 15.26-28). Mud33.
Fig. 20. *Nv*. aff. *pakistanensis* 5?. M04-12BC.

All P1 elements, all ×80.

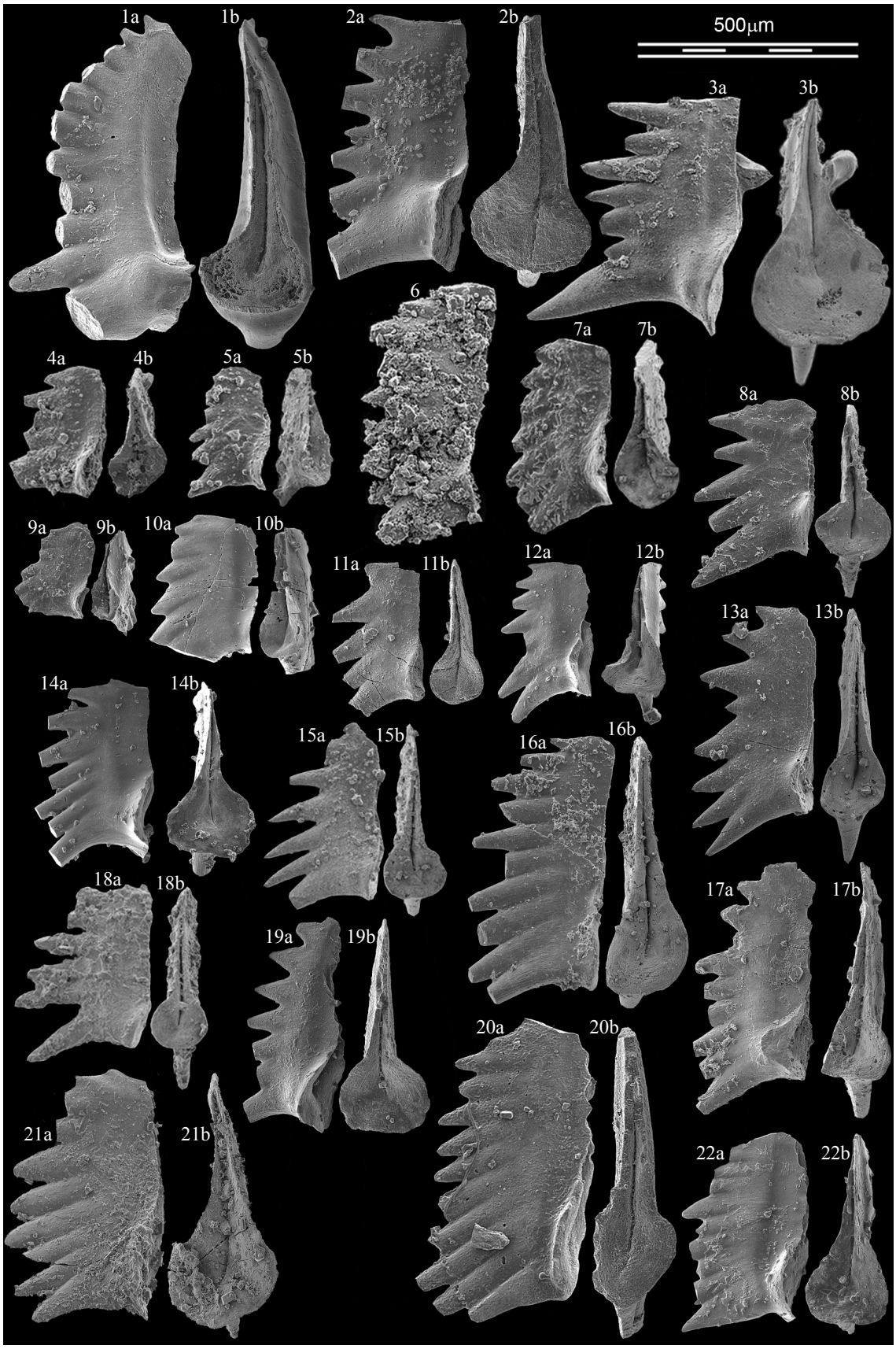
1a
1b
2a
2b
500µm
3a
3b
6
7a
7b
4a
4b
5a
5b
8a
8b
9a
9b
10a
10b
11a
11b
12a
12b
13a
13b
14a
14b
15a
15b
16a
16b
18a
18b
17a
17b
19a
19b
20a
20b
21a
21b
22a
22b

PLATE 3

PLATE 4

Figs. 1-6. *Ns*. *robustus*. 1-5: Mud33; 6: M04-10.
Fig. 7. *Ns*. n. sp. 1. M03-16A.
Fig. 8. *Ns*. *dieneri* morphotype 6. M03-11.
Fig. 9. *Ns*. *dieneri* morphotype 5. M03-11.
Fig. 10. *Nv*. *waageni* morph 6. M03-16A.
Fig. 11. *Ns*. *dieneri* morphotype 1?. M03-11.
Figs. 12, 13. *Ns*. *dieneri* morphotype 3. Both M04-10.
Figs. 14?, 19. *Ns*. *dieneri* morphotype 4. 14: M03-11; 19: Mud33.
Fig. 15. *Nv*. n. sp. S. M03-16A.
Fig. 16. *Ns*. cf. *concavus*. Mud33.
Fig. 17. *Ns*. *dieneri* morphotype 2. M05-10.
Fig. 18. *Ns*. *dieneri* morphotype 7. M05-10.

All P1 elements, all ×80.

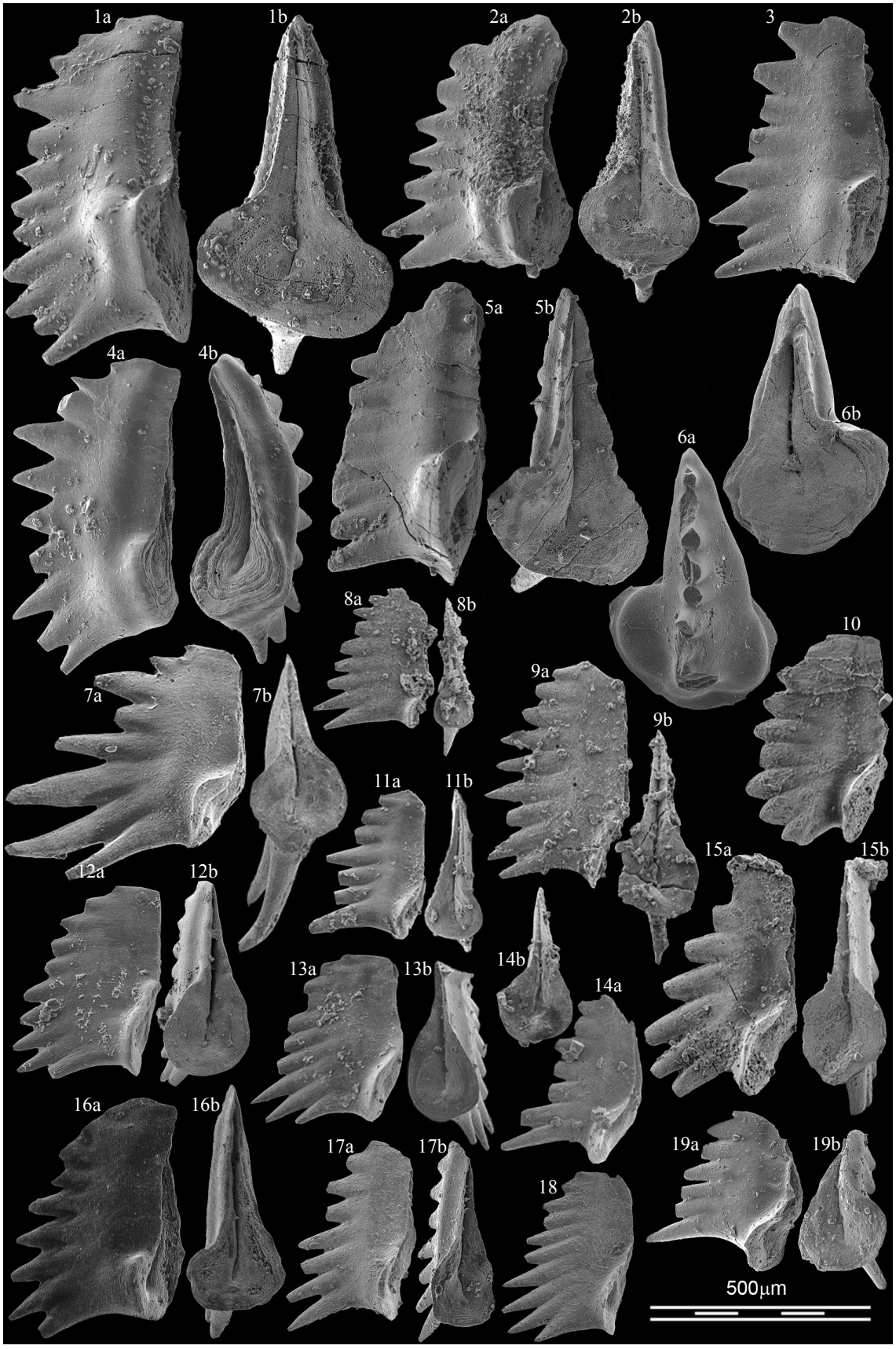
1a
1b
2a
2b
3
4a
4b
5a
5b
6a
6b
7a
7b
8a
8b
9a
9b
10
11a
11b
12a
12b
13a
13b
14a
14b
15a
15b
16a
16b
17a
17b
18
19a
19b
500μm

PLATE 4

PLATE 5

Figs. 1-3. *Discretella discreta*. 1: M06-13B; 2, 3: M04-14C.
Figs. 4-10, 12, 13. *Borinella nepalensis*. 4, 9, 12: M03-13; 5: M08-12C; 6-8: M03-12C; 10: XXX; 13: M03-14.
Fig. 11. *Eurygnathodus hamadai*. M06-13B.

All P1 elements, all ×80.

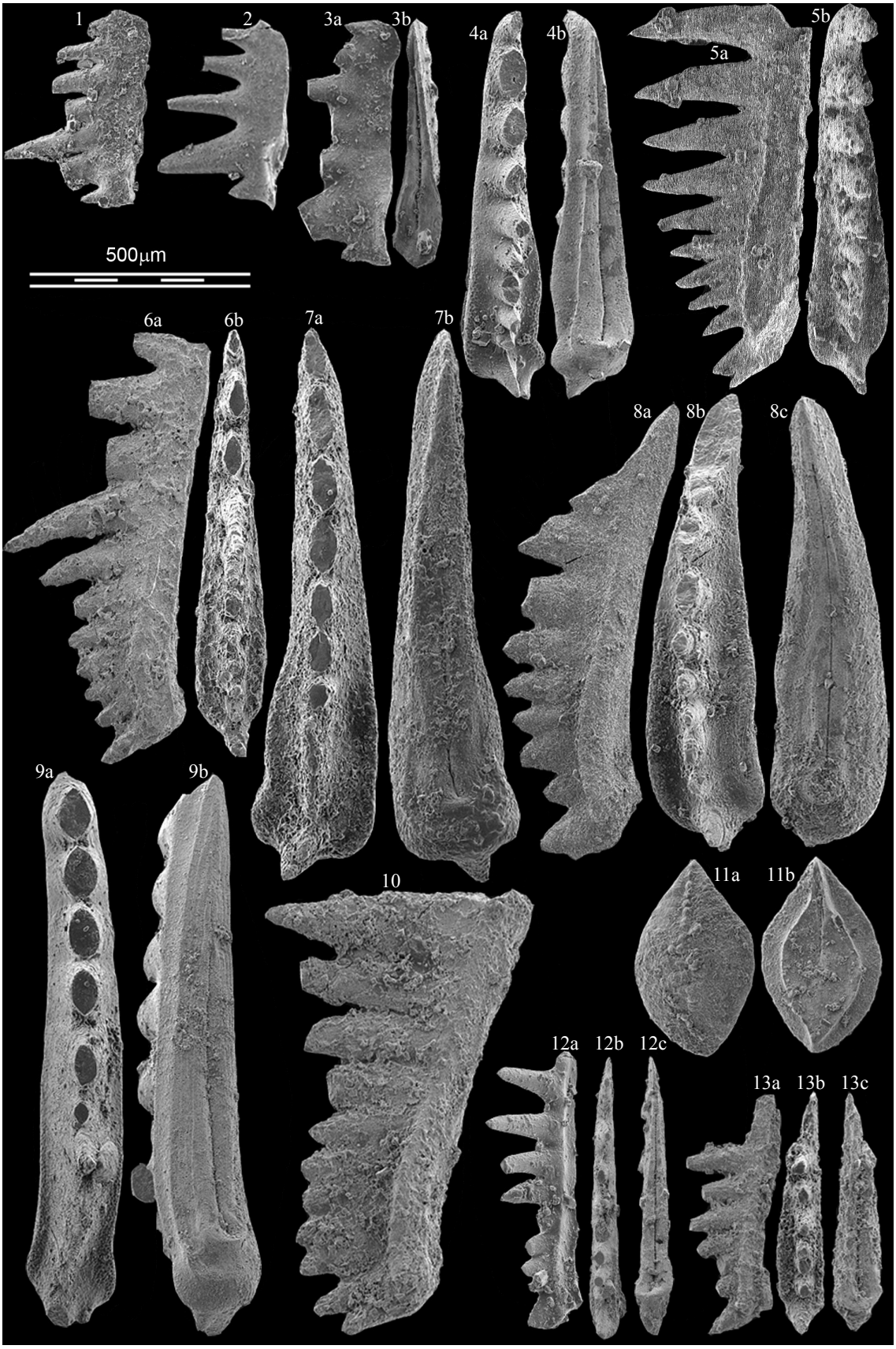
1
2
3a
3b
4a
4b
5a
5b
500μm
6a
6b
7a
7b
8a
8b
8c
9a
9b
10
11a
11b
12a
12b
12c
13a
13b
13c

PLATE 5

PLATE 6

Figs. 1-5, 7-9, 12, 13. *Borinella nepalensis*. 1-5, 7, 8, 12: M08-12C; 9, 13: M06-13A1.
Figs. 6, 10. *Ng*. ex gr. *carinata*. Both M03-13A.
Fig. 11. *Eurygnathodus* cf. *costatus*. M04-12BC.

All P1 elements, all ×80.

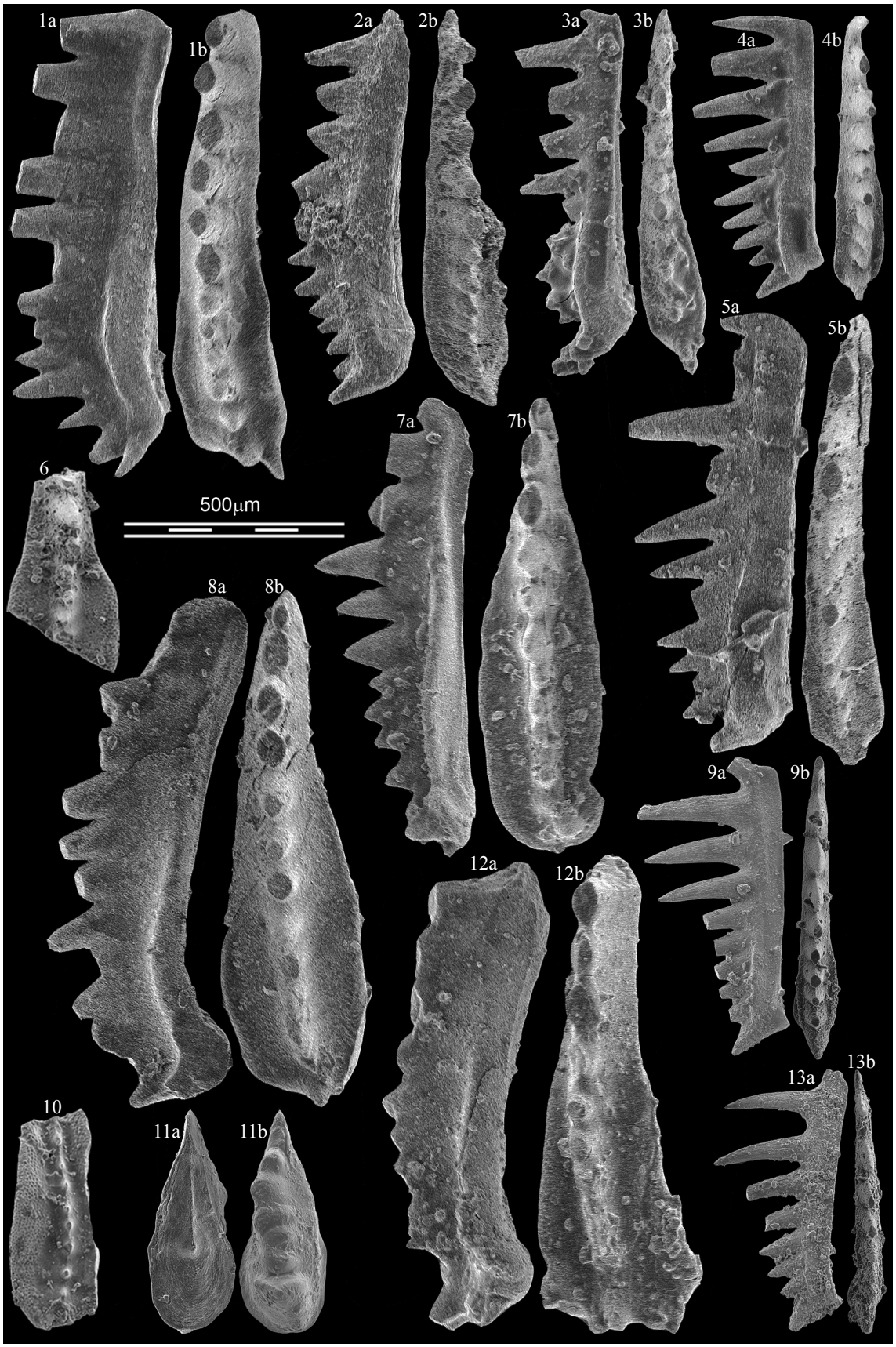
1a
1b
2a
2b
3a
3b
4a
4b
5a
5b
6
7a
7b
500μm
8a
8b
9a
9b
10
11a
11b
12a
12b
13a
13b

PLATE 6

PLATE 7

Figs. 1, 2. *Ns*. *cristagalli* Huckriede. 1: M04-10; 2: Mud33.
Fig. 3. *Ns*. aff. *cristagalli* morphotype 1. Mud10.
Figs. 4, 5. *Ns*. aff. *cristagalli* morphotype 3. 4: Mud33, 5: M03-11.
Figs. 6-13, 15. *Ns*. aff. *cristagalli* morphotype 2. 6, 8, 10, 12, 13, 15: Mud33; 7: M03-11; 9: M04-10; 11: M05-10.
Fig. 14. *Ns*. aff. *cristagalli* morphotype 4. Mud33.

All P1 elements, all ×80.

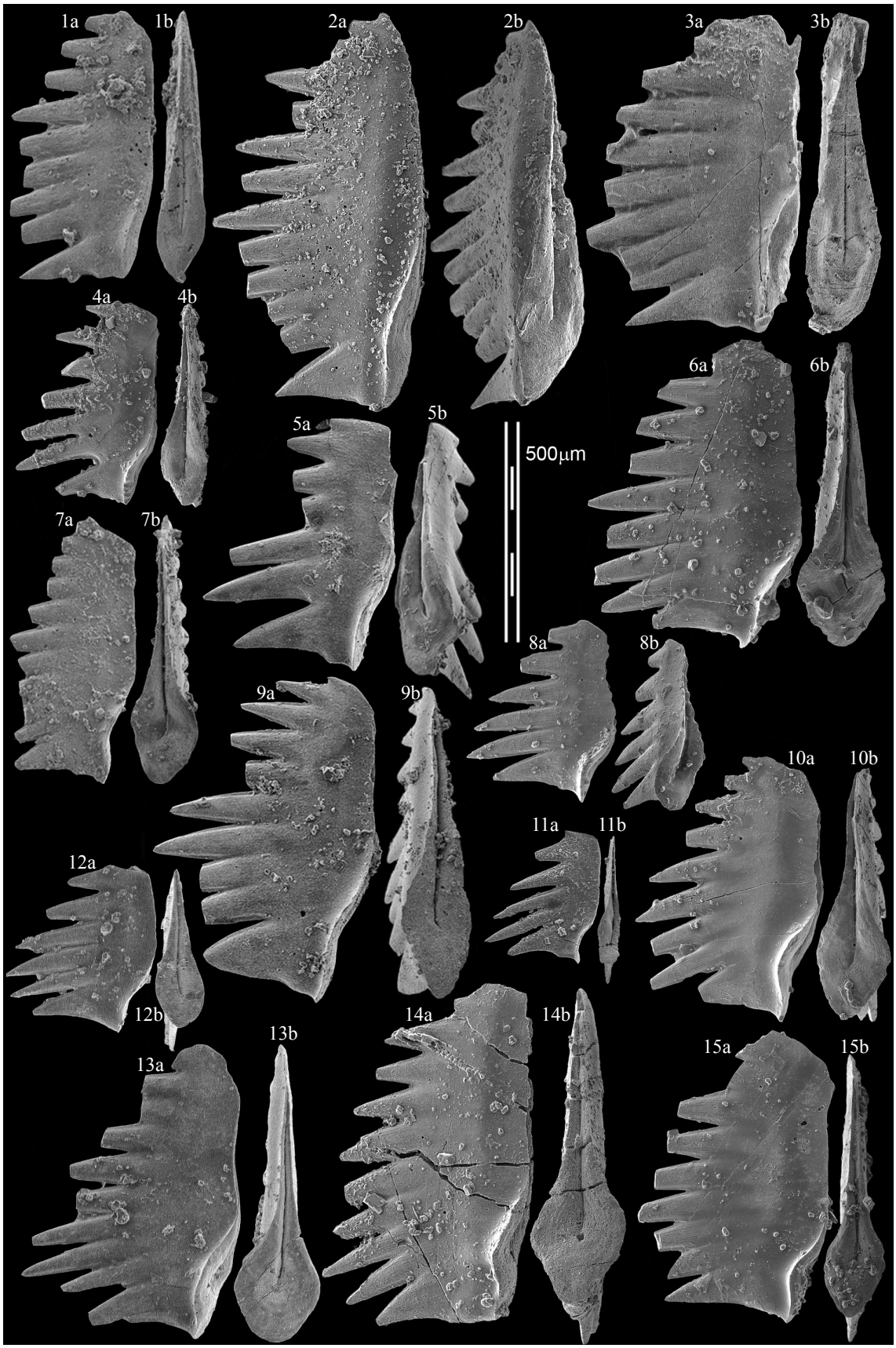
1a
1b
2a
2b
3a
3b
4a
4b
5a
5b
500µm
6a
6b
7a
7b
8a
8b
9a
9b
10a
10b
11a
11b
12a
12b
13a
13b
14a
14b
15a
15b

PLATE 7

PLATE 8

Figs. 1, 12. *Ns*. aff. *cristagalli* morphotype 4. 1: Mud33, 12: M05-10.
Fig. 2. *Ns*. aff. *cristagalli* morphotype 2. M05-10.
Figs. 3, 4. *Ns*. aff. *cristagalli* morphotype 5. 3: Mud9; 4: Mud33.
Figs. 5, 10. *Ns*. aff. *cristagalli* morphotype 6. 5: Mud33, 10: M05-10.
Figs. 6, 8. *Ns*. aff. *cristagalli* morphotype 10. Both Mud33.
Fig. 7. *Ns*. aff. *cristagalli* morphotype 9. Mud33.
Figs. 9, 11. *Ns*. aff. *cristagalli* morphotype 7. Both Mud33.

All P1 elements, all ×80.

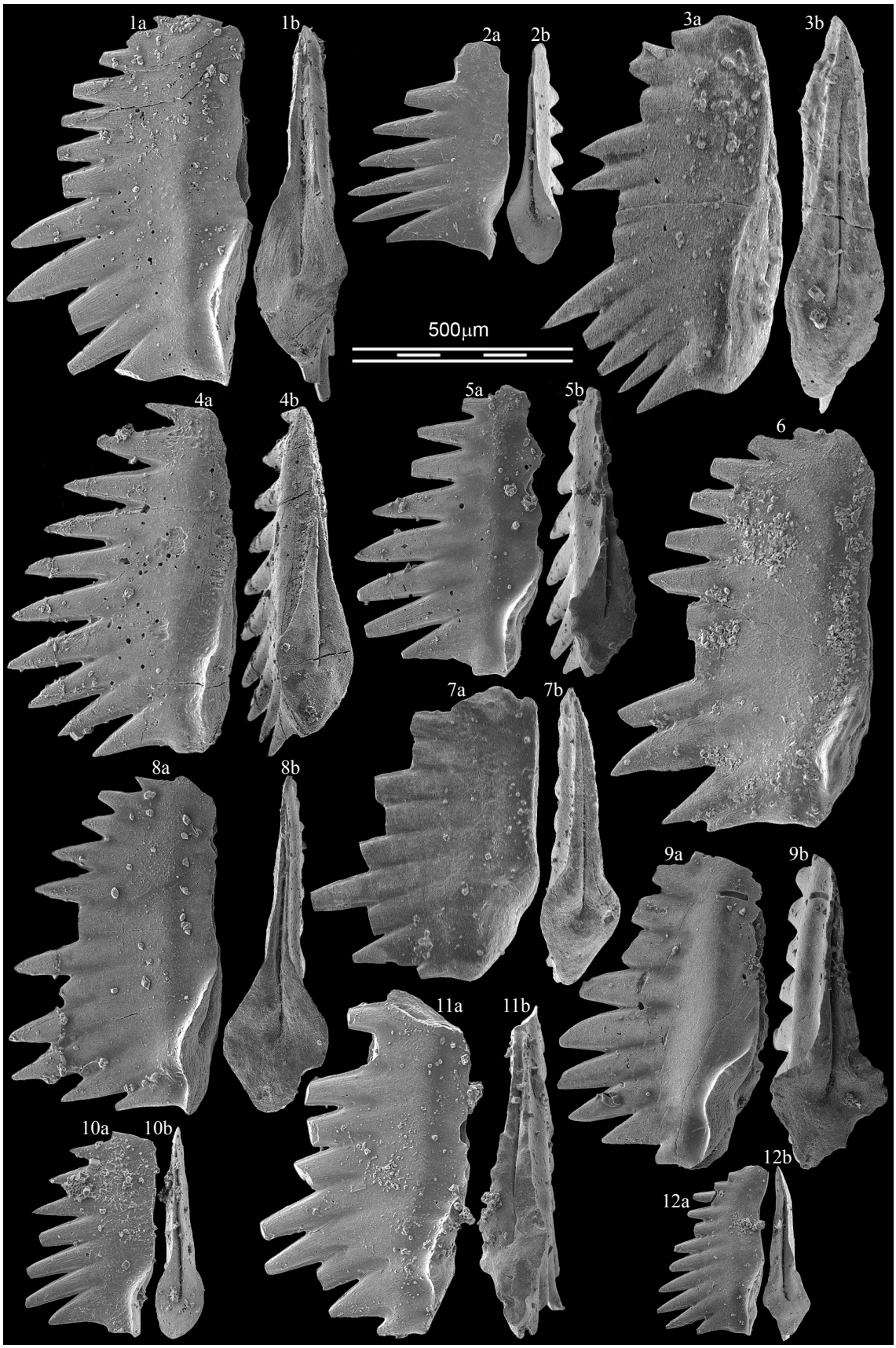
1a
1b
2a
2b
3a
3b
500μm
4a
4b
5a
5b
6
7a
7b
8a
8b
9a
9b
10a
10b
11a
11b
12a
12b

PLATE 8

PLATE 9

Figs. 1-3, 5, 6, 9. *Ns*. n. sp. U. 1: M04A-13A2; 2, 6: M03-15; 3, 5, 9: M03-16A.
Figs. 4, 7, 8, 10-12. *Ns*. *spitiensis* Goel. 4, 8, 10: M03-16A; 7, 11, 12: M03-15.

All P1 elements, all ×80.


1a
1b
2a
2b
3a
3b
500μm
4a
4b
5a
5b
6
7
8a
8b
9a
9b
10a
10b
11a
11b
12a
12b

PLATE 9

PLATE 10

Fig. 1. *Ns*. cf. *spitiensis* Goel. Mud33.
Fig. 2. *Ns*. n. sp. 2. M03-16A.
Fig. 3. *Ns*. n. sp. 3. M05-10.
Fig. 4. *Nv*. *pakistanensis* 4. M03-12C.
Figs. 5, 6. *Ns*. n. sp. S. Both M03-16A.
Fig. 7?, 11.transitional to *Nv*. *waageni* 9. 7: M04-14A; 11: M04-12BC.
Fig. 8. *Nv*. aff. *pakistanensis* 1. M04-13B1.
Fig. 9. *Nv*. *posterolongatus*. M03-13A.
Fig. 10. *Nv*. aff. *pakistanensis* 2. M03-13A.

All P1 elements, all ×80.


1a
1b
2a
2b
3a
3b
6a
6b
5a
5b
4a
4b
7
10a
9a
9b
10b
8a
8b
11a
11b
500µm

PLATE 10

PLATE 11

Fig. 1. *Nv*. *latiformis* 2?. M03-13B.
Fig. 2, 6. *Nv*. *pakistanensis* 2?. 2: M04-13A;.6: M04A-13A1.
Figs. 3?, 10, 13. *Nv*. *pakistanensis* 4. 3: M04A-13B1; 10, 13: M04A-13A3.
Figs. 4, 9. *Nv*. aff. *pakistanensis* 4. 4: M04A-13A1; 9: M04A-13A2.
Fig. 5. transitional between *Ns*. *spitiensis* and *Ns*. n. sp. S.
Figs. 7, 8. *Nv*. *pakistanensis* 3. 7: M04A-13A1; 8: M03-13A.
Fig. 11. *Nv*. *waageni* 10. M04A-13A3.
Fig. 12. *Nv*. *waageni* 9. M08-12C.
Fig. 14. *Nv*. aff. *posterolongatus*. M04A-13A3.

All P1 elements, all ×80.

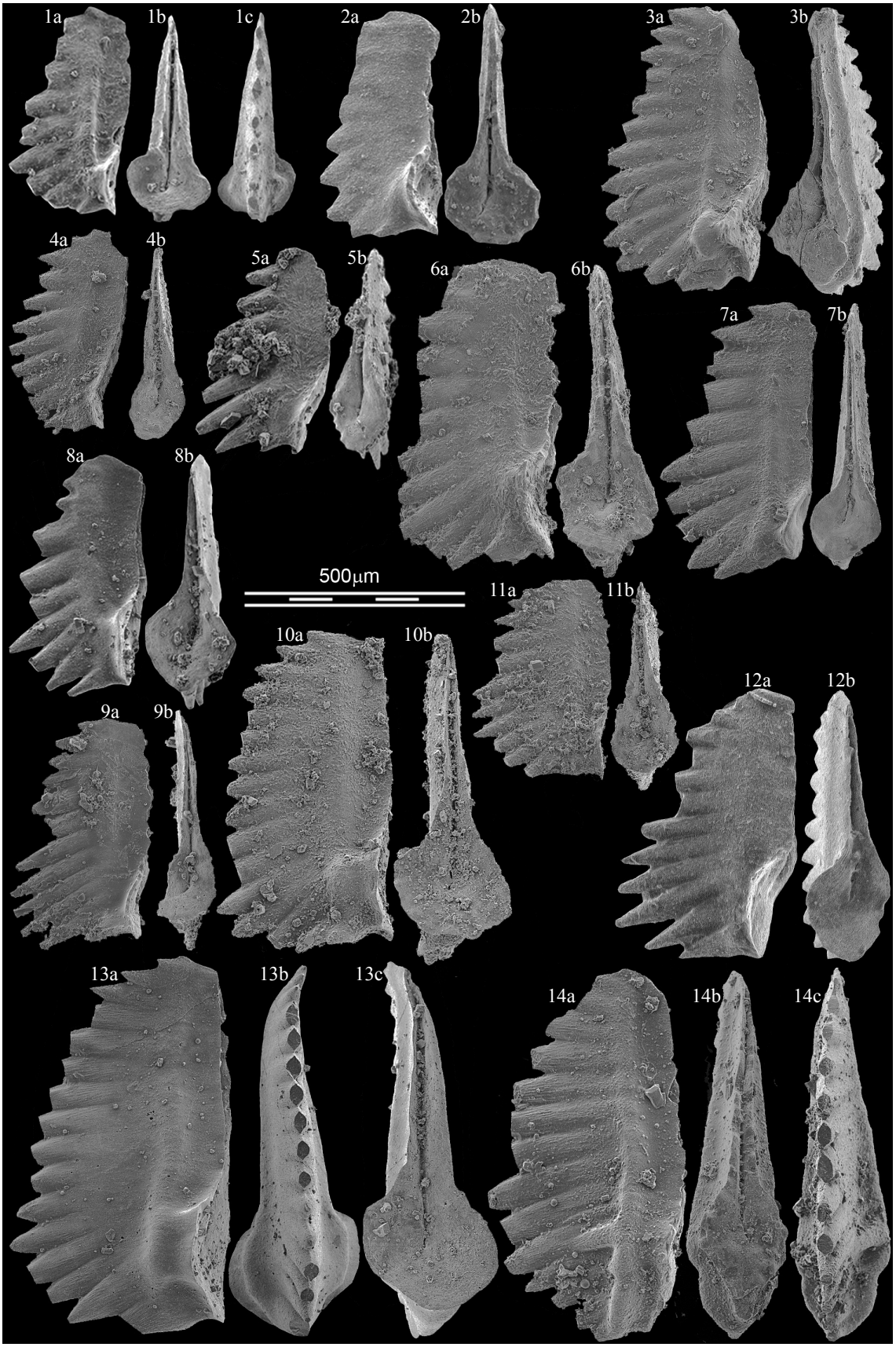
1a
1b
1c
2a
2b
3a
3b
4a
4b
5a
5b
6a
6b
7a
7b
8a
8b
500μm
11a
11b
10a
10b
12a
12b
9a
9b
13a
13b
13c
14a
14b
14c

PLATE 11

PLATE 12

Fig. 1. *Nv*. *latiformis* 1. M03-13A.
Figs. 2, 6?. *Nv*. *latiformis* 2. 2: M03-13A; 6: M03-15.
Fig. 3. *Nv*. *waageni* 3. M03-13B.
Fig. 4. *Nv*. *waageni* 6. M03-15.
Fig. 5. *Nv*. *waageni* 9. M03-16A.
Figs. 7?, 8. *Nv*. *waageni* 2. 7: M03-14A; 8: M04-14C.
Figs. 9, 15, 17. *Nv*. *waageni* 4. 9: M03-16A; 15: M03-14A; 17: M04-14C.
Figs. 10-13, 14?. *Nv*. *waageni* 5. 10: M04-15B; 11: M03-15; 12, 13, 14: M03-16A.
Fig. 16. *Nv*. *waageni* 8. M04-13A3.

All P1 elements, all ×80.

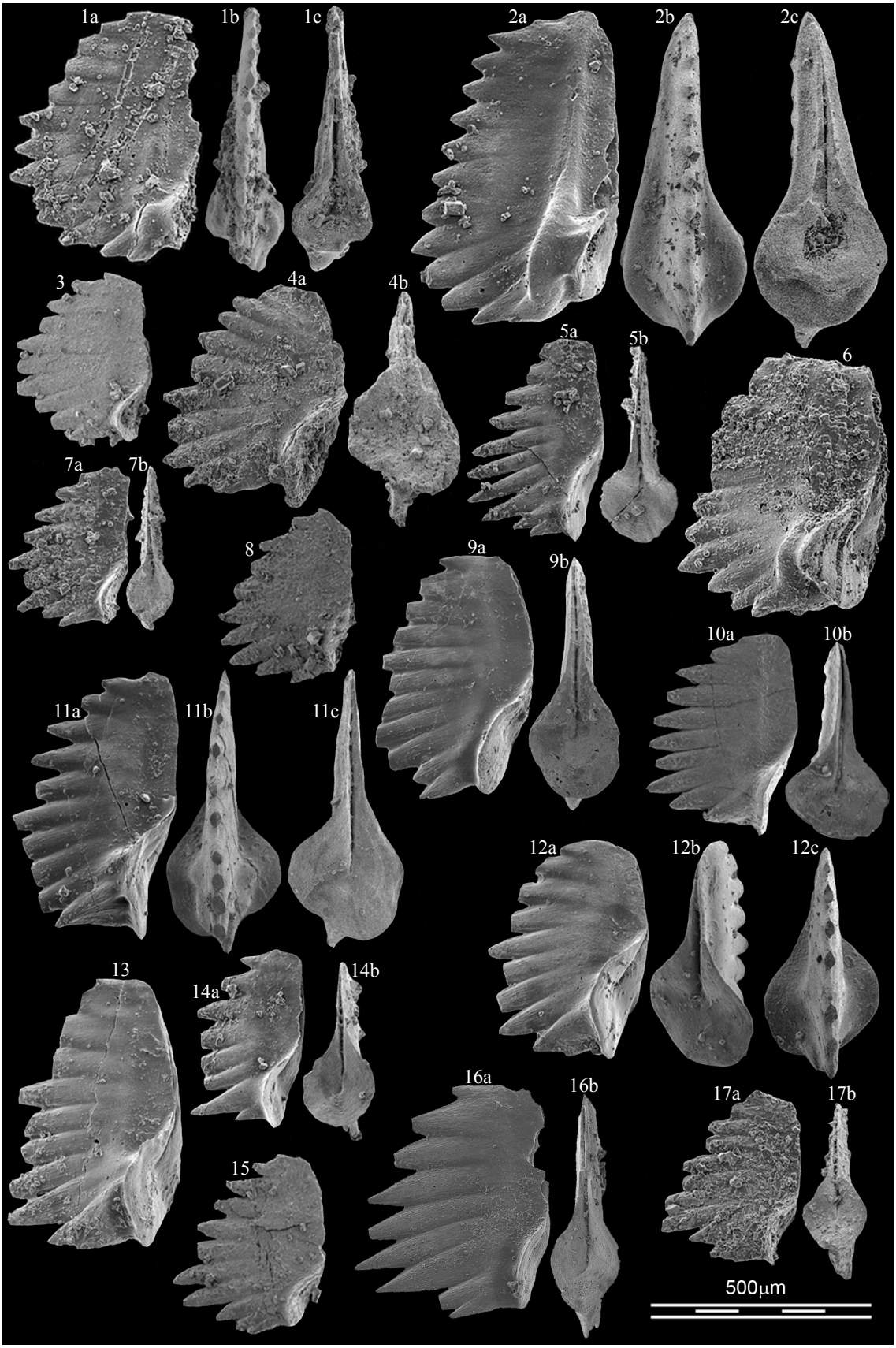
1a
1b
1c
2a
2b
2c
3
4a
4b
5a
5b
6
7a
7b
8
9a
9b
10a
10b
11a
11b
11c
12a
12b
12c
13
14a
14b
15
16a
16b
17a
17b
500μm

PLATE 12

PLATE 13

Figs. 1-4. *Nv*. *waageni* 3. 1, 3, 4: M03-14A; 2: M04A-13B1.
Fig. 5. *Nv*. *waageni* morph indet. M03-14A.
Figs. 6, 7?, 8, 9, 11?, 12?, 13, 14?, 16?, 17, 20-22, 23?, 24, 25, 28?. *Nv*. aff. *pakistanensis* 5. 6, 8, 9, 14, 17, 21, 23-25: M05-10; 7, 11-13, 16, 20, 22, 28: Mud33.
Figs. 10, 15. *Nv*. aff. *pakistanensis* 7. Both M05-10.
Figs. 18, 26?. *Nv*. aff. *pakistanensis* 4. Both M05-10.
Fig. 19?, 27?, 29. *Ns*.? n .sp. 4. All Mud33.

All P1 elements, all ×80.

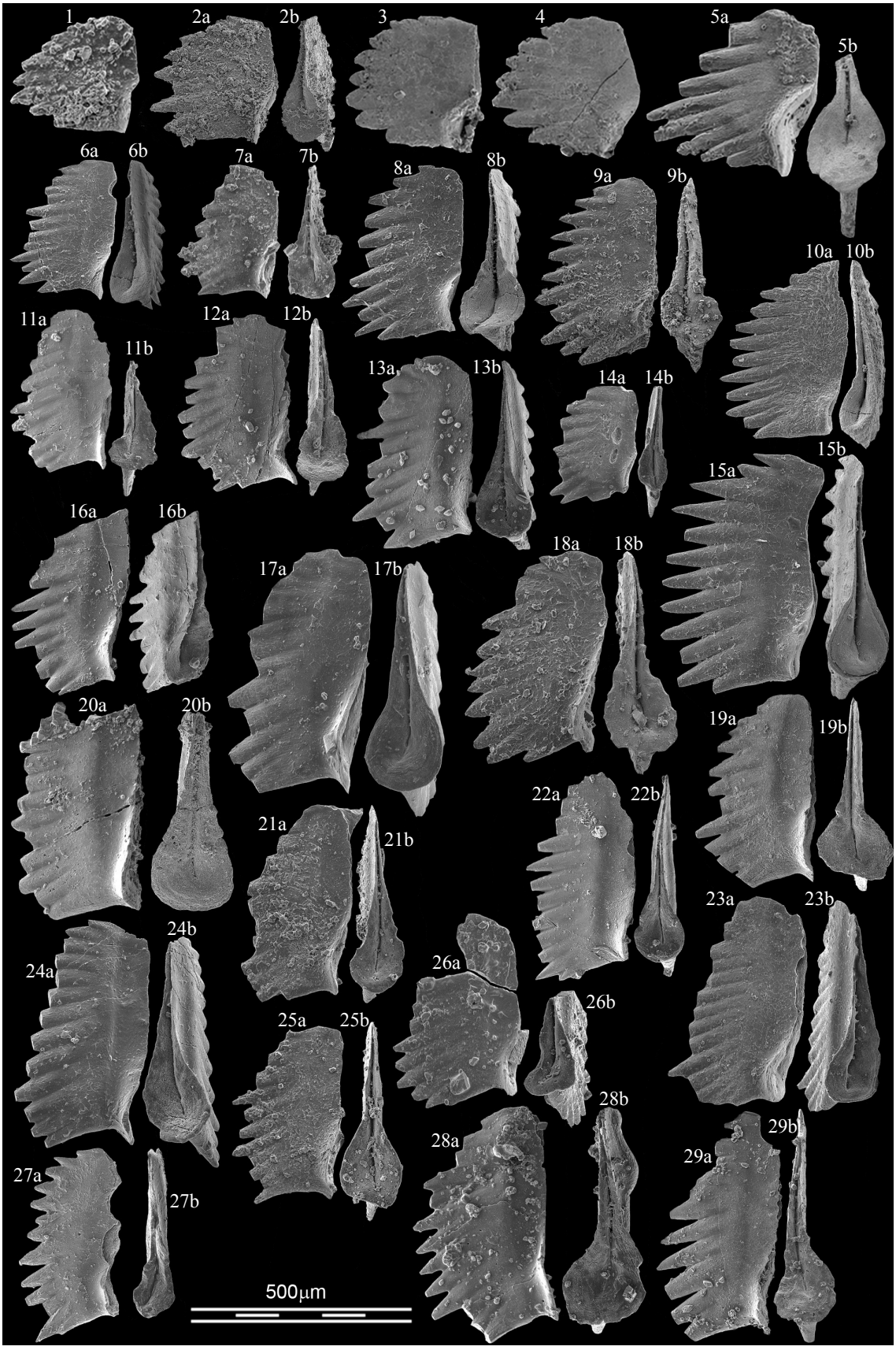
1
2a
2b
3
4
5a
5b
6a
6b
7a
7b
8a
8b
9a
9b
10a
10b
11a
11b
12a
12b
13a
13b
14a
14b
15a
15b
16a
16b
17a
17b
18a
18b
19a
19b
20a
20b
21a
21b
22a
22b
23a
23b
24a
24b
25a
25b
26a
26b
27a
27b
28a
28b
29a
29b
500μm

PLATE 13

PLATE 14

Figs. 1, 5, 7?. *Ns*. aff. *dieneri* ?. 1, 5: M05-10; 7: M04-10.
Figs. 2, 4. *Nv*. aff. *waageni* 6. 2: Mud33; 4: M05-10.
Figs. 3, 12, 21. *Nv*. aff. *waageni* 5. All Mud33.
Figs. 6, 8?, 9, 10?, 11, 13?, 15?, 16, 22?, 24, 25. *Nv*. aff. *waageni* 4. 6, 10, 13, 15: M05-10; 8, 9, 11, 16, 22, 24, 25: Mud33.
Figs. 14, 20. *Nv*. aff. *waageni* 1. 14: M05-10; 20: Mud33.
Figs. 17, 18. *Nv*. aff. *waageni* 2. Both Mud33.
Figs. 19, 23. *Nv*. aff. *waageni* 3. Both Mud33.

All P1 elements, all ×80.

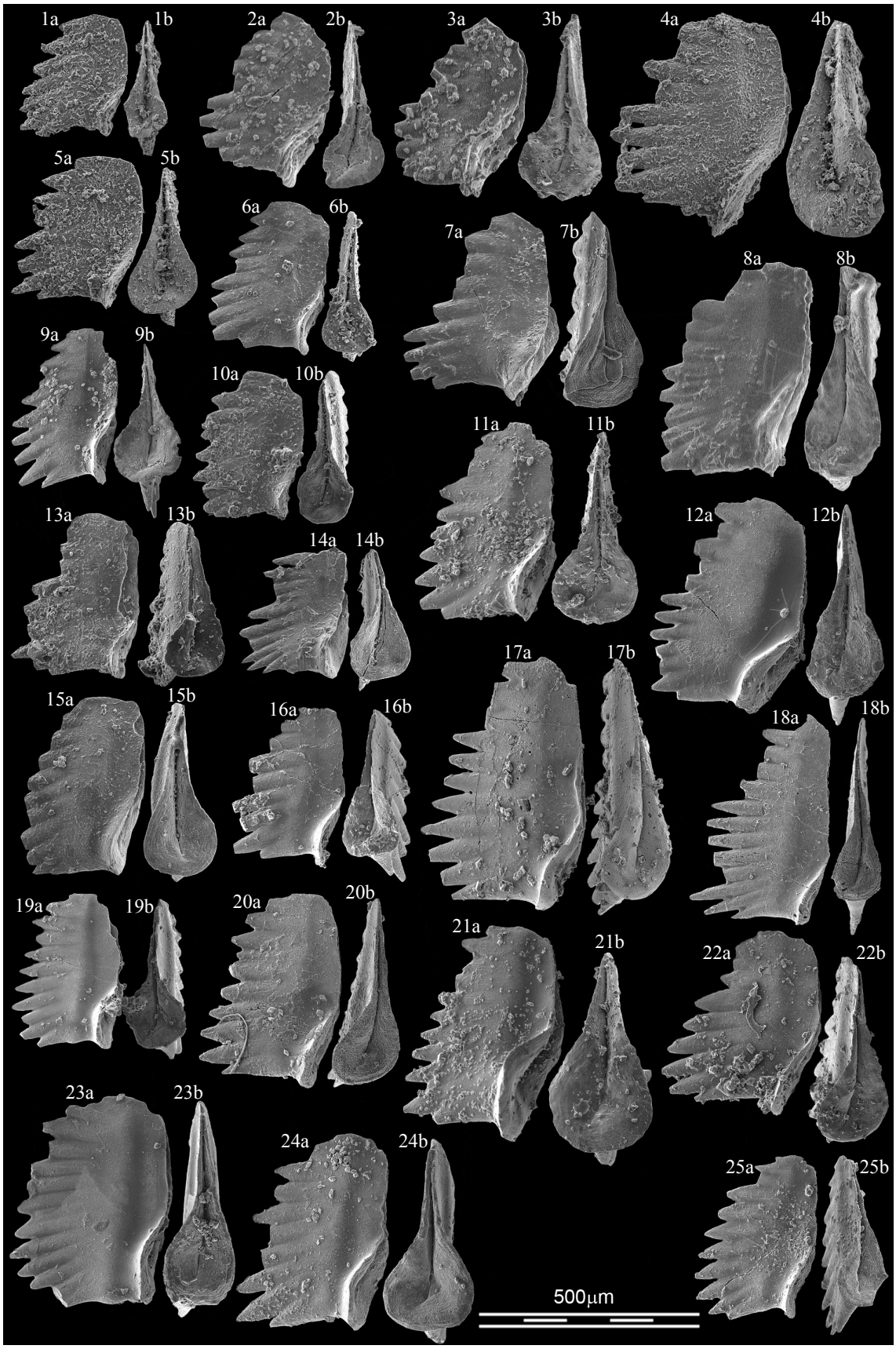
1a
1b
2a
2b
3a
3b
4a
4b
5a
5b
6a
6b
7a
7b
8a
8b
9a
9b
10a
10b
11a
11b
12a
12b
13a
13b
14a
14b
15a
15b
16a
16b
17a
17b
18a
18b
19a
19b
20a
20b
21a
21b
22a
22b
23a
23b
24a
24b
25a
25b
500μm

PLATE 14

Objects without names cannot be talked about or written about; without description they cannot be identified and such knowledge as may have accumulated regarding them is sealed.

Gahan (1923:73), quoted in Winston (1999:115)

CHAPTER 5

Gahan, A. B. 1923. The role of the taxonomist in present day entomology. Proc., Entomological Society of Washington 25: 68-78.

Winston, J. E. 1999. Describing Species: Practical Taxonomic Procedure for Biologists. Columbia University Press, New York.

Early Triassic conodont faunas from the Dienerian/Smithian boundary beds at Waili (Guangxi, China)

N. Goudemand[1], H. Bucher[1]

[1]Paläontologisches Institut und Museum der Universität Zürich, Karl Schmid-Strasse 4, CH-8006 Zürich, Switzerland.

Bed by bed conodont sampling around the Induan/Olenekian boundary at a section near Waili, northern Guangxi, South China led to rich and well-preserved collections that enabled the description of one new genus (*Larenella*), 23 new species, as well as about 40 other new forms let in open nomenclature. Based on our revised taxonomy, we recognize 5 informal biozones (in ascending order: the *Neospathodus circulocta-vus* beds, the *Larenella chaohuense* 2 beds, the *Novispathodus gnomarcuatus* beds, the *Larenella* beds and the *Eurygnathodus costatus* beds), which correlate very well with the revised sequences of both Mud and Chaohu, the two GSSP candidates sections for the definition of the IOB. These results partly confirm the lateral reproducibility of the biochronological scheme recently proposed for Mud. Furthermore, here too the first typically Smithian faunas occur within the *Nv. gnomarcuatus* sp. nov. (previously *Nv*. aff. *waageni* 1) beds and this strongly suggest that the IOB should optimally be placed just below this horizon.

Key words: Early Triassic, Induan/Olenekian boundary, GSSP, conodonts.

The marine Permo-Triassic boundary (PTB) record is well preserved in South China and has attracted much attention, especially since the official approval of the Meishan section as the Global Stratotype Section and Point (GSSP) for the base of the Triassic (Yin *et al*., 2001). Similarly, a section at Chaohu, Anhui Province (Tong *et al*., 2003, 2004) has been proposed as the GSSP for the definition of the Induan-Olenekian boundary (IOB). Indeed, the sedimentary record in Chaohu is nearly complete from the PTB to the base of the Middle Triassic and quite rich in fossils including ammonoids, bivalves and conodonts. In particular, thousands of thermally altered (black) but fairly well-preserved conodonts were recovered over the last years from this area (Zhao *et al*., 2007, 2008a, 2008b), and the produced IOB conodont sequence in Chaohu is considered by many to be the most complete. However, like in Meishan, the ammonoid record of Chaohu is very poor: ammonoids are usually too badly preserved for allowing any reliable determination. Since 2004, some of us have been investigating extensively other regions of South China, especially northwestern Guangxi and southern Guizhou, in order to re-assess previously documented ammonoid successions (Chao 1950, 1959). These investigations led to the discovery of several new Early Triassic ammonoid faunas (Brayard *et al*., 2007; Brayard and Bucher, 2008; Brühwiler *et al*., 2008; Bucher *et al*., in prep.). Many conodonts were also recovered from these

sections, which allowed the construction of intercalibrated ammonoid-conodont scales for the Early Triassic (Goudemand *et al*., in prep.). In this Chapter 4, we present the first conodont results concerning the Jinya/Waili area (northwestern Guangxi). We here focus on the taxonomy and biochronology of the IOB conodont faunas, which we then compare with those from the two GSSP candidates: Chaohu (China) and Mud (Himashal Pradesh, India).

2. Geological setting

During Early Triassic times the Waili area was located close to the equator, on the eastern side of the Tethys Ocean (e.g. Smith *et al*., 1994) (Fig. 1). The Jinya/Waili area is located within the Nanpanjiang Basin in the northwestern Guangxi Province, South China (Fig. 2). A composite section of this area with the main lithological and formational subdivisions is shown in Fig. 3. Late Permian skeletal reef limestones of the Wujiaping Fm. are overlain by the ~80 m thick, ammonoid- and conodont-rich Early Triassic mixed carbonate-siliciclastic series of the Luolou Fm. (see Galfetti *et al*., 2008 for a comprehensive description). The described faunas were retrieved from rocks collected

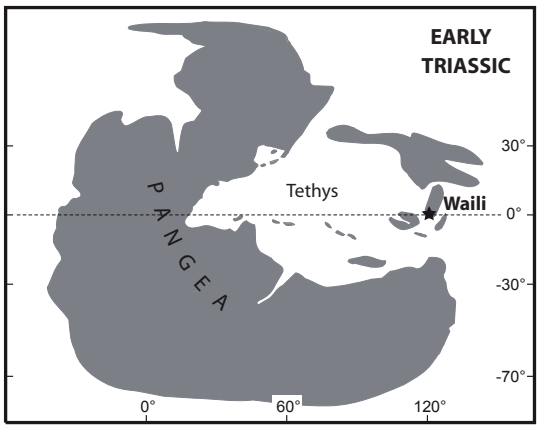

Fig. 1. Simplified Early Triassic palaeogeography (modified after Brayard et al., 2006) and position of South China Block.

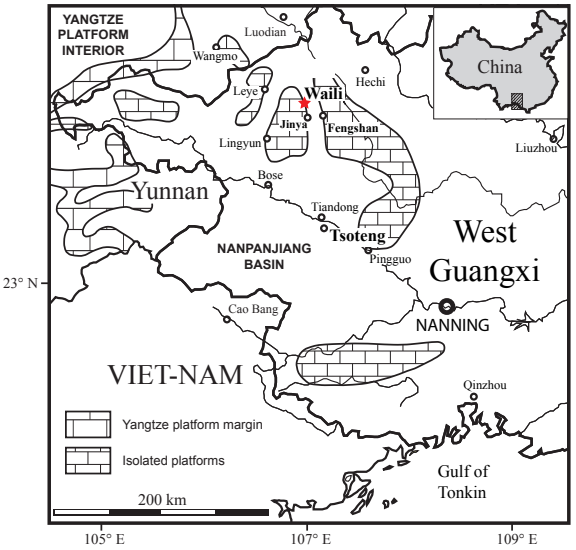

Fig. 2. Location of the Waili cave section, Waili/Laren, northwestern Guangxi, South China.

at the 'cave section' (*ibid*) within the uppermost part of Unit II (*ibid*) up to three meters below the prominent "*Flemingites rursiradiatus*" beds (see Fig. 4). These rocks represent 4 meters of strata straddling the IOB.

3. New conodont faunas

Figure 4 gives the detailed conodont stratigraphic distributions within the critical interval at Waili.

We have recently (Goudemand *et al*., Chapter 4) started to differentiate numerous new morphotypes of the important *Neospathodus* ex gr. *dieneri*, *Ns*. ex gr. *cristagalli*, *Novispathodus* ex gr. *pakistanensis* and *Nv*. ex gr. *waageni* taxa. Here, we distinguish 5 new morphotypes of *Ns*. *dieneri*.

Based on well preserved specimens from Beds W146-C7 and W147-C2, we also formally describe 6 new species that correspond to the forms previously assigned to *Novispathodus* aff. *waageni* (morphotype 1) and *Nv*. aff. *pakistanensis* (morphotype 5). These new forms are known also from Mud, Spiti, India and from Chaohu, South China and allow defining an informal earliest Smithian biozone (*Nv*. *gnomarcuatus* beds,

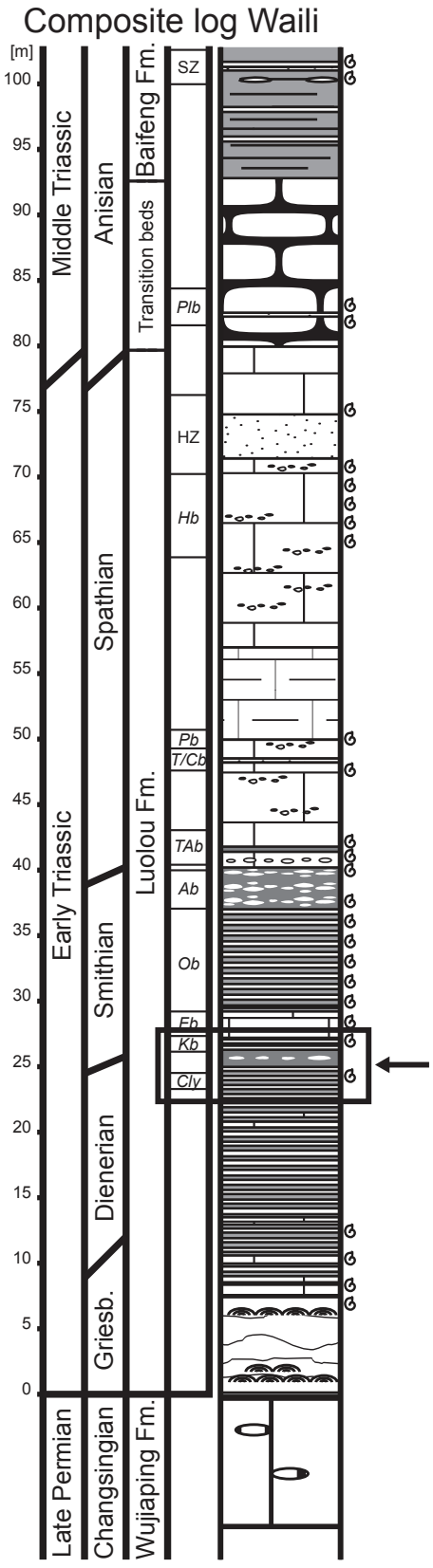

Fig. 3. Composite stratigraphic section at Waili/Laren, northwestern Guangxi, South China (see Galfetti *et al*., 2008 for a detailed description).

see below).

Seventeen additional new species are described too. Most of these belong to *Larenella* gen. nov., a new genus with close affinities with both *Guangxidella* and *Wapitiodus*, by which the P1 element is a robust, segminate element. Relatively abundant and very well preserved specimens of this group occur in samples WAI61 and W148-C3, which allows their description herein. Relatively rare specimens of some of these new species occur also in Mud, Spiti (see below). This observation was made rather late during completion of the present study and after completion of our description of the material from Mud (Goudemand et al., Chapter 4). This explains why they were not described in the latter. Nevertheless, a completed, emended occurrence table of the Mud material is provided here (Fig. 5) and discussed below.

Strikingly, relatively many ellisonid P1 elements were recovered from the Waili cave section (see Pl. 10). These forms are otherwise very rare and barely documented in the literature. Consequently most of these are new. Apparently some of them occur also in Chaohu (Zhao, unpublished material) and they may have some biostratigraphic value (see below in part 6).

4. Discussion

Based on figure 4 (confirmed occurrences only), we recognize five local maximal horizons in the Waili cave section. An informal biozone can be associated with each of these local maximal horizons. These are color coded in figures 4-6. Obviously the same colors are used also for Mud and Chaohu in order to visually enhance correlations. Pending thorough assessment of their lateral reproducibility in other basins (ongoing work), these biozones are not introduced as formal zones and are here termed ‘beds’ instead. They are association zones sepa-

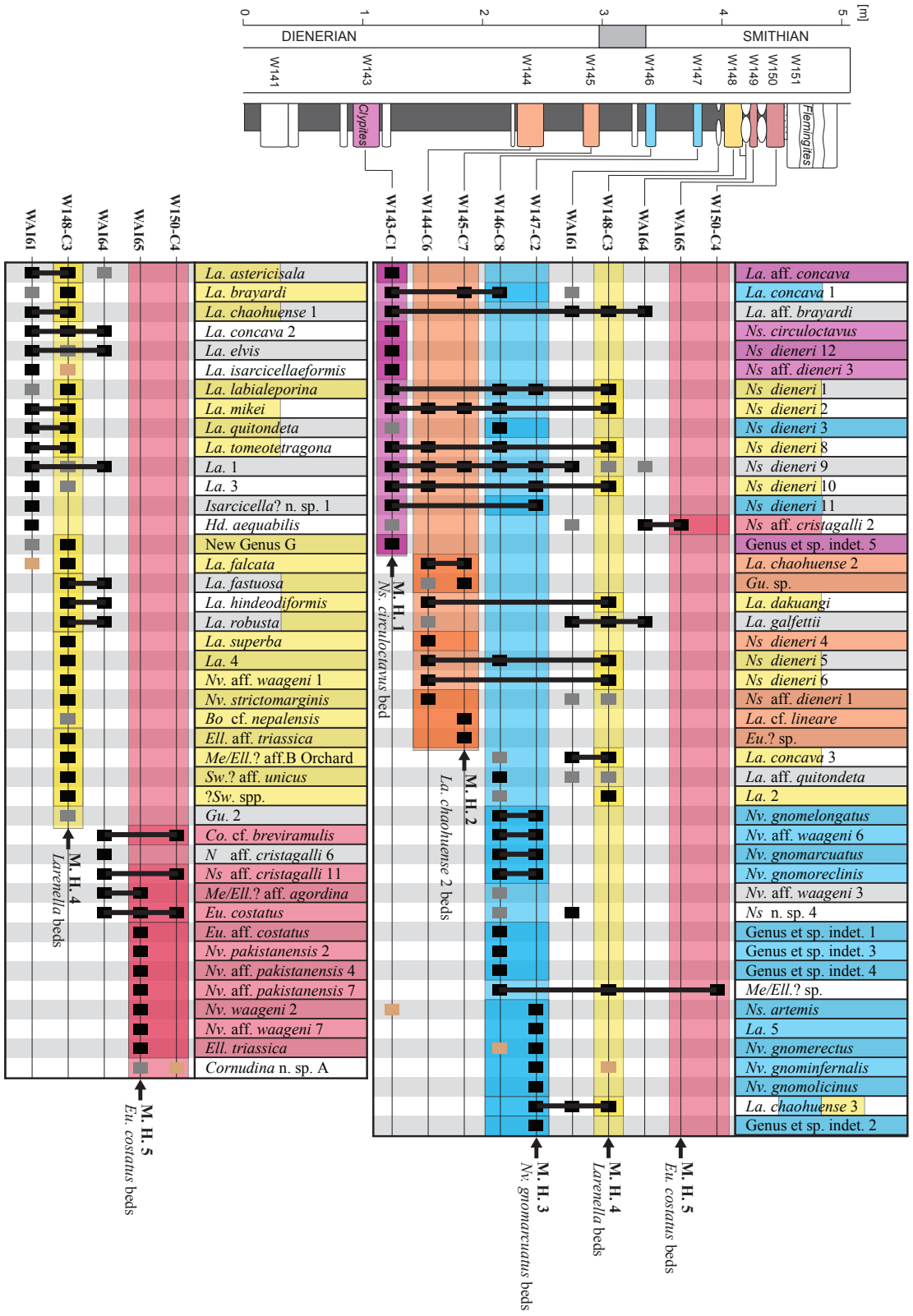

Fig. 4. Detailed stratigraphic section of the Dienerian/Smithian boundary at Waili/Laren with the distribution of conodont taxa and indicated local maximal horizons. Black rectangles correspond to confirmed occurrences, gray (50%) rectangles indicate occurrences based on fragmentary or poorly preserved material, and light gray (25%) rectangles indicate occurrences of new, undescribed specimens showing affinity with the corresponding taxa.

rated by interval of uncertainty, and each one is characterized by the exclusive occurrence of species and/or pairs of species. Instead of listing below all characteristic elements for each association zone, the reader is referred to figure 4, where the latter are displayed in a color-coded, domino-like way in the upper row (see Chapter 4 for explanations). For instance the local co-occurrence of *La*. *mikei* (yellow lower half) with *La*. *fastuosa* (yellow upper half) identifies the *Larenella* beds (coded in yellow). *La*. *superba* (all yellow) is in itself a characteristic element of the latter zone.

In ascending order, we have the following local faunal succession: the *Neospathodus circuloctavus* beds, the *Larenella chaohuense* 2 beds, the *Novispathodus gnomarcuatus* beds, the *Larenella* beds and the *Eurygnathodus costatus* beds. Note that strictly speaking, WAI61 and WAI64 are two additional local maximal horizons. Yet, a closer look shows that the former differs from the *Larenella* beds only by a few species whose range can be considered to be underestimated, and the corresponding questionable occurrences suggest that it actually belongs to the *Larenella* beds. The latter in turn contains a mixed fauna with affinities with both the *Larenella* beds and the *Eu*. *costatus* beds. Because this sample corresponds to ammonoids matrices that were sampled (see Brayard and Bucher, 2008) within and on the upper surface of Bed W148-C3 (*Larenella* beds), in contact with the somewhat nodular limestone horizon WAI65 (*Eu*. *costatus* beds), it is not clear whether this mixing is due to sampling or whether it actually reflects co-occurrence of these faunas during a certain amount of time. In the latter case it would deserve a separate association zone.

Figures 5 and 6 give the detailed conodont stratigraphic distributions at the IOB GSSP candidates sections of Mud and Chaohu (West Pingdingshan). Mud's occurrence table is a revised version of the one we published recently (Goudemand *et al*., Chapter 4). It takes into account the new species we create herein. We were not able to see Chaohu's collections yet, so Figure 6 integrates only determinations made from illustrations (Zhao *et al*., 2005, 2007, 2008a, b, and unpublished material). The *Novispathodus gnomarcuatus* beds and the *Eurygnathodus costatus* beds are easily recognized in all sections. As previously stated (Goudemand *et al*., Chapter 4), the *Novispathodus gnomarcuatus* beds have a Smithian affinity and correspond to an upper bound for the location of the IOB. In Mud, it is not possible to set any lower bound using only conodonts but ammonoids enable to constrain the IOB within a 10cm-thick interval below the *Nv. gnomarcuatus* beds. Waili's *La*. *chaohuense* 2 beds, whose fauna is dominated by the 'Dienerian' *Ns*. ex gr. *dieneri* and does not contain any conodont of obvious Smithian affinity, should most probably be considered Dienerian in age. This would constrain the IOB in Waili within a 40cm-thick interval between Bed W145 and Bed W146. Note that about one and half meter below this interval, Bed W143 (*Ns. circuloctavus* beds) contains *Clypites* (not *Hedenstroemia hedenstroemi*, corrected after Brayard and Bucher, 2008), a typical Dienerian ammonoid. In Chaohu, such lower bound could potentially be provided by the relative early occurrences of '*Ns*'. *chaohuensis* and *Ns. chii* in Bed 23 (see Fig. 6, M. H. 1) and Beds 23-24 respectively. Yet, the former occurs also much higher, up to the *Larenella* beds in Waili; and the latter is too poorly illustrated and described. If our understanding of *Ns. chii* is correct, then it occurs also in Bed 10 (sample Mud33, *Nv. gnomarcuatus* beds) in Mud. It does not seem to occur in Waili. Our *Ns*. *artemis* sp. nov., which is morphologically close, occurs in Bed W147 within the *Nv. gnomarcuatus* beds. Hence, as far as enabled by the limited illustrated data, the IOB in Chaohu appears relatively badly constrained.

La. *chaohuense* 2, a characteristic el-

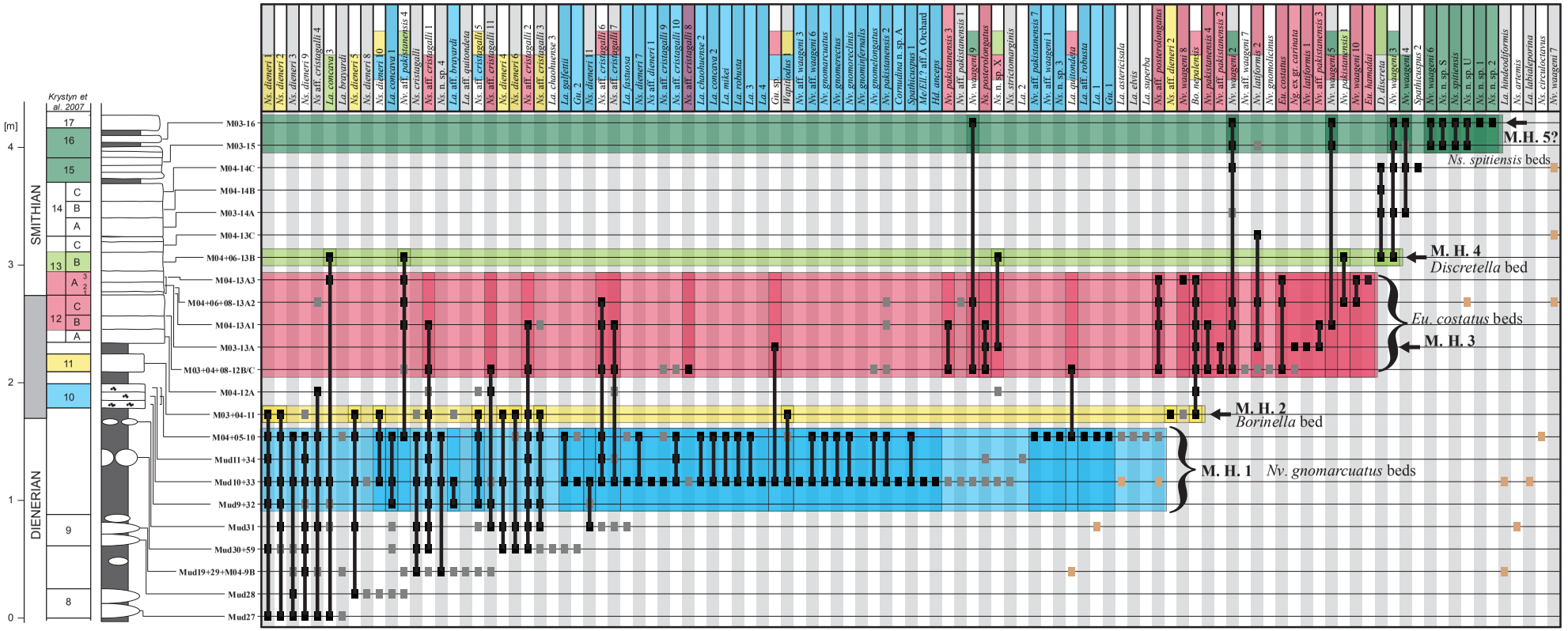
Krystyn et al. 2007
[m]
SMITHIAN
DIENERIAN
M03-16
M03-15
M04-14C
M04-14B
M03-14A
M04-13C
M04+06-13B
M04-13A3
M04+06+08-13A2
M04-13A1
M03-13A
M03+04+08-12B/C
M04-12A
M03+04-11
M04+05-10
Mud11+34
Mud10+33
Mud9+32
Mud31
Mud30+59
Mud19+29+M04-9B
Mud28
Mud27
M.H. 5?
Ns. spitiensis beds
M. H. 4
Discretella bed
Eu. costatus beds
M. H. 3
M. H. 2
Borinella bed
M. H. 1
Nv. gnomarcuatus beds

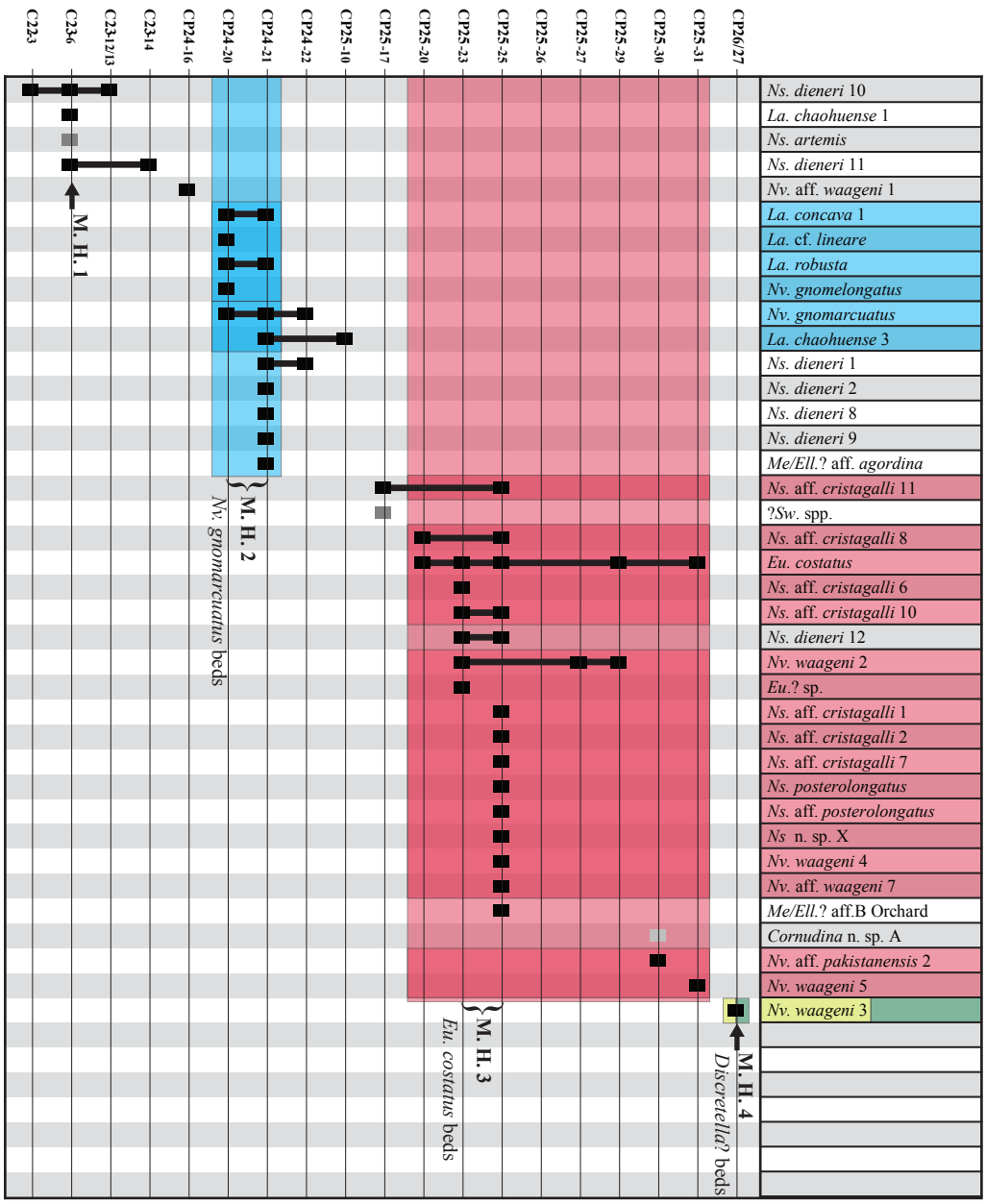

Fig. 6. Detailed stratigraphic section of the Dienerian/Smithian boundary at Chaohu with the revised (and probably incomplete) distribution of conodont taxa and indicated local maximal horizons.

ement of the correlative zone in Waili, occurs in Bed 10 in Mud. This suggests that: 1) its range is still too poorly documented; 2) it is diachronous between Waili and Mud; 3) Bed 10 in Mud is partly condensed (relative to Waili) and correlates both with the *Nv. gnomarcuatus* beds and the *La*. *chaohuense* 2 beds of Waili.

A broken segminiplanate element assigned to *Bo*. cf. *nepalensis* co-occurs in Bed W148 with the last representatives of the *dieneri* group (*Ns*. *dieneri* 1, 2, 5, 6, 10). This association is a characteristic element of the *Borinella* beds in Mud and it suggests that the *Larenella* beds of Waili correlate with the latter. Note that *Bo*. *nepalensis* is

Fig. 5. Detailed stratigraphic section of the Dienerian/Smithian boundary at Mud, Spiti with the distribution of conodont taxa and indicated local maximal horizons.

considered a boreal species. This very rare and still questionable occurrence is the first report of this species in the equatorial realm. Note that there is no equivalent of either the *Larenella* beds or the *Borinella* beds in Chaohu.

Above the *Eu. costatus* beds, we recognized two local maximal horizons in Mud (Goudemand *et al.*, Chapter 4) to which we respectively associated the *Discretella* beds and the *Ns. spitiensis* beds. *Nv*. *waageni* 3 (alias '*Ns*. *waageni eowaageni*', type subspecies, not the presumed early forms, which are here assigned to *Nv*. *gnomarcuatus* sp. nov.) occurs there from the base of the Discretella beds and ranges into the *Ns*. *spitiensis* beds. Hence, its occurrence from Bed 26 at the West Pingdingshan section suggests that one or both association zones occur in Chaohu too. In the Waili cave section, the *Flemingites* beds were not sampled but these beds are easily traced over large distances within the Jinya/Waili area and samples from other nearby localities show that in this region too this species occurs above the *Eu*. *costatus* beds, within the *Flemingites* beds, together with *Discretella discreta*.

To summarize, the conodont sequence of the IOB interval at the Waili section agrees very well with that in Mud (so far the best known sequence for this boundary) and is of similar biochronological resolution. The proposed biochronological scheme is thus laterally reproducible over large distances across the Tethys. It needs to be now confirmed in other places, in particular in the Salt Ranges from where we have large collections of beautifully preserved conodonts (in particular topotype material of some of the most important taxa of this interval), and where the ammonoid biozonation around the Dienerian/Smithian boundary is currently the best resolved (Brühwiler and Bucher, accepted).

Finally, note that besides these important biostratigraphical considerations, the rich collections of Waili and in particular the discovery of the *Larenella* group have also numerous implications for our understanding of the conodont radiation during this critical time interval. This is partly discussed in part 6 and will be developed in a future, synthetic paper.

5. Conclusions

Several new, well-preserved conodont faunas have been recovered from a section near the village of Waili, northwestern Guangxi, South China. They led to the description of one new genus and 23 new species, as well as about 40 other new forms let in open nomenclature. It enabled us to recognize 5 informal biozones (in ascending order: the *Neospathodus circuloctavus* beds, the *Larenella chaohuense* 2 beds, the *Novispathodus gnomarcuatus* beds, the *Larenella* beds and the *Eurygnathodus costatus* beds). At least one additional, overlying biozone (the '*Nv*. *waageni* 3 and *Discretella*' beds) is known from nearby, correlatable sections. The proposed biochronological scheme is recognized also in the two IOB GSSP candidate sections of Mud and Chaohu. The latter is considered to be less resolved and less constrained in terms of location of the boundary itself. In Waili, the IOB is located within a 40cm-thick interval between Bed W145 and Bed W146.

6. Systematic palaeontology (N. Goudemand)

Suprageneric classification mostly follows Donoghue *et al.* (2009).

Class CONODONTA Eichenberg, 1930
Division PRIONIODONTIDA Dzik, 1976
Order OZARKODINIDA Dzik, 1976
Superfamily GONDOLELLOIDEA (Lindström, 1970)
Family GONDOLELLIDEA Lindström, 1970

Subfamily CORNUDININAE Orchard, 2005

Genus CORNUDINA Hirschmann, 1959

Type species and holotype. *Ozarkodina breviramulis* Tatge, 1956, p. 139, pl. 5, fig. 12a-b.
Type stratum and locality. Lower Muschelkalk, Kalkwerk Quarry, Trubenhausen, Germany.

Original diagnosis and type species. Based on a small angulate P2 element with a large and prominent medial cusp and very short upturned processes (Hirschmann, 1959, p. 44).
Multielement diagnosis. We follow here the interpretation of *Cornudina* by Orchard (2005), where the P1 element has a long cusp, at least twice the length of the adjacent denticles, a very short anterior process, and a broadly excavated basal cavity (Orchard 2005).
Remarks. As noted by Orchard (2005, 2007), it is not certain whether this genus (as reconstructed from Spathian collections) belongs to *Cornudina*. This is particularly true for the forms described from the Smithian (see below; see also *Cornudina* sp. A Goudemand and Orchard in Chapter 4) for which no multi-element reconstruction is available yet.

Cornudina*? cf. *breviramulis Tatge, 1956 – Pl. 10, figs. 21, 22.

Specimen on Pl. 10, fig. 21 has a very prominent, unfortunately broken cusp, short posterior and anterior processes and a broad basal cavity and as such it fits the above genus diagnosis. It even closely resembles *Cornudina breviramulis* as illustrated by Koike (1996) except that this element is bilaterally subsymmetrical. Specimen on Pl. 10, fig. 22 on the other hand is clearly asymmetrical, as reflected by its sheared elliptical basal cavity and it is suggestive of a P2 element. It also resembles *Cornudina breviramulis* even more closely than the latter specimen. Consequently we assign them (with some reserve, given the considerable stratigraphic gap with other reported occurrences) to this species, in P1 and P2 positions respectively.
Orchard (2007) reported unusual elements from the late Smithian and early Spathian of North America that he tentatively assigned to *Sweetocristatus*? sp. His illustrated specimen seems to be more laterally flattened than ours but both forms share similarities in their denticulation and overall shape and would be related.

***Cornudina*? sp.** – Pl. 10, fig. 19.

The only available posterior part of this element resembles that of an element found by Zhao at Chaohu in subbed 25-12 (unpublished material), which itself may belong to *Cornudina*.

New Genus G spp. – Pl. 10, figs. 10, 12, 16, 24.

Included here are forms whose P1 element is short with a usually inverted basal cavity of lenticular shape, pointed at both ends, that extends beneath the entire unit. The four or five, broad and long denticles are strongly recurved to the posterior and the posteriormost denticle has usually a subtriangular shape that recalls the otherwise unrelated *Ns. cristagalli* Huckriede. The lower margin is slightly to strongly convex.
Some forms resemble elements assigned by Koike to *Cornudina* (compare for instance Pl. 10, fig. 24 with Koike, 1996, fig. 3, part 2; or Pl. 10, fig. 10 with Koike, 1996, fig. 4, part 11). Yet, though they may fit the original diagnosis of the latter genus (see above), they are clearly excluded from it following our interpretation of that genus (see multi-element diagnosis): the cusp is neither much longer nor broader than adjacent denticles and the basal cavity is not broadly excavated but usually inverted or very shallow (Pl. 10, figs. 12, 16). Koike illustrated only lateral views, which does not allow deciding whether some of his elements may actually belong to or be related with the present genus.

Genus NEOSTRACHANOGNATHUS Koike, 1998

Type species and holotype. *Neostrachanognathus tahoensis* Koike, 1998, p. 127-128, fig. 9.
Type stratum and locality. Taho Limestone (Spathian), Tahokamigumi, Japan.

Original diagnosis and type species. Koike described the genus as a quadrimembrate apparatus composed of an adenticulated and three denticulated nongeniculate coniform elements (Koike, 1998), but his reconstruction was incomplete.
Multielement diagnosis. Agematsu *et al*. (2008) reconstructed the apparatus of the type species

from natural assemblages: the apparatus is bilaterally symmetrical and consists of 7 pairs of elements, three of them being pectiniform elements (P1-3). The S1-4 elements are bipennate ramiforms (e.g. *Oncodella obuti* Buryi 1979) that strongly resemble homologous elements of the Cornudinidae (Orchard, 2007).

***Neostrachanognathus*? sp.** – Pl. 10, fig. 18.

The single occurrence of this badly preserved coniform specimen resembling the P1 element of *N. tahoensis* suggests that the genus is maybe older than previously assumed. This genus is probably a derivative of *Cornudina* (Goudemand *et al*., Chapter 4).

Subfamily MULLERINAE Orchard, 2005

Though they do not necessarily possess the characteristic tertiopedate S3 element, both *Larenella* gen. nov. and *Wapitiodus* are here considered as early representative of this subfamily (see below).

Genus GUANGXIDELLA Zhang and Yang, 1991

Type species and holotype. *Guangxidella typica* Zhang and Yang, 1991, pp. 35-37.
Type stratum and locality. Lower Triassic Luolou Formation, *N. waageni* Zone, Zuodeng (Tsoteng),Tiandong County, Guangxi, Province, South China.

Diagnosis. Zhang and Yang (1991, pp. 33-36) introduced the genus as a seximembrate apparatus, whose P1 element is segminate, anteriorly bent, with distinct midlateral ribs which disappear posteriorly (Zhang and Yang, 1991). It was later reinterpreted as septimembrate by Orchard (2005). Following our revision of the architecture of the superfamily (Goudemand et al., Chapter 1), we reinterpret Zhang and Yang' elements as following: their P2 (*op*. *cit*., Pl. 1, figs. 3, 5) is a S2, their S2 (fig. 8) is probably the S3 (fig. 9 is also a S3 but it may belong to another apparatus), and their S3 (fig. 10) is a S4. The P2 and S1 elements are missing in their reconstruction. It is expected that the P2 element is similarly arched and bowed as the P1 element and bears rather discrete denticles (see Pl. 11, fig. 14).
Remarks. The P2 element of *Wapitiodus*, as reconstructed and defined by Orchard (2005) would differ only in having a more developed latero-posterior process. Other elements of the apparatus of *Guangxidella* closely resemble those of *Wapitiodus* (see below) and presumably those of *Larenella* gen. nov., with the notable exception of the S3 element: in *Guangxidella*, a third downwardly and inwardly directed process arises directly from the cusp (Orchard, 2005); in *Wapitiodus* the bifurcation of the antero-lateral process is located at the second denticle anterior of the cusp and in *Larenella*, this bifurcation may have been located at the cusp (like *Guangxidella* and other members of the Mullerinae subfamily) or at the first, second (like *Wapitiodus*) or even third denticle anterior of it.

***Guangxidella* sp.** - Pl. 8, fig. 23.

This element has a very large cusp that is oriented perpendicular to the base, and a rounded basal cavity. Orchard and Zonneveld (2009, p. 780) observed that elements sharing these features were associated with *Gu*. *bicuspidata* (Müller, 1956) in topotype material from Nevada and suggested that such elements should be assigned to *Guangxidella* (see also Goudemand *et al*., Chapter 4).

Genus LARENELLA gen. nov.

Derivation of name. from the type locality at Laren/Waili, Guangxi Province, South China.
Type species and holotype. *Larenella dakuangi* sp. nov. (see below).
Type stratum and locality. Luolou Formation, Laren/Waili, Western Guangxi, South China.

Multielement diagnosis. A 15-element apparatus in which the segminate, usually robust P1 element has typically a subterminal cusp whose base is slightly to conspicuously inflated laterally. Posteriorly the basal margin of the cusp is often deflected inwards and downwards, which may affect the profile of the basal cavity: in the strongest cases the basal cavity is heart-shaped; otherwise it may be subcircular or flattened posteriorly. In elements where midlateral thickening develops and extends posteriorly, this typical 'cleft lip' may partly disappear and the basal cavity tends to be rounded. The other elements have rather discrete denticles, which are very similar to those of *Wapitiodus* (see below). The S3 element has a well-developed secondary anterior process branching either from the first, second or third denticle anterior of the cusp. In some species it may even branch directly from the cusp (in which case this process becomes a third process

and the element is said to be tertiopedate).
Remarks. The P1 and S3 elements are distinctive. The apparatus is otherwise very similar to *Guangxidella* and *Wapitiodus*, to which it is clearly related. Specific assignment of the variants of the S3 element remains unclear. Species with bifurcation of the anterior process of the S3 element on the second or third denticle anterior of the cusp differ from *Wapitiodus* species only in having a short segminate P1 element; their apparatus closely resembles that of *Neospathodus* from which they are thought to have originated (*Ns*. ex gr. *dieneri*) within the Dienerian. Similarly, species with a tertiopedate S3 element would differ from *Guangxidella* species only on the basis of their P1 element; the latter genus may actually have derived from those forms later on. The other S3 variant appears to be transitional.
Many S1 elements in our collections from this section lack the distinctive discrete denticulation but some of these may however belong to species of the present genus. These elements have a second, tiny antero-lateral process wearing up to two denticles and they hence resemble homologous elements of early representatives of *Novispathodus* (the latter is less abundant in the corresponding beds but however present; consequently it is still unclear whether the corresponding S1 may actually all belong to him). Yet, at least in our sample W146-C8, as well as in somewhat coeval (occurrence of *Larenella dakuangi* sp. nov.) collections from Thailand (Savage and Orchard, unpublished), specimens of what is thought to be the typical S1 of *Larenella* closely resemble the homologous element of *Neospathodus* (see below), with more discrete denticles and a second antero-lateral process which is more developed and bears two denticles.

***Larenella astericisala* sp. nov.**- Pl. 7, figs. 14, 15; Pl. 6, fig. 3.

Derivation of name. from the Latin *ala* for 'wing'. For the resemblance of the posterior denticulation with the wings on Asterix' helmet.
Holotype. PIMUZ XXX. Pl. 7, fig. 15.
Type locality. Sample W148-C3, Waili cave section, northwestern Guangxi, South China.
Formation and stratigraphic level. Luolou Fm., top of unit II, earliest Smithian.
Material. More than 10 specimens in samples WAI61, W148-C3, WAI64, Waili, China.

Diagnosis. The P1 position is occupied by a short segminate element that closely resembles *La. mikei* sp. nov., but differs in having a higher, peculiar denticulation (see below).
Description. Short segminate element with a length/height ratio of about 0.9-1:1 and about 8-10 subequally high denticles that are fused for half or two-thirds of their height. The denticles tend to radiate, being slightly inclined to the anterior anteriorly and slightly reclined posteriorly. At mid-height, especially posteriorly, above the basal cavity, the unit is usually slightly to conspicuously inflated (see for instance Pl. 6, fig. 3). As a consequence the posterior margin of the cusp is basally convex, whereas it is recurved posteriorly and thus concave in its upper part. The lower margin is straight anteriorly and slightly upturned posteriorly beneath the subcircular basal cavity. Apparently the more inflated the posterior part or the more conspicuous the lateral thickening, the more laterally expanded the basal cavity, which is then zero- or eight-shaped.

***Larenella brayardi* sp. nov.**- Pl. 5, fig. 12.

Derivation of name. in honor of Arnaud Brayard for his outstanding contributions to the study of Early Triassic ammonoids, especially in the Jinya/Waili area.
Holotype. PIMUZ XXX. Pl. 5, fig. 12.
Type locality. Sample W148-C3, Waili cave section, northwestern Guangxi, South China.
Formation and stratigraphic level. Luolou Fm., top of unit II, earliest Smithian.
Material. 3 specimens from samples WAI61 and W148-C3, Waili, China. 3 specimens from samples Mud27 and Mud33, Mud, Spiti, India.

Diagnosis. The P1 position is occupied by a short segminate element that closely resembles *La. quitondeta* sp. nov., but differs in having a small posterior denticle behind the cusp. The denticles are also less fused (their free tips are not subtriangular as in the latter) and somewhat more reclined or recurved posteriorly.
Description. Short and robust segminate element with a length/height ratio of about 1.2:1. The anterior process has about 7 subequal denticles which are suberect anteriorly and progressively more reclined to the posterior. The reclined cusp is not conspicuous compared with the denticles to its anterior. At the posterior end however, an additional, distinctly smaller, posteriorly recurved denticle stands behind the cusp. The upper margin of the rounded basal cavity is inflated. The robust unit is conspicuously thickened at mid-height. The upper margin of this rib is not marked as the elements gets rather continuously thicker from the tips of the denticles downwards but the lower margin is abrupt and the anterior process

is much thinner (constricted) below this level (posteriorly the basal cavity starts flaring out at about the same height). Consequently the lower margin of the rib is much more visible than the upper one in lateral view. Note that this is principally true for most representatives of the genus.
Remarks. The orientation of the posterior denticles recalls the Spathian *Ns*.? *triangularis* (Bender, 1968; revised by Orchard, 1995) but they miss the characteristic lateral fold on each side of the subterminal cusp of the latter. Dagis illustrated a similar but less robust element from Smithian strata of Siberia (Dagis, 1984, Pl. XV, fig. 2) and assigned it to *Ns*. aff. *triangularis*. Yet, its basal cavity is broken and it is illustrated only in lateral view, which precludes any reliable assignment.

Larenella* aff. *brayardi - Pl. 5, figs. 9, 15.

The denticulation of these *Larenella* specimens closely resembles that of specimens from Spiti assigned to *Neospathodus*? cf. *concavus* (Goudemand *et al*., Chapter 4, Pl. 2, fig. 5). Yet, they differ in having a shorter anterior process that is not downarched. They also resemble *La*. *quitondeta* sp. nov. in having relatively broad denticles whose free tips are subtriangular. They most closely resemble *La*. *brayardi* sp. nov. but differ in having less recurved and more fused denticle and in missing the small posterior denticle behind the cusp.

***Larenella*? *chaohuense* (Zhao & Orchard) 2007**- Pl. 7.

The original diagnosis referred to short segminate elements with a length/height ratio of ~1:1.4, and 5-8 variably discrete, erect to slightly reclined, pointed to apically rounded denticles. Denticles are subequal in width and length, the basal margin is straight anteriorly and upwardly deflected in the posterior part, the basal cavity is broadly expanded and rounded (Zhao et al., 2007). Herein we differentiate three different morphotypes and assign a related form to a new species (see below).

morphotype 1 – Pl. 7, figs. 1, 3, 4?, 6.

2007 *Neospathodus chaohuensis* n. sp., Zhao and Orchard, Pl. 1, figs. 6A, 6B.

Like the holotype, this morphotype has posteriorly reclined denticles, a very large, height-shaped basal cavity and an inward deflection of the posterior basal margin of the cusp (hence the eight shape of the cavity, see also *Larenella*'s 'hare lip'). The free tips of the mostly fused denticles are subtriangular in shape. One specimen (Pl. 7, fig. 4) is distinctly more elongate, has more denticles and a straight anterior lower margin. It is assigned to this species with question mark. Note the 'muffin belly'-shaped anterior extension beyond the lower margin. This feature is often encountered within the present genus.

morphotype 2 – Pl. 7, figs. 7, 11, 12.

? *Neospathodus chaohuensis*, Goudemand and Orchard, Chapter 4, Pl. 2, figs. 7, 8.

This morph invariably has upright denticles. Furthermore the denticles are higher and narrower than in *morphotype 1* and of subequal height. The basal cavity is not as large as in the latter and more zero-shaped than eight-shaped. The anterior lower margin is variably straight or slightly upturned. These elements are homeomorphs of the unpublished earliest Spathian *Novispathodus* aff. *brevissimus*.

morphotype 3 – Pl. 7, figs. 5, 13?, 16.

? *Neospathodus* aff. *dieneri*, Goudemand and Orchard, Chapter 4, Pl. 3, fig. 14.
1997 *Neospathodus dieneri*, Paull *et al*., fig. 2G.

This morphotype is very close to *morphotype 2* but the broader denticles are slightly reclined to the posterior and their height decreases more to the anterior than in the latter. The lower margin is straight anteriorly, upturned beneath the posterior third of the unit and again straight or slightly downturned at the posterior end. Goudemand and Orchard illustrated a similar element with more recurved denticles (Chapter 4, Pl. 3, fig. 14) that is somehow transitional between *Ns. dieneri* and this morphotype. The specimen illustrated by Paull *et al*. from Alberta (1997, fig. 2G) is very similar. The aboral view is missing but the characteristic 'harelip' of the present group is clearly recognizable in the lateral view. One of our specimens (Pl. 7, fig. 13) has upright, rather discrete denticles and resembles *Ns*. aff. *cristagalli* morphotype 2 (see below) but its posterior part differs from the latter and is identical to that of the present form.

***Larenella*? *concava* (Zhao & Orchard) 2007**- Pl. 3.

The original diagnosis referred to relatively large and long segminate elements with a length/height [not length/width] ratio of ~1.6:1 [not 1.9-2.6:1], and about 9-10 denticles, the sixth denticle from the posterior end being large and conspicuous and similar in size to that of the cusp. Also, the basal margin is slightly or conspicuously concave below the anterior four-fifths of the blade; the basal cavity is rounded with a shallow medium pit.
Remarks. The lower profile is judged to be less diagnostic than previously assumed: several very different pectiniform elements belonging to unrelated species have a concave lower profile.
The generic assignment is based on the robust aspect of the unit, the nature of the basal cavity and the presence in some specimens of a faint inward deflection posteriorly above the edge of the cup.
The variation observed in our Chinese material led us to differentiate at least 3 morphotypes and to assign one closely related specimen to a separate species (in open nomenclature).

morphotype 1 – Pl. 3, figs. 1, 4, 5?, 6.

2005 *Neospathodus* n. sp. E, Zhao, Pl. 11, figs. 3a-c, 6a, b.
2007 *Neospathodus concavus* n. sp., Zhao and Orchard, Pl. 1, figs. 1A-C.
? *Neospathodus concavus*, Goudemand and Orchard, Chapter 4, Pl. 2, fig. 1.

This morphotype corresponds roughly to the holotype. The element is robust, variably elongate (Pl. 3, figs. 1, 2 have a markedly smaller length/height ratio than in the original diagnosis), and has usually 7-9 denticles (but one large specimen from Spiti has 12 denticles, see Goudemand *et al*., Chapter 4). The most diagnostic feature is the presence of a fifth or sixth denticle from the posterior end that is usually the broadest and is at least as large as the cusp. The lower margin of the anterior process is slightly to conspicuously concave but in some specimens only the anteriormost part of the unit is significantly downturned. As a consequence, elements where this part is broken may have an apparent straight basal margin. It might be the case for the specimen illustrated on Pl. 3, fig.5. The presence, location and size of a broad fifth or sixth denticle seem to be linked with the location and amplitude of the downturning of the anterior process.

morphotype 2 – Pl. 3, fig. 8.

? *Neospathodus* cf. *concavus*, Goudemand and Orchard, Chapter 4, Pl. 2, fig. 2.

This morphotype corresponds to short forms (length/height ratio is ~1.1) where the lower margin of the anterior process is conspicuously downcurved beneath the anterior third of the unit. There is no markedly broader denticle above this downturning (all denticles are subequally broad) and behind the latter, all denticles are similarly reclined posteriorly (hence subparallel) and rather discrete.

morphotype 3 – Pl. 8, fig. 5?, Goudemand and Orchard, Chapter 4, Pl. 2, fig. 4.

2005 *Neospathodus* n. sp. K, Zhao, Pl. 11, figs. 7a, b, 8a, b.
? *Neospathodus* cf. *concavus*, Goudemand and Orchard, Chapter 4, Pl. 2, fig. 1.

This morphotype was considered as a separate species by Zhao in his PhD thesis (2005), apparently on the basis of the absence of a wide sixth denticle. It is not clear from his illustrations of two specimens with broken denticles but the seventh denticle might be broader and larger than the others in both elements. Though we consider this feature as important for the recognition of the species, this is not the only one (see *morphotype 2*) and we already mentioned that this character is variable. This morphotype differs from *morphotype 1* in having strongly fused and strongly recurved posterior denticles. In the latter morphotype the denticles are only slightly reclined (not recurved) to the posterior.
Some specimens (Goudemand *et al*., Chapter 4, Pl. 2, fig. 4; Zhao, 2005, Pl. 11, fig. 8) closely resemble *N*. n. sp. Q Orchard and Zonneveld (2009) from Ganoid Ridge, Wapiti Lake area, Canada. It is still unclear whether the variability of the lower margin should include such elements where the downturning point is located more posteriorly, but both taxa are probably related.

***Larenella*? cf. *concava* (Zhao & Orchard) 2007**- Pl. 3, fig. 2.

This specimen has a substraight lower margin and its fifth denticle though being slightly broader than adjacent denticles is markedly smaller than the cusp. Nevertheless this element closely resembles elements of *Larenella*? *concava* and

it probably belongs to this species.

***Larenella*? aff. *concava* (Zhao & Orchard) 2007**- Pl. 3, fig. 3.

This specimen differs from *Larenella*? *concava* in having a big and strongly reclined cusp, behind which sits a twice smaller terminal denticle.

***Larenella dakuangi* sp. nov.**- Pl. 5, figs. 1, 4.

Derivation of name. Named for Kuang Guodun, alias 'DaKuang' who guided us through the geology of Guangxi. Note that the Chinese phoneme 'Kuang' may also mean 'basket' or 'eye socket', hence 'dakuang' is evocative of a big cup, a feature of this species.
Holotype. PIMUZ XXX. Pl. 5, fig. 1.
Type locality. Sample W148-C3, Waili cave section, northwestern Guangxi, South China.
Formation and stratigraphic level. Luolou Fm., top of unit II, earliest Smithian.
Material. 5 specimens from samples W144-C6 and W148-C3, Waili, China.

Diagnosis. The P1 position is occupied by a segminate element that resembles *La*. *concava* (morphotype 3) but differs in having a deep cavity, a rather straight lower margin and in being shorter than the latter.
Description. Segminate element with a length/height ratio of about 1.4-1.5:1 and about 7-10 denticles that are slightly reclined anteriorly and recurved (see holotype) posteriorly. Their height gradually decreases towards the anterior. The lower margin is straight anteriorly and either straight or slightly upturned posteriorly beneath the large, subcircular and deep basal cavity. The posterior margin of the basal cavity might be deflected inward and downward. The basal cavity together with the terminal cusp (sometimes also with the penultimate denticle) tend to form a conical shape that is readily distinguished from the rest of the unit. This feature is reminiscent of some forms of *La*. *chaohuense* (see for instance Pl. 7, figs. 1, 5). The latter differ in having larger, eight-shaped basal cavities. Specimens like Pl. 4, fig. 13 might be transitional between both species.
Remarks. This species is known also from Thailand where it occurs in presumed Dienerian (?) strata with the ramiform elements of the present genus (Orchard, pers. comm., 2010; Orchard and Savage, in prep.).

***Larenella elvis* sp. nov.**- Pl. 4, fig. 7.

Derivation of name. in honor of Elvis Presley. For the strongly reclined posterior denticles that recall Elvis'hairstyle.
Holotype. PIMUZ XXX. Pl. 4, fig. 7.
Type locality. Sample WAI61, Waili cave section, northwestern Guangxi, South China.
Formation and stratigraphic level. Luolou Fm., top of unit II, earliest Smithian.
Material. 3 specimens from samples WAI61, W148-C3 and WAI64, Waili, China. 1 specimen from sample M05-10/1, Mud, Spiti, India.

Diagnosis. The P1 position is occupied by a segminate element that resembles *La*. *mikei* sp. nov. but differs in having an additional, strongly reclined denticle posterior of the cusp.
Description. Segminate element with a length/height ratio of about 1.6:1 and about 9 subequal, somewhat radiating denticles. The strongly posteriorly reclined cusp is slightly bigger than the denticles of the anterior process. The posteriormost denticle is strongly recurved posteriorly in its basal part and then somewhat upturned, so that the posterior margin is S-shaped. The posterior margin is also inwardly deflected at its base. The lower margin is straight or slightly concave anteriorly and slightly upturned posteriorly beneath the subheart-shaped and asymmetrical basal cavity
Remarks. A similar element has been illustrated by Orchard and Zonneveld from the Wapiti lake area, Canada (Orchard and Zonneveld, 2009, Fig. 15, parts 6, 7, *Wapitiodus*? n. sp. A). The latter has a more developed anterior process that is slightly downarched and its basal cavity is not heart-shaped but pointed posteriorly. The present species resembles also the Spathian *Ns*. *triangularis* (Bender, 1968; revised by Orchard, 1995), especially in its posterior configuration, but differs in being much lower, longer, and conspicuously thickened at mid-height ('larenellid' rib, see *La*. *brayardi* sp. nov.).
Two presumably teratological specimens of the present species are illustrated on Pl. 4, figs. 8, 9 where the cusp and the penultimate denticle are markedly separated from the other denticles.

***Larenella falcata* sp. nov.**- Pl. 3, fig. 14.

Derivation of name. from the Latin for 'sickle-shaped, curved'. It refers to the shape of the P1 element.
Holotype. PIMUZ XXX. Pl. 3, fig. 14.
Type locality. Sample W148-C3, Waili cave section, northwestern Guangxi, South China.
Formation and stratigraphic level. Luolou Fm., top of unit II, earliest Smithian.

Material. 1 very nicely preserved specimen (see holotype).

Diagnosis. The P1 position is occupied by a segminate element that most closely resembles *La*. *concava* (morphotype 1) but differs in having almost completely fused denticles.
Description. Rather long segminate element with a length/height ratio of about 1.6 and about 10 broad, slightly reclined and almost completely fused denticles. In lateral view, the free tips of the denticles are low, asymmetrical, leant back obtuse triangles. Both upper and lower margins are conspicuously concave, the major deflection being located at the 6th denticle, whose free tip differs from others by forming a subequilateral triangle. The upper margin is more concave than the lower margin and in front of the 6th denticle, the size of the denticles rapidly decreases towards the anterior. Consequently, in lateral view, the overall shape recalls a sickle. The basal cavity is big and rounded with a shallow pit. Above it the base of the cusp is conspicuously inflated (see *La*. *dakuangi* sp. nov.).
Remarks. This specimen resembles also *Guangxidella*? sp. 2 Goudemand and Orchard (Goudemand *et al*., Chapter 4, Pl. 3, fig. 1) but the broken denticles of the latter look more discrete, its cusp is conspicuously bigger than the other denticles and the constricted basal configuration is also slightly different. Yet, both elements are probably related. A paratype of '*Neoprioniodus*' *bicuspidatus* Müller (1956, Pl. 95, figs. 16, 17) differs in having an asymmetrical basal cavity, a conspicuous terminal cusp that is fused with the penultimate denticle and more differentiated denticles. The denticles of *Guangxidella typica* Zhang and Yang (1991, Pl. 1, figs. 1, 2) are even more discrete. *Wapitiodus robustus* Orchard (2005, Text-fig. 24) is also somewhat similar but the present species is relatively shorter and higher and the whole anterior process is conspicuously downarched whereas the latter species has a (sub)straight (see also Orchard and Zonneveld, 2009, Fig. 14, parts 25-27) and elongate P1 element. Since the most resembling forms are assigned either to *Guangxidella* or to *Wapitiodus*, the present species may be transitional to one of these genera.
It is also worth mentioning that the holotype is preserved with some remains of the basal body. Another element in our collection apparently resembles the present species but differs in having a conspicuous cusp which is about twice broader than the denticles anterior of it. It looks as if the penultimate denticle has been once broken and was later overgrown and fused with the cusp. An incipient denticle develops also below the free apex of the cusp (that is, on a line perpendicular to the main axis of the cups and passing by the tip of the adjacent denticle).

***Larenella fastuosa* sp. nov.**- Pl. 3, fig. 10; Pl. 6, fig. 7.

Derivation of name. from the Latin for 'proud, haughty'.
Holotype. PIMUZ XXX. Pl. 3, fig. 10.
Type locality. Sample W148-C3, Waili cave section, northwestern Guangxi, South China.
Formation and stratigraphic level. Luolou Fm., top of unit II, earliest Smithian.
Material. More than 10 specimens from samples W148-C3 and WAI64, Waili, China and from sample Mud33, Mud, Spiti, India.

Diagnosis. The P1 position is occupied by a short segminate element that most closely resembles *La*. *mikei* sp. nov., but differs in having a big terminal cusp and denticles of the anterior process which are subequally broad and whose height decreases gradually to the anterior. It also closely resembles *La*. *labialeporina* sp. nov. but the latter has a bigger, heart-shaped basal cavity and the deflection of the posterior margin of its cusp is more conspicuous (see below).
Description. Short segminate element with a length/height ratio of about 1.2:1 and about 7 mostly fused, apically pointed denticles. The subequally broad denticles are suberect anteriorly and gradually more reclined to the posterior. Only the terminal cusp is broader and higher than the other denticles. The lower margin is straight to slightly concave anteriorly and upturned posteriorly beneath the rather large, subcircular basal cavity. The basal posterior margin of the cusp may be slightly deflected inward and downward.
Remarks. A specimen (Pl. 4, fig. 4) has a tiny denticle burgeoning on the posterior margin of the cusp. Another specimen (Pl. 4, fig. 12) resembles the present species but is a bit more elongate and has an additional strongly reclined denticle posterior of the cusp, as if the tiny burgeon of the former had grown into a 'real' denticle. Such elements may deserve assignment to a separate species. A similar 'trend' is observed in several forms (see Pl. 4, figs. 3, 6, 7, 11).

***Larenella galfettii* sp. nov.**- Pl. 5, fig. 8.

Derivation of name. Named for Thomas Galfetti for his contribution to the study of the Early Triassic period, especially his work in the Jinya/Waili area.
Holotype. PIMUZ XXX. Pl. 5, fig. 8.
Type locality. Sample W148-C3, Waili cave section, northwestern Guangxi, South China.
Formation and stratigraphic level. Luolou Fm., top of unit II, earliest Smithian.
Material. More than 10 specimens from samples WAI61, W148-C3 and WAI64, Waili, China and from samples Mud33 and M05-10, Mud, Spiti, India.

Diagnosis. The P1 position is occupied by a short segminate element that resembles *La*. *mikei* sp. nov., but differs in having more numerous and higher denticles, a sinuous lower margin and a basal cavity that is less upturned and lacks the downward deflection posteriorly. It also resembles *La*. *astericisala* sp. nov. but it is lower and longer and the posterior margin of its terminal cusp is substraight.
Description. Short segminate element with a length/height ratio of about 1.4:1 and about 10 subequal and slightly radiating denticles. Maximal height is about at mid-length of the unit. The lower margin is sinuous, being slightly concave anteriorly, convex at mid-length (including in the anterior part of the basal cavity), and straight to slightly downcurved beneath the posterior part of the slightly asymmetrical, rounded, rather flat basal cavity. The element is conspicuously thickened at mid-height (flange).

***Larenella hindeodiformis* sp. nov.**- Pl. 6, fig. 12, 15.

Derivation of name. For its superficial resemblance with elements of the older *Hindeodus* genus.
Holotype. PIMUZ XXX. Pl. 6, fig. 12.
Type locality. Sample WAI64, Waili cave section, northwestern Guangxi, South China.
Formation and stratigraphic level. Luolou Fm., top of unit II, earliest Smithian.
Material. 5 specimens from samples W148-C3 and WAI64, Waili, China.

Diagnosis. The P1 position is occupied by a short segminate or segminiscaphate element that most closely resembles *La*. *labialeporina* sp. nov., but differs in being more elongate and in having a big terminal cusp that is straight. Furthermore the unit is conspicuously thickened at mid-height, especially posteriorly above the basal cavity.
Description. Segminate or segminiscaphate element with a length/height ratio of about 1.4-1.5:1 and 9-11 erect denticles, which are somewhat bullet-shaped. The straight to slightly reclined, terminal cusp is conspicuously broader and higher than the otherwise subequal denticles of the anterior process. The lower margin is straight or slightly upturned anteriorly and somewhat S-shaped beneath the big and shallow basal cavity (the anterior part of the basal cavity is upturned and the posterior part is straight). The basal cavity is zero- or eight-shaped in aboral view. It is often asymmetrical being sheared along the antero-posterior axis (the zero-shape is then slightly reclined).
Remarks. Some elements like the one illustrated on Pl. 6, fig. 15 have the 'hare lip' deflection of the posterior margin that is somewhat typical of the genus. Those elements are then very similar to the closely related *La*. *labialeporina* sp. nov.
This element is somewhat homeomorph of some Griesbachian hindeodid forms, except that in *Hindeodus* the 'false' cusp is located anteriorly and the basal cavity much bigger.

***Larenella isarcicellaeformis* sp. nov.**- Pl. 6, fig. 17.

Derivation of name. For its superficial resemblance with elements of the Griesbachian *Isarcicella* genus.
Holotype. PIMUZ XXX. Pl. 6, fig. 17.
Type locality. Sample WAI61, Waili cave section, northwestern Guangxi, South China.
Formation and stratigraphic level. Luolou Fm., top of unit II, earliest Smithian.
Material. 1 very nicely preserved specimen (see holotype).

Diagnosis. The P1 position is occupied by a rather long segminate (bisegminate?) element that most closely resembles *La*. *hindeodiformis* sp. nov. and *Gu*.? sp. 2 Goudemand and Orchard (Goudemand et al., Chapter 4, Pl. 3, fig. 1) but differs in having a very asymmetrical, wide basal cavity, the less developed lateral lobe of which bears one denticle. *Isarcicella*? n. sp. 1 bears a denticle on the outer lobe of its more asymmetrical cup. As in *Gu*.? sp. 2 the lower margin of the present species is slightly concave anteriorly and its basal part conspicuously constricted (see also below *La*. *superba* sp. nov. whose denticulation is clearly different).
Description. Segminate element with a length/height ratio of about 1.6-1.7:1 and about 12 erect denticles on the blade. The posteriormost three denticles are broken in the present specimen, but they might have been higher than the other

denticles anterior of them, in a similar way as *La*. *hindeodiformis* sp. nov. The terminal and penultimate denticles are fused. The anterior process is slightly downarched. The lower margin is slightly upturned beneath the wide, conspicuously asymmetrical basal cavity. The inner lobe of the cup (on the concave side of the slightly bowed element) is less developed than the inner side and bears a denticle. The anterior process is laterally compressed in front of the cup and the corresponding denticles tend to get more flattened (elliptical or lenticular in cross-section) towards the anterior.
Remarks. This element is somewhat homeomorph of the Griesbachian *Isarcicella staeschei* Dai and Zhang (1989), except that in the latter a prominent and posteriorly reclined 'false' cusp is located anteriorly. Though their posterior configuration differs, it also recalls the early Spathian *Icriospathodus crassatus* Orchard (1995) and *Ic.*? *zaksi* Buryi (1979; the latter bearing similarly a denticle on one lobe of the cup), especially in oral view.

***Larenella labialeporina* sp. nov.**- Pl. 6, fig. 5.

Derivation of name. from the Latin for 'hare lip'.
Holotype. PIMUZ XXX. Pl. 6, fig. 5.
Type locality. Sample W148-C3, Waili cave section, northwestern Guangxi, South China.
Formation and stratigraphic level. Luolou Fm., top of unit II, earliest Smithian.
Material. 3 specimens from samples W148-C3 and WAI61, Waili, China.

Diagnosis. The P1 position is occupied by a short segminate or segminiscaphate element that most closely resembles *La*. *fastuosa* sp. nov. or *La*. *hindeodiformis* sp. nov., but differs in having a eight- or heart-shaped basal cavity, and the deflection of the posterior margin of the cusp is well marked and extends both downward to the basal cavity (hence the marked heart-shape of the latter) and upward up to the apical third of the cusp.
Description. Short segminate or segminiscaphate element with a length/height ratio of about 1.2:1 and about 8 mostly fused, apically pointed denticles. The denticles are suberect. The terminal cusp is conspicuously broader and higher than the otherwise subequal denticles of the anterior process. The cusp is substraight for about two-thirds of its height and slightly recurved to the posterior for its upper third. Its posterior margin is characteristically deflected inward from the posterior margin of the basal cavity to the point where the cusp is slightly recurved. As a consequence the subflat and upturned basal cavity is eight-shaped. Its upper margin is conspicuously inflated. The lower margin is convex being upturned both anteriorly and posteriorly.

***Larenella*? cf. *lineare* (Zhao & Orchard) 2007** - Pl. 3, fig. 7.

This robust specimen might be a broken specimen of *La*.? *concava* but its very long and posteriorly reclined denticles closely resemble those of the holotype of '*Ns*.' *linearis*. Its lower margin however is partly broken anteriorly and it cannot be asserted whether it was straight.

***Larenella mikei* sp. nov.**- Pl. 6, figs. 1, 2, 4.

2007 *Neospathodus* n. sp. T, Orchard, fig. 2.

Derivation of name. Named for Mike Orchard, who first recognized that such elements deserved assignment to a new species.
Holotype. PIMUZ XXX. Pl. 6, fig. 1.
Type locality. Sample WAI61, Waili cave section, northwestern Guangxi, South China.
Formation and stratigraphic level. Luolou Fm., top of unit II, earliest Smithian.
Material. More than 10 specimens from samples W148-C3 and WAI61, Waili, China and from samples Mud33, M05-10, Mud, Spiti, India.

Diagnosis. The P1 position is occupied by a short segminate element that most closely resembles *La*. *chaohuense* (morphotype 1) but differs in having an irregular anterior denticulation and a less broad and less deep basal cavity that is rather subcircular in outline.
Description. Short segminate element with a length/height ratio of about 1.2:1 and about 7 mostly fused, apically pointed denticles. The denticles are suberect anteriorly and gradually more reclined to the posterior. The terminal cusp is about as high as the penultimate denticle. The breadth and height of the denticles are irregular but the maximal height is usually at the posterior end. The lower margin is straight anteriorly and upturned posteriorly beneath the large, subcircular to zero-shaped basal cavity. The basal posterior margin of the cusp is deflected inward and downward and as a consequence the basal cavity appears heart-shaped in posterior view. In lateral view, the anterior margin has the 'muffin belly' shape that we already mentioned as some-

what typical of the genus.
Remarks. This species is known also from the Arctic (Orchard, 2007) where it occurs in Dienerian strata (Diener creek, *Candidus* Zone; Orchard, pers. comm., 2010).

***Larenella quitondeta* sp. nov.**- Pl. 5, figs. 13, 16.

Derivation of name. from the Latin for 'the one who clips'. For its resemblance with hair clippers.
Holotype. PIMUZ XXX. Pl. 5, fig. 16.
Type locality. Sample WAI61, Waili cave section, northwestern Guangxi, South China.
Formation and stratigraphic level. Luolou Fm., top of unit II, earliest Smithian.
Material. 5 to 10 specimens from samples WAI61, W148-C3 and WAI64, Waili, China and from sample M05-10, Mud, Spiti, India.

Diagnosis. The P1 position is occupied by a short segminate element that is readily recognized by its broad, suberect and fused denticles whose free tips are equilaterally triangular.
Description. Short segminate element with a length/height ratio of about 1.2-1.3:1 and about 8-9 mostly fused, conspicuously broad, subequally high, and suberect or slightly radiating denticles whose free tips are equilaterally triangular. The posterior margin is substraight to slightly angled at mid-height. The lower margin is substraight anteriorly and slightly upturned posteriorly beneath the drop-shaped and flat basal cavity.
Remarks. Similar elements are known from the Arctic, where they occur in Dienerian strata (Diener creek, *Candidus* Zone; Orchard, pers. comm., 2010). Dagis illustrated the lateral view of a similar element from Siberia (*Ns*. sp. A, Dagis, 1984, Pl. VIII, fig. 8; early Smithian) but the absence of additional views precludes any confident assignment to the present species.

Larenella* aff. *quitondeta - Pl. 6, fig. 9.

This specimen shares with *La. quitondeta* sp. nov. the same denticulation and basal configuration but differs in having relatively smaller denticles, a more upturned basal cavity and a much shorter anterior process.

***Larenella*? *superba* sp. nov.**- Pl. 6, fig. 8.

Derivation of name. From the Latin for'proud, splendid'.
Holotype. PIMUZ XXX. Pl. 6, fig. 8.
Type locality. Sample W148-C3, Waili cave section, northwestern Guangxi, South China.
Formation and stratigraphic level. Luolou Fm., top of unit II, earliest Smithian.
Material. 1 very nicely preserved specimen (see holotype).

Diagnosis. The P1 position is occupied by a segminate element that most closely resembles *Wapitiodus robustus* Orchard (2005) but it is much shorter. It resembles also *Gu*.? sp. 2 Goudemand and Orchard (Goudemand et al., Chapter 4, Pl. 3, fig. 1) but differs in having less numerous, shorter denticles. The shape of its big terminal cusp is reminiscent of that of *Guangxidella* species in looking as if it were formed by the fusion of two denticles where the anterior one were distinctly smaller. Yet, it is more stubbed than the one of the latter and less than the one of *Wapitiodus robustus*.
Description. Segminate element with a length/height ratio of about 1.4:1 and about 6-8 denticles. The anterior process is downarched at about two-thirds from the posterior (5th denticle). The 5th denticle at the anterior deflection is erect and triangular. The denticles to its posterior are gradually larger and more reclined to the posterior so that the posterior upper margin remains substraight, even at the big terminal cusp: the posterior edge of the cusp is straight and makes an angle of about 20 degrees with the vertical axis but its anterior edge is largely recurved to the posterior, which gives the corresponding knife-shape much *belly* (see *Ns*. *artemis* sp. nov.). The lower margin is slightly upturned beneath the big, circular, and flat basal cavity. The unit is (like most of *Larenella* and *Wapitiodus* species) conspicuously thickened at mid-height on its lateral flanks and posteriorly around the cusp.

***Larenella*? *tomeotetragona* sp. nov.** - Pl. 7, figs. 2, 8, 9.

Derivation of name. From the Greek for 'cutting tooth, incisor' and 'square'. It refers to the shape of the denticles.
Holotype. PIMUZ XXX. Pl. 7, fig. 8.
Type locality. Sample WAI61, Waili cave section, northwestern Guangxi, South China.
Formation and stratigraphic level. Luolou Fm., top of unit II, earliest Smithian.
Material. More than 10 specimens from samples WAI61and W148-C3, Waili, China.

Diagnosis. This species is closely related to *Larenella*? *chaohuensis*, from which it differs only by its broad, squared denticulation.
Description. The P1 position is occupied by a

short segminate element with a length/height ratio of ~1.1, and 5 to 6 distinctly broad and fused denticles. The lower margin is V-shaped, being about 30 degrees upturned both anteriorly (beneath two-thirds of the unit) and posteriorly (beneath the one-third of the unit, which corresponds to the basal cavity). The laterally flattened, and subequally broad denticles tend to radiate from the tip of this V. Their free tips have a diagnostic shape: they are squared with rounded corners. The basal cavity is very large and eight-shaped in aboral view. Posteriorly the waist of this eight-shape corresponds to an inward and downward directed deflection of the posterior margin of the cusp.

Discussion. As for *La*.? *chaohuensis*, the generic assignment is based on the robust nature of the P1 and the 'hare lip'-like posterior deflection, which is characteristic of the genus. Yet, this still needs to be assessed through a multi-element reconstruction.

***Larenella*? n. sp. 1** - Pl. 4, figs. 3, 11.

? *Neospathodus* n. sp. 3, Goudemand and Orchard, Chapter 4, Pl. 10, fig. 3.

These short segminate elements share a circular basal cavity, posteriorly reclined and subequal denticles and an incipient denticle budding at mid-height of the posterior margin.

***Larenella*? n. sp. 2** - Pl. 4, fig. 2; Pl. 5, fig. 11.

These short, possibly teratological, segminate elements have a drop-shaped basal cavity and four high, broad, and suberect denticles in front of which a few, tiny denticles may develop. Dagis illustrated a similar (also teratological?) specimen (Dagis, 1984, Pl. VIII, fig. 1), in which the anteriormost three denticles are high and broad and a couple of much smaller denticles are grown posteriorly.

***Larenella* n. sp. 3** - Pl. 5, figs. 6, 7.

These segminate elements have more erect, posterior denticles than *La*. *dakuangi* sp. nov. or *La*. *mikei* sp. nov. The 'hare lip' deflection is well marked, which is reminiscent of *La*. *labialeporina* sp. nov. but their terminal cusp appears less prominent than in the latter and their basal cavity is not as large. Their lower margin is slightly concave anteriorly but their posterior configuration is clearly different than *La*. *concava*. Paull *et al*. (1997, fig. 2G) illustrated a similar specimen from Alberta, but additional views would be necessary to confirm this assignment.

***Larenella*? n. sp. 4** - Pl. 9, fig. 24.

This comb-shaped element somewhat recalls the older *Sweetospathodus kummeli* from which it differs in being shorter, higher and much more robust (length/height ratio ~1.3:1). The basal cavity is also less inverted than in the latter and the erect and subequal denticles are here rounded in cross-section whereas those of *Sw*. *kummeli* are laterally flattened and sharp-edged. A very conspicuous mid-lateral rib extends on both flanks from the anterior end to the posterior fifth of the element (it stops in front of the cusp). It is thickest at mid-length or slightly posteriorly. The lower margin is slightly upturned at both ends, otherwise substraight. The basal cavity is drop-shaped. This element recalls *La*. *galfettii* sp. nov. from which it differs in having erect denticles and a substraight lower margin and a faint 'hare lip' deflection of the posterior margin. Hence we tentatively assign it to *Larenella*.

***Larenella*? n. sp. 5** - Pl. 2, fig. 18.

This very robust P1 element resembles *La*. *hindeodiformis* sp. nov. or *La*. *isarcicellaeformis* sp. nov. in oral view but clearly differs in being much higher with a length/height ratio of about 1:1 and in having only 5 big denticles. The terminal cusp is conspicuously broader than the other denticles, being apparently fused with what might have been a distinct posterior denticle in earlier growth stages. As in *La*. *isarcicellaeformis* sp. nov., the most developed lobe of the big, asymmetrical basal cavity bears a lateral process with one small denticle. The aboral part of the anterior process is constricted (a common feature of *Larenella* species).

Remarks.

-*Neospathodus biangularis* Wang and Cao, 1981, Pl. II, figs. 22, 23. In the original description, the basal cavity of the robust P1 elements is said to be 'swallowtail'-like. This suggests that the typical 'harelip' was present on the posterior

margin and we therefore include this species in *Larenella*.
-*Neospathodus robustus* Koike, 1982, Pl. VI, figs. 32-35 (=*N*s. *cyclodontus* Zhao and Orchard, 2008b, Pl. 1, fig. 8). This very robust element clearly resembles elements of *Larenella* and is here considered to belong to this genus.

Subfamily NEOGONDOLELLINAE Hirsch, 1994

Genus NEOSPATHODUS Mosher, 1968

Type species and holotype. *Spathognathodus cristagalli* Huckriede, 1958, pp. 161-162, pl. 10, fig. 15.
Type stratum and locality. Lower 'Ceratitenschichten', Mittiwali near Chhidru, Salt Range, Pakistan.

Original diagnosis and type species. The type species is a segminate P1 element with a width: height:length ratio of 1:3:4, a posterior lower margin that is upturned beneath the posterior one-third of the element, and a short-terminal cusp (Mosher, 1968, pp. 929-930).
Multielement diagnosis. see Orchard, 2005 and subsequent reinterpretation by Goudemand *et al*., Chapter 1.
Remarks. Segminate P1 elements of this time interval are typically assigned to *Neospathodus*. New, unpublished material suggests that their multi-element apparatuses rather belong to several, distinct genera. Pending reconstruction of these apparatuses and subsequent taxonomic revision of their generic assignment, the following taxa are provisory included in this genus and the specific determination is based solely on the morphology of the P1 element.

***Neospathodus artemis* sp. nov.** - Pl. 8, figs. 12-14.

Derivation of name. in honour of Artemis, the goddess of the chase. It refers to the shape of the cusp, which is like the blade of a 'trailing point hunter' knife.
Holotype. PIMUZ XXX. Pl. 8, fig. 13.
Type locality. Sample W147-C2, Waili cave section, northwestern Guangxi, South China.
Formation and stratigraphic level. Luolou Fm., top of unit II, earliest Smithian.
Material. 5 specimens from sample W147-C2, Waili, China.

Diagnosis. The P1 position is occupied by a short segminate element that most closely resembles *Ns. dieneri* but differs in having a large and characteristic cusp that is laterally flattened, sharp-edged and knife-shaped. More exactly the cusp resembles the blade of a so called 'trailing point hunter' knife, whose orientation is such that the *edge* (cutting surface) is anterior and the *spine* (thicker portion of the blade) is posterior. In elements like the holotype the cusp seems to be '*swaged*', which means that the posterior margin is sharp-edged too.
Description. The P1 segminate element has a relatively small length/height ratio (~0.8-0.9). The 3-5 denticles of the anterior process are discrete, rounded in cross-section and pointed at their tips. Their height decreases rapidly towards the anterior and the upper margin has a nice convex shape at all stages of growth. The conspicuous and characteristic cusp is terminal, higher and broader than the other denticles. In cross-section it is rather rounded or elliptical at its base and progressively more lenticular towards the apex, with sharp-edged posterior and anterior margins. All denticles are slightly recurved posteriorly. Especially the posterior margin of the cusp is slightly concave and consequently the tip of the latter trails more posteriorly than the generalized axis of the posterior margin ('trailing point'; the *point* is the apex of a blade). The lower margin is substraight anteriorly and conspicuously upturned below the subcircular basal cavity.
Discussion. Note that in blades design, a 'trailing point hunter' configuration has enhanced slicing properties (more *belly*, or cutting edge, while the weak *point* is put out of the way). The *swage* reduces the cross sectional area of the *point* without loosing too much thickness. This improves thrusting insertion.
Ns. chii has also a conspicuous, thin, cusp that is elliptical in cross-section, but the latter species differs in its broad and deep basal cavity and its subequally high anterior denticles. The present species may find its origin in *Ns*. aff. *cristagalli* 2 Goudemand and Orchard (Goudemand *et al*., Chapter 4), which is closely similar except for the terminal cusp of the latter which is conspicuously smaller than the denticles of the anterior process.

***Neospathodus circuloctavus* sp. nov.** - Pl. 9, figs. 6, 7, 12.

Derivation of name. from the Latin for 'circle' and 'eighth'. It refers to the 45-degree (eighth of a circle)-oriented basal cavity.
Holotype. PIMUZ XXX. Pl. 9, fig. 7.
Type locality. Sample W143-C1, Waili cave section, northwestern Guangxi, South China.
Formation and stratigraphic level. Luolou Fm., top of unit II,

late Dienerian.
Material. 10 specimens from sample W143-C1, Waili, China.

Diagnosis. The P1 position is occupied by a short segminate element that most closely resembles *Ns. dieneri* but differs in having upright, straight denticles and a basal cavity that is strongly upturned so that its planar margin makes an angle of about 45-60 degrees with the horizontal anterior lower margin.
Description. Short segminate element with 6-7 straight, upright denticles. Lower margin straight anteriorly and abruptly upturned posteriorly as the basal cavity's lower margin makes an angle of 45-60 degrees with the anterior lower margin. Upper margin rather arcuate with maximal height above the lower margin deflection at the anterior edge of the rather broad and subcircular basal cavity. The posterior margin of the terminal cusp is substraight and starts right at the posterior edge of the cup (in related species like *Ns. dieneri*, the base of the cusp is posteriorly expanded).

***Neospathodus* aff. *cristagalli* (Huckriede) 1958** – Pl. 9.

Several morphotypes of the P1 element corresponding to *N*. ex gr. *cristagalli* has been recently differentiated by Goudemand *et al*. (Chapter 4). These forms have commonly a broad, subtriangular cusp, a complex ('cristagallid', see Goudemand *et al*., Chapter 4) basal cavity, and laterally flattened, sharp-edged denticles.

morphotype 2 – Pl. 9, figs. 14, 15.

1970 *Neospathodus cristagalli* n. sp., Sweet, Pl. 1, figs. 14, 15.
2005 *Neospathodus* cf. *cristagalli* - Orchard, Text-fig. 14, p. 89.

The overall shape of this rather short morphotype (length/height ratio: ~1.2-1.4:1) is close to that of *morphotype 1* but the basal cavity occupies only one-third to half of the length of the element, is oval, posteriorly rounded and only partly inverted. The cusp is markedly shorter and usually broader than the denticles to the anterior but it tends to be more slender than in *N. cristagalli* and it is usually not conspicuously separated from the anterior denticles.

morphotype 11 new –Pl. 9, figs. 18, 19.

? *Ns.* aff. *cristagalli* morph 2, Goudemand and Orchard, Chapter 4, Pl. 7, figs. 10, 11.

This morphotype is very close to *morphotype 2* and *morphotype 6* but differs in having denticles that are reclined and/or recurved to the posterior. Elements like Pl. 9, fig. 4 (possibly also fig: 3) are thought to be the corresponding juveniles. With their more discrete denticles they clearly resemble also *Ns. dieneri* (morphotype 2) but the 'cristagallid' configuration of the basal cavity and the laterally flattened denticles place these elements in the *cristagalli* group.

***Neospathodus dieneri* Sweet 1970** – Pl. 4.

The P1 element is a relatively short (length/height ratio is about 1-1.2:1) segminate element. Typically, the outer margin of the circular basal cavity is somewhat swollen and the rather discrete denticles are rounded in cross-section.
Based on the size of the terminal cusp relative to those of the anterior process, Zhao & Orchard (in Zhao et al., 2007) distinguished three morphotypes. Based on material from Mud (Spiti, northern India), we have recently introduced several new morphotypes (see Goudemand *et al*., Chapter 4). Here, we further differentiate several additional morphotypes. As for the description of the Spiti material, we retain these in open nomenclature pending a thorough revision based on the topotype material (Salt Range, Pakistan).

morphotype 1 –Pl. 8, figs. 11?, 16, 17?.

This morphotype has a terminal cusp that is larger than the other denticles whose height decreases gradually towards the anterior.

morphotype 2 –Pl. 8, fig. 7.

This morphotype has a terminal cusp that is about as large as the adjacent denticle and subparallel to it. In lateral view the maximal height is at the first or second denticle anterior of the cusp. As in *morphotype 1*, the denticles are rather discrete. In our view, the sole comparison of the relative lengths of the cusp and the adjacent anterior denticle is not sufficient and we differentiate here several morphotypes that share this particular character (see *morphotypes 8-12*).

morphotype 3 –Pl. 9, fig. 8.

1970 *Neospathodus dieneri* n.sp., Sweet, Pl. 1, figs. 1, 4.

This morphotype corresponds to the holotype of the species, not to Zhao and Orchard's illustrated specimen (see Goudemand *et al*., Chapter 4). This more discrete, slightly more erect specimen could be a juvenile specimen.

morphotype 6 –Pl. 9, figs. 16, 17.

Close to *morphotype 2*, this morphotype has erect, straight denticles. One specimen (Pl. 9, fig. 17) has a conspicuous downturning of the lower margin anteriorly that is reminiscent of the *La*.? *concava* morphotype 2, to which it may be related. The basal cavity of the latter as illustrated here is markedly different of the typical cavity of *Ns*. *dieneri* but it is not excluded that juvenile specimens of *La*.? *concava* resembled *Ns. dieneri*, possibly *morphotype 6*. In which case at least some specimens included here may belong to *La*.? *concava*.

morphotype 8 new –Pl. 8, figs. 6, 10; Pl. 9, fig. 9.

This morphotype is very close to *morphotype 2* but it has more numerous denticles and consequently a conspicuously larger length/height ratio (~1.25:1). The juvenile specimens (Pl. 9, fig. 9) have more discrete denticles than *morphotype 2* and bigger elements get progressively more fused, but never as *morphotype 5*, which is also markedly lower (~1.6:1).

morphotype 9 new –Pl. 8, figs. 1-3, 4?, 9.

This morphotype is very close to the holotype of the species (*morphotype 3*) but the cusp is subequal to the adjacent anterior denticle. The denticles are more fused and more erect than in *morphotype 2*. *Ns*. *svalbardensis* Trammer (in Birkenmaier and Trammer, 1975) differs in having a downturned posterior lower margin and being usually mid-laterally thickened. Some robust specimens like Pl. 8, fig. 3 have a posterior configuration (slight inward and downward deflection of the basal posterior margin) that recalls the *Larenella* group with which they may be transitional.

morphotype 10 new –Pl. 8, fig. 8.

This morphotype differs from *morphotype 2* in having relatively higher and more erect denticles. The lower margin is convex.

morphotype 11 new –Pl. 8, figs. 15, 21.

This short and high morphotype differs from both *morphotype 2* and *morphotype 10* in having broader and more fused denticles, whose cross-section is more elliptical than is typical of *Ns*. *dieneri*. The orientation of the denticles is similar to that of *morphotype 2*. The lower margin of the anterior process is slightly concave.

morphotype 12 new – Pl. 9, fig. 5.

This morphotype differs from *morphotype 2* in its substraight posterior margin (as in *Ns*. *dieneri* morphotype 7 whose cusp is however smaller than the denticles to the anterior). The broad triangular shape of the cusp is somewhat reminiscent of *Ns*. n. sp. U (Goudemand *et al*., Chapter 4).

***Neospathodus* aff. *dieneri* Sweet 1970** – Pl. 9.

morphotype 3 –Pl. 9, fig. 13.

This element resembles a rather erect and fused *Ns*. *dieneri* (morphotypes 3, 8 or 9) but differs in having apically recurved denticles. This element also resembles the element numbered 20 on the same plate, but the latter has straight, erect denticles that broaden towards the anterior.

***Neospathodus*? n. sp. 4 Goudemand and Orchard** – Pl. 9, fig. 21.

This specimen strongly resembles elements illustrated by Goudemand and Orchard (Goudemand *et al*., Chapter 4) from Spiti and temporary assigned to *Ns*.? n. sp. 4.

Subfamily NOVISPATHODINAE Orchard, 2005

Genus NOVISPATHODUS Orchard, 2005

Type species and holotype. *Neospathodus abruptus* Orchard, 1995, pp. 118-119, figs. 3.23-24.
Type stratum and locality. Jabal Safra, Oman.

Revised multielement diagnosis. see Goudemand et al., Chapter 1.

***Novispathodus gnomarcuatus* sp. nov.**- Pl. 1, figs. 1, 4, 12, 13, 16, 17, 20, 23, 27-29, 31.

2008 *Neospathodus waageni eowaageni* – Zhao *et al*., fig. 3, parts 2-4.
1977 Neospathodus waageni – Goel, Pl. 2, fig. 2.
? *Nv.* aff. *waageni* 1, Goudemand and Orchard, Chapter 4, Pl. 14, fig. 20.

Derivation of name. from the Latin for 'dwarf' and 'arcuate'. The first root is common to all these new forms that are illustrated on Plate 1 and refers to their dwarfed aspect compared with their younger relatives. The second root specifically refers to the distinctive arcuate upper margin of the P1 element of this species.
Holotype. PIMUZ XXX. Pl. 1, fig. 29.
Type locality. Sample W147-C2, Waili cave section, northwestern Guangxi, South China.
Formation and stratigraphic level. Luolou Fm., top of unit II, earliest Smithian.
Material. More than 20 specimens from samples W146-C7 and W147-C2, Waili, China and from samples Mud33 and M05-10, Mud, Spiti, India.

Diagnosis. The P1 position is occupied by a short segminate element that closely resemble *Nv*. *gnomelongatus* sp. nov., but their length/height ratio is distinctly smaller (~1:1) and their denticles are not reclined posteriorly but rather straight, upright.
Description. About 10-12 upright, mostly fused, narrow denticles whose cross-section is subcircular. Lower margin straight or slightly upturned posteriorly. Upper margin distinctly arcuate with maximal height at about one third from the posterior end of the unit. The basal cavity is rounded, sometimes partly inverted.
Remarks. Note that the high variability of this morphotype may allow further differentiation.
It is not clear yet how *Nv*. *waageni* and *Nv*. *pakistanensi*s are related to each other (see my remarks in Goudemand *et al*., Chapter 4) but the same relationship may exist between *Nv*. *gnomelongatus* sp. nov. and *Nv*. *gnomarcuatus* sp. nov.

***Novispathodus gnomelongatus* sp. nov.**- Pl. 1, figs. 2, 6-9, 21, 22.

2009 *Neospathodus pakistanensis* – Orchard, fig. 8.10.
2008 *Neospathodus posterolongatus* – Zhao *et al*., fig. 3, parts 7, 8.
? *Nv.* aff. *pakistanensis* 5, Goudemand and Orchard, Chapter 4, Pl. 13, figs. 6, 8.

Derivation of name. from the Latin for 'dwarf' and 'elongate'.
Holotype. PIMUZ XXX. Goudemand *et al*., Chapter 4, Pl.13, fig. 8.
Type locality. Sample M05-10. Mud, Himashal Pradesh, Northern India.
Formation and stratigraphic level. Mikin Fm., Bed 10, top of 'Ambites beds', earliest Smithian.
Material. More than 20 specimens from samples W146-C7 and W147-C2, Waili, China and from samples Mud33 and M05-10, Mud, Spiti, India.

Diagnosis. The P1 position is occupied by a short segminate element that closely resembles *Nv*. aff. *pakistanensis morphotype 4* Goudemand and Orchard (Goudemand *et al*., Chapter 4) but differs in having a terminal cusp.
Description. Short segminate element with a length/height ratio of about 1.4-1.5 and 9-12 posteriorly reclined, mostly fused, narrow denticles. Lower margin straight, except for the posterior part of the subcircular or drop-shaped basal cavity that can be downcurved in a manner that is highly reminiscent of *Nv*. *pakistanensis*, to which this species is probably related. Upper margin substraight, except for the terminal cusp that is slightly smaller than the denticles of the anterior process. Maximal height at the 4th or 5th denticle from the posterior end.
Discussion. Small variants like that figured by Orchard (2009, fig. 8.10), by Zhao et al. (*supra*) or like that figured by Goudemand and Orchard (Chapter 4, Pl. 13, fig. 6) may be juveniles of this species. They closely resemble *N*. *dieneri* morphotype 5 Goudemand and Orchard (*ibid*) and some could be juveniles of this species too, which suggests a close relationship between both forms. They more superficially resemble *N*. aff. *cristagalli* morphotypes 2 and 4 (compare with Goudemand *et a*l., Chapter 4, Pl. 7, figs. 6, 14) but besides their relative tiny size, differ also in having more numerous denticles and a basal cavity that is rounded and in lateral view posteriorly straight or downcurved.

***Novispathodus gnomerectus* sp. nov.**- Pl. 1, figs. 3, 10, 11, 14.

? *Nv.* aff. *waageni* 2, Goudemand and Orchard, Chapter 4, Pl. 14, figs. 17, 18.

Derivation of name. from the Latin for 'dwarf' and 'erect'.
Holotype. PIMUZ XXX. Pl. 1, fig. 10.
Type locality. Sample W147-C2, Waili cave section, northwestern Guangxi, South China.
Formation and stratigraphic level. Luolou Fm., top of unit II, earliest Smithian.
Material. 5 to 10 specimens from sample W147-C2, Waili,

China and from samples Mud33 and M05-10, Mud, Spiti, India.

Diagnosis. The P1 position is occupied by a short segminate element that differs from *Nv*. *gnomarcuatus* sp. nov. only in having a bigger length/height ratio (~1.5:1) and more numerous denticles.
Description. About 12-15 usually upright, mostly fused, narrow denticles whose cross-section is subcircular. Lower margin straight anteriorly and slightly upturned posteriorly. Upper margin slightly convex with maximal height at mid-length of the unit. The rounded basal cavity is flat or partly inverted (in which case it is upturned posteriorly and somehow resembles the basal cavity of typical *cristagalli* elements except that it is rounded; compare in particular with *N*. aff. *cristagalli* morphotype 2 Goudemand and Orchard in Goudemand *et al*., Chapter 4, Pl. 7), but a similar variation is also observed in populations of *Nv. gnomarcuatus* sp. nov. (see above). *Nv*. *gnomelongatus* sp. nov. closely resembles but it has posteriorly reclined denticles (see also *Nv*. *gnomoreclinis* sp. nov.).

***Novispathodus gnominfernalis* sp. nov.**- Pl. 1, fig. 5.

? *Nv.* aff. *waageni* 5, Goudemand and Orchard, Chapter 4, Pl. 14, figs. 3, 12, 21.

Derivation of name. from the Latin for 'dwarf' and 'lower'.
Holotype. PIMUZ XXX. Pl. 1, fig. 5.
Type locality. Sample W147-C2, Waili cave section, northwestern Guangxi, South China.
Formation and stratigraphic level. Luolou Fm., top of unit II, earliest Smithian.
Material. 5 specimens from sample W147-C2, Waili, China and from samples Mud33 and M05-10, Mud, Spiti, India.

Diagnosis. The P1 position is occupied by a short segminate element that differs from *Nv*. *gnomarcuatus* sp. nov. by having a big and strongly upturned basal cavity. The upper margin is straight and makes an angle of about 20 degrees with the anterior lower margin (the height of the denticles diminish regularly towards the anterior end).
Description. Segminate element with a length/height ratio of about 1.7:1. About 10-12 upright, mostly fused, narrow denticles whose cross-section is subcircular. Lower margin straight anteriorly and strongly upturned (about 45 degrees with the anterior lower margin) posteriorly beneath the basal cavity. The substraight upper margin with maximal height just in front of the slightly smaller, terminal cusp makes an angle of about 20 degrees with the anterior lower margin. The basal cavity is flat and rounded and its orientation recalls *Ns*. *circuloctavus*.
Remarks. Specimens from Spiti (Goudemand *et al*., Chapter 4, Pl. 14, figs. 3, 12, 21) have higher denticles (hence a much lower length/height ratio of 1.4) and hence closely resemble *Nv*. *strictomarginis* sp. nov. to which they may be transitional. Despite the name (see etymology) they are included in this species too.

***Novispathodus gnomolicinus* sp. nov.**- Pl. 1, fig. 30.

Derivation of name. from the Latin for 'dwarf' and 'bent or turned upward'.
Holotype. PIMUZ XXX. Pl. 1, fig. 30.
Type locality. Sample W147-C2, Waili cave section, northwestern Guangxi, South China.
Formation and stratigraphic level. Luolou Fm., top of unit II, earliest Smithian.
Material. 2 specimens from sample W147-C2, Waili, China.

Diagnosis. The P1 position is occupied by a short segminate element that resembles *Nv*. *gnomarcuatus* sp. nov. and *Nv*. *gnomerectus* sp. nov., but differs by having a conspicuously upturned anterior lower margin.
Description. Segminate element with a length/height ratio of about 1.3:1. About 14 upright, mostly fused, narrow denticles whose cross-section is subcircular. Convex lower margin that is slightly upturned posteriorly beneath the basal cavity and strongly upturned anteriorly. Substraight or arcuate upper margin. The terminal cusp is smaller than the denticles to its anterior. The basal cavity is rounded and slightly inverted.

***Novispathodus gnomoreclinis* sp. nov.**- Pl. 1, figs. 28, 36.

? *Nv.* aff. *waageni* 4, Goudemand and Orchard, Chapter 4, Pl. 14, figs. 6, 11, 24, 25.

Derivation of name. from the Latin for 'dwarf' and 'leaning back'.
Holotype. PIMUZ XXX. Goudemand *et al*., Chapter 4, Pl.14, fig. 11.
Type locality. Sample Mud33. Mud, Himashal Pradesh, Northern India.
Formation and stratigraphic level. Mikin Fm., Bed 10, top of 'Ambites beds', earliest Smithian.
Material. More than 10 specimens from samples W146-C7 and W147-C2, Waili, China and from samples Mud33 and

M05-10, Mud, Spiti, India.

Diagnosis. The P1 position is occupied by a short segminate element that is very similar to *Nv*. *gnomarcuatus* sp. nov., but here the denticles are posteriorly reclined and laterally flattened, and the lower margin is distinctly upturned beneath the posterior third of the element.
Description. About 9-11 posteriorly reclined, mostly fused denticles whose cross-section is elliptical. Basal cavity rounded. Lower margin straight anteriorly and S-shaped upturned posteriorly, as is otherwise typical of the *Nv*. *waageni*'s basal cavity. Posteriorly the tangent of the lower margin is either horizontal (the posterior part of the basal cavity is straight) or oriented slightly aborally (the posterior part of the basal cavity is downcurved). The posterior margin is straight. Convex upper margin with maximal height at about one third from the posterior end of the unit.
Discussion. Elements having a bigger length/height ratio and a lower margin that is more downarched posteriorly (typical '*pakistanensis*' feature) have been here assigned to *Nv*. *gnomelongatus* sp. nov.

***Novispathodus* aff. *pakistanensis* (Sweet) 1970** – Pl. 4.

***morphotype 4*? ** – Pl. 4, fig. 15.

This element closely resembles *Nv*. aff. *pakistanensis* morphotype 4 (see Goudemand *et al*., Chapter 4). It differs in having larger denticles that are also more reclined (hence the length/height ratio is similar around 1.5:1). Unfortunately the denticles are partly broken but the maximal height might have been on the 5th denticle, in which case the upper margin was possibly more arcuate than is typical of *Nv*. *pakistanensis* and more like the one of *Nv*. *waageni*. The lower margin is slightly concave beneath the rounded basal cavity.

***morphotype 7*? ** – Pl. 10, fig. 2.

This conspicuously thickened specimen resembles a very robust version of *Nv*. aff. *pakistanensis* as described and illustrated by Goudemand and Orchard (Goudemand *et al*., Chapter 4, Pl. 13, figs. 10, 15).

***Novispathodus strictomarginis* sp. nov.**- Pl. 10, figs. 3, 6.

Derivation of name. from the Latin for 'straight' and 'margin'; for both the straight (but oblique) upper margin of the P1 element and its straight (horizontal) lower margin posterior of the pit.
Holotype. PIMUZ XXX. Pl. 10, fig. 6.
Type locality. Sample W148-C3, Waili cave section, northwestern Guangxi, South China.
Formation and stratigraphic level. Luolou Fm., top of unit II, earliest Smithian.
Material. 2 specimens from sample W148-C3, Waili, China.

Diagnosis. The P1 position is occupied by a short segminate element that resemble *Nv*. *gnominfernalis* sp. nov., but differs by having a basal cavity whose posterior part is straight.
Description. Segminate element with a length/height ratio of about 1.2-1.5:1 and 11-12 suberect, mostly fused denticles whose cross-section is subcircular. Lower margin straight anteriorly and strongly S-shaped upturned posteriorly beneath the basal cavity: beneath the anterior part of the cup, the lower margin makes an angle of about 45 degrees with the anterior lower margin and beneath the posterior part of the basal cavity it is again parallel to the anterior lower margin. The upper margin is substraight posterior of the deflection of the lower margin and anterior of it, that is from the 5th or 6th denticle from the posterior, it drops regularly with an angle of about 20 degrees. The denticles tend to be broader in the anterior part of the element. The basal cavity is circular and folded in the middle (at the pit): the anterior part makes an angle of about 135 degrees with the posterior part.

***Novispathodus* aff. *waageni* (Sweet) 1970** – Pl. 14.

***morphotype 1* revised** – Pl. 9, fig. 22.

2008 *Neospathodus waageni eowaageni* – Zhao *et al*., fig. 3, part 1.
? *Nv.* aff. *waageni* 1, Goudemand and Orchard, Chapter 4, Pl. 14, fig. 14.

Forms of *Nv*. aff. *waageni* morphotype 1 where the denticles are upright have been here assigned to a new species (see above *Nv*. *gnomarcuatus* sp. nov.). The present form has posterior denticles that are recurved to the posterior.

morphotype 6 – Pl. 1, figs. 15, 27.

1977 *Neospathodus waageni* – Goel, Pl. 2, fig. 4.
? *Nv.* aff. *waageni* 6, Goudemand and Orchard, Chapter 4, Pl. 14, figs. 2, 4.

This morphotype is similar to *Nv*. *gnominfernalis* sp. nov., but maximal height is at midlength rather than posteriorly. The lower margin is convex, being upturned both posteriorly and anteriorly and the denticles tend to radiate. Similar elements were reported by Goel (1977) from a section at Khar. This morphotype somewhat resembles *Nv*. *waageni* morphotype 6 but the posterior denticulation, especially the size and orientation of the posteriormost denticle differs markedly: in the latter it is strongly reclined and recurved posteriorly and here it is only slightly reclined and of subtriangular shape.

morphotype 7 **new** – Pl. 10, figs. 1, 4.

The shortest of these specimens (Pl. 10, fig. 1) closely resembles *Nv*. *waageni* but is conspicuously arched laterally, has a more elongate, somewhat rhomboid basal cavity and a flange is markedly developed on its flanks. The lower margin is substraight or slightly upturned beneath the basal cavity. The second specimen (fig. 4) has two more denticles and resembles an elongate version of the former.

Subfamily Uncertain

Genus BORINELLA Budurov and Sudar, 1994.

Type species and holotype. *Neogondolella buurensis* Dagis, 1984, pp.12-13, pl. XI, figs. 1, 2.
Type stratum and locality. Buur River basin, Taion-Uiolaakh River, *Hedenstromia hedenstromi* Zone.

Multielement diagnosis. Orchard (2005) observed that the limited material of '*Neogondolella*' *buurensis* available for study resembles elements of *Wapitiodus* (which is here regarded as synonymous with *Guangxidella*). In a more recent paper, Orchard (2007) wrote that "the multielement apparatus of *Borinella chowadensis* [..] is the same as that of *Neogondolella*". Pending reconstruction of its apparatus, its suprageneric assignment remains uncertain but a derivation from *Neogondolella* is the most plausible hypothesis.

Borinella **cf.** ***nepalensis*** **(Kozur & Mostler)** 1976 – Pl. 2, fig. 17.

Only the anterior part of this specimen remains. The broken denticles seem bigger towards the anterior (generic assignment) and the profile suggest that this specimen is a quite broad variant of this species. Without the missing posterior part, any reliable assignment is impossible.

Genus EURYGNATHODUS Staesche, 1964.

Type species and holotype. *Eurygnathodus costatus* Staesche, 1964, pp.269-271, Pl. 28, figs. 1-4.
Type stratum and locality. middle Campil Member, St. Vigil, Enneberg, South Tyrol.

Eurygnathodus costatus Staesche, 1964 – Pl. 2, figs. 1-11.

The smooth *Eu*. *hamadai* was not found in the collections from the 'Waili cave' section. Yet, it does co-occur with the costate *Eu*. *costatus* in correlative (ammonoid-based correlation) beds of neighbouring sections.

Eurygnathodus **aff.** ***costatus*** – Pl. 2, fig. 12.

This small segminate specimen resembles the co-occuring *Eu*. *costatus* in lateral view and has also a broad basal cavity but the denticulation is different: compared with similarly small elements of the latter species (see Pl. 2, figs. 10, 11), this specimen is higher, much thinner and lacks the distinctive transverse ribs.

Eurygnathodus**? sp.** – Pl. 2, fig. 13.

This broken specimen has a broad, large, flat basal cavity that resembles that of *Eurygnathodus*, to which it is tentatively assigned. This very robust, globular form is however very different to other known representatives of the genus and corresponds either to a new species or to a new genus. The denticulation also clearly differs in consisting of a main row of small, spiky denticles (no ribs), and an additional node or denticle laterally at mid-length of the unit, which are somehow reminiscent of the Griesbachian *Isarcicella*. This element also resembles '*Neospathodus*' n. sp. G from Chaohu (Zhao, 2005, Pl. 6, figs. 7a-c; co-occurs with *Eu. costatus* in subbed 25-23 at

Chaohu, West Pingdingshan section), to which it may be related, but it differs in having a posterior process.

New Genus D – Pl. 11, fig. 3.

This S2 element has a bifurcated antero-lateral process as new genus B Goudemand and Orchard (Chapter 4) but the nature of this bifurcation is different: it is not Y-shaped but rather like an inverted T and the anteriormost denticles are recurved to the posterior. The only remaining process bears numerous, high and strongly fused denticles which form a relatively high crest.

New Genus E – Pl. 11, fig. 7.

This S3 or S4 element is laterally flattened, has a big and broad cusp that is strongly recurved to the posterior. The anterior process is about half the length of the posterior one and it is strongly bowed laterally, whereas the latter is straight. The denticles of the anterior process are suberect in lateral view and recurved inward and posteriorly. The denticles of the posterior process are strongly reclined to the posterior. The lower margin is slightly upturned at the posterior end and more conspicuously upturned at the antero-lateral end. Fused clusters of S3 and S4 elements have been recently described from the same interval of the same section (Goudemand *et al*., Chapter 1). It showed that S3 and S4 elements are almost identically shaped. Such elements are rather abundant in association with P1 elements of the *Ns*. *dieneri* and *Ns*. *cristagalli* groups but it is still uncertain to what apparatus they belong.

New Genus F – Pl. 12, figs. 28, 29.

These P2 elements have strongly fused, irregular denticles. The subequilaterally triangular free apices of the anterior process of the specimen illustrated on fig. 29 suggest a close relationship with *La*. *robusta*. The curved, latero-posteriorly projected denticles of the posterior process recall elements assigned here to *La*. n. sp. 1. The peculiar shape of these P2 elements might be the basis for a separate generic assignment of the yet unknown, corresponding multi-element apparatus.

Gen. et sp. indet. 1 – Pl. 2, fig. 14.

This broken (anguli?-)scaphate element has a big cusp and discrete denticles.

Gen. et sp. indet. 2 – Pl. 2, fig. 15.

This possibly teratological, aborally broken element has a long, narrow, longitudinal groove on the posterior margin of the cusp.

Gen. et sp. indet. 3 – Pl. 2, fig. 16.

This very peculiar, possibly teratological, carminiscaphate element has a huge cusp (broken at about mid-height) that is slightly recurved to the posterior. In oral or aboral view, the element is somewhat drop-shaped and the flat basal cavity occupies the entire aboral surface. At the posterior end there is small denticle that is recurved to the anterior. The anterior process is conspicuously downarched and bears two fused denticles that are recurved to the posterior in a manner such that the anterior process resembles a fish tail.

Gen. et sp. indet. 4 – Pl. 2, fig. 19.

This short and very thin slightly angulate element has a big terminal, subtriangular cusp and three smaller denticles. The cusp and the anterior denticles are strongly reclined to the posterior. This P2 element resembles elements assigned to *Cornudina latidentata* by Kozur and Mostler (1970, Pl. 1, fig. 21).

Gen. et sp. indet. 5 – Pl. 9, fig. 20.

This short, comb-like element is reminiscent of both *Sweetospathodus kummeli* (but it is much shorter) and *Discretella* spp. The high, rather discrete denticles are pointed apically, some are even subtriangular in shape and they get broader toward the anterior. Maximal height is at mid-length and the upper margin is arcuate. The lower margin is downwardly convex, almost V-shaped, with a clear angle between the anterior process and the posterior part beneath the inverted basal cavity.

Superfamily POLYGNATHACEA Ulrich & Bassler, 1926

Genus ISARCICELLA Kozur, 1975.

Type species and holotype. *Spathognathodus isarcica* Huckriede, 1958, pp. 162, Pl. 6, figs. 7a-c.
Type stratum and locality. Seiser beds (Griesbachian), Pufelsbach, Gröden, South Tirol.

Diagnosis and type species. The P1 position is occupied by a scaphate element with a very wide and inflated cup bearing lateral nodes or denticles on one or both sides.

***Isarcicella*? n. sp. 1** - Pl. 6, fig. 16.

This segminate element has a very asymmetrical, wide basal cavity, the more developed lateral lobe of which bears one denticle. The length/height ratio is about 1.4:1 and it bears 7-8 suberect denticles. The posterior end of the blade is laterally (inwardly) deflected and bears denticles whose height decreases rapidly. The anterior process, whose anteriormost part is partly broken, is about half the length of the unit and hence much larger than is typical in *Isarcicella*. The lower margin is straight anteriorly and S-shaped beneath the wide, conspicuously asymmetrical and inflated basal cavity. The outer side of the cup (convex side of the slightly asymmetrical element) is much more developed laterally than the inner side and bears a prominent denticle. The anterior process is laterally compressed in front of the cup and the corresponding denticles are elliptical or lenticular in cross-section. The typical very prominent 'false cusp', which usually occupies most of the anterior process in front of the cup, is missing but it is not excluded that it is only broken off. Consequently, and despite the huge stratigraphic gap between this occurrence and the youngest known occurrence of *Isarcicella* in the late Griesbachian and the unusual length of the anterior process, this specimen is tentatively assigned to the present genus and not considered as a homeomorph of for instance *Isarcicella staeschei* Dai and Zhang (1989), which it most closely resembles. Note that specimens of the related form *Hindeodus* sp. were found also by Orchard and Savage in the already mentioned Dienerian (?) material from Thailand (Orchard, 2010, pers. comm.). These occurrences need to be confirmed by resampling in order to exclude any contamination (both faunas are very well preserved and show no sign of reworking). Yet, it seems that both genera survived after the late Griesbachian at least up to the late Dienerian and early Smithian respectively, but such younger representatives are very rare, in contrast with Griesbachian times when anchignathodontids dominated the conodont faunas of tropical seas (Alps, China).

Suborder PRIONIODININA

Genus ELLISONIA Müller, 1956.

The type species (*E. triassica*) was described from Smithian strata in Nevada. The most recent suprageneric classification of euconodonts by Donoghue *et al*. (2008) suggests that latest Permian *Merrillina* rather belongs to suborder Ozarkodinina, which would weaken Kozur's hypothesis (2004, p. 54) of *Ellisonia* and *Hadrodontina* (both genera of the suborder Prioniodinina) evolving from *Merrillina* in the Lower Triassic. Yet, their homology assignments relative to these genera are not convincing and pending reassessment of their cladistic analysis, the latter hypothesis is retained. Consequently, as explained by Orchard (2007), it is not clear yet whether earliest Triassic representatives should be assigned to the one or the other genus.

Ellisonia triassica Müller, 1956 – Pl. 11, fig. 10.

Koike (2004) reconstructed the apparatus of this species recently from a natural assemblage. The present specimen strikingly resembles its S4 element (*ibid*, fig. 7, part 7).

Ellisonia* aff. *triassica *sensu* Koike, 2004 – Pl. 11, fig. 11.

Koike (2004) reconstructed the apparatus of this species. The present specimen is probably a S3 element (*ibid*, fig. 8, part 5).

Merillina*?/*Ellisonia*? aff. *agordina Perri and Andraghetti, 1987 – Pl. 10, fig. 23.

The overall shape of this P1 element resembles the homologous element (*supra*, Pa element) of *Ellisonia agordina* in having 4 subequal denticles which are strongly recurved to the posterior. Yet, the present element is not bowed laterally (con-

trary to *E. agordina*, which is almost angulate, the denticles of this element lie more or less in the same plane) and the elliptical lower surface is not reversed with an expanded zone of recessive basal margin but rather scaphate.
This element co-occurs with *Eu*. *costatus*. Another specimen has been found also in Jinya (sample J290-C3; Goudemand, in prep.), again in co-occurrence with *Eu*. *costatus*. Apparently a similar element with 5 denticles has been found by Zhao in Chaohu in subbed 25-17 (sample CP25-4, unpublished) within the occurrence interval of *Eu*. *costatus*. Dagis (1984) assigned a similar element from the early Smithian (*Hedenstromia hedenstromi* Zone) of Siberia to '*Sweetocristatus*' *borealis* (*ibid*, Pl. X, fig. 4; see also below). The latter has 6 denticles.

***Merillina*?/*Ellisonia*? aff. sp. B** Orchard, 2007 – Pl. 10, fig. 15.

This element strongly resembles the Dienerian element illustrated by Orchard (*ibid*), but differs in having a slightly more developed anterior process and more fused posterior process. A similar element has been found by Zhao in Chaohu in subbed 25-25 (unpublished). Another possibly related specimen is reported by Koike from early Smithian rocks of Malaysia (Koike, 1982, Pl. VII, fig. 7). He assigned this specimen to *Cornudina breviramulis minor* Kozur and Mostler (1970) but it more closely resembles the Griesbachian *Me*.?/*Ell*.? *peculiaris* and might be better assigned to the present genus.

***Merillina*?/*Ellisonia*? sp.** – Pl. 10, fig. 13; Pl. 12, fig. 22.

These laterally flattened elements have a very big cusp.

Genus HADRODONTINA Staesche, 1964.

Hadrodontina aequabilis Staesche, 1964 – Pl. 10, fig. 25.

This element fits the description of the P1 element of *Hd. aequabilis* as reconstructed by Perri (1991). A second, similar element (Pl. 10, fig. 17) has an inverted basal cavity and is hence assigned to *Hd*. aff. *aequabilis*.

Genus SWEETOCRISTATUS Szaniawski, 1979.

The original diagnosis refer to an angulate P1 element "with reclined cusp, well-developed, high anterior process and shorter posterior process which is bent downwardly [...]. Both processes denticulated. Basal cavity in advanced forms prominent, flaring beneath the cusp, narrowing more strongly anteriorly than posteriorly; in primitive forms, small, elongated." (Szaniawski, 1979).

Sweetocristatus*? aff. *unicus Dagis, 1984 – Pl. 10, fig. 9.

This laterally flattened element has a big, reclined cusp, a high anterior process wearing broad denticles and a shorter, smaller posterior process beneath which the lower margin is slightly downcurved. The basal cavity is large, S-shaped, extends beneath the entire unit, and tapers at both ends. This description fits at least superficially the diagnosis of *Sweetocristatus*, but the cavity does not quite flare as much as seems typical of the genus. The present generic assignment stems from the similarity of this specimen with the holotype of *Sweetocristatus unicus* Dagis (*supra*, Pl. X, fig. 6). Yet, the denticulation of the latter clearly differs from the present specimen in being much more discrete and the denticle of the anterior process of *Sw. unicus* appears markedly separated from the cusp, which is not the case here. This element also resembles a *Novispathodus* P2 element with broad denticles, but its basal cavity is significantly different and the unit is not angulate.

***?Sweetocristatus* spp.** – Pl. 10, figs. 14, 20.

Elements grouped here share some (superficial) affinity with *Sweetocristatus* or at least with elements assigned to this genus by Dagis (1984) but are not considered to belong to the latter: both elements have a posterior process that exceeds the anterior process in length; hence, the question mark to the left of the genus name. The element on Pl. 10, fig. 14 resembles the element assigned by Dagis to *Sweetocristatus borealis* (*ibid*, Pl. X, fig. 4) and to which we compared our element on Pl. 10, fig. 23, here assigned to *Merillina*?/*Ellisonia*? aff. *agordina*. The posterior process is more developed and more reclined

than the element on Pl. 10, fig. 23, and the basal cavity is pointed posteriorly beneath it. Yet, compared to Dagis' specimen it is not arched; its lower margin is straight. The second specimen (Pl. 10, fig. 20) is arched and its denticulation is somewhat reminiscent of *Sw. unicus* to which it is possibly related; but again its posterior process is much larger than the anterior one. It also resembles an element assigned by Dagis to *Sw. borealis* (*ibid*, Pl. X, fig. 2), but this assignment is precluded both by the bad preservation of the aboral surface of our specimen and by the lack of additional views on Dagis' illustration plate. Note that the shape of the cusp strongly resembles that of the element on Pl. 12, fig. 18, which could be the corresponding P2 element.

Acknowledgements

This research is supported by the Swiss NSF project 200020-113554 (to H.B.). We are much indebted to the following colleagues: Arnaud Brayard (CNRS, Dijon) and Thomas Galfetti (Zurich) were of great support during fieldwork; Leonie Pauli and Julia Huber (Zurich) dissolved and concentrated the conodont samples; Peter Strauss (GSC, Vancouver) helped with some of the SEM photographs; Séverine Urdy (Zurich) helped with the preparation of the plates; Mike Orchard (GSC, Vancouver) discussed some of the results.

References

Agematsu, S., M. J. Orchard, AND K. Sashida. 2008. Reconstruction of an apparatus of *Neostrachanognathus tahoensis* from Oritate, Japan and species of *Neostrachanognathus* from Oman. Palaeontology, 2008(?):1-11?

Bender, H. 1968. Zur Gliederung der Mediterranen Trias II. Die Conodontenchronologie der Mediterranen Trias. Annales Géologiques des Pays Hélléniques, 19:465-540.

Birkenmajer, K., AND J. Trammer. 1975. Lower Triassic Conodonts from Hornsund, South Spitsbergen. Acta Geologica Polonica, 25(2):299-308.

Brayard, A., AND H. Bucher. 2008. Smithian (Early Triassic) ammonoid faunas from northwestern Guangxi (South China): Taxonomy and Biochronology. Fossils and Strata, 55:179 pp.

Brayard, A., H. Bucher, T. Brühwiler, T. Galfetti, N. Goudemand, G. Kuang, G. Escarguel, AND J. Jenks. 2007. *Proharpoceras* Chao: a new ammonoid lineage surviving the end-Permian mass extinction. Lethaia, 40:175-181.

Brayard, A., H. Bucher, G. Escarguel, F. Fluteau, S. Bourquin, AND T. Galfetti. 2006. The Early Triassic Ammonoid Recovery: Paleoclimatic Significance of Diversity Gradients. Palaeogeography, Palaeoclimatology, Palaeoecology.

Brühwiler, T., A. Brayard, H. Bucher, AND K. Guodun. 2008. Griesbachian and Dienerian (Early Triassic) ammonoid faunas from northwestern Guangxi and southern Guizhou (South China). Palaeontology, 51(5):1151-1180.

Brühwiler, T., AND H. Bucher. accepted. Systematic palaeontology. , Smithian (Early Triassic) ammonoids from the Salt Range, Pakistan.

Buryi, G. I. 1979. Lower Triassic Conodonts of Southern Primor›ye, Trudy Instituta Geologii i Geofiziki [Proceedings of the Institute of Geology and Geophysics of the Siberian Department of the USSR Academy of Sciences].Volume 412. Nauka Publishers, Moscow.

Chao, K. 1950. Some new ammonite genera of Lower Triassic from western Kwangsi. Palaeontological Novitates, 5:1-11.

Chao, K. 1959. Lower Triassic ammonoids from Western Kwangsi, China. Palaeontologia Sinica. New Series B, 9:355 pp.

Dagis, A. A. 1984. Lower Triassic Conodonts from Northern Central Siberia. Nauka Publishers, Moscow, 554.

Dai, J., AND J. Zhang. 1989. Description of new genus and species : Conodonts, p. 220-238. *In* L. Zishun (ed.), Study on the Permian-Triassic Biostratigraphy and Event Stratigraphy of Northern Sichuan and Southern Shaanxi.Volume Series 2, Number 9. Geological Publishing House, Beijing.

Donoghue, P. C. J., M. A. Purnell, R. J. Aldridge, AND S. Zhang. 2008. The interrelationships of ‹complex› conodonts (Vertebrata). Journal of Systematic Palaeontology, 6(2):119-153.

Dzik, J. 1976. Remarks on the evolution of Ordovician conodonts. Acta Palaeontologica Polonica, 21:395-455.

Eichenberg, W. 1930. Conodonten aus dem Culm des Harzes. Palaeontol. Zeitschr., 12:177-

182.

Galfetti, T., H. Bucher, R. Martini, P. A. Hochuli, H. Weissert, S. Crasquin-Soleau, A. Brayard, N. Goudemand, T. Brühwiler, AND G. Kuang. 2008. Evolution of Early Triassic outer platform paleoenvironments in the Nanpangjiang Basin (South China) and their significance for the biotic recovery. Sedimentary Geology, 204:36-60.

Goel, R. K. 1977. Triassic Conodonts from Spiti (Himachal Pradesh), India. Journal of Paleontology, 51(6):1085-1101.

Hirsch, F. 1994. Triassic conodonts as ecological and eustatic sensors, p. 949-959, Pangea: Global Environments and Resources.Volume Memoir 17. Canadian Society of Petroleum Geologists.

Hirschmann, C. 1959. Über Conodonten aus dem oberen Muschelkalk des Thüringer Beckens. Freiberger Forschungshefte, 76:35-86.

Huckriede, R. 1958. Die Conodonten der mediterranen Trias und ihr stratigraphischer Wert. Paläontologisches Zeitschrift, 32(3/4):141-175.

Koike, T. 1982. Triassic Conodont Biostratigraphy in Kedah, West Malaysia. Contributions to the Geology and Palaeontology of Southeast Asia, 23:9-65.

Koike, T. 1996. Skeletal Apparatuses of Triassic Conodonts of *Cornudina*. Prof. H. Igo Commem. Vol.:113-120.

Koike, T. 1998. Triassic Coniform Conodont Genera *Aduncodina* and *Neostrachanognathus*. Paleontological Research, 2(2):120-129.

Koike, T., S. Yamakita, AND N. Kadota. 2004. A natural assemblage of *Ellisonia* sp. cf. *E. triassica* Müller (Conodonta) from the Permian-Triassic boundary in the Suzuka Mountains, Central Japan. Paleontological Research, 8(4):241-253.

Kozur, H. 1975. Beiträge zur Conodontenfauna des Perm. Geol. Paläont. Mitt. Innsbruck, 5(4):1-44.

Kozur, H. 2004. Pelagic Uppermost Permian and the Permian-Triassic Boundary Conodonts of Iran. Part I: Taxonomy. Hallesches Jahrbuch für Geowissenschaften, Reihe B, 18:39-68.

Kozur, H., AND H. Mostler. 1970. Neue Conodonten aus der Trias. Ber. Nat.-Med. Ver. Innsbruck, 58:429-464.

Kozur, H., AND H. Mostler. 1976. Neue Conodonten aus dem Jungpaläozoikum und der Trias. Geol. Paläont. Mitt. Innsbruck, 6(3):1-33.

Lindström, M. 1970. A Suprageneric Taxonomy of the Conodonts. Lethaia Norwegia, 3:427-445.

Mosher, L. C. 1968. Triassic Conodonts from Western North America and Europe and Their Correlation. Journal of Paleontology, 42(4):895-946.

Müller, K. J. 1956. Triassic Conodonts from Nevada. Journal of Paleontology, 30(4):818-830.

Orchard, M. J. 1995. Taxonomy and Correlation of Lower Triassic (Spathian) Segminate Conodonts from Oman and Revision of Some Species of Neospathodus. Journal of Paleontology, 69(1):110-122.

Orchard, M. J. 2005. Multielement conodont apparatuses of Triassic Gondolelloidea, p. 73-101. *In* M. A. Purnell and P. C. J. Donoghue (eds.), Conodont Biology and Phylogeny: Interpreting the Fossil Record.Volume 73. Special Chapter 4s in Palaeontology.

Orchard, M. J. 2007. Conodont diversity and evolution through the latest Permian and Early Triassic upheavals. Palaeogeography, Palaeoclimatology, Palaeoecology, 252:93-117.

Orchard, M. J., AND J.-P. Zonneveld. 2009. The Lower Triassic Sulphur Mountain Formation in the Wapiti Lake area: lithostratigraphy, conodont biostratigraphy, and a new biozonation for the lower Olenekian (Smithian). Canadian Journal of Earth Sciences, 46:757-790.

Paull, R. K., R. A. Paull, AND T. S. Laudon. 1997. Conodont Biostratigraphy of the Lower Triassic Mackenzie Dolomite Lentil, Sulphur Mountain Formation in the Cadomin Area, Alberta. Bulletin of Canadian Petroleum Geology, 45(4):708-714.

Perri, M. C. 1991. Conodont Biostratigraphy of the Werfen Formation (Lower Triassic), Southern Alps, Italy. Bolletino della Società Paleontologica Italiana, 30(1):23-46.

Perri, M. C., AND M. Andraghetti. 1987. Permian-Triassic Boundary and Early Triassic Conodonts from the Southern Alps, Italy. Rivista Italiana di Paleontologia e Stratigrafia, 93(3):291-328.

Smith, A. G., D. G. Smith, AND B. M. Funnell. 1994. Atlas of Mesozoic and Cenozoic Coastlines. Cambridge University Press, Cambridge.

Staesche, U. 1964. Conodonten aus dem Skyth von Südtirol. Neues Jahrbuch für Geo-

logie und Paläontologie. Abhandlungen, 119(3):247-306.

Sweet, W. C. 1970. Uppermost Permian and Lower Triassic Conodonts of the Salt Range and Trans-Indus Ranges, West Pakistan, p. 207-275. *In* B. Kummel and C. Teichert (eds.), Stratigraphic Boundary Problems: Permian and Triassic of West Pakistan.Volume Special Publication 4. The University Press of Kansas.

Szaniawski, H., AND K. Małkowski. 1979. Conodonts from the Kapp Starostin Formation (Permian) of Spitsbergen. Acta Palaeontologica Polonica, 24:231-264.

Tatge, U. 1956. Conodonten aus dem germanishen Muschelkalk. Paläontologisches Zeitschrift, 30(1/2):108-127.

Tong, J., Y. D. Zakharov, M. J. Orchard, H. Yin, AND H. J. Hansen. 2003. A Candidate of the Induan-Olenekian Boundary Stratotype in the Tethyan Region. Science in China (series D), 46(11).

Tong, J., Y. D. Zakharov, M. J. Orchard, H. Yin, AND H. J. Hansen. 2004. Proposal of Chaohu Section as the GSSP Candidate of the Induan-Olenekian Boundary. Albertiana, 29:13-28.

Ulrich, E. O., AND R. S. Bassler. 1926. A classification of the toothlike fossils, conodonts, with descriptions of American Devonian and Mississippian species. Proceedings of the United States National Museum, 68:1-63.

Wang, Z.-h., AND Y.-y. Cao. 1981. Early Triassic Conodonts from Lichuan, Western Hubei. Acta Pal. Sinica, 20(4):363-375.

Yin, H. F., K. X. Zhang, J. N. Tong, Z. Y. Yang, AND S. B. Wu. 2001. The Global Stratotype Section and Point (GSSP) of the Permian-Triassic Boundary. Episodes, 24(2):102-114.

Zhang, S., AND Z. Yang. 1991. On Multielement Taxonomy of the Early Triassic Conodonts. Stratigraphy and Paleontology of China, 1:17-47.

Zhao, L., M. J. Orchard, J. Tong, Z. Sun, J. Zuo, S. Zhang, AND A. Yun. 2007. Lower Triassic conodont sequence in Chaohu, Anhui Province, China and its global correlation. Palaeogeography, Palaeoclimatology, Palaeoecology, 252:24-38.

Zhao, L., J. Tong, AND M. J. Orchard. 2005. Study on the Lower Triassic conodont sequence and the Induan-Olenekian boundary in Chaohu, Anhui Province. PhD thesis, China University of Geosciences Press, Wuhan, Hubei, China, 140 p.

Zhao, L., J. Tong, Z. Sun, AND M. J. Orchard. 2008a. A detailed Lower Triassic conodont biostratigraphy and its implications for the GSSP candidate of the Induan-Olenekian boundary in Chaohu, Anhui Province. Progress in Natural Science, 18:79-90.

Zhao, L., J. Tong, S. Zhang, AND Z. Sun. 2008b. An update of conodonts in the Induan-Olenekian boundary strata at West Pingdingshan section, Chaohu, Anhui Province. Journal of China University of Geosciences, 19(3):207-216.

PLATE 1

Figs. 1, 4, 12, 13, 16, 17, 20, 23, 27-29, 31. *Novispathodus gnomarcuatus* sp. nov., P1 elements. All W147-C2, except 20, 27, 28: W146-C8.

Figs. 2, 6-9, 18?, 21, 22, 25? *Novispathodus gnomelongatus* sp. nov., P1 elements. All W147-C2, except 21, 22, 25: W146-C8.

Figs. 3, 10, 11, 14, 24? *Novispathodus gnomerectus* sp. nov., P1 elements. All W147-C2.

Fig. 5. *Novispathodus gnominfernalis* sp. nov., P1 element. W147-C2.

Figs. 15, 27. *Novispathodus* aff. *waageni* morph 6, P1 elements. 15: W147-C2, 27: W146-C8.

Figs. 19?, 28, 36, 37? *Novispathodus gnomreclinis* sp. nov., P1 elements. 19: W147-C2; 28, 36, 37: W146-C8.

Fig. 26. *Novispathodus* aff. *waageni* morph indet., P1 element. W146-C8.

Fig. 30. *Novispathodus gnomolicinus* sp. nov., P1 element. W147-C2.

Figs. 32-35. *Novispathodus* sp. indet. P2 elements. 32-34: W147-C2; 35: W146-C8.

All ×80.

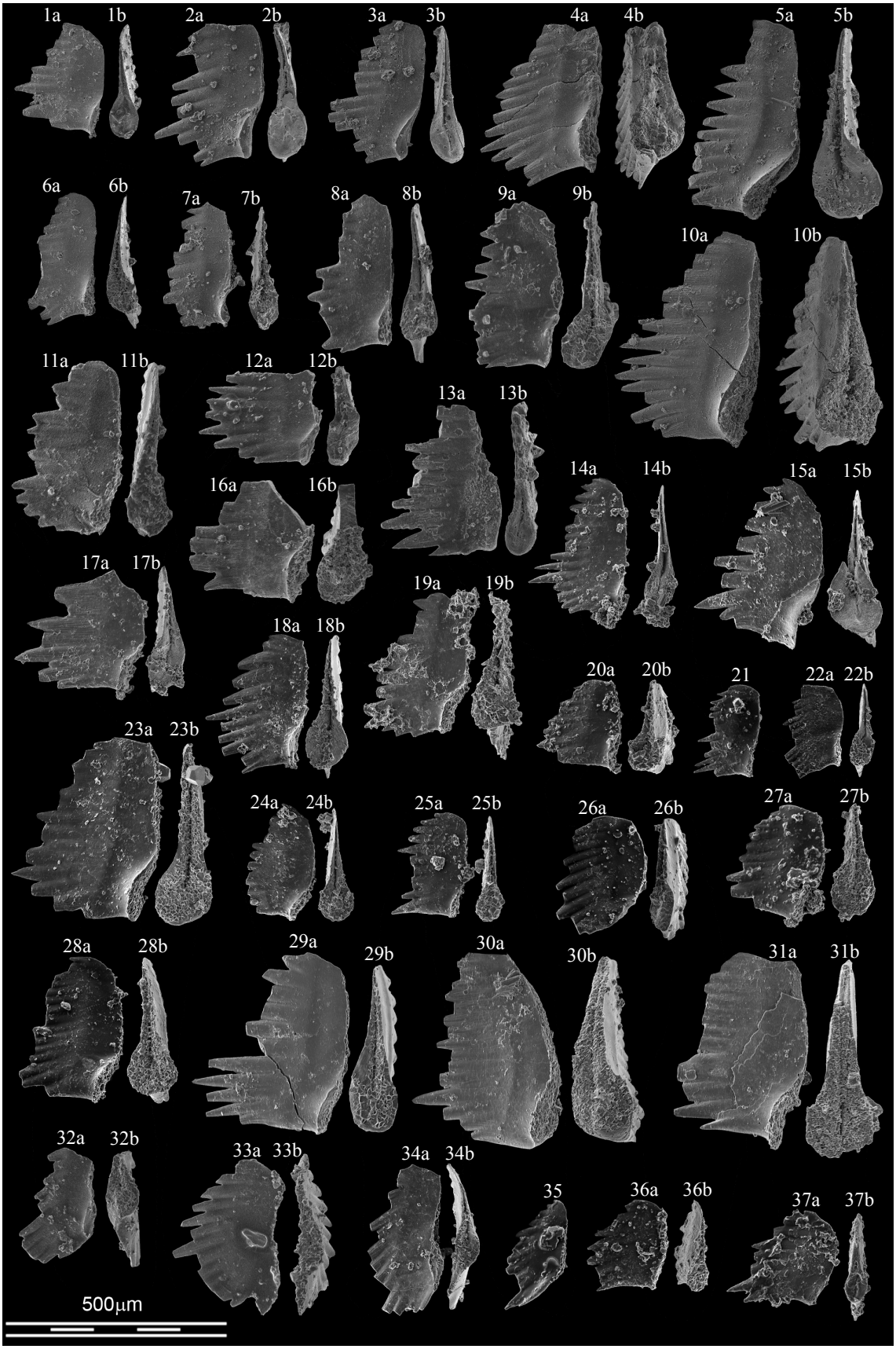
1a 1b 2a 2b 3a 3b 4a 4b 5a 5b
6a 6b 7a 7b 8a 8b 9a 9b
10a 10b
11a 11b 12a 12b
13a 13b
14a 14b 15a 15b
16a 16b
17a 17b
19a 19b
18a 18b
20a 20b 21 22a 22b
23a 23b
24a 24b 25a 25b 26a 26b 27a 27b
28a 28b 29a 29b 30a 30b 31a 31b
32a 32b 33a 33b 34a 34b 35 36a 36b 37a 37b
500μm

PLATE 1

PLATE 2

Figs. 1-11. *Eurygnathodus costatus*. 1-4: WAI64; 5-9: WAI65; 10, 11: W150-C4.
Fig. 12. *Eu*. aff. *costatus*. WAI65.
Fig. 13. *Eurygnathodus*? sp. W145-C7.
Fig. 14. Gen. et sp. indet. 1. W146-C8.
Fig. 15. Gen. et sp. indet. 2. W147-C2.
Fig. 16. Gen. et sp. indet. 3. W146-C8.
Fig. 17. *Borinella* cf. *nepalensis*. W148-C3.
Fig. 18. La.? n. sp. 5. W147-C2.
Fig. 19. Gen. et sp. indet. 4. W146-C8.

All ×80. All P1 elements.

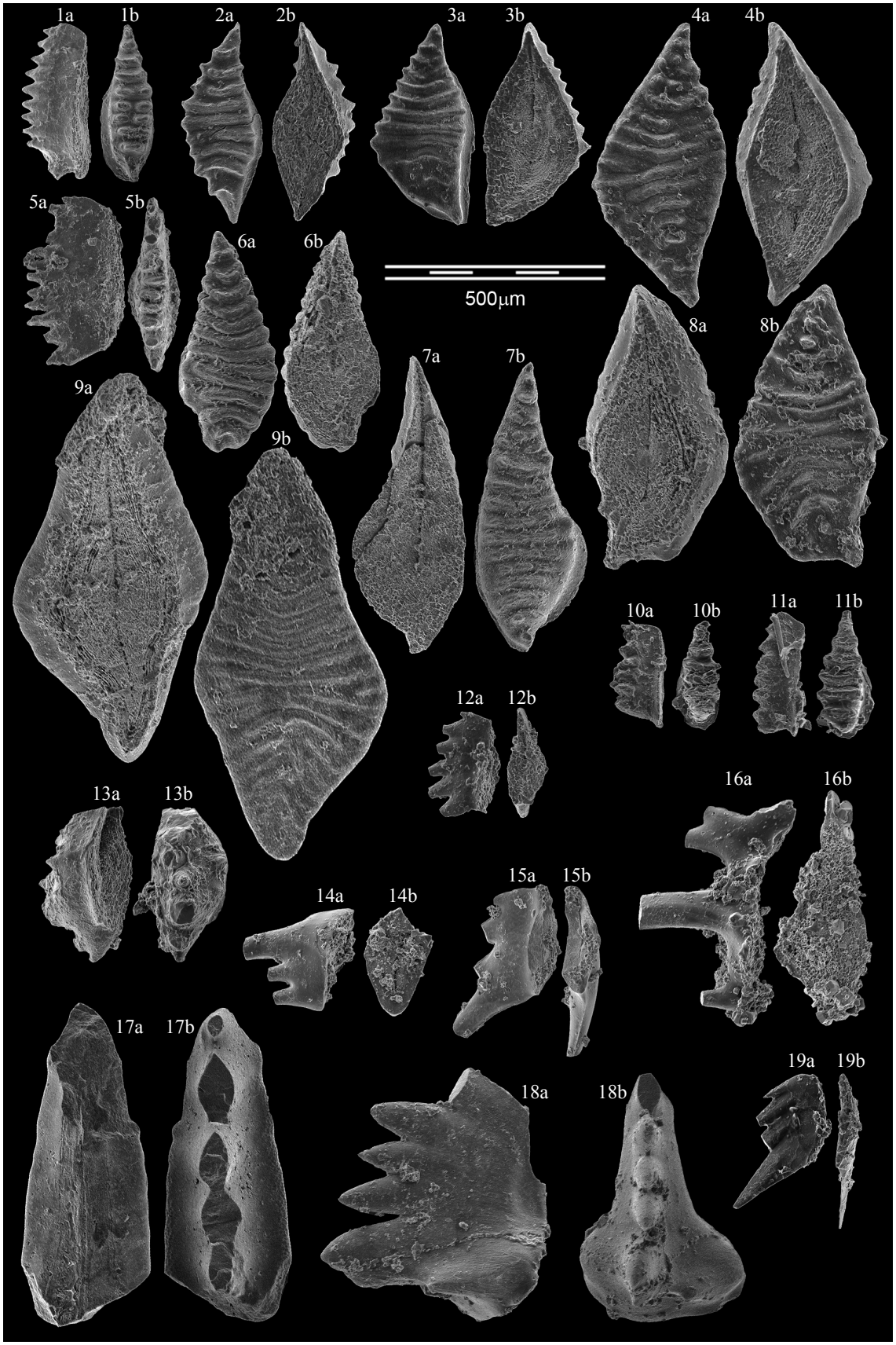
1a
1b
2a
2b
3a
3b
4a
4b
5a
5b
6a
6b
500μm
8a
8b
7a
7b
9a
9b
10a
10b
11a
11b
12a
12b
13a
13b
16a
16b
15a
15b
14a
14b
17a
17b
19a
19b
18a
18b

PLATE 2

PLATE 3

Figs. 1, 4, 5?, 6. *Larenella*? *concava* morph 1. 1, 4: W146-C8; 5: W145-C7; 6: W143-C1.
Fig. 2. *Larenella*? cf. *concava*. W146-C8.
Fig. 3. *Larenella*? aff. *concava*. W143-C1.
Fig. 7. *Larenella*? cf. *linearis* Zhao and Orchard. W145-C7.
Fig. 8. *Larenella*? *concava* morph 2. W148-C3.
Fig. 9. *Larenella* aff. *falcata*. WAI61.
Fig. 10. *Larenella fastuosa* sp. nov. W148-C3.
Fig. 11. transitional between *La*. *concava* and *La*. *astericisala* sp. nov. W148-C3.
Figs. 12, 13. *La*. cf. *galfettii* sp. nov. 13: W148-C3, 12: WAI61.
Fig. 14. *Larenella falcata* sp. nov. W148-C3.

All ×80. All P1 elements.


1a
1b
2a
2b
3a
3b
4a
4b
5a
5b
6a
6b
7a
7b
8a
8b
9a
9b
10a
10b
500μm
11a
11b
12a
12b
13a
13b
14a
14b

PLATE 3

PLATE 4

Fig. 1. transitional? between *Ns*. *dieneri* 9 and *La*.? n. sp. 1. W148-C3.
Fig. 2. *Larenella*? n. sp. 2. W148-C3.
Figs. 3, 6?, 11. *Larenella*? n. sp. 1. 3, 6: WAI61; 11: W148-C3.
Fig. 4. *Larenella fastuosa* sp. nov. W148-C3.
Fig. 5. *Larenella*? cf. n. sp. 4. W148-C3.
Fig. 7. *Larenella elvis* sp. nov. WAI61.
Figs. 8, 9. teratological? specimens of *Larenella elvis*?. 8: WAI61, 9: W148-C3.
Fig. 10. Ns. cf. dieneri 9?. WAI64.
Fig. 12. *Larenella* aff. *fastuosa* sp. nov. W148-C3.
Fig. 13. transitional between *La*. *dakuangi* sp. nov. and *La*. *chaohuense*. W148-C3.
Fig. 14. *Nv*.? aff. *gnomerectus*. W146-C8. The basal cavity and the denticles recall *Nv*. *gnomerectus* sp. nov. Yet, the denticles are not erect but reclined to the posterior.
Fig. 15. *Nv*. aff. *pakistanensis* 4?. WAI65.
Fig. 16. *Neospathodus* cf. *dieneri* morph 8. W148-C3.
Fig. 17. *Merillina*?/*Ellisonia*? aff. n. sp. B Orchard (2007). W148-C3.

All ×80. All P1 elements.


1a
1b
2a
2b
3a
3b
4a
4b
5
6a
6b
7a
7b
8a
8b
9a
9b
10a
10b
11a
12a
12b
13a
13b
500μm
14a
14b
11b
15a
15b
16a
16b
17a
17b

PLATE 4

PLATE 5

Figs. 1, 4. *Larenella dakuangi* sp. nov. 1: W148-C3, 4: W144-C6.
Figs. 2, 3. *Larenella*? *concava* morph 3. 2: W148-C3, 3: WAI61.
Fig. 5. *Larenella* cf. *galtettii* sp. nov. W144-C6.
Figs. 6, 7. *Larenella* n. sp. 3. Both WAI61.
Fig. 8. *Larenella galfettii* sp. nov. W148-C3.
Figs. 9, 15. *Larenella* aff. *brayardi*. 9: W148-C3, 15: WAI61.
Fig. 10. transitional? to *Larenella quitondeta* sp. nov. WAI61.
Fig. 11. *Larenella*? n. sp. 2. W148-C3.
Fig. 12. *Larenella brayardi* sp. nov. W148-C3.
Figs. 13, 14?, 16. *Larenella quitondeta* sp. nov. 13, 16: WAI61; 14: W148-C3.

All ×80. All P1 elements.

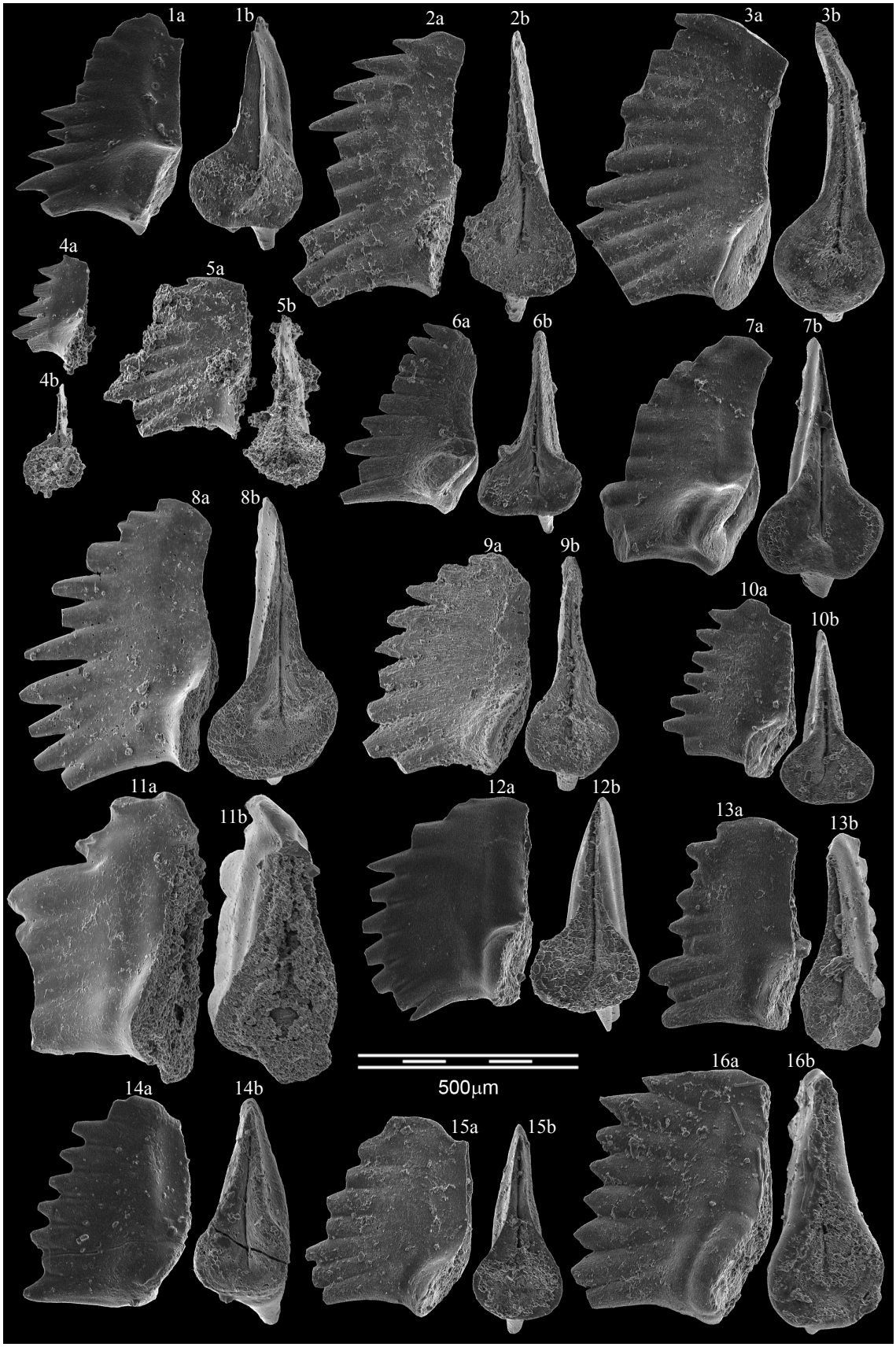
1a
1b
2a
2b
3a
3b
4a
4b
5a
5b
6a
6b
7a
7b
8a
8b
9a
9b
10a
10b
11a
11b
12a
12b
13a
13b
14a
14b
15a
15b
16a
16b
500μm

PLATE 5

PLATE 6

Figs. 1, 2, 4. *Larenella mikei* sp. nov. 1, 4: WAI61; 2: W148-C3.
Fig. 3. *Larenella astericisala* sp. nov. W148-C3.
Fig. 5. *Larenella labialeporina* sp. nov. W148-C3.
Fig. 6. *Larenella galfettii* sp. nov. W148-C3.
Fig. 7. *Larenella fastuosa* sp. nov. W148-C3.
Fig. 8. *Larenella superba* sp. nov. W148-C3.
Fig. 9. *Larenella* aff. *quitondeta*. W146-C8.
Figs. 10, 11. transitional? between *La*. *galfettii* sp. nov. and *La*. *robusta* (Koike, 1982). Both W148-C3.
Figs. 12, 14?, 15. *Larenella hindeodiformis* sp. nov. 12, 15: WAI64; 14: W148-C3.
Fig. 13. transitional? between *La*. *mikei* sp. nov. and *La*. *hindeodiformis* sp. nov. WAI64.
Fig. 16. *Isarcicella*? n. sp. 1. WAI61.
Fig. 17. *Larenella isarcicellaeformis* sp. nov. WAI61.

All ×80. All P1 elements.

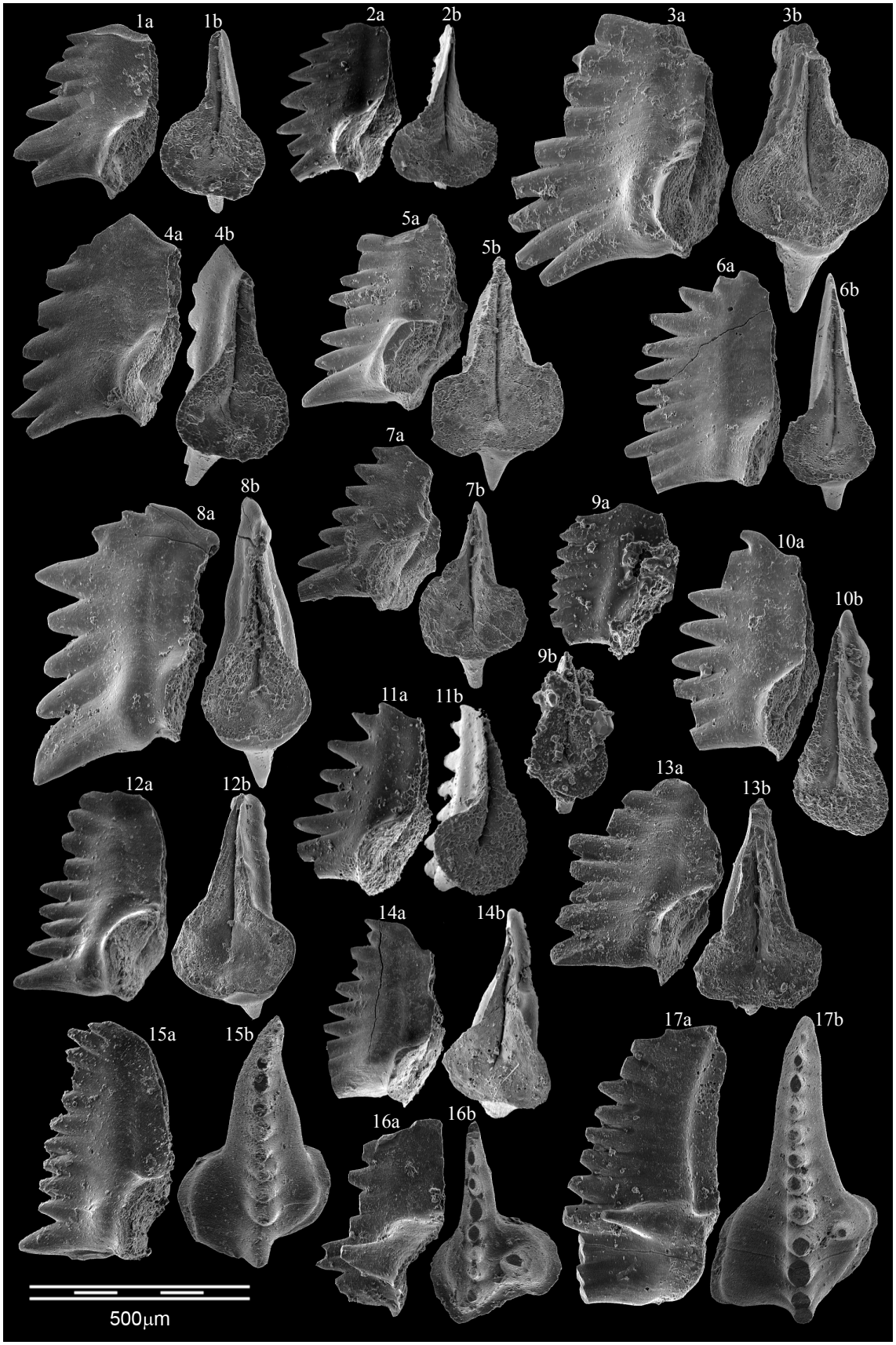
1a
1b
2a
2b
3a
3b
4a
4b
5a
5b
6a
6b
7a
7b
8a
8b
9a
9b
10a
10b
11a
11b
12a
12b
13a
13b
14a
14b
15a
15b
16a
16b
17a
17b
500μm

PLATE 6

PLATE 7

Figs. 1, 3, 4?, 6. *Larenella*? *chaohuense* morph 1. 1, 4: WAI61; 3, 6: W148-C3.
Figs. 2, 8, 9. *Larenella*? *tomeotetragona* sp. nov. 2, 9: W148-C3; 8: WAI61.
Figs. 5, 13?, 16. *Larenella*? *chaohuense* morph 3. 5: W148-C3; 13: W147-C2; 16: WAI61.
Figs. 7, 11, 12. *Larenella*? *chaohuense* morph 2. 7: W145-C7; 11, 12: W144-C6.
Fig. 10. *Nv*. aff. *waageni* 6?. W146-C8.
Figs. 14, 15, 17. *Larenella astericisala* sp. nov. All W148-C3.

All ×80. All P1 elements.

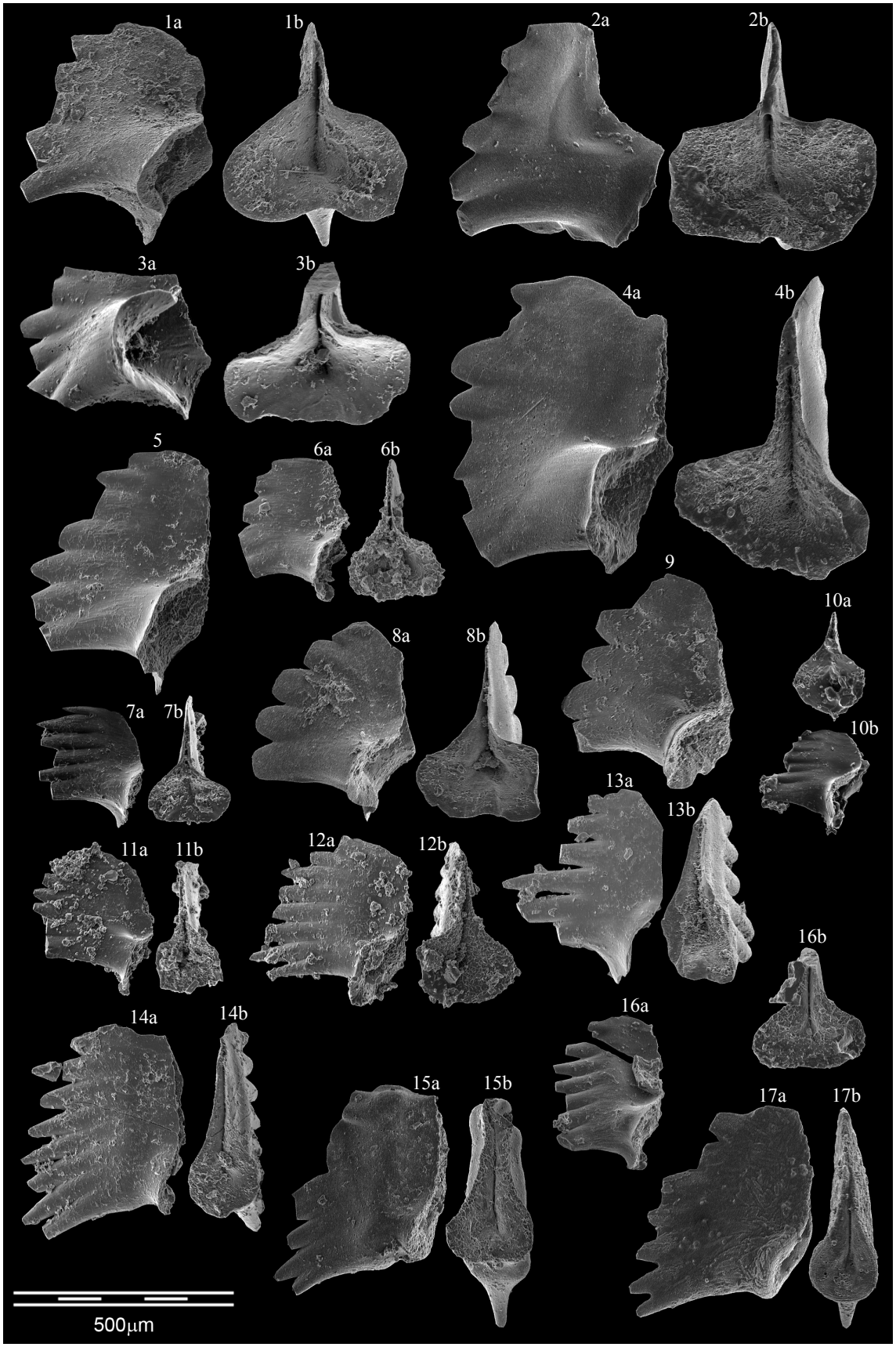
1a
1b
2a
2b
3a
3b
4a
4b
5
6a
6b
9
10a
8a
8b
7a
7b
10b
13a
13b
11a
11b
12a
12b
16b
14a
14b
16a
15a
15b
17a
17b
500μm

PLATE 7

PLATE 8

Figs. 1-3, 4?, 9. *Neospathodus dieneri* morph 9. 1: WAI64; 2, 3, 9: W148-C3; 4: W146-C8.
Fig. 5. Larenella? concava morph 3? W146-C8.
Figs. 6, 10. *Neospathodus dieneri* morph 8. 6: W143-C1; 10: W148-C3.
Fig. 7. *Neospathodus dieneri* morph 2. W148-C3.
Fig. 8. *Neospathodus dieneri* morph 10. W147-C2.
Fig. 11?, 16, 17?. *Neospathodus dieneri* morph 1. All W147-C2.
Figs. 12-14. *Neospathodus artemis* sp. nov. All W147-C2.
Figs. 15, 18, 21. *Neospathodus dieneri* morph 11. 15, 18: W147-C2; 21: W143-C1.
Figs. 19, 22. *Larenella*? sp. Both W147-C2.
Fig. 20. *Wapitiodus*? sp. W143-C1.
Fig. 23. *Guangxidella*? sp. W144-C6.

All ×80. All P1 elements.


1a
1b
2a
2b
3a
3b
4a
4b
5a
5b
6a
6b
9a
9b
7a
7b
8a
8b
10a
10b
11
12a
12b
14a
14b
13a
13b
15a
15b
17a
17b
16a
16b
18a
18b
19
21a
21b
20
22a
22b
23a
23b
500μm

PLATE 8

PLATE 9

Figs. 1?, 2?, 10?, 11?, 14, 15. *Neospathodus* aff. *cristagalli* morph 2. 1, 2, 11: W143-C1; 10: WAI61; 14: WAI65; 15: WAI64.
Figs. 3?, 4?, 18, 19. *Neospathodus* aff. *cristagalli* morph 11. 3, 4, 19: W150-C4; 18: WAI64.
Fig. 5. *Neospathodus dieneri* morph 12. W143-C1.
Figs. 6, 7, 12. *Neospathodus circuloctavus* sp. nov. All W143-C1.
Fig. 8. *Neospathodus dieneri* morph 3?. W143-C1.
Fig. 9. *Neospathodus dieneri* morph 8. W143-C1.
Fig. 13. *Neospathodus* aff. *dieneri* morph 3. W143-C1.
Figs. 16, 17. *Neospathodus dieneri* morph 6. W148-C3.
Fig. 20. Gen. et sp. indet. 5. W143-C1.
Fig. 21. *Ns*. n. sp. 4 Goudemand and Orchard. WAI61.
Fig. 22. *Nv*. aff. *waageni* 1. W148-C3.
Fig. 23. *Nv*. aff. *gnominfernalis* sp. nov. W148-C3.
Fig. 24. *Larenella*? n. sp. 4. W148-C3.
Fig. 25. gen. et sp. indet. juvenile. W148-C3.

All ×80. All P1 elements.


1a
1b
2a
2b
3a
3b
4a
4b
5a
5b
6a
6b
7a
7b
8a
8b
9a
9b
10a
10b
11a
11b
12a
12b
13a
13b
14a
14b
15a
15b
16a
16b
17a
17b
18a
18b
19a
19b
20a
20b
21a
21b
22a
22b
23a
23b
24a
24b
25a
25b
500μm

PLATE 9

PLATE 10

Figs. 1, 4. *Novispathodus* aff. *waageni* morph 7 new. Both WAI65.
Fig. 2. *Novispathodus* aff. *pakistanensis* morph 7?. WAI65.
Figs. 3, 6. *Novispathodus strictomarginis* sp. nov. Both W148-C3.
Figs. 5. *Larenella astericisala*? sp. nov., juvenile. WAI61.
Figs. 7, 8. transitional? between *Ns*. *dieneri* 9 and *La*. *galfettii* sp. nov. Both W148-C3.
Fig. 9. *Sweetocristatus*? aff. *unicus* Dagis (1984). W148-C3.
Figs. 10, 12, 16, 24. New genus G spp. All W148-C3.
Fig. 11. *Larenella*? aff. n. sp. 1 Dagis (1984). W148-C3.
Fig. 13. *Merillina*?/*Ellisonia*? sp., P2? element. W148-C3.
Fig. 14. ?*Sweetocristatus* sp.. W148-C3.
Fig. 15. *Merillina*?/*Ellisonia*? aff. sp. B Orchard (2007). W148-C3.
Fig. 17. *Hadrodontina* aff. *aequabilis*. WAI61.
Fig. 18. ?*Neostrachanognathus* sp. W150-C4.
Figs. 19?. *Cornudina*? sp. broken specimen. W150-C4.
Figs. 21, 22. *Cornudina*? cf. *breviramulis*. WAI64.
Fig. 20. ?*Sweetocristatus* sp.. W148-C3.
Fig. 23. *Merillina*?/*Ellisonia*? aff. *agordina*. WAI64.
Fig. 25. *Hadrodontina aequabilis*. WAI61.

All ×80. All P1 elements (except Figs. 13?, 14?).


1a
1b
2a
2b
3a
3b
4a
4b
5a
5b
6a
6b
7a
7b
8a
8b
9a
9b
10a
10b
11a
11b
12a
12b
13a
13b
14a
14b
15
16a
16b
17a
17b
18a
18b
19a
19b
20a
20b
21a
21b
22a
22b
23a
23b
24
25a
25b
500µm

PLATE 10

PLATE 11

Figs. 1, 5. Genus C Goudemand and Orchard (Chapter 4), S3 elements. 1: W147-C2, 5: W146-C8.
Figs. 2, 12. Genus B Goudemand and Orchard (Chapter 4), S2 elements. 2: W147-C2, 12: WAI61.
Fig. 3. New Genus D, S2 element. W145-C7.
Figs. 4, 9. *Novispathodus* spp., resp. S1 and S2 elements. 4: WAI61, 9: W148-C3.
Fig. 6. *Neospathodus*, S3 element. W147-C2.
Fig. 7. New Genus E, S3/4 element. WAI64.
Fig. 8. *Guangxidella*?/*Larenella*? sp., typical tertiopedate S3 element of the Mullerinae subfamily. W145-C7.
Fig. 10. *Ellisonia triassica* Müller (1956), S4? element. WAI65.
Fig. 11. *Ellisonia* aff. *triassica* sensu Koike (2004), S3? element. W148-C3.
Fig. 13. *Larenella* sp., S0 element. W148-C3.
Fig. 14. *Guangxidella*? sp., P2? element. The overall shape of this slightly angulate element suggests a homology as a P2 element. The cusp and anterior process are similar to the homologous element in *Wapitiodus* as reconstructed by Orchard (2005). Yet, the posterior 'process' as well as the aboral surface more strongly resemble some P1 elements of the closely related *Guangxidella*, hence the tentative assignment. W145-C7.
Figs. 15-17. *Neospathodus*? spp., P2 elements. Note the bifurcation of the anterior process in fig. 17. All W148-C3.


1
2
3a
3b
4
5
7a
7b
8
6
9
12
11a
11b
10
14a
14b
16a
16b
17
13b
13a
15
500μm

PLATE 11

PLATE 12

Figs. 1, 3, 4, 6?, 13, 20. *Larenella*? spp., P2 elements. 1, 3, 6: W146-C8; 4, 13: W147-C2; 20: W148-C3.
Figs. 2, 5, 7?, 9-12, 14-19, 21, 23, 25, 27. unassigned P2 elements. 2, 7: W146-C8; 5, 12: W147-C2; 9, 10: W144-C6; 11, 14-16, 18, 19, 21, 23, 25, 27: W148-C3; 17: WAI61.
Fig. 8, 22, 24. *Merillina*?/*Ellisonia*? spp., P1/2 elements. 8: W150-C4, 22: W148-C3, 24: W146-C8.
Fig. 26. *Novispathodus* sp., P2 element. W148-C3.
Figs. 28, 29. New Genus F, P2 elements. Both W148-C3.


1a
1b
2a
2b
3a
3b
4
5a
5b
6
7a
7b
8a
8b
11a
11b
10a
10b
13a
13b
9a
9b
12a
12b
17a
17b
16a
16b
14a
14b
15a
15b
18a
18b
21a
21b
22
20a
20b
19a
19b
23a
23b
24a
24b
28a
28b
29a
29b
25a
25b
26a
26b
27a
27b
500μm

PLATE 12

ACKNOWLEDGEMENTS

This dissertation would not have been possible without the support and enthusiasm of my advisor Prof. Hugo Bucher (PIMUZ). He is warmly thanked for the friendly, stimulating atmosphere he instilled to our research group.

I'm very indebted to my committee members: Mike Orchard (GSC, Vancouver) for introducing me to the multi-element taxonomy of Early Triassic conodonts and for his great sense of hospitality, Leopold Krystyn (Vienna) for our collaboration on the material from Spiti, and Christoph Zollikofer (AIM, Zurich) for his help and interest.

My best thanks also to: Jim Jenks (Salt Lake City), Kuang Guodun (Nanning), Li Guobiao (Lhasa), Wan Xiaoqiao (Beijing), Aymon Baud (Lausanne), Arnaud Brayard (Dijon, formerly PIMUZ), Thomas Galfetti (Zurich, formerly PIMUZ) and Thomas Brühwiler (Zurich, formerly PIMUZ) for their help before, during and after fieldwork in the US, South China, and Tibet; all those members of PIMUZ who brought me conodont samples from all over the world; Peter Krauss (GSC, Vancouver) for teaching me how to process conodont samples properly; Julia Huber and Leonie Pauli (PIMUZ) for processing my numerous conodont samples properly; Hans Thierstein (ETHZ) for granting access to his lab's SEM; Sandra Hermann (ETHZ) for her help and advices with the SEM; Paul Tafforeau (ESRF, Grenoble), Claude Monnet (PIMUZ), and Renaud Lebrun (Montpellier, formerly AIM) for their help with the 3d model; and all other current and alumni members of PIMUZ who supported me in many ways.

My special thanks to those of my colleagues who eventually became some of my closest friends, especially Séverine Urdy for her unshakable help and encouragement.

CURRICULUM VITAE

GOUDEMAND Nicolas

Date of birth:	02.12.1974
Place of birth:	Chalons en Champagne (France)
Nationality:	French

Education

Since 2005	PhD Student at the Paleontological Institute and Museum, Univ. Zurich.
2000-05	Doctoral Degree in Technical Sciences, ETH Zurich. PhD at the Centre for Structure Technologies, IMES, ETHZ. Title: *3D-3C Speckle Interferometry: Optical Device for Measuring Complex Structures*. Main advisors: Prof. Paolo Ermanni (ETHZ), Prof. Pierre Jacquot (EPF Lausanne).
1998-2003	Research Assistant at the Centre for Structure Technologies, IMES, ETH Zurich: definition and management of research projects, coaching of mechanical engineering students, supervision of the optical methods' laboratory.
1998	DEA (French Master Degree) in "Image and Photonics", Louis Pasteur University (ULP), Strasbourg, France.
1995-98	Engineer's Degree in Physics, Ecole Nationale Supérieure de Physique de Strasbourg (ENSPS), France.
1998	Diploma Thesis, ENSPS, *Automatic Recognition of Insulators for Robotic Maintenance of Electric Power Distribution Lines*, performed at the Super-Mechatronics Research Lab, Yaskawa Electric Corp., Yahatanishi-ku, Kitakyushu, Japan.
1996	Licence (Bsc) in Physics at the Louis Pasteur University (ULP), Strasbourg, France.
1995	Deug A (intermediate degree in Mathematics and Physics) at Orsay University, France.
1992-95	Maths Sup, Maths Spé P': two-year intensive post A-level preparatory courses for entrance exams to the Grandes Ecoles d'Ingénieurs, Savigny sur Orge, France.
1992	Baccalauréat C, equivalent to A-levels in Mathematics, Physics and Chemistry, Savigny sur Orge, France.

Publications during promotion

Articles

Bucher H., Hochuli P.A., Schaltegger U., Ovtcharova M., Galfetti T., Brayard A., **Goudemand N.** & Guex J., 2007. *Timing of recovery from the end-Permian extinction: Geochronologic and biostratigraphic constraints from south China: Comment*. doi: 10.1130/G23609C.1. Geology.

Brayard A., Bucher H., Brühwiler T., Galfetti T., **Goudemand N.**, Jenks J., Escarguel G. and Guodun K., 2007. *Proharpoceras Chao: The last Permian ammonoid survivor*. Lethaia, 40, 175-181.

Galfetti T., Bucher H., Ovtcharova, M., Schaltegger U., Brayard A., Brühwiler T., **Goudemand N.**, Weissert H., Hochuli P. A., Cordey F. and Guodun K., 2007. *Timing of the Early Triassic carbon cycle perturbations inferred from new U-Pb ages and ammonoid biochronozones*. Earth and Planetary Science Letters, 258, 593-604.

Li Guobiao, Wan Xiaoqiao, Jiang Ganqing, Hu Xiumian, **Goudemand N.**, Han Hongdou, Chen Xi, 2007. *Late Cretaceous foraminiferal faunas from the Saiqu 'melange' in southern Tibet*. Acta Geologica Sinica-English edition, 81(6), 917-924.

Galfetti T., Bucher H., Martini R., Hochuli P.A., Weissert H., Crasquin-Soleau S., Brayard A., **Goudemand N.**, Brühwiler T., Guodun Kuang, 2008. Evolution of Early Triassic outer platform paleoenvironments in the Nanpanjiang Basin (South China) and their significance for the biotic recovery. Sedimentary Geology 204 (2008), 36–60.

Li Guobiao, Wan Xiaoqiao, Liu Wencan, Bucher H., Li Hongsheng, **Goudemand N.**, 2009. *A new Cretaceous age for the Saiqu „mélange," Southern Tibet: evidence from Radiolaria*. Cretaceous Research, 30(2009), 35-40.

Monnet, C., Zollikofer, C., Bucher, H. & **Goudemand N.**, 2009. *Three-dimensional morphometric ontogeny of coiled molluscs by micro-computed tomography and geometric analysis*. Palaeontologia Electronica, 12(3), 12A.

Brayard A., Escarguel G., Bucher H., Monnet C., Brühwiler T., **Goudemand N.**, Galfetti T., Guex J., 2009. *Good Genes and Good Luck: Ammonoid Diversity and the End-Permian Mass Extinction*. Science, 325(2009), 1118-1121.

Brühwiler T., **Goudemand N.**, Galfetti T., Bucher H., Baud A., Ware D., Hermann H., Hochuli P. A., Martini R., 2009. *The Lower Triassic sedimentary and carbon isotope records from Tulong (South Tibet) and their significance for Tethyan palaeoceanography.* Sedimentary Geology, 222(2009), 314-332.

Brühwiler T., Bucher H., **Goudemand N.**, 2010. *Smithian (Early Triassic) ammonoids from Tulong, South Tibet*. Geobios, 43, 403-431.

Brühwiler T., Ware D., Bucher H., Krystyn L., **Goudemand N.**, 2010. *New Early Triassic ammonoid faunas from the Dienerian/Smithian boundary beds at the Induan/Olenekian GSSP candidate at Mud (Spiti, Northern India)*. Journal of Asian Earth Sciences, 39(6), 724-739.

Brühwiler, T., Bucher, H., Brayard, A., **Goudemand, N.** 2010. *High-resolution biochronology and diversity dynamics of the Early Triassic ammonoid recovery: the Smithian faunas of the Northern Indian Margin*. Palaeogeography, Palaeoclimatology, Palaeoecology. doi:10.1016/j.palaeo.2010.09.001.

Kaim, A., Nützel, A. Bucher, H., Brühwiler, Th., **Goudemand N.**, 2010. *Early Triassic (Late Griesbachian) gastropods from South China (Shanggan, Guangxi)*. Swiss Journal of Geoscience, 103, 121-128.

Urdy, S., **Goudemand N.**, Bucher, H. & Chirat, R. 2010. Allometries and the morphogenesis of the molluscan shell: a quantitative and theoretical model. Journal of Experimental Zoology (Mol. Dev. Evol.), 314B.

Urdy, S., **Goudemand N.**, Bucher, H. & Chirat, R. 2010. Growth dependent phenotypic variation of molluscan shell shape: a theoretical and empirical comparison using gastropods. Journal of Experimental Zoology (Mol. Dev. Evol.), 314B.

Brühwiler T., Bucher H., **Goudemand N.**, Galfetti T. (submitted). *Smithian (Early Triassic) ammonoid faunas from Exotic Blocks from Oman: taxonomy and biochronology*. Palaeontographica.

Forel, M.B., Crasquin, S., Brühwiler, T., Goudemand, N., Bucher, H., Baud, A., Randon, C., (submitted). *Ostracod recovery after Permian-Triassic boundary mass-extinction in South Tibet*. Palaeogeography, Palaeoclimatology, Palaeoecology.

Urdy, S., **Goudemand N.**, Bucher, H. (submitted). *Growth dynamics within a population of Hexaplex trunculus (Muricidae, Gastropoda) reared in laboratory*.

Urdy, S., **Goudemand N.**, Bucher, H. (submitted). *Growth dynamics and recurrent patterns of covariation among shell characters: a case study on living gastropods*.

Hofmann R., **Goudemand N.**, Wasmer M., Bucher H., Hautmann M. (submitted). *New trace fossil evidence indicates fast recovery from the end-Permian mass extinction*.

Hautmann M., Bucher H., Brühwiler T., **Goudemand N.**, Kaim A., Nützel A. (accepted). *An unusually well preserved mollusc fauna from the Earliest Triassic of South China and its implications for benthic recovery after the end-Permian biotic crisis*. Geobios.

Monnet C., Klug C., **Goudemand N.**, De Baets K., Bucher H. (accepted). *Quantitative Biochronology of Devonian ammonoids from Morocco and comments on the Unitary Association method*. Lethaia.

Goudemand N., Orchard M.J., Urdy S., Bucher H., Tafforeau P., (submitted). *Synchrotron light gives euconodonts new bite: indirect evidence for a lingual cartilage*.

Goudemand N., Orchard M., Tafforeau P., Urdy S., Brühwiler T., Brayard A., Galfetti T. & Bucher H., (submitted) *Early Triassic conodont clusters from South China: revision of the architecture of the 15-element apparatuses of the superfamily Gondolelloidea*.

Goudemand N., Orchard M., Bucher H., Jenks J., (submitted). *The elusive origin of* Chiosella timorensis *(Conodonts, Triassic)*.

Goudemand N., Orchard M., Krystyn L.,Brühwiler T., **Ware D., Bucher H.**, (submitted). *New Early Triassic conodont faunas from the Dienerian/Smithian boundary beds at Muth (Himashal Pradesh, India)*.

Goudemand N., Bucher H., (submitted). *New Early Triassic conodont faunas from the Dienerian/Smithian boundary beds at Waili (Guangxi, China)*.

Abstracts

Goudemand N., Orchard M., Li G., Galfetti T., Bucher H., 2006. *A new early Spathian (Early Triassic) conodont succession from North America*, abstract for *The Boreal Triassic* conference, Longyearbyen, Svalbard, Arctic Norway, 15-20 August 2006, NGF Abstracts and Proceedings, 3: 54.

Goudemand N., Orchard M., Li G., Galfetti T., Bucher H., 2006. *A new early Spathian (Early Triassic) conodont succession from North America*, abstract for the 1st ICOS meeting (First International Conodont Symposium), Leicester, UK, 17-22 July 2006, abstracts and proceedings, p. 35.

Brayard A., Bucher H., Escarguel G., Galfetti T., Hochuli P.A., Brühwiler T., **Goudemand N.**, 2007. *The Early Triassic ammonoid recovery in time and space and its relationship with major changes in the geological record*, 1st International Symposium of Paleobiogeography, Paris.

Brühwiler T., Bucher H., **Goudemand N.** and Brayard A., 2007. *Smithian (Early Triassic) ammonoid faunas of the Tethys: new preliminary results from Tibet, India, Pakistan and Oman*. The global Triassic, Lucas G.L. & Spielmann J.A. eds., New Mexico Museum of Natural History and Science Bulletin, 41: 25-26.

Brühwiler T., **Goudemand N.**, Galfetti T. and Bucher H., 2007. *Early Triassic ammonoid biostratigraphy and a new high-resolution carbon isotope record from Tulong area, South Tibet*. 5th Swiss Geoscience Meeting, Geneva.

Galfetti T., Bucher H., Ovtcharova M., Schaltegger U., Brayard A., Brühwiler T., **Goudemand N.**, Weissert H., Hochuli P.A., Cordey F., Guodun K., 2007. *Early Triassic timescale and new U-Pb ages from South China: first calibration of the Early Triassic carbon cycle perturbations*, The Global Triassic, Lucas G.L. & Spielmann J.A. eds., New Mexico Museum of Natural History & Science, Bull. 41: 312-39.

Ovtcharova M., Bucher H., Galfetti T., Schaltegger U., Brayard A., **Goudemand N.**, Stracke A., 2008. *Tracing magmatic sources of ash beds in the Late Permian to Middle Triassic Nanpanjiang Basin (South China): insights from Hf isotopes on zircons from volcanic ash beds*. Goldschmidt Conference, Vancouver, Canada, .

Urdy S., **Goudemand N.**, Bucher H., Monnet C., 2008. *Molluscan shell shape: patterns of variation and growth models*. 2nd Euro Evo Devo Conference, Gent, Belgium, July 29-August 1st, 2008.

Brayard A., Escarguel G., Bucher H., Brühwiler T., **Goudemand N.**, 2008. *Integrated regional diversity analysis of the Early Triassic ammonoid recovery.* GSA Joint Annual Meeting, Houston, Texas, October 5-9, 2008.

Brühwiler T., Bucher H., Brayard A., **Goudemand N.**, Galfetti T., Hermann E., Hochuli P.A., 2008. *Smithian Ammonoids: The First Diver-*

sity Peak In Ammonoid Recovery Following the Permian-Triassic Mass Extinction. GSA Joint Annual Meeting, Houston, Texas, October 5-9, 2008.

Bucher H., Hochuli P.A., Escarguel G., Hautmann M., **Goudemand N.**, Brühwiler T., Brayard A., Hermann E., Galfetti T., Ware D., 2008. *The Early Triassic Biotic Recovery: a multiproxy approach.* GSA Joint Annual Meeting, Houston, Texas, October 5-9, 2008.

Goudemand N., Orchard M., Bucher H., Brayard A., Brühwiler T., Galfetti T., Hochuli P.A., Hermann E., Ware D., 2008. *Smithian-Spathian Boundary: The Biggest Crisis in Triassic Conodont History.* GSA Joint Annual Meeting, Houston, Texas, October 5-9, 2008.

Hautmann M., Bucher H., Nützel A., Brühwiler T., **Goudemand N.**, Brayard A., 2008. *Recovery of Benthos Versus Nekton after the End-Permian Mass Extinction Event. A Preliminary Comparison.* GSA Joint Annual Meeting, Houston, Texas, October 5-9, 2008.

Hermann E., Hochuli P.A., Bucher H., Brühwiler T., **Goudemand N.**, Roohi G., 2008. *Major Climatic Change at the Smithian/Spathian Boundary – Evidence from Low Palaeolatitudinal Records.* GSA Joint Annual Meeting, Houston, Texas, October 5-9, 2008.

Urdy S., **Goudemand N.**, Bucher H. Monnet C., 2008. *Growth models of recent gastropods shells: implication for ammonoids.* GSA Joint Annual Meeting, Houston, Texas, October 5-9, 2008.

Hermann E., Hochuli P.A., Bucher H., Brühwiler T., **Goudemand N.** & Roohi G., 2008. *Evidence for major climatic change at the Smithian- Spathian boundary from low palaeolatitudinal records.* 6th Swiss Geoscience Meeting, Lugano.

Goudemand N., Orchard, M., Bucher H., Brayard A., Brühwiler T., Galfetti T., Hermann E., Hochuli P.A. & Ware D., 2008. *Smithian-Spathian boundary: The biggest crisis in Triassic conodont history.* 6th Swiss Geoscience Meeting, Lugano. **Award** for best paper and presentation, a prize for young researchers from the Commission of the Swiss Palaeontological Memoirs.

Stephen D. A., Menlove L., **Goudemand N.**, Bylund K. G., Brayard A., McShinsky R. D., Bucher H., Jenks J., 2009. *Early Triassic conodonts in the Pahvant range of central Utah*. GSA, Rocky Mountain Section, 61st Annual Meeting, May 11-13, 2009.

Brayard A., Escarguel G., Bucher H., Monnet C., Brühwiler T., **Goudemand N.**, Galfetti T., Guex J., 2009. *Dynamiques évolutives après une extinction de masse : le feu d'artifices des ammonoïdes au Trias inférieur*. Prospectives en Paléontologie et Palynologie, 4ème congrès A.P.F. (Association Paléontologique Française), Lille, France, June 2-5, 2009.

Stephen D. A., Menlove L., **Goudemand N.**, Brayard A., 2009. *Early Triassic conodonts in Central and Western Utah*. NAPC (North American Paleontological Convention), Cincinnati, Ohio, June 21-26, 2009.

Bucher H., **Goudemand N.**, Brühwiler T. & Ovtcharova M., 2009. *High-resolution biochronology and taxonomic richness of Early Triassic ammonoids and conodonts: Why methodology matters*. NAPC (North American Paleontological Convention), Cincinnati, Ohio, June 21-26, 2009.

Goudemand N., Orchard M., Tafforeau P., Urdy S., Brühwiler T., Bucher H., Brayard A., Galfetti T., 2009. *Early Triassic conodont clusters from South China: Revision of the architecture of the 15-element apparatuses of the Gondolelloidea superfamily*. International Conodont Symposium (ICOS) 2009 Abstracts, Calgary, Alberta, Canada, July 12-17, 2009. Permophiles, 53, Supplement 1, ISSN 1684-5927, June 2009, pp. 16-17.

Goudemand N., Orchard M., Tafforeau P., 2009. *An animated functional model of the Lower Triassic* Novispathodus *apparatus based on X-ray synchrotron microtomography and computer graphics*. International Conodont Symposium (ICOS) 2009 Abstracts, Calgary, Alberta, Canada, July 12-17, 2009. Permophiles, 53, Supplement 1, ISSN 1684-5927, June 2009, pp. 17-18.

Goudemand N., Orchard M., Tafforeau P., Urdy S., Brühwiler T., Bucher H., Brayard A., Galfetti T., Monnet C., Lebrun R. & Zollikofer C., 2009. *Paleobiology of Early Triassic conodonts: implications of newly discovered fused clusters imaged by X-ray synchrotron microtomography*. 7th Swiss Geoscience Meeting, Neuchâtel. **Award** for best paper and presentation, a prize for young researchers from the Commission of the Swiss Palaeontological Memoirs.

Brühwiler T., Bucher H., **Goudemand N.**, Ware D., Hermann E., 2009. *Smithian ammonoids (Early Triassic): explosive evolutionary radiation following the Permian/Triassic mass*

extinction. 7th Swiss Geoscience Meeting, Neuchâtel.

URDY S., **GOUDEMAND N.**, BUCHER H.& MONNET C., 2009. *How do recurrent patterns of covariation in molluscan shells connect to growth dynamics?* 7th Swiss Geoscience Meeting, Neuchâtel.

HOFMANN R., HAUTMANN M., **GOUDEMAND N.**, WASMER M., BUCHER H., 2010. *Complex colonisation patterns of benthic communities in the immediate aftermath of the end-Permian mass extinction: New data from the Dolomites.* IGCP 572: Recovery of ecosystems after the P-Tr mass extinction: Field workshop in Oman, Gutech of Muscat, Oman, 20-26 February, 2010, abstract book.

HAUTMANN, M., BUCHER, H., BRÜHWILER T., **GOUDEMAND N.**, KAIM A., NÜTZEL A., 2010. *An unusually well preserved mollusc fauna from the Earliest Triassic of South China: a unique window into the early survival phase after the end-Permian mass extinction event*. IGCP 572: Recovery of ecosystems after the P-Tr mass extinction: Field workshop in Oman, Gutech of Muscat, Oman, 20-26 February, 2010, abstract book.

OVTCHAROVA M., BUCHER H., **GOUDEMAND N.**, SCHALTEGGER U., BRAYARD A., GALFETTI T., 2010. *New U/Pb ages from Nanpanjiang Basin (South China): implications for the age and definition of the Early-Middle Triassic boundary*. European Geosciences Union, General Assembly 2010, Geophysical Research Abstracts, Vol. 12, EGU2010-12505-3, Vienna, Austria, 02-07 May, 2010.

URDY, S., GOUDEMAND, N., BUCHER, H., MONNET, C., 2010. *Recurrent patterns of covariation in ammonoid shell characters: How do they relate to growth dynamics?* 8th international symposium- Cephalopods, Past and Present, Dijon, France, Aug. 30-Sept. 3, 2010.

WARE, D., BUCHER, H., BRÜHWILER, T., GOUDEMAND, N., 2010. *Dienerian (early Triassic) ammonoid successions of the Tethys: preliminary results from Pakistan and India*. 8th international symposium- Cephalopods, Past and Present, Dijon, France, Aug. 30-Sept. 3, 2010.

URDY, S., GOUDEMAND, N., BUCHER, H., MONNET, C., 2010. *Recurrent patterns of covariation in ammonoid shell characters: How do they connect to growth dynamics?* 80. Jahrestagung der Paläontologischen Gesellschaft, Munich, Germany, 5-8 Oct., 2010.

POSTERS

URDY S., **GOUDEMAND N.**, BUCHER H., CHIRAT R., 2006. *Growth dependent phenotypic variation: quantitative theoretical approach of mollusc shell morphogenesis*, abstract for the First and Founding Meeting of the European Society for Evolutionary Developmental Biology (EED), Prague, Czech Republic, 16-19 August, 2006. **Award** for best student poster presentation.